Regulation of phosphatidylinositol 3-kinase (PI3K/Akt) pathway in chicken and duck cells and its implications for influenza A virus pathogenesis

By

Sanjeeva Kumar **B.V.Sc. & A.H., M.V.Sc.**

Thesis submitted to the University of Nottingham for the degree of Doctor of Philosophy

School of Veterinary Medicine and Science

The University of Nottingham

March-2018

For my dearest parents for their motivation,

My beloved wife Suhasini for her love and support

And my lovely daughter and son for their cooperation

during the course of this work

Abstract

Wild aquatic birds, particularly ducks are considered as the major reservoirs of low-pathogenic avian influenza A viruses (LPAIAVs). Occasional spill-over to susceptible hosts like chicken and turkeys results in severe disease especially when infected with high pathogenic H5N1 virus subtypes that evolve from their progenitors LPAIAVs in gallinaceous birds, gaining zoonotic significance. Disparate disease outcomes between chicken and ducks to avian influenza virus (AIV) infection suggest potential species differences in mounting antiviral response. Mammalian studies indicate that influenza A virus non-structural protein 1 (NS1) interacts with vital host proteins to interfere with and hijack cellular functions for viral replication advantage. NS1 has been shown to bind to PI3K/Akt (phosphatidylinositol-3-kinase) p85beta subunit resulting in pathway activation. The PI3K/Akt pathway is crucial in the regulation of cellular differentiation, proliferation and survival through inhibition of pro-apoptotic factors. However, there are few studies of regulation of PI3K/Akt signalling in avian hosts, and in particular of its role in AIV replication. Understanding the host cellular response to AIV infections is key for developing effective control measures. Therefore, the present study investigated the regulation of PI3K/Akt regulation in avian cells and its implications for influenza A virus replication.

Infection of primary chicken or duck embryo fibroblast (CEF/DEF) cells with A/mallard duck/England/7277/06(H2N3) virus demonstrated activation of PI3K/Akt only in the chicken but not in duck cells. The virus induced PI3K/Akt pathway activation was further confirmed by infecting cells with different low pathogenic

avian influenza (LPAI) virus subtypes. Chemical inhibition of PI3K/Akt by treating infected CEFs with LY294002 resulted in significantly higher apoptosis induction and reduced infectious virus production compared to uninhibited control cells. These results suggest that activation of the PI3K/Akt pathway in infected chicken cells results in improved cellular survival allowing for enhanced virus replication.

Analysis of previously published transcriptome data from IAV infected chicken and duck lung cells revealed higher expression of phosphatase and tensin homolog (PTEN) a potent PI3K/Akt negative regulator and down regulation of cytoskeletal actin remodelling associated genes like Cdc42 and RAC 1 in duck compared to chicken cells. Previous studies on AIV morphogenesis have shown roughly spherical budding virion morphology in CEFs while elongated in duck cells and speculated host factors responsible for virus morphogenesis. Based on these observations, repercussions of PI3K/Akt activation on cytoskeletal actin remodelling and virus morphogenesis in H2N3 virus infected CEFs and DEFs was studied. The results revealed loss of actin filament integrity and recorded perfectly spherical budding virion morphology upon PI3K/Akt inhibition in CEF cells. While duck cells still produced elongated viruses irrespective of PI3K/Akt inhibitor or mock treatment. Strikingly, a complete loss of cytoskeletal actin architecture was observed in virus infected duck cells irrespective of inhibitor or mock treatment.

Analysis of chicken and duck PI3K/Akt p85β sequence revealed amino acid changes that may interfere AIV-NS1 binding and activation of PI3K/Akt. In particular, a highly acidic glutamic acid

(E) amino acid residue at 475 position was observed across all major mammalian and avian hosts studied except ducks in which E475 residue was substituted with a non-polar valine (V) residue (E475V). However, these in silico experimental observations require further investigations.

Infection of CEFs with LPAI viruses resulted in activation of PI3K/Akt for a shorter duration while recombinant H5N1 virus infection resulted in prolonged pathway activation. Infection of CEFs with chimeric(c) H9N2 virus carrying segment 8 (NS) from H5N1 (50-92) confirmed the potential contribution of H5N1-NS segment for prolonged PI3K/Akt activation. A comparative AIV NS1 sequence analysis from LPAI and HPAI viruses, revealed several amino acid differences that might contribute to prolonged PI3K/Akt activation. Interestingly, an additional SH3-binding motif-1 was observed in H5N1 (50-92) virus NS1 in comparison to other four viruses used in the study upon in silico protein binding site predictions.

In conclusion, the present study revealed lack of PI3K/Akt activity despite AIV infection in duck fibroblast cells. There is an indication that there may be differences in the p85β subunit underlying these differences in the ducks conferring disease resistance compared to chickens. The study signifies host-specific viral replication strategy that may find potential use in disease control interventions in the future.

Author’s declaration

I declare that the work in this thesis was carried out in accordance with the regulations of the University of Nottingham. The work is original and has not been submitted for any other degree at the University of Nottingham or elsewhere.

Name: SANJEEVA KUMAR

Signature & date:

Conferences, Posters and Oral Presentations

1) "Potential role of Toll-like receptor-3 in influenza virus pathogenesis in chickens." Sanjeeva Kumar, Sujith Sebastian, Sharon M Brookes, Ian H Brown, Kin-Chow Chang, Suresh V Kuchipudi. Poster presentation at Society for General Microbiology (SGM) Annual Conference 2015. March 30th -2nd April 2015 at international convention Birmingham, United Kingdom.

2) "The role of the PI3K-Akt pathway in influenza virus replication in chicken cells" Sanjeeva Kumar, Rathnapraba S, Vijayarani K, Raja S, Kumanan K, Kin-Chow Chang, Janet Daly and Suresh V Kuchipudi. Poster presentation, Emerging viruses Conference, March 27th -29th July 2015 at School of Veterinary Medicine & Science, University of Nottingham, United Kingdom.

3) "Highly pathogenic H5N1 and novel H7N9 avian influenza viruses induce differential innate response in chicken cells" Sanjeeva Kumar, Sebastian S,brookes SM,Brown IH, Kin-Chow Chang and Suresh V Kuchipudi. Poster presentation. Emerging viruses Conference from March 27th -29th July 2015, at School of Veterinary Medicine & Science, University of Nottingham, United Kingdom.

4) "Role of PI3K a host cellular signalling pathway in innate immune response to influenza virus infection in chicken cells" Sanjeeva Kumar, Kin-Chow Chang, Holly Shelton, Suresh V Kuchipudi and Janet Daly. Poster presentation. Microbiology Society Annual Conference, March 21st -24th at international convention Liverpool, United Kingdom.

5) "In-vitro assessment of PI3K/AKT regulation in influenza virus infected primary chicken fibroblast cells" Sanjeeva Kumar, Holly Shelton, Suresh V Kuchipudi, Kin-Chow Chang and Janet Daly. Oral Presentation, Microbiology Society focused meeting on molecular biology and pathogenesis of avian viruses. 27th -29th July 2016 at Charles Darwin House, London, United Kingdom.

6) "Differential phosphatase and tensin homologue (PTEN) expression in chicken and duck cells may explain the differences in antiviral response between these species" Sanjeeva Kumar, Holly Shelton, Suresh V Kuchipudi, Kin-Chow Chang and Janet Daly. Oral Presentation, Microbiology Society Annual Conference, April 3rd–6th 2017 at ICC Edinburgh, United Kingdom.

7) "Regulation of the phosphatidylinositol-3-kinase (PI3K-Akt) pathway in influenza A virus-infected avian cells" Sanjeeva Kumar, Kin-Chow Chang, Suresh V Kuchipudi, Holly Shelton and Janet Daly. Presented at Global Alliance for Research on Avian Diseases-2018 (GARAD-18) conference. January 17th-19th 2018 at Hanoi, Vietnam.

8) "Regulation of the phosphatidylinositol-3-kinase (PI3K-Akt) pathway in influenza A virus-infected avian cells". Janet M Daly, Sanjeeva Kumar, Holly Shelton, Suresh V Kuchipudi, Kin-Chow Chang, Stephen P Dunham. Poster presentation, 10 th International Symposium on Avian Influenza 15 - 18 April 2018 the Grand Hotel, Brighton, UK.

9) "Virus-host co-evolution in influenza A virus reservoir species". Sanjeeva Kumar, Holly Shelton, Suresh V Kuchipudi, Stephen P Dunham, Janet M Daly Kin-Chow Chang. Poster presentation.

10th International Symposium on Avian Influenza15 - 18 April 2018 the Grand Hotel, Brighton, UK.

10) "Influenza A viruses activate host PI3K/Akt survival pathway for "pro-viral" advantage in chicken but not in duck cells" Sanjeeva Kumar, Holly Shelton, Suresh V Kuchipudi, Kin-Chow Chang and Janet Daly. Oral presentation. 5th international One Health Congress, Saskatoon, Canada during 22-25th June 2018.

Acknowledgments

I am very grateful to my supervisors, Dr. Janet M Daly and Dr. Suresh V Kuchipudi for their enormous scientific, technical and personal supervision and support, without which this thesis would not have been possible. I consider working with both of them as one of the greatest privilege of my professional life. My Deepest regards also to my supervisory committee members, Prof. Kin-Chow Chang and Dr. Holly Shelton for their excellent support and valuable inputs throughout the study. It was with the kind support from Dr. Holly that I could make short visits to the Pirbright institute for virus rescue and TOCs works, indeed a big thank you for all your kind heart Dr. Holly. I wish to take this opportunity to extend my sincere thanks to Dr. Stephen Dunham for providing me with AIV H2 primary antibody and for all his valuable and fruitful discussions during the group meetings. My sincere thanks are also due to Dr. Lisa Chakrabarti, for allowing me to use the protein blot modules. I wish also to thank Dr. Tania Dottorini, for helping me with *in-silico* protein-protein interaction modelling, and also extend my deepest regards to my PhD bioinformatics friend Sankalp Arya for helping me analysing microarray data.

I also wish to thank Denise Christie, the technician in School of Biomedical Science, University of Nottingham for her technical support with the Electron Microscopy work, to Belinda Wang, A43 technician in charge and I wish to express my genuine gratefulness to all my fellow postgrads, in the Vet School who directly or indirectly touched my heart during my time at Nottingham.

Funding indeed is a vital component of the project, I whole heartedly thank Indian council of agricultural research (ICAR) New Delhi, India for awarding me with ICAR-international fellowship towards my subsistence allowance at Nottingham and University of Nottingham for awarding me with Special scholarship that covered my tuition fees for the entire period of my study at Nottingham. Again my special thanks to Dr. Suresh V Kuchipudi for all his untiring efforts for securing special scholarship for me. I wish to thank my employer and all my colleagues at The Institute of Animal Health & Veterinary Biologicals, Hebbal, Bangalore, India for granting me study leave for perceiving full time PhD programme at University of Nottingham. I have been very fortunate to have had the generous support of my colleagues back home in India, Dr.M.D.Venkatesha, Shivaraj Murag, Shesha Rao, Shankar Bajantri and list is on… friends and family members, too numerous to mention here. But I wish to thank my lab mates at Nottingham especially Phangxiang chang,

Sujith Sabestian, Awatif Belkheri, Lamyaa Al-Dalwai, Ge Wu, Anitha Varghese, Irene, Sadie, Maha (One more name missing!), my Portuguese pubmate Ivo, and of course Barney the 'King' for their fabulous friendship and cooperation throughout the course of my study. My love to a battalion of JNV school friends, Ambaray, Shivanand, Nagaraj, Uday to name a few, who withstood the test of time and supported me morally 'yet times financially'!.

I wish to express my deepest gratitude to my beloved father who is now over 100 years and my mother, 90+ years, who have been a constant support throughout my career. To my elder brothers Shri. Shivasharanapp and Santosh, sisters who all are my constant source of refilling motivation and encouragement. I would have been worthless without the support of my lovely caring wife Suhasini and my sweet little daughter Manushka and son Siddhant for being so wonderful, understanding and willing to accept the many hours I have had to devote to my research, to their neglect. I extend my kind regards to my mother in-law and brother in-law Harish, who all have supported enormously throughout my study.

Table of contents

Abstract iii

Author's declaration vi

Conferences, Posters and Oral Presentations vii

Acknowledgments x

Table of contents xiii

List of figures xxiv

List of tables xxx

List of abbreviations xxxi

Chapter 1. Introduction 1

1.1 Influenza overview 2

1.2 Type A Influenza viruses 7

1.3 Influenza A virus taxonomy 7

1.3.1 Unified nomenclature system for identification of H5N1 viruses 9

1.4 Properties of influenza A virus 10

1.4.1 Structure and genomic architecture 10

1.4.2 Viral ribonucleoprotein complex 14

1.4.3 Molecular organisation of influenza A viral genome 14

1.5 Replication of IAVs 20

1.5.1 Virus attachment and uncoating 20

1.5.2 Viral RNA synthesis 20
1.5.3 Protein synthesis, packaging, budding and release of virus particles. 21
1.6 Genetic variations in influenza A virus 22
1.6.1 Antigenic drift and shift in influenza A virus 23
1.7 Determinants of influenza A virus host range 26
1.8 Influenza A virus transmission 27
1.9 Influenza A virus pathogenicity determinants 28
1.10 Immune response to influenza A virus 30
1.10.1 Adaptive immune response to influenza virus infection 31
1.10.2 Unique features of avian immune system 32
1.10.3 Differences in the outcome of influenza A virus infected chickens and ducks or derived cells 33
1.11 Emergence of highly pathogenic influenza viruses from their progenitor low pathogenicity influenza A viruses 35
1.12 Host cell signalling pathways and IAV infections 36
1.12.1 Phosphatidylinositol 3-kinase pathway and influenza A virus infection 38
1.12.2 PI3K/Akt pathway mediated signal transduction loop 40
1.12.3 PI3K/Akt pathway mediated apoptosis regulation 42
1.12.4 Negative regulators of PI3K/Akt activation 44

1.13 Cell cytoskeleton reorganisation by PI3K/Akt and its implications for budding virus morphogenesis..... 45
1.14 Importance of adopting species specific cell culture system for study of signalling pathways during AIV infections 46
1.15 Study hypothesis..... 49
1.15.1 Aims and objectives of the study 49
Chapter 2. General Materials and Methods.....50
2.1 Influenza viruses used in the study..... 51
2.1.1 Propagation of virus stocks in eggs 51
2.1.2 Preparation and maintenance of chicken and duck primary embryo fibroblast cells..... 53
2.1.3 Standard protocol adopted for propagation of cells..... 54
2.1.4 Cryopreservation and revival of cells..... 56
2.1.5 Titration of influenza viruses 56
2.1.6 Immuno–cytochemical staining for detection of IAV NP protein in the infected cells 57
2.1.7 Determination of MOI and viral focus forming units..... 58
2.2 Experimental infection of cells IAVs 60
2.3 Statistical analysis of data 61
Chapter 3. Regulation of phosphatidylinositol-3-kinase (PI3K/Akt) pathway in H2N3 or H6N1 virus-infected chicken and duck embryo fibroblast cells 63

3.1 Introduction 64
3.1.1 PI3K/Akt pathway in virus-induced pathogenesis 64
3.1.2 PI3K/Akt pathway activation by influenza A virus and its implications on virus propagation 67
3.1.3 Importance of IAV induced PI3K/Akt activation for viral replication 69
3.1.4 Species specificity, a crucial factor to consider for studying host cellular signalling mechanism 71
3.2 Aims and objectives 73
3.2.1 Aims 73
3.2.2 Objectives 73
3.3 Materials and Methods 74
3.3.1 Cell lysate preparation for protein expression 74
3.3.2 Total protein quantification 74
3.3.3 SDS-Polyacrylamide gel electrophoresis 75
3.3.4 Protein transfer onto PVDF membrane and blocking 76
3.3.5 Incubation with primary and secondary antibodies 77
3.3.6 Chemiluminescent development 78
3.3.7 Determination of binding specificity of rabbit origin primary pAkt (Ser473) antibody for use in avian cells 78
3.3.8 Titration of LY294002 or Wortmannin dose for use in cell culture 79

3.3.9 Titration of infectious virus production in MDCK cells 80
3.3.10 Measurement of cell metabolic activity 81
3.3.11 Measurement of activated caspase 3/7 activity 82
3.3.12 Preparation of tracheal organ cultures 83
3.3.13 Propagation and infection with H2N3 virus of chicken macrophage (HD11) cells 85
3.4 Results 86
3.4.1 CEF cells produce higher titres of IAV than DEF cells 86
3.4.2 AIV infection induces activation of the PI3K/Akt pathway in chicken embryo fibroblast cells 87
3.4.3 Titration of effective dose of LY294002 or wortmannin for PI3K/Akt inhibition and cytotoxicity assessment 88
3.4.4 Binding and entry of influenza A virus does not transiently activate the PI3K/Akt pathway 91
3.4.5 Influenza virus entry into cells is independent of PI3K activity 92
3.4.6 Post-infection inhibition of the PI3K/Akt pathway results in a significant reduction in infectious virus output in CEF cells 94
3.4.7 Influenza A virus infection does not induce the PI3K/Akt signalling pathway in DEF cells 95
3.4.8 PI3K/Akt inhibition leads to enhanced caspase-mediated apoptosis in H2N3 virus infected CEFs 96

3.4.9 Chemical inhibition of PI3K activity leads to reduced cellular metabolic activity in H2N3 virus infected chicken embryo fibroblast cells 98
3.4.10 Activation of the PI3K/Akt pathway was not observed in HD11 (chicken macrophage) cell line despite virus infection 100
3.4.11 The PI3K/Akt pathway is actively regulated in chicken tracheal organ cultures (TOCs) 101
3.5 Discussion 103
3.5.1 Activation of the PI3K/Akt in CEF and DEF cells 103
3.5.2 Effect of PI3K/Akt activation on virus propagation..... 104
3.5.3 IAV infected duck cells exhibited no evidence of PI3K/Akt activation..... 105
3.5.4 Apoptosis regulation in IAV infected CEF and DEF cells 106
3.5.5 Evaluation of continuous cells and ex-vivo organ culture models for study of PI3K/Akt activation 108
3.5.6 Conclusions..... 109
Chapter 4. Transcriptomic insights into the interplay of PI3K/Akt pathway, actin remodelling and AIV morphogenesis 112
4.1 Introduction 113
4.1.1 Deciphering functional genomics knowledge from transcriptome data of IAV infected avian lung cells..... 113

4.1.2 High throughput gene expression profiling 114
4.1.3 Avian specific transcriptomic studies 115
4.1.4 IAV mediated PI3K/Akt activation and apoptosis..... 118
4.1.5 PI3K/Akt role in cytoskeletal actin remodelling 119
4.2 Aims and objectives..... 122
4.2.1 Aims 122
4.2.2 Objectives 122
4.3 Materials and Methods 123
4.3.1 Microarray experimental design and data processing..... 123
4.3.2 Transcriptomic data analysis and interpretation 124
4.3.3 Immunofluorescence staining of CEFs and DEFs for actin-staining and H2N3 viral morphogenesis 125
4.3.4 Electron microscopy of H2N3 virus infected CEF cells 129
4.3.5 Preparation of samples for transmission electron microscopy..... 129
4.4 Results..... 133
4.4.1 H2N3 virus infected chicken and duck lung cells display equivalent PI3K/Akt stimulatory gene cluster expression..... 133
4.4.2 Host anti-apoptosis gene cluster expression revealed higher basal expression of adaptor protein Growth factor receptor-bound protein 2 (GRB2) 134

4.4.3 PI3K/Akt negative regulator phosphatase and tensin homolog (PTEN) was constitutively over expressed in duck compared to chicken cells 135
4.4.4 Higher expression of cell division control protein 42 homolog (Cdc42) and Ras-related C3 botulinum toxin substrate 1(RAC1) observed in chicken but not in duck cells 137
4.4.5 Five key PI3K/Akt associated genes differentially expressed in chicken and duck lung cells 139
4.4.6 PI3K/Akt inhibition resulted in cytoskeletal actin disruption and cytosolic viral cargo retention in CEFs 140
4.4.7 Complete loss of actin integrity observed in H2N3 virus infected duck fibroblast cells 146
4.4.8 PI3K/Akt inhibition influenced budding virus morphology in chicken cells 148
4.5 Discussion 150
Chapter 5. Innate response to avian influenza viruses and importance of NS1–p85β interactions in PI3K/Akt activation in chicken cells 154
5.1. Introduction 155
5.1.1 Innate immune response to avian influenza virus 155
5.1.2 IAV NS1 in host innate response and PI3K activation 156

5.1.3 The p85β-NS1 interaction and its significance in PI3K activation..... 160
5.2 Aims and objectives..... 163
5.2.1 Aim..... 163
5.2.2 Objectives 163
5.3 Materials and Methods 164
5.3.1 Infection of chicken fibroblast cells and collection of cell lysates 164
5.3.2 RNA extraction, cDNA conversion and gene expression studies. 164
5.3.3 Host immune related gene expression analysis..... 167
5.3.4 Recombinant influenza virus rescue 169
5.3.5 Recombinant viruses used in the present study 170
5.3.6 PI3K–p85β and AIV NS1 sequence analysis..... 174
5.4 Results..... 176
5.4.1 TLR expression was significantly higher compared RLR and NLR responses 176
5.4.2 LPAI viruses induced more potent Mx1 and OAS response than an H5N1 virus. 178
5.4.3 LPAI and HPAI viruses differentially induce pro-inflammatory cytokine response in infected CEFs..... 180

5.4.4 Recombinant H5N1 and rH9N2 viruses differentially activate PI3K/Akt pathway 182
5.4.5 H5N1 NS1 is responsible for prolonged PI3K activation.... 183
5.4.6 Infectious virus production was significantly reduced in PI3K/Akt inhibited cH9N2 virus infected CEF cells..... 185
5.4.7 AIV NS1 sequence analysis revealed variations in genetic constitution between HPAI and LPAI viruses. 186
5.4.8 Presence of an additional SH3 binding motif 1 (SH3 bmf1) may contribute for prolonged PI3K/Akt activation in rH5N1 infected cells. 188
5.4.9 Duck PI3K-p85β subunit exhibits sequence diversity compared to chicken. 190
5.4.10 Protein structural modelling suggested E475V is bound on the helix outside the P85β–NS1 interaction site 192
5.4.11 In silico analysis revealed role of chicken p85β E475 residue in conferring protein binding sites on iSH2 domain 193
5.5 Discussion 196
5.5.1 Host cytokine response to influenza virus infection..... 196
5.5.2 Differences in the rH5N1 and LPAI mediated PI3K/Akt activation and AIV NS1 contributions. 197
5.5.3 Differences in the genetic constellation of AIV NS1 and PI3K activation. 198

5.5.4 Diversity in duck PI3K-p85 may potentially hinder pathway activation 200

Chapter 6. General Discussion 202

6.1 General discussion 203

6.2 Summary and future scope of the study 211

Appendices 213

References 221

List of figures

Figure 1-1: Schematic depiction of international system of nomenclature for influenza viruses 8
Figure 1-2: Schematic structural illustration of influenza A virus 11
Figure 1-3: Schematic illustration of influenza virus vRNA segment ..12
Figure 1-4: Organization of protein coding open reading frames (ORF) in Influenza A virus genome 13
Figure 1-5: Schematic illustration of influenza A viral ribonucleoprotein (vRNP).....14
Figure 1-6: Schematic illustration showing influenza A virus HA protein 16
Figure 1-7: Antigenic drift and shift in influenza A viruses 25
Figure 1-8: Host spectrum of influenza A viruses.....27
Figure 1-9: Influenza A virus pathogenesis comparison between LPAIV and HPAIV in chicken and ducks.....35
Figure 1-10: Classification of mammalian PI3K family and its domain structure modified and adopted from Thorpe et al. (2015).....40
Figure 1-11: Schematic representation of phosphoinositide-3 kinase (PI3K/Akt) signalling pathway.....42

Figure 1-12: Apoptosis regulation by effector kinase Akt (activated Akt) downstream of PI3K 44
Figure 2-1: Representative imaging technique adopted for imaging 96 well plate for virus titration studies. 60
Figure 3-1 Formation of second messenger PIP3 molecule and recruitment of downstream effector kinase. 65
Figure 3-2: Time course activation of the PI3K pathway in influenza A virus infected MDCK, A549 or glial cells. 69
Figure 3-3: Infectious virus production in H2N3 virus infected chicken and duck fibroblast cell supernatants. 86
Figure 3-4: Western blot analysis of uninfected or LPAI H2N3 or LPAI H6N1 virus infected CEF cells. 88
Figure 3-5: Titration of LY294002 and wortmannin dose for inhibition of the PI3K/Akt pathway. 89
Figure 3-6: Titration of infectious virus output in supernatants derived from LY294002 treated CEF cells. 90
Figure 3-7: Measurement of cytotoxicity following treatment of CEF cells with 20 μM LY294002 chosen for inhibition of the PI3K/Akt pathway. 91
Figure 3-8: Protein expression profiling of LPAI H2N3 virus infected CEF cells up to 1 hour post-infection. 92

Figure 3-9: Immunocytochemical staining of CEF cells treated with LY294002 for one hour before H2N3 virus infection depicting comparable virus infectivity. 93
Figure 3-10: Titration of infectious virus in supernatants derived from CEF cells treated with LY294002 before H2N3 virus infection. 94
Figure 3-11: Effect of inhibition of the PI3K/Akt pathway on infectious virus output from infected CEFs. 95
Figure 3-12: Western blotting to determine PI3K/Akt pathway regulation in DEF cells. 96
Figure 3-13: Measurement of activated caspase 3/7 activity in H2N3 virus infected or uninfected and PI3K inhibitor or carrier treated chicken and duck embryo fibroblast cells at 24 and 48 hpi. 98
Figure 3-14: Measurement of cell metabolic activity in H2N3 virus infected or uninfected and PI3K inhibitor or carrier treated CEF and DEFs at 24 and 48 hpi. 100
Figure 3-15: Western blot analysis of cell lysates derived from H2N3 virus infected or uninfected HD11 cells. 101
Figure 3-16: Western blot analysis of H2N3 virus or uninfected chick embryo tracheal organ cultures..... 102

Figure 4-1: Combined global gene expression pattern in IAV infected primary chicken and duck lung cells. 117
Figure 4-2: Regulation of PI3K activation by PTEN and PDK1. 119
Figure 4-3: Pictorial depiction showing measurement of grey value from H2N3 virus infected CEF or DEF cells 128
Figure 4-4: IGF-1 signalling (PI3K activation initiator) gene cluster expression..... 134
Figure 4-5: Beclin-2 associated death (BAD) promoter phosphorylation and associated host anti-apoptotic response. 135
Figure 4-6: PTEN-dependent cell cycle arrest and apoptosis. 137
Figure 4-7: Expression of small GTPases involved in actin remodelling and cytoskeletal regulation in chicken and duck lung cells. 138
Figure 4-8: H2N3 virus infected (1MOI) or uninfected control CEF cells. 142
Figure 4-9: CEF cells infected with H2N3 virus (1MOI) and LY294002 treated or mock treated 2 hpi. 143
Figure 4-10: H2N3 virus infected (1MOI) or uninfected control DEF cells. 144
Figure 4-11: DEF cells infected with H2N3 virus (1MOI) and LY294002 treated or mock treated 2 hpi. 145

Figure 4-12: Comparative cytosolic retention of HA (H2) antigen in H2N3 virus infected CEF and DEF cells. 146
Figure 4-13: Comparative mean fluorescence intensity of actin from H2N3 virus infected and uninfected DEF cells. 147
Figure 4-14: Morphogenesis of H2N3 virus in PI3K/Akt inhibitor treated chicken fibroblast cells. 149
Figure 5-1: Distribution of domains and binding motifs. 161
Figure 5-2: p85β-iSH2 protein-protein interaction interface showing the amino acid residues involved in the complex formation. 162
Figure 5-3: Illustration of recombinant virus rescue. 169
Figure 5-4: Expression of innate immune sensors of viral nucleic acids in AIV infected chicken cells. 178
Figure 5-5: Induction of type-I interferon (IFN) response to HPAI H5N1 and LPAI virus infection. 180
Figure 5-6: Pro-inflammatory cytokine expression in LPAI and HPAI virus infected chicken cells. 182
Figure 5-7: Akt phosphorylation in recombinant virus infected CEF cells. 183
Figure 5-8: Prolonged activation of PI3K as evidenced by the presence of pAKT at 24 hpi in PR8 TRIG infected CEF's. 185

Figure 5-9: Significant reduction in virus titre in PI3K/Akt inhibitor-treated cells compared to the untreated cell. 186
Figure 5-10: HP and LPAI NS1 sequence homology analysis reveal three tyrosine residue modifications. 188
Figure 5-11: Positions of protein binding regions between HPAI H5N1 (50-92) and H2N3 virus NS1. 190
Figure 5-12: PI3K-p85β sequence analysis reveals a conserved Glutamic acid (E475) residue replaced by non-polar valine (E475V) in ducks. 192
Figure 5-13: PI3K p85β-NS1 protein-protein interaction model. 193
Figure 5-14: PI3K-p85β sequence-based protein binding site prediction 195

List of tables

Table 1-1: Member of the family Orthomyxoviridae and their host range 6

Table 1-2: Summary of influenza A virus major proteins and their functions modified from Bouvier and Palese (2008) 19

Table 3-1: Primary antibodies used in this study 78

Table 4-1: Preparation of resin solvent mix 130

Table 4-2: Summary of differentially expressed genes in both cells 140

Table 5-1: SYBR green-based RT-qPCR cycling profile..... 167

Table 5-2: List of primers used in the study..... 168

Table 5-3: Details of plasmids used and the concentrations. 172

Table 5-4: The details of virus rescue combinations study 174

List of abbreviations

Acronym	Meaning
ºC	degree Celsius
µl	microlitre(s)
µM	micromolar
AAF	Amnio-allantoic fluid
AI	avian influenza
AIV	avian influenza virus
IAV	Influenza A virus
cDNA	complementary deoxyribonucleic acid
CEF	chicken embryo fibroblast cells
Cq	quantification cycle
DEF	duck embryo fibroblasts
DEPC	diethylpyrocarbonate
DMEM	Dulbecco's modified Eagle's medium
DMSO	dimethylsulphoxide
dNTP	Premix of sodium salts of dATP, dCTP, dGTP and dTTP
DNA	deoxyribonucleic acid
FCS	foetal calf serum
FFU	focus forming units
g	gravitational force
HA	haemagglutinin
HCl	hydrochloric acid
HRP	horseradish peroxidise
hrs	hours
HPAI	highly pathogenic avian influenza
IFN	interferon
IM	infection medium
IVT	*in-vitro* transcription
kDa	kilodalton
L	litre(s)
LPAI	low pathogenicity avian influenza
mab	monoclonal antibody
MDCK	Madin-Darby canine kidney
mg	milligram(s)
min	minutes(s)
ml	millilitre(s)

List of abbreviations (continued)

Acronym	Meaning
mM	milli molar
MOI	multiplicity of infection
mRNA	messenger RNA
MTT	3-(4,5-dimethylthiazol-2-yl)-2,5-diphenyl tetrazolium bromide
NA	neuraminidase
nm	nanometers
NP	nucleoprotein
nt	nucleotides
PBS	phosphate buffered saline
PCR	polymerase chain reaction
RNA	ribonucleic acid
RPM	revolutions per minute
RT-PCR	reverse transcriptase polymerase chain reaction
s	seconds
SAα2,3Gal	Sialic acid linked to galactose by α2,3 linkage
SAα2,6Gal	Sialic acid linked to galactose by α2,6 linkage
Tris	tris (hydroxymethyl) aminomethane
Tris HCl	tris hydrochloride
TBS	Tris buffered saline
TBS-T	Tris buffered saline with 0.1% Tween-20

Chapter 1. Introduction

1.1 Influenza overview

The term "*influenza*" originated from an Italian word "*influentia*" used for describing a contagious respiratory disease epidemic in Europe. There is evidence that 'influenza-like illness' has existed for centuries with a low frequency of occurrence causing infrequent fatalities. However, the causative agent was isolated only in the early 20th century (Potter, 2001). Influenza viruses are now one of the most important viral pathogens of human and veterinary significance, posing a major public health concern globally. The 1918 *'Spanish flu'* is considered the most devastating outbreak in the history of influenza; it is estimated to have caused 21 to 100 million deaths (Holtenius and Gillman, 2014). The continued occurrence of epidemics and pandemics underlines the importance of influenza infections.

The historical description for the beginning of avian influenza (AI) dates back to 1878 when Perroncito first described a contagious poultry disease associated with high mortality in northern Italy. Initially called 'fowl plague' (avian pasteurellosis), it was confused with the acute septicaemic form of fowl cholera. In 1880, Rivolta and Delprato differentiated the disease from fowl cholera based on the clinical and pathological signs and termed it *Typhus exudatious*

gallinarum. Although Centanni and Suvunzzi in 1901 showed that fowl plague was caused by a filterable virus, it was only in 1955 that the so–called classical fowl plague virus was shown to be caused by influenza type A virus based on the presence of influenza type A specific ribonucleoprotein (Schäfer, 1955). The term fowl plague was substituted by the term highly pathogenic avian influenza (HPAI) virus during the first international symposium on influenza in the year 1981 as reviewed by Sonnberg et al. (2013).

Influenza viruses are classified in the *"Orthomyxoviridae"* family, *"orthos"* in Greek meaning 'straight or correct' and "*myxa*" meaning 'mucus'. Orthomyxoviruses are enveloped viruses with a negative-sense, single-stranded and segmented ribonucleic acid (RNA) genome (Cheung and Poon, 2007). The family *Orthomyxoviridae* includes seven genera, namely: Alphainfluenzavirus, Betainfluenzavirus, Deltainfluenzavirus, Gammainfluenzavirus, Isavirus, Thogotovirus and Quaranjavirus. Isaviruses mainly infect salmon, and Thogoto viruses predominantly infect invertebrate hosts like ticks and other insects. The Quaranja virus genus has three member species, Quaranfil virus, the type species, which infects humans, Johnston Atoll virus and Lake Chad virus (Presti et al., 2009).

Classification of influenza viruses into A, B, C and D is based on serological differences in the nucleoprotein (NP) and membrane matrix (M) proteins. Hause et al. (2013) recently identified a new genus in the Orthomyxoviridae family, distantly related to human influenza C virus, designated as influenza D virus. The novel influenza D virus was first isolated in pigs with influenza-like illness. However, serological studies suggest cattle as the possible reservoir (Chiapponi et al., 2016). The nucleoprotein antigen is common to all strains of the specific type but is distinct from other types or genera. Influenza A and B viruses possess eight segments in the viral core, while influenza C and D viruses have only seven segments. Haemagglutinin-esterase-fusion (HEF) protein functionally corresponds to HA and NA of influenza A and B viruses (Table 1-1). Although influenza A, B, C and D viruses are capable of infecting multiple hosts including humans and avian species, only influenza A viruses infect a wide host range, including both aquatic and terrestrial species. Influenza B viruses are mostly restricted to humans. Barring humans, only seals are known to be susceptible to influenza B virus infections (Osterhaus et al., 2000). Influenza C viruses are rare compared to both influenza A and B viruses, and mostly infect humans with occasional spill over into pigs (Guo et al., 1983, Matsuzaki et al., 2002) causing only mild clinical

manifestations (Matsuzaki et al., 2006). To date influenza D virus antibodies were detected in humans, sheep, goat and horses, but not in chicken serum samples (Quast et al., 2015).

Table 1-1: Member of the family Orthomyxoviridae and their host range

Genus	Type species	No of gene segments	Surface glycoproteins	Host range
Influenza A virus	Influenza A virus	8	HA and NA	Humans, pig, birds, horse & other species e.g dog
Influenza B virus	Influenza B virus	8	HA and NA	Humans and seals
Influenza C virus	Influenza C virus	7	HEF	Humans and pigs
Influenza D virus	Bovine influenza D virus	7	HEF	Pigs and Cattle
Isavirus	Infectious salmon anaemia virus	8	HEF	Atlantic salmons
Thogoto virus	Thogoto virus, Dhori virus	6-7	Glycoprotein (GP)	Ticks, mosquitos and mammals
Quaranji virus	Quaranfil virus	6	Glycoprotein (GP)	Humans and ticks

1.2 Type A Influenza viruses

Influenza A viruses (IAVs) are medically important pathogens infecting humans, pigs, horses, dogs, sea mammals and a wide range of terrestrial and aquatic birds. Phylogenetic studies indicate the existence of species-specific lineages of viral genes (Webster et al., 1992). Aquatic birds were thought to serve as a reservior for all the genetic diversity in influenza A viruses (Yoon et al., 2014). However, the recent identification of two influenza A virus subtypes in bats (Tong et al., 2013) raises doubts on aquatic birds being the only repository for genetic diversity among all the circulating IAVs.

1.3 Influenza A virus taxonomy

Influenza A virus subtypes are differentiated based on antigenic variations in their surface glycoproteins haemagglutinin (HA) and neuraminidase (NA). Influenza A virus isolates are identified by adopting a standard approach which uses influenza virus host origin, geographical location, strain number, year of isolation and HA and NA subtype number in parentheses (Figure 1-1). Host origin is excluded in describing human influenza virus isolates. Currently, 16 different H types and 9 different N types have been identified in water birds. Conventional classification of influenza A viruses was based on antigenic properties while recent classification systems have adopted phylogenetic analysis of the nucleotide and deduced amino acid sequences of the HA and NA genes (Fouchier et al., 2005). Avian influenza viruses of the H5 and H7 subtypes are also

classified based on presence of a multibasic cleavage site in the HA and their virulence in chickens. Those that cause clinical disease with high mortality are known as highly pathogenic avian influenza (HPAI) viruses, whereas those which cause mild or no clinical signs in chickens are classified as low pathogenicity avian influenza (LPAI) viruses (Rebel et al., 2011). Both HPAI and LPAI viruses spread rapidly in poultry flocks, but only H5 and H7 subtypes are known to cause severe disease with up to 90–100% mortality in chickens, often within 24–48 hours after contracting the virus.

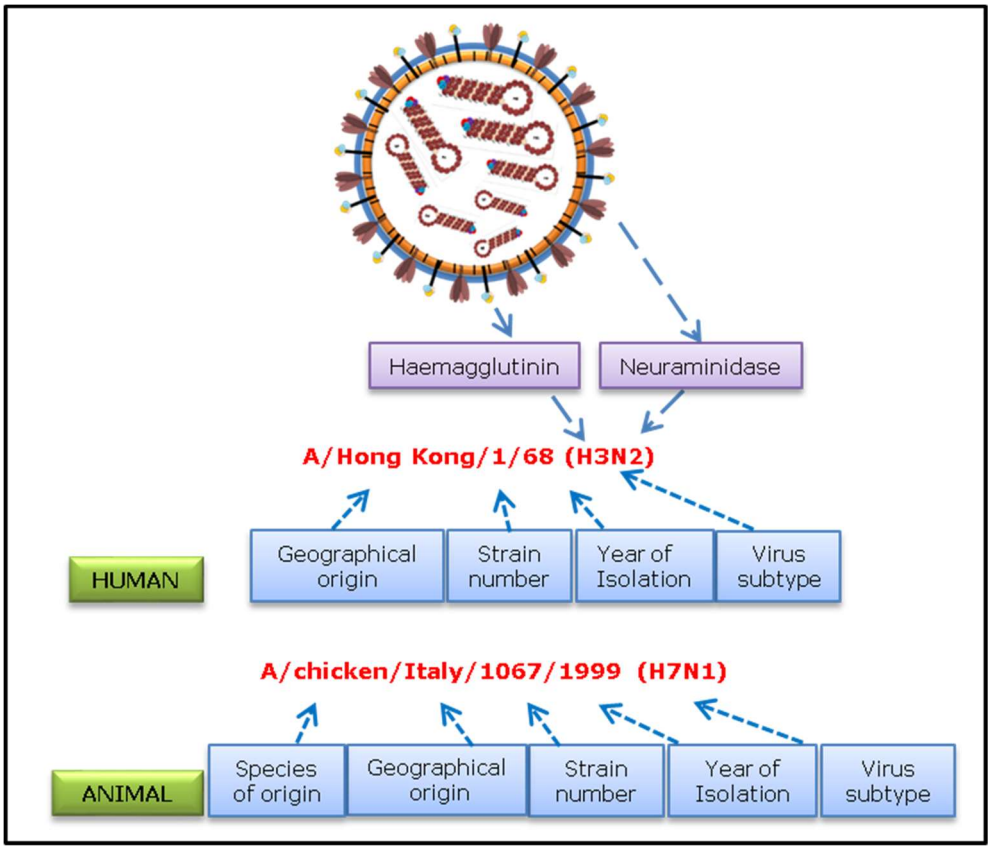


Figure 1-1: Schematic depiction of international system of nomenclature for influenza viruses

1.3.1 Unified nomenclature system for identification of H5N1 viruses

Emergence of multiple lineages of HPAI H5N1 viruses has proved difficult for analysis, comparison and discussion of various lineages due to different provincial nomenclature. The international consultative group along with the evolution working group of World Health Organisation (WHO), the World Organisation for Animal Health (OIE) and the Food and Agriculture Organisation (FAO) proposed a unified nomenclature system for identification of HPAI viruses (WHO/OIE/FAO, 2014). While most of the viral segments have been replaced by many different genotypes because of continuous reassortment, the haemagglutinin (HA) of H5N1 identified in 1996 is still similar in the majority of isolates. Hence the H5 HA was taken as standard to which all the evolving strains can be compared. A standard clade nomenclature system was adopted that allows unique identification of each new isolate. The criteria set for defining the clade is the sharing of a common node in the phylogenetic tree. A monophyletic group with a bootstrap value ≥ 60 at the clade defining node and with an average percentage pairwise nucleotide distance between and within clades of > 1.5% and <1.5%, respectively.

1.4 Properties of influenza A virus

1.4.1 Structure and genomic architecture

IAVs measure approximately 100 nm in diameter or filaments as long as 300 nm, surrounded by a lipid membrane envelope derived from the host cell membrane (Bouvier and Palese, 2008). The influenza A viral genome is organized into eight different segments which are polymerase basic (PB1 and PB2), polymerase acidic (PA), haemagggglutinin (HA) nucleoprotein (NP) neuraminidase (NA), matrix (M) and non-structural. In total, the genome is approximately 13600 nucleotides long (Inoue et al., 2010). The virus envelope incorporates surface glycoproteins HA, NA as surface projections, and matrix protein 2 (M2). Rod-shaped HA spikes and mushroom-shaped NA spikes (~10 to 14 nm length) are anchored by a short sequence of hydrophobic amino acids in the lipid bilayer (Simms and Jeggo, 2014). The lipid bilayered viral envelope is derived from host plasma membrane. Surface proteins HA, NA and M2 are in the lipid bilayer. Rod–like HA spikes constitute approximately 80% of the total surface proteins. The mushroom–shaped NA spikes represent 17% with the rest consisting of M2 ion channel proteins (Spackman, 2008, Samji, 2009). The morphology of the virus is a genetic trait and may be influenced by several viral proteins including HA, NA, matrix (M) proteins (Cheung and Poon, 2007). A schematic structural organisation of influenza A virus has been shown in Figure 1-2.

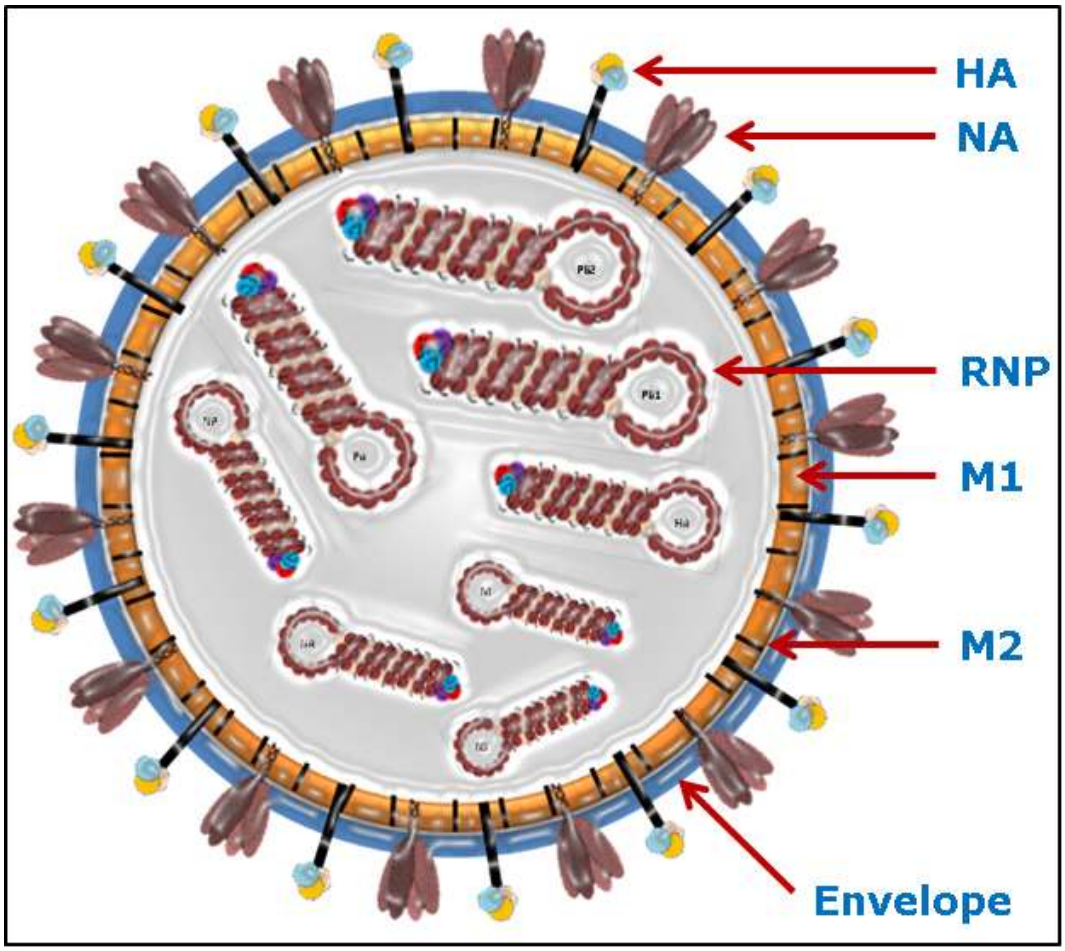


Figure 1-2: Schematic structural illustration of influenza A virus

Each viral segment consists of terminal non-coding regions. The 5' terminal has 13 conserved nucleotides whereas the 3' terminal has 12. The extreme ends are conserved regions in all the segments followed by a segment-specific non-coding region (Hoffmann et al., 2001). The terminal 5' and 3' regions (U12 and U13, respectively) are essential as they contain promoter sequences that are recognized by the polymerase complex PB1,

PB2 and PA for initiation of transcription and replication (Bae et al., 2001, Coloma et al., 2009). A short sequence of untranslated region (UTR) exists between the highly conserved non-coding region and a large central coding region in each gene at both 5′ and 3′ terminals; these, along with terminal coding regions and specific nucleotides, form the viral packaging signals (Hutchinson et al., 2010) (Figure 1-3).

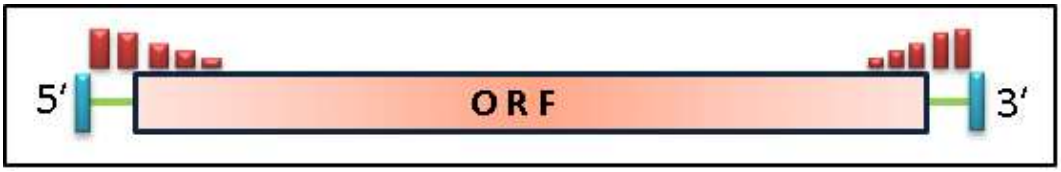


Figure 1-3: Schematic illustration of influenza virus vRNA segment

A large open reading frame (ORF, faint box) flanked by short UTRs (green line) encompassing terminal promoter sequence (blue boxes) that forms the polymerase binding site and is similar in all the segments. Specific packaging signals (red wedges) overlap the UTRs and terminal coding regions. Illustration modified from Hutchinson et al. (2010).

The eight genome segments code for at least ten important viral proteins. They are surface glycoproteins haemagglutinin and neuraminidase, RNA polymerase complex comprising of polymerase basic-1 (PB1) polymerase basic-2 (PB2) and polymerase acidic (PA), nucleoprotein (NP), matrix (M) proteins M1 and M2 and non-structural proteins NS1 and nuclear export protein (NEP). Since the discovery of the first accessory protein PB1-F2 (a pro-apoptotic protein) in some strains of influenza A virus translated on segment 2 of PB1 (Chen et al., 2001, Wise et al., 2009), six more proteins PB1-N40, PA-X, PA-N155, PA-N182, M42 and NS3 have been found translated on different viral segments (Jagger et al., 2012, Vasin et al., 2014) (Figure 1-4).

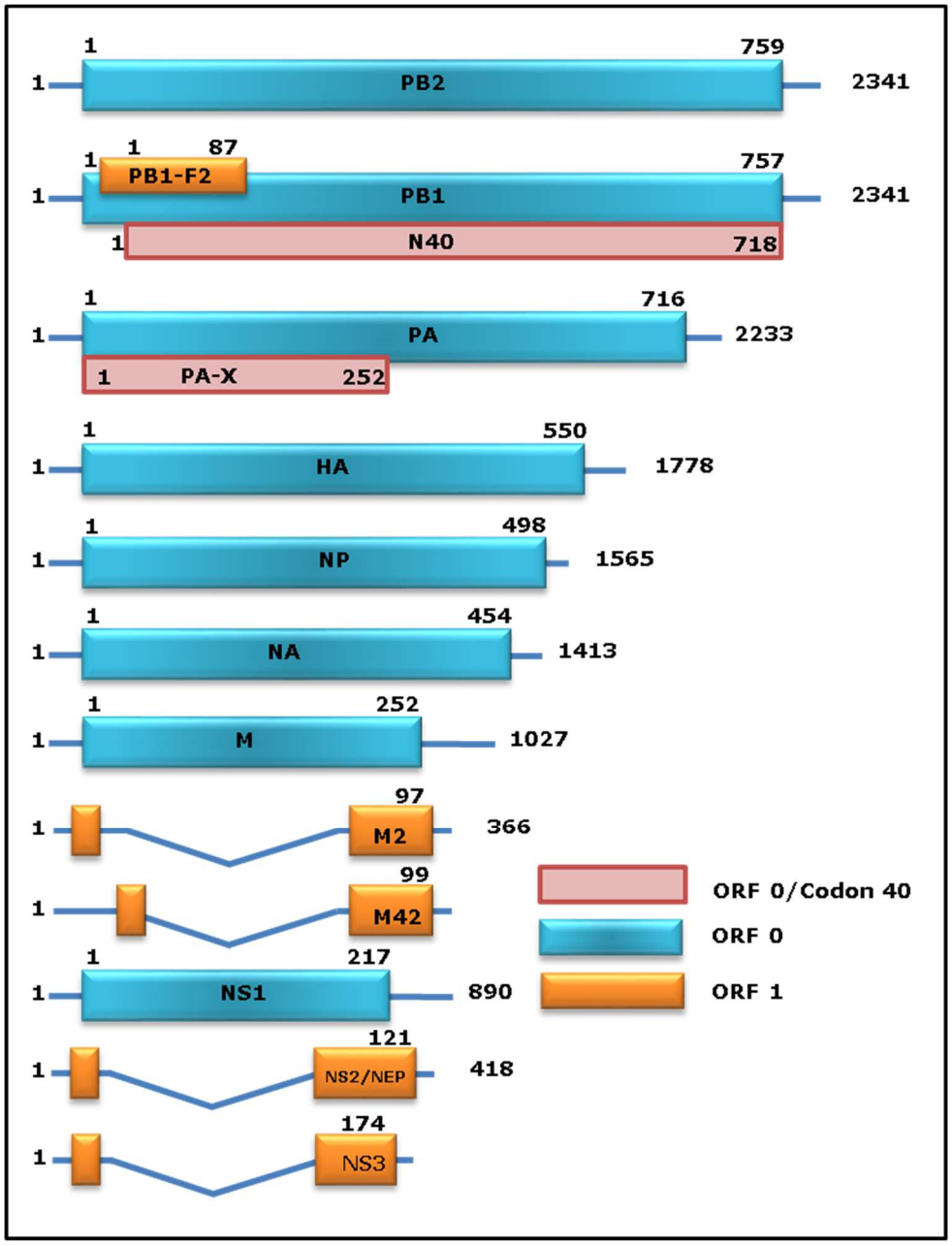


Figure 1-4: Organization of protein coding open reading frames (ORF) in Influenza A virus genome

RNA segments (in nucleotides) shown as slender lines and their encoded proteins (in amino acids) in box shapes. Two proteins PB1 and N40 are translated from ORF0 and PB1-F2 translated from ORF 1. NEP (non-structural protein-2), NS3, M2 and M42 proteins are coded by spliced mRNAs (Introns denoted by 'V' shaped lines). Illustration modified from Vasin et al. (2014).

1.4.2 Viral ribonucleoprotein complex

Each viral RNA (vRNA) genome segment is bound to the nucleoprotein (NP) on the backbone and RNA polymerases to form the ribonucleoprotein (RNP) complex. Each RNP complex is encapsulated by a trimeric polymerase complex (PB1, PB2 and PA), which is essential for initiation of viral replication (Figure 1-5) (Digard et al., 1999). The length of the viral RNP varies between 30 and100 nm and corresponds to the length of each viral segment (Noda and Kawaoka, 2010). The progeny viruses released from the plasma membrane of the infected host cells must contain eight vRNA segments to be infectious.

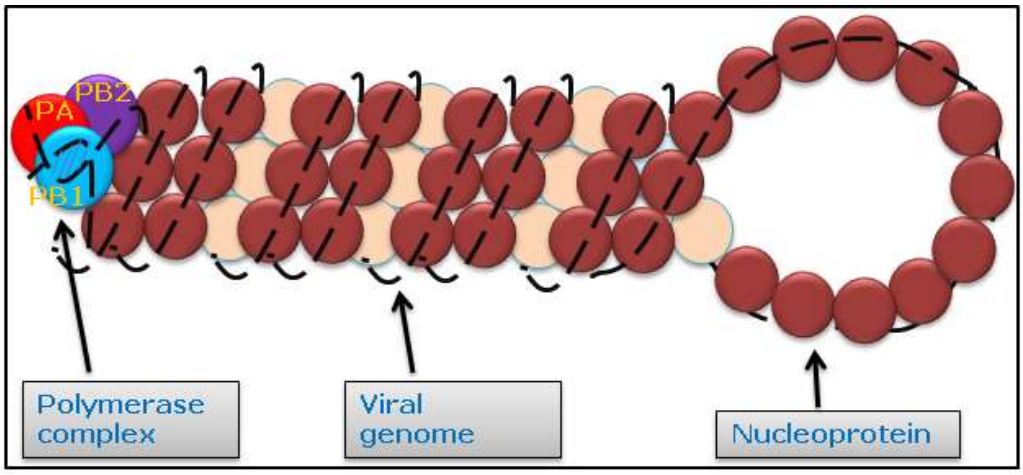


Figure 1-5: Schematic illustration of influenza A viral ribonucleoprotein (vRNP) Discontinuous black lines represent single stranded viral genome. Nucleoprotein monomers represented as chocolate spheres running as the backbone to vRNA molecule. Folding of RNP into double helical structure gives it a characteristic 'hairpin appearance'. Short duplex formation between the 5' and 3' ends facilitates the binding site for heteromeric RNA-dependent RNA polymerases. Illustration modified from Portela and Digard (2002).

1.4.3 Molecular organisation of influenza A viral genome

All eight viral RNA (vRNA) segments invariably are composed of NP and polymerase complex. The polymerase complex synthesizes three types of RNAs, viral RNA (vRNA), complementary RNA (cRNA) and messenger

RNA (mRNA). PB2 recognizes the cap structure in the host mRNA to generate primers for initiation of transcription. PA is responsible for vRNA replication (Kawaguchi et al., 2005). Together, PB2, PB1, PA and NP are responsible for viral genome transcription and replication in the infected host cells. Viral mRNA segments 1, 4, 5 and 6 are monocistronic hence encode only one protein each, namely PB2, HA, NP and NA, respectively. Polymerase basic-1 (PB1) the second segment encodes for two minor proteins: PB1-F2 known for pro-apoptotic activity and N40 translated from a single mRNA by an alternative open reading frame. PA-X, a minor protein encoded by PA gene segment, has shown to contribute to virus growth and suppression of host antiviral immune response (Hayashi et al., 2015). Mutations in the heterotrimeric polymerase complex contribute to host adaptation; particularly the PB2 protein is selected during mammalian adaptation. Long et al. (2016) have shown presence of species-specific differences in the host acidic leucine rich nuclear phosphoprotein 32A protein (ANP32A) is responsible for suboptimal activity of avian virus polymerase in mammalian cells because of the presence of an additional 33 amino acids between the leucine-rich repeats (LRR) and carboxy-terminal low-complexity acidic region domains.

Haemagglutinin exists as a homo-trimer, responsible for viral attachment to sialic acid receptors on host target cells. HA is synthesised as a precursor polypeptide HA_0 of about 560 amino acids. Cleavage of HA_0 yields HA1 and HA2 subunits exposing a "fusion peptide" at the amino terminal of HA2 for

membrane fusion (Figure 1-6), a prerequisite for viral infectivity. Cleavage also promotes the native HA molecule to undergo a conformational change because of the endosomal acidic environment and is essential for fusion between the host cell and viral particle (Skehel et al., 1982). As previously mentioned, the presence of an HA_0 cleavage site is particularly important in influenza A virus pathotyping of H5 and H7 subtype isolates. Mutations in the amino acid sequences of antigenic sites recognised by host immune sensors, cleavage sites for host proteases, and fusion peptides that mediate endosomal fusion of viral envelope in low endosomal pH may have a potential impact on the pathogenicity and host range of influenza A viruses (Sriwilaijaroen and Suzuki, 2012). The HA molecule preferentially binds to either α 2,3 or α 2,6- sialic acid linkage determining the receptor specificity of influenza virus (Connor et al., 1994).

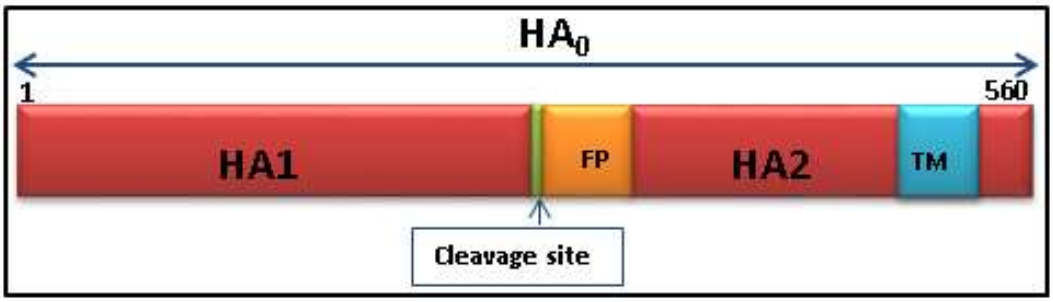


Figure 1-6: Schematic illustration showing influenza A virus HA protein

HA1 is the sialic acid receptor domain, HA2 constitutes fusion protein (FP) exposed upon cleavage and a transmembrane domain (TM).

The nucleoprotein (NP) serves as the backbone of the influenza A virus RNA genome, and is essential for viral transcription and replication. NP has a specific role in "switchover" of RNA polymerase from transcription to replication. NP also has nuclear localisation signals and is regarded as a

"shuttle protein"; nuclear transport of incoming vRNPs is mediated through NP (Martin and Helenius, 1991a). Neuraminidase (NA) exists as a homo-tetramer consisting of four domains: a globular head; a thick stalk; a transmembrane domain; and a cytoplasmic domain. NA is an integral protein in the viral structure and replication process. The progeny virus anchors to sialic acid on the cell surface. In order to release the virus from host cells, neuraminidase is responsible for cleavage of the α-ketosidic linkage between the terminal sialic acid and an adjacent D-galactose or D-galactosamine residue (Colman et al., 1981) leading to release of virus from the cell surface.

The matrix (M) protein segment encodes for two proteins, matrix protein 1 and 2 (M1 and M2). The M1 lies just beneath the lipid envelope and is multifunctional in nature; it binds to RNA in a sequence non-specific manner and inhibits viral transcription (Watanabe et al., 1996). M2 protein, a homo-tetramer, is an integral membrane protein and functions as an ion channel for acidification of the interior of the viral particle during release of viral segments in the host cell (Shaw et al., 2008, Szewczyk et al., 2014). Histidine (His37) and tryptophan (Trp41) amino acid residues present in the transmembrane domain of the M2 protein are essential for pH-regulated proton conductance. M2 also maintains a high pH in the Golgi vesicles to stabilise the conformation of newly synthesized HA molecule during intracellular transport for viral assembly (Takeuchi and Lamb, 1994). The smallest segment in the influenza A viral genome encodes for

two non-structural proteins; non-structural protein 1 (NS1) and nuclear export protein (NEP). NS1 accumulates mainly in the nucleus and regulates cellular and viral protein expression by binding to different RNA molecules (Greenspan et al., 1988). NEP contains a nuclear export signal (NES) hence facilitates vRNP export (O'Neill et al., 1998). Recent studies suggest a role for NS1 in the regulation of innate immune response (Cheung et al., 2002). A summary of important influenza viral proteins and their functions is detailed in Table 1-2.

Table 1-2: Summary of influenza A virus major proteins and their functions modified from Bouvier and Palese (2008)

Segment	Segment length	Encoded proteins	Protein length (aa)	Protein function
1	2341	PB2	759	Polymerase subunit; mRNA cap recognition
2	2341	PB1	757	Polymerase subunit; RNA elongation, endonuclease activity
		PB1-F2	87	Pro-apoptotic activity
		N40	718	Polymerase complex interaction
3	2233	PA	716	Polymerase subunit; protease activity
		PA-X	252	Modulates the host response and viral virulence
4	1778	HA	550	Surface glycoprotein; major antigen, receptor binding and fusion activities
5	1565	NP	498	RNA binding protein; nuclear import regulation
6	1413	NA	454	Surface glycoprotein; sialidase activity, virus release
7	1027	M	252	Matrix protein; vRNP interaction, RNA nuclear export regulation, viral budding
		M2	97	Ion channel; virus uncoating and assembly
		M42	99	Functionally replaces M2 in M2-null viruses
8	890	NS1	230	Interferon antagonist protein; regulation of host gene expression
		NEP (NS2)	121	Nuclear export of RNA

1.5 Replication of IAVs

Different steps involved in the replication of influenza A viruses are explained briefly below.

1.5.1 Virus attachment and uncoating

Effective membrane interaction is essential for establishing influenza virus infection. Influenza viral glycoprotein HA spikes bind to the sialic acid receptors. HA binding facilitates virus entry into the cell through receptor-mediated endocytosis (Sieczkarski and Whittaker, 2002). Once the virus is endocytosed, low pH in the endosomal compartment along with the hydrogen ion pump mediated by the M2 ion channel triggers a conformational change in the HA, exposing the fusion peptide in HA2, which mediates fusion of the viral envelope with the endosomal membrane. Internal acidification of the virus via the M2 channel disrupts protein–protein interactions, allowing viral ribonucleoproteins (RNPs) to be released into the host cell cytoplasm (Stegmann, 2000, Martin and Helenius, 1991b).

1.5.2 Viral RNA synthesis

Viral ribonucleoproteins released from the endosome are trafficked to the host cell nucleus, mediated by nuclear localisation signals present on viral proteins. The viral enzyme RNA dependent RNA polymerase a component of the vRNP trafficked into the nucleus, utilises negative sense vRNA as template for transcribing two positive sense RNA species. The mRNA for translation of viral proteins and

complementary RNA for transcribing negative sense genomic vRNA as reviewed by Bouvier and Palese (2008). Addition of the cap structure to the viral mRNA is mediated through PB1 and PB2 proteins, which "snatch" the capped primers from host cell pre-mRNA transcripts for initiating vRNA transcription in a process known as "cap snatching" (Krug, 1981). The viral polymerase transcribes a stretch of five to seven uracil residues forming an adenosine string in positive sense viral mRNA called the poly (A) tail (Li and Palese, 1994). The polyadenylated and capped, viral-origin mRNA is mobilized to the cytoplasm and translated. Nuclear export of vRNA segments is mediated by viral proteins M1 and NEP, mediating the M1-RNP export through nucleoporins into the host cell cytoplasm (Cros and Palese, 2003).

1.5.3 Protein synthesis, packaging, budding and release of virus particles.

Haemagglutinin, NA and M2 envelope proteins are synthesised from viral-origin mRNA on the membrane-bound ribosomes in the endoplasmic reticulum, where they are folded and transported to the Golgi apparatus for post translational modification. All three proteins are believed to have apical sorting signals that direct them to the cell membrane for virion assembly. M1 plays a key role in bridging the contact between the RNP–NEP complex and envelope-bound HA, NA and M2 proteins for packaging at the host cell membrane (Knipee and

M.Howley, 2013). Packaging of virus particles has been described as a highly organised and selective process; discrete packaging signals from all the vRNA segments ensure that a full set of genome segments are incorporated into the budding virion particle (Watanabe et al., 2003, Fujii et al., 2003). The vRNP are incorporated in a specific pattern in which seven RNPs surround the central one (Noda, 2015). Budding and release of progeny virus occurs at the host cell membrane. Accumulation of M1 protein at the cytoplasmic phase of the lipid layer initiates the budding process. HA spikes continue to bind the newly-formed virion particles with sialic acid receptors on the cell surface. The sialic acid receptors are destroyed by cleavage of sialic acid surface glycoprotein by sialidase activity of the NA to release progeny virions from the host cell (Cabezas, 1991, Colman et al., 1981).

1.6 Genetic variations in influenza A virus

RNA viruses are highly prone to genetic variations. These mutations are predominantly observed due to the lack of proof reading mechanism (exonuclease activity) during viral replication. Influenza A viruses may constantly acquire genetic diversity through different mutational process like antigenic drift, shift and reassortment.

1.6.1 Antigenic drift and shift in influenza A virus

The progressive occurrence and accumulation of point mutations in the HA and NA genes over a period of time gives rise to "antigenic drift", resulting in antigenic changes in the progeny virus. However, the progeny virus is still closely related to the parent virus. These virus antigenic changes are responsible for evasion of host immune responses (Webster and Govorkova, 2014). Antigenic shift is the process of acquiring an abrupt major change in the genetic constitution of the virus. The shift process results in a new virus subtype or a virus with different surface glycoprotein combination (HA and NA) to that of the parent viruses. Two or more different influenza virus subtypes when co-infected in the same cell can result in "antigenic shift". Having a segmented genome therefore confers an evolutionary advantage by allowing genetic reassortment which may result in the emergence of new subtypes of virus that could be more pathogenic or may broaden its host range (Neumann et al., 2009). Although, influenza A viruses continuously undergo antigenic drift, antigenic shift occurs occasionally. An illustration of typical genetic reassortment is shown in Figure 1-7. Pigs have been postulated as a "mixing vessel" as they can be infected by both avian and human subtypes. Hence they play important intermediary role in virus reassortment (Hass et al., 2011, Ma et al., 2008). The 2009 pandemic H1N1 emerged as a consequence of genetic reassortment

between pigs, human and avian virus subtypes (Schrauwen and Fouchier, 2014). The immunologically naïve human population helped the virus to rapidly spread and infect causing a pandemic. However, recent studies with H5N1 virus subtype suggested acquiring minimal adoptational mutations upon direct transmission from avian reservoirs shown as discontinuous lines in (Figure 1-7) (Herfst et al., 2012).

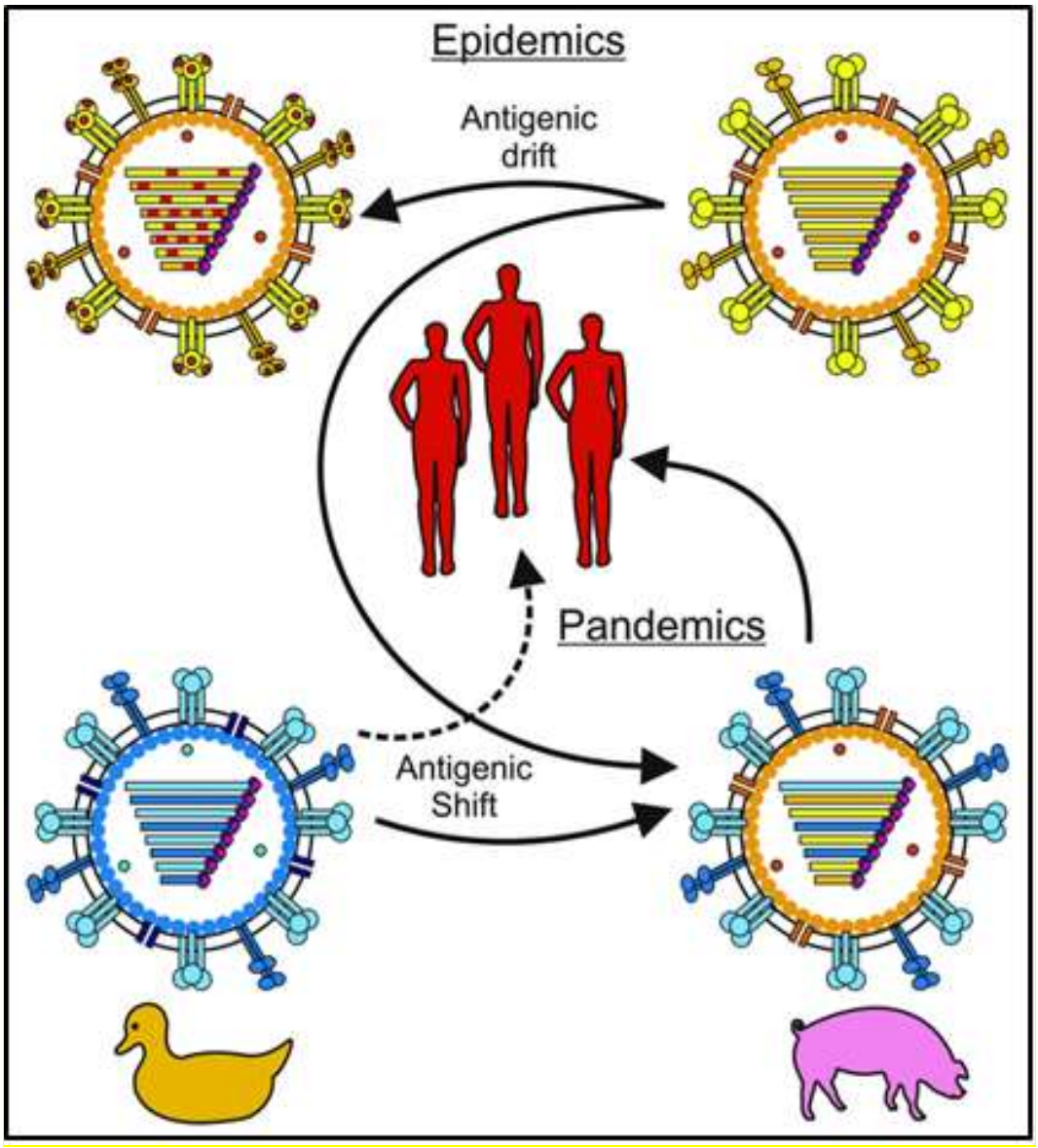


Figure 1-7: Antigenic drift and shift in influenza A viruses
Antigenic drift is the continuous or gradual acquisition of minor mutations in the genetic constitution of a virus, while a more rapid and a major compositional change results in the emergence of a novel virus subtype that is distinct from its progenitors. Novel virus subtypes may be responsible for causing a pandemic outbreak in the immunologically naïve population. Pigs serve as mixing vessels for emergence of novel virus subtypes when simultaneously infected by two or more virus subtypes favouring exchange of viral segments. Illustration modified from van de Sandt et al. (2012).

1.7 Determinants of influenza A virus host range

Influenza A viruses have been isolated from wide host range. Extensive surveillance in birds has led to the understanding that low pathogenicity influenza viruses are ubiquitous in most bird species (Webster et al., 1992) and sustained outbreaks have been observed in other mammalian hosts including humans, pigs, horses, seals, and minks (Parrish et al., 2015). A representative illustration showing the host range and directions of virus spread is shown in Figure 1-8. Avian origin viruses preferentially bind to neuraminic acid α 2, 3 galactose (SA α 2, 3) receptors. In contrast, human influenza viruses bind to neuraminic acid α 2,6–galactose (SA α 2,6) receptors (Yang et al., 2015, de Graaf and Fouchier, 2014). Horses have SA α 2,3 receptors (Muranaka et al., 2011, Daly et al., 2011). However, both type of receptors are extensively distributed in respiratory tract in pigs (Nelli et al., 2010), thus, facilitating pigs to act as a 'mixing vessel' for both avian and human influenza viruses. Mutations in the influenza viral HA may also play a key role in changing the binding affinity from SA α 2,3 to α SA α 2,6 leading to the extension of host range. A comparative study of chicken and duck tracheal distribution of SA receptor showed dominance of SA α 2,6 receptors in chicken but SA α 2,3 receptors in ducks (Kuchipudi et al., 2009). However, widespread enteric distribution of both SA α 2, 3 and SA α 2,6 receptors was observed in both chickens and ducks. The co-

expression of both receptors may enhance the possibility of co-infection of cells with both human and avian type viruses leading to evolution of novel influenza viruses.

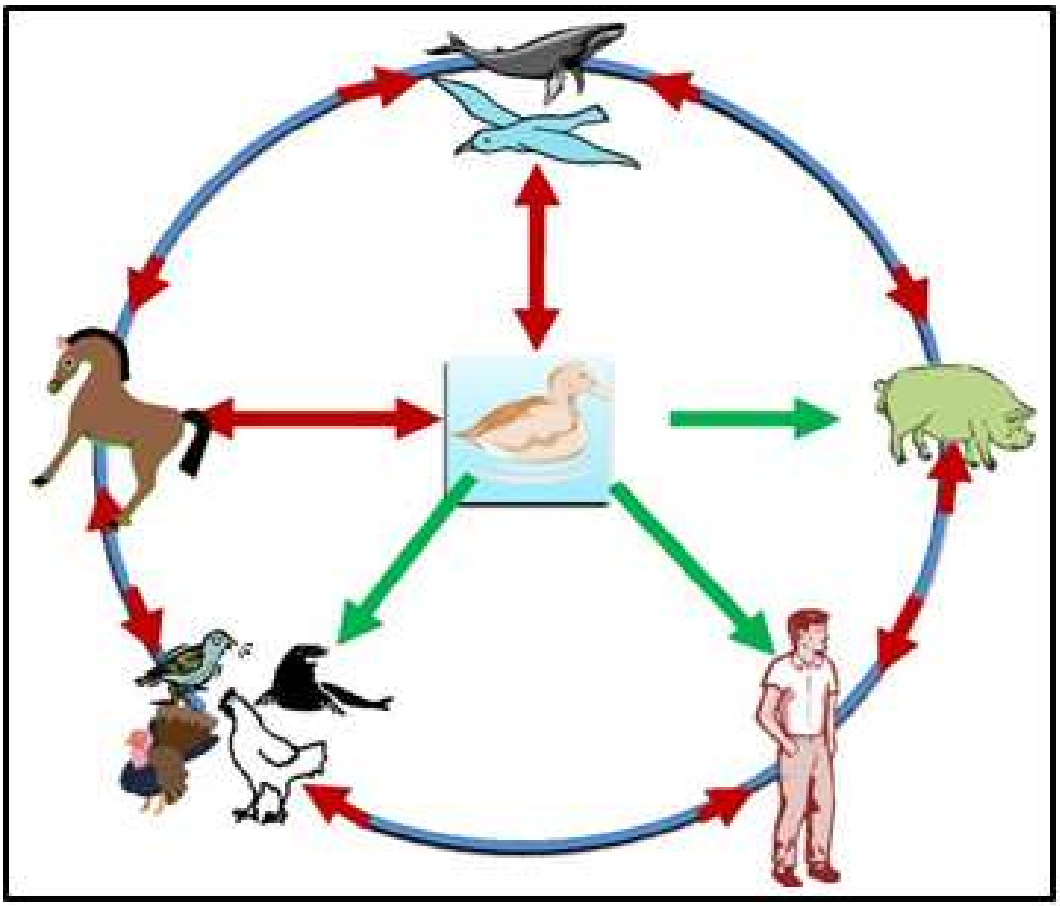


Figure 1-8: Host spectrum of influenza A viruses
Aquatic birds serve as a primary reservoir of most known influenza viruses and are a major source of influenza viruses to other mammalian hosts. IVAs also transmit between other mammalian and avian hosts as shown by arrows. Green arrows indicates unidirectional spread, Red arrow indicates bidirectional virus spread. Illustration modified from Webster et al. (1992).

1.8 Influenza A virus transmission

Influenza A viruses are transmitted from infected to healthy susceptible host through various routes. Direct contact with infected birds or animals, contact with contaminated fomites, droplet infection, faeco-oral route and inhalation of virus laden aerosols all

contribute to the spread of influenza virus. Inhalation of aerosols and infectious respiratory droplets is considered as an important route of spread in mammalian hosts (Herfst et al., 2012, Tellier, 2009). Migratory mallard ducks are believed to play a role in the spread of viruses to new geographical areas (Stallknecht and Brown, 2009). Humans can be infected with certain avian influenza viruses such as HPAI viruses from infected poultry. However, some HPAI viruses can spread through aerosols and faeco-oral route between birds (Tellier, 2006, Herfst et al., 2012, Guan et al., 2013). Aerosol transmission is particularly important in poultry farmers who are constantly exposed to poultry birds. Subsequent adaptation of avian virus in humans may lead to future pandemics.

1.9 Influenza A virus pathogenicity determinants

Haemagglutinin protein needs to be cleaved by host proteases for infectivity and spread. Presence of basic amino acid residues at the HA0 cleavage site, to an extent determines the pathogenicity. Most low pathogenicity influenza viruses possess arginine as the only basic amino acid residue in the HA_0 cleavage site that limits the site for cleavage by host cellular proteases. As a result, virus replication is limited to specific tissues or organs, mostly in the respiratory or/and digestive tracts depending on the species (Abdelwhab el et al., 2013).

Addition of one or more basic amino acid residues at the cleavage site results in cleavage by several common ubiquitously distributed endogenous proteases that recognise a multi-basic cleavage site allowing the virus to spread and replicate in broad range of tissues, causing widespread damage (Adams and Sandrock, 2010). Typical monobasic sequence is PEKQTR that is recorded in most low pathogenicity viruses, however high pathogenicity viruses specifically of subtype H5 and H7 may contain multibasic cleavage site typically representing PQRESRRKK- however variations have been observed in the number of basic amino acid insertions in the cleavage site (Khaliq et al., 2015). The AIVs with potential of becoming highly pathogenic subtypes are restricted to H5 and H7 types to date (Krauss and Webster, 2010). It is thought that continuous mutations leading to accumulation of basic amino acid residues at the HA0 cleavage site in low pathogenicity H5N1 viruses may lead to emergence of high pathogenicity H5N1 viruses through the process of adaptation in the poultry birds (Mundt et al., 2009).

Presence of HA_0 cleavage site sequence may not always be sufficient to change the phenotype of virus from LPAI to HPAI virus (Stech et al., 2009, Wasilenko et al., 2008), as other viral proteins like NS1 and viral polymerase complex PB1, PB2 and PA and NP have also been shown to play crucial role in modulating pathogenicity. While HA binds the virus to host cells through SA receptors, NA

cleaves SA from glycoprotein carbohydrate chains, liberating progeny viruses from the cell surface. NA activity should balance HA activity for efficient viral entry and exit, imbalance in the NA activity may lower the virulence (Kamal et al., 2014).

1.10 Immune response to influenza A virus

Immune competent infected host cells mount the first line of defense against invading influenza virus by activating the innate immune system. Host immune regulation is aimed at reducing viral replication and eliminating the virus from host cells. The principal immune effector cells of the innate immune system recognize pattern associated molecular patterns (PAMPs) like viral proteins or intermediary double stranded viral RNA (dsRNA) molecules through pattern recognition receptors (PRRs). Toll–like receptors, NK cell receptors and mannose-binding receptors are important PRRs (Pasare and Medzhitov, 2005). Monocytes and neutrophils are directed to influenza virus-infected cells for rapid viral clearance by phagocytosis of virus–infected cells (Iwasaki and Pillai, 2014). If the influenza virus establishes infection despite these barriers, the responsibility of viral clearance is taken over by adaptive immunity.

The interferons produced by APCs may stimulate dendritic cells (DCs) presenting the antigen to CD4+ and CD8+ T cells prompting the activation of adaptive immune response (Kreijtz et al., 2011).

The PRRs detect viral pathogens through recognition of pathogen associated molecular patterns (PAMPs) leading to the activation of transcription factors and expression of interferons (Chen et al., 2013). PRRs like toll–like receptors (TLRs), retinoic acid inducible gene-I (RIG-I), melanoma differentiation-associated gene 5 (MDA5) and NOD-like receptors (NLR) are crucial in sensing intracellular viral components. RIG-I is the main cytosolic PRR that selectively senses dsRNA for induction of an antiviral response. The classical immune pathways explained above are reasonably well understood in mammalian hosts however, there may be subtle differences in the avian species.

1.10.1 Adaptive immune response to influenza virus infection

Adaptive immunity is mediated by T lymphocytes and a humoral response represented by B lymphocytes producing virus-specific antibodies. Influenza A virus infection induces a specific antibody response against the two surface glycoproteins HA and NA. HA antibodies bind to the HA trimer thereby inhibiting viral attachment and therefore neutralise the influenza virus. However, not all antibodies that bind to HA neutralise the biological activity, binding antibodies like IFNβ or glatiramer acetate facilitate antigen flagging. HA-specific antibodies also facilitate viral component clearance by phagocytosis. Antibodies directed against NA limit the virus spread by inhibiting the sialidase activity of NA. Furthermore,

antibodies are also directed against matrix protein and nucleoprotein. The major histocompatibility complex (MHC) class II presents processed exogenous antigens to CD4(+) T-lymphocytes. Hence, MHC class II are critical for mounting antigen-specific host immune response. The cluster of differentiation (CD) CD4+ T helper cells direct Th1/Th2 cells for to cytokine production. Th1 cells aid in the production of IFN-gamma (γ) and IL-2, both of which regulate the cellular response. While, activated Th2 cells produce Interleukin- 4 (IL-4) and IL-13 which promote B cell responses. Induction of cytotoxic CD8+ T cells exert cytolytic activity on virus infected cells (Braciale et al., 2012).

1.10.2 Unique features of avian immune system

The common reptilian ancestry between avian and mammalian hosts probably carry many similar immunological features. However, avian specific evolutionary adaptational requirements mean they acquired distinct immunological strategies compared to their mammalian counterparts, makes birds immunologically unique. Birds lack functional eosinophils and neutrophils are functionally replaced by heterophils. The Bursa of Fabricius replaces lymph nodes necessary for B cell development (Karel Antoni Schat, 2014). The birds respiratory or lung system is extended in thoracic and abdominal cavity called as air sacs. The economic importance and availability of inbred lines have bolstered most avian immunological

research in chickens in the recent past. However, a few comparative studies between chicken and ducks or cells derived from these species have revealed presence of novel differences in host antiviral defence mechanisms in these two species. Reduced IFN response was observed upon silencing of MDA5, CARDIF, and chicken IRF3 indicating their involvement in influenza viral sensing (Liniger et al., 2012). Chickens, unlike ducks, lack RIG-I, and recruit MDA5 for cytosolic recognition of viral components for type- I interferon induction (Kaiser, 2010, Chen et al., 2013). A study showed preferential recognition of shorter dsRNA by MDA5 highlighting its importance in mounting antiviral immune response in chickens (Hayashi et al., 2014).

1.10.3 Differences in the outcome of influenza A virus infected chickens and ducks or derived cells

Outcome of influenza A virus infection predominantly depends on two important factors, the virus subtype involved and host species affected. AIV infection triggers a cascade of cellular events in both chickens and ducks, ducks tends to be asymptomatic when infected while chicken show sever clinical disease (Figure 1-9) (Capua and Alexander, 2009). HPAI viruses replicated more rapidly in chickens when compared to LPAI viruses hence rapidly reaching to high titres in the infected chicken cells (Kuchipudi et al., 2012a). Further, HPAIV infection resulted in higher immune-related cytokine activation

compared to LPAIV infection in chicken lung cells (Kuchipudi et al., 2014). Similarly, IFNβ and IL-6 levels were elevated in H5N1 virus infected chicken embryo fibroblast (CEF) cells compared to duck embryo fibroblast (DEF) cells (Liang et al., 2011). HPAI H5N1 virus infection resulted in the down-regulation of signal transducer and activator of transcription-3 (STAT-3) expression, resulting in elevated STAT-3 mediated pro-inflammatory response in chicken primary cells compared to duck cells, which showed no changes in constitutive basal expression pattern (Kuchipudi et al., 2014).

Infection of chicken and duck peripheral blood mononuclear cells (PBMC) with low pathogenicity H11N9 virus revealed higher expression of IFNβ, IFN-gamma, IL-1β and IL-6 in chickens, while expression of these cytokines was unaffected in duck PBMCs (Adams et al., 2009). Interferon-induced transmembrane protein (IFITM) 1, 2 and 3 were strongly upregulated in ducks compared to chickens when infected with HPAI H5N1 virus, suggesting IFITM and the RIG-I protein family mediate cyto-protective role in ducks (Smith et al., 2015). It has been shown that duck cells undergo rapid apoptosis and produce less infectious virus particles compared to chicken cells when infected (Kuchipudi et al., 2012a, Al-Mubarak et al., 2015). All these findings highlight the importance of differential immune regulation in chicken and ducks and induction of clinical signs in chickens when infected. The key factors and the precise mechanisms underlying

these disparate disease outcomes between chicken and ducks are not fully understood.

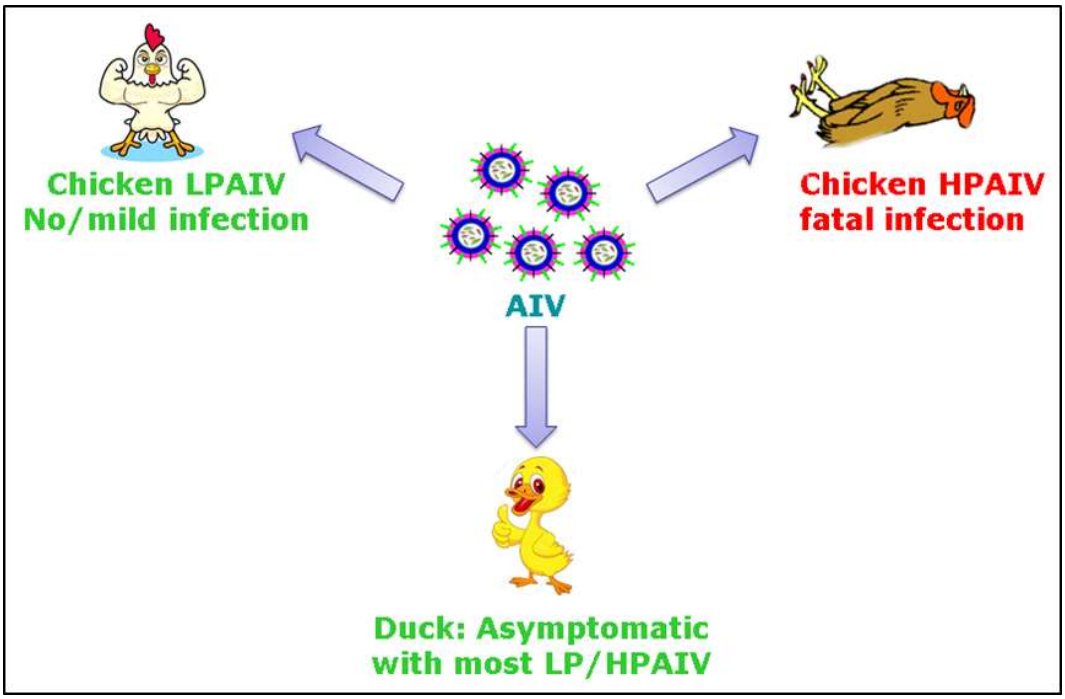


Figure 1-9: Influenza A virus pathogenesis comparison between LPAIV and HPAIV in chicken and ducks

1.11 Emergence of highly pathogenic influenza viruses from their progenitor low pathogenicity influenza A viruses

Although low pathogenicity viruses evolve and circulate in wild bird populations, the HPAI viruses evolve in gallinaceous birds like domestic chicken and turkeys causing severe disease. Persistent, asymptomatic infection of poultry flocks with low pathogenicity H5 or H7 subtype viruses are of particular concern, due to their ability to evolve into high pathogenicity influenza viruses from these progenitors. The process of switching from LPAI to HPAI virus is possibly multifactorial and not a clearly understood mechanism. Immense production stress under intensive farming conditions in

artificial ecosystem, the availability of susceptible host density for efficient virus transmission and rapid passage of the virus, uniform physiological status and age structure of the susceptible birds, which may not be available to the virus in natural ecosystem, may all predispose LPAI virus to switch to HPAI (Monne et al., 2014). Differential host response and virus-host interactions in chickens compared to ducks may all play critical role in favouring the emergence of high pathogenicity avian influenza viruses, however this needs to be elucidated.

1.12 Host cell signalling pathways and IAV infections

The cellular signalling pathways are essential in signal transduction and regulation of physiological homeostasis in cells. The host signalling molecules can be classified into three groups: cell membrane receptors, cytoplasmic adaptor molecules including kinases, and nuclear transcription factors (Dai et al., 2011). Recent research highlights the alteration of several host signalling pathways during influenza A virus infections. The viral proteins are shown to interact with host proteins and exploit different cellular signalling pathways during influenza A virus infection and hijack the host cellular machinery for viral protein synthesis. Following influenza A virus infection host pathways like phosphatidylinositol 3 kinase (PI3K/Akt), nuclear factor kappa b (NF-kB), mitogen activated

protein kinase (MAPK) and Toll like receptor/ retinoic acid inducible gene-1 (TLR/RIG-I) signalling cascades are reported to be altered. The regulation of these pathways was shown to be important in viral entry, efficient replication, and pathogenesis of virus, as reviewed by Gaur et al. (2011). These cellular signalling pathways have been extensively studied under different disease processes like cancer and infectious disease biology. The NF-kB transcriptional pathway is regulated by IKK. Upon activation, IKK phosphorylates and degrades IkB, releasing the active form of nuclear factor. Activated NF-kB regulates interferon beta (IFN beta) gene expression. Mitogen activated protein kinases are essential in conversion of extracellular signals into cellular responses (Karin and Ben-Neriah, 2000, Dong et al., 2002).

Recent studies have shown the activation of PI3K/Akt pathway as a strategy used by viruses to reduce apoptosis to prolong virus replication in the infected cells. Phosphorylated Akt leads to inhibition of activation of pro-apoptotic proteases, as reviewed by Dai et al. (2011). PI3K/Akt are part of an important intracellular signalling pathway that plays a key role in regulating cell growth, differentiation and survival (Diehl and Schaal, 2013). Recent studies indicate activation of the PI3K/AKT pathway by PR8 H1N1, H3N2, H7N7 and H5N3 viruses in MDCK or A549 cells (Hirata et al., 2014, Zhirnov and Klenk, 2007, Shin et al., 2007b, Ehrhardt et al., 2006). Presence of

phosphorylated Akt is the indirect indication of the activation of PI3K pathway. It is noted that inhibition of the PI3K pathway resulted in reduced virus output in mammalian cells (Shin et al., 2007b). The dsRNA signalling through TLR3 leads to the activation of interferon regulatory factor 3 (IRF3). Sarkar et al. (2004) have shown the role of PI3K/Akt for IRF 3 mediated induction by dsRNA. However, the regulation and the role of the PI3/Akt signalling pathway in avian cells is not yet fully elucidated.

1.12.1 Phosphatidylinositol 3-kinase pathway and influenza A virus infection

PI3K/Akt are a family of cellular heterodimeric enzymes that function downstream of receptor tyrosine kinases (RTKs) and are classified into I, II & III classes based on the catalytic subunit, sequence homology and their substrate specificity (Zvelebil et al., 1996). Class I are divided further into class IA and IB. Class IA consists of one of the catalytic subunits p110α, p110β or p110δ that have both protein and lipid kinase activity (Dhand et al., 1994) and a common regulatory subunit p85 to form the dimer (Otsu et al., 1991, Vanhaesebroeck et al., 1997b). The regulatory subunit helps p110 in stabilisation and recruiting it to the phosphorylated tyrosine residues or adaptor proteins and has five isoforms (p85α, p85β, p55α, p50α and p55γ) (Vanhaesebroeck et al., 2010). The N-terminal SH3 (Src homology3) domain in the p85β subunit is followed by a BH (Bcl-

2 homology) domain and two SH2 domains nSH2 (N-terminal SH2) and cSH2 (C-terminal SH2). Between nSH2 and CSH2 lies the coiled coil structure iSH2 (inter-SH2) domain. The class IB PI3Ks or PI3Kγ consists of only one catalytic subunit, p110γ, associated with regulatory subunits p101 or p84 (Suire et al., 2005), that functions downstream of G-protein coupled receptors (GPCR). PI3K class II and III are ubiquitously expressed and predominantly mediate protein trafficking and cellular homeostasis.

All PI3K catalytic subunits have a core structure consisting of a C2 domain, a helical domain and a catalytic domain. Class I PI3Ks use phosphatidylinositol-4,5-bisphosphate as the substrate and exist in a complex with a regulatory subunit, either a p85 isoform (for p110α, p110β and p110δ) or p101 or p87 (for p110γ). All p85 isoforms have two Src homology 2 (SH2) domains, but p101 and p87 lack SH2 domains. Class II PI3Ks use phosphatidylinositol as a substrate, and lack regulatory subunits and have amino- and carboxy-terminal extensions that may mediate protein–protein interactions. Class III PI3K has one catalytic member, vacuolar protein sorting 34 (Vps34), which uses phosphatidylinositol as a substrate and binds Vps15. Vps15 has an inactive catalytic domain, HEAT domains that facilitate protein–protein interactions and WD repeats. The WD repeats are essential for interaction with RAB5–GTP and the yeast guanine nucleotide-binding protein 1a (Gpa1) and

autophagy-related protein 14 (Atg14). BH, BCR homology domain; P, Pro-rich region; SH3, Src-homology 3 domain (Figure 1-10) (Thorpe et al., 2015).

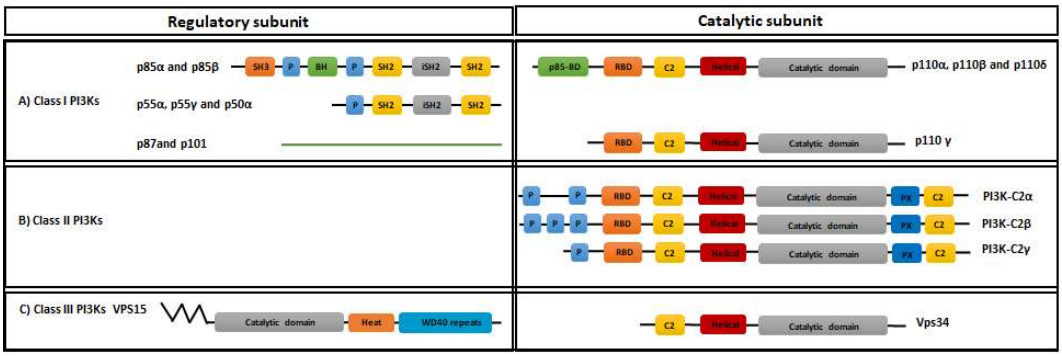


Figure 1-10: Classification of mammalian PI3K family and its domain structure modified and adopted from Thorpe et al. (2015)

1.12.2 PI3K/Akt pathway mediated signal transduction loop

PI3Ks are activated by autophosphorylated surface receptor kinases (RTKs) upon insulin or associated growth factor stimulation, mediated through adaptor proteins like insulin receptor substrates (IRS). The interaction between PI3K and autophosphorylated RTKs leads to phosphorylation at fifth position in the inositol ring giving rise to phosphatidylinositol monophosphate (PIP1), which is phosphorylated again at fourth position forming PIP2 (4,5 biphosphate). Finally, phosphorylation at the 3'-position of the inositol ring in PIP2 leads to the generation of 'second messenger' phosphatidylinositol 3, 4, 5-triphosphate (PIP3) that recruits pleckstrin homology (PH) domain containing kinase Akt/protein kinase B (PKB). Akt serves as a major effector kinase and is activated by phosphorylation at threonine at 308 by PDK1 and serine at 473

amino acid positions (Brazil et al., 2004). Mammalian target of rapamycin complex2 (mTORC2) is a key mediator of Akt phosphorylation. The mTORC2 mediates phosphorylation of Akt at a serine residue S473 as well as serine residue S450. Phosphorylation of these two serine sites stimulates phosphorylation of Akt by PDK1 at a threonine T308 residue that leads to full Akt activation (Figure 1-11) (Sarbassov et al., 2005). Phosphorylation activation of Akt inhibits GTPase-activating protein tuberous sclerosis complex 2 (TSC2) by forming a complex with TSC1 leading to lowered intrinsic GTPase activity of Rheb. Activation of the PI3K/Akt negatively regulates glycogen synthase kinase-3β (GSK3β) essential for glycogen metabolism and cytoskeletal organisation. Inhibition of GSK3β leads to accumulation of β-catenin, which integrates with various transcription factors (TCFs) and facilitate carcinogenesis related gene expression. Activated Akt mediates phosphorylation inhibition of pro-apoptotic factors like caspases and beclin associated death (Bad) promoters leading to apoptosis prevention (Ji and Liu, 2008) (Figure 1-11).

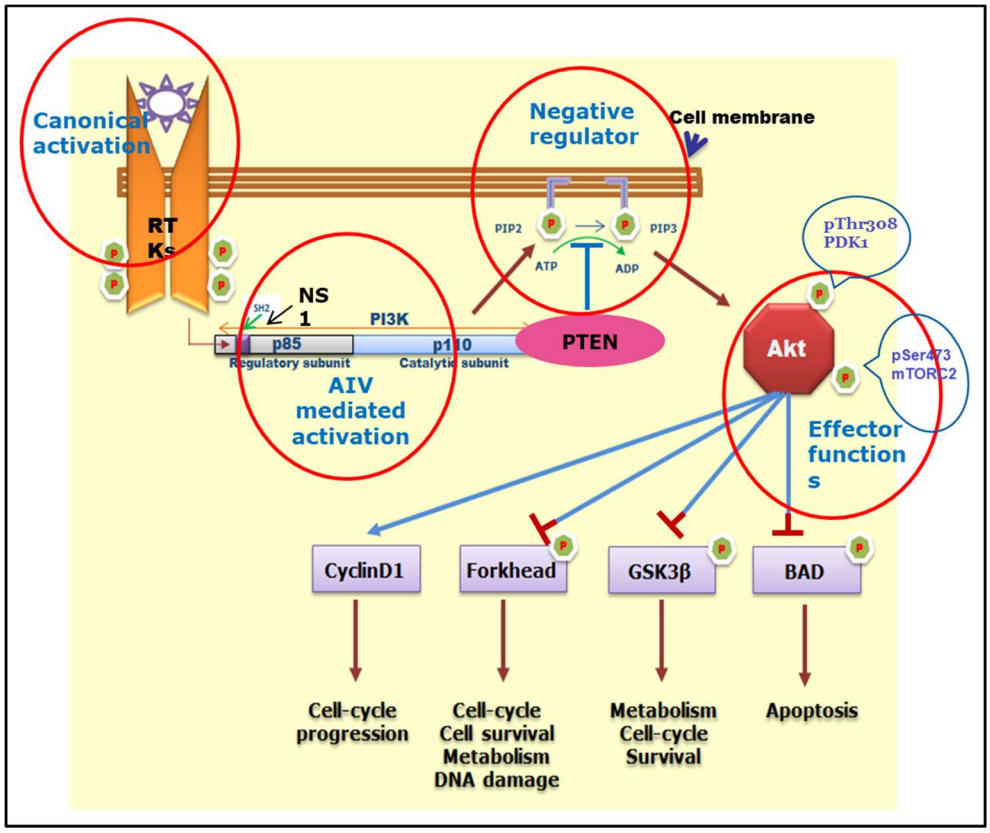


Figure 1-11: Schematic representation of phosphoinositide-3 kinase (PI3K/Akt) signalling pathway

PI3K is activated upon stimulation by growth factor receptors or adaptor proteins which have phosphorylated tyrosine residues, a conformational change in the dimers take place and leads to activation. Activated PI3K gives rise to second messenger protein 'PIP3' on the plasma membrane. PIP3 recruits PH domain containing Akt protein. Akt is phosphorylated at Ser308 and Ser473 positions for its complete activation. Activated Akt then activates or inhibits downstream target proteins such as Bad, Caspase-9, GSK3β, to regulate cellular proliferation, differentiation, migration and apoptosis. PTEN down-regulates PI3K/Akt activity by degrading PIP3 to PIP2 by eliminating phosphoric acid at the 3' end.

1.12.3 PI3K/Akt pathway mediated apoptosis regulation

Diverse cellular death stimuli activate intrinsic apoptotic pathway leading to the loss of mitochondrial membrane integrity and release of cytochrome-C, which then activates caspase mediated cellular death (Figure 1-12). IAV proteins interact with host cellular molecules that regulate induction of apoptosis cascade.

Dysregulation of apoptosis machinery partly influences disease severity in influenza virus infected cells (Iwai et al., 2013). Infection of MDCK-SIAT1 cells with influenza A and B viruses exhibited activation of PI3K/Akt survival pathway. The PR8 virus with mutated viral segments failed to activate PI3K/Akt pathway resulting in pronounced caspase mediated apoptosis induction compared to wild-type lab adapted IAV strain PR8, implying that PI3K activation suppresses apoptosis (Shin et al., 2007a). PR8 SH3-motif-1 exhibited crucial role in mitochondrial membrane disruption, and cytochrome-C release and BAX mediated apoptosis induction (Lu et al., 2010). PI3K activation site specific mutation in the NS1 protein of A/Udorn/72 (H3N2) virus contradicts the above observation, as MRC-5 and A549 cells infected with a virus carrying altered NS1 protein showed similar levels of apoptosis compared to wild-type virus infected cells (Jackson et al., 2010). It has been demonstrated that until the mid-stage of infection cycle, the anti-apoptotic process is mediated by PI3K/Akt signalling predominantly mediated by NS1 (Ehrhardt et al., 2007b), while pro-apoptotic factor p53 is activated in the late stage of infection (Zhirnov and Klenk, 2007).

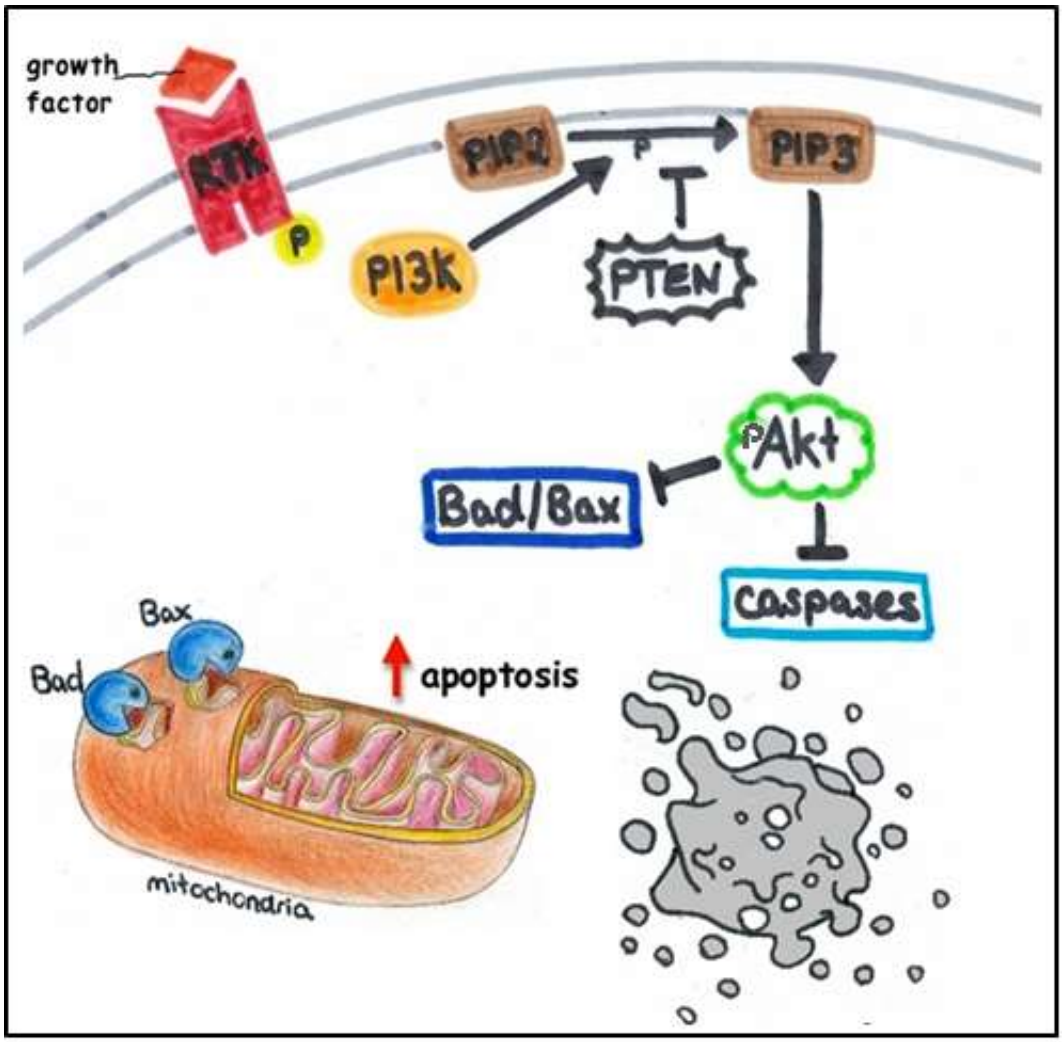


Figure 1-12: Apoptosis regulation by effector kinase Akt (activated Akt) downstream of PI3K

Phosphorylation of effector Akt kinase in turn leads to phosphorylation inhibition of pro-apoptotic factors like beclin associated death promoters (Bad) and caspases leading to arrest of apoptosis. Image graphics adapted from, https://commons.wikimedia.org/wiki/File:PTEN-Akt_interactions.

1.12.4 Negative regulators of PI3K/Akt activation

The PI3K/Akt pathway is tightly controlled by several feedback mechanisms. Phosphatases like PDK1, phosphatase and tensin homologue deleted on chromosome 10 (PTEN), SH2 containing inositol phosphatase (SHIP) and skeletal muscle and kidney enriched inositol (SKIP) have emerged as important negative regulators of

PI3K activity by de-phosphorylation of PIP3 'second messenger' to PIP2 (Figure 1-11). However, tumour suppressor PTEN has shown to be the major phosphatase in controlling PI3K activity (Leslie and Downes, 2004). PI3K-PTEN interaction axis has been identified as novel therapeutic signature for targeted PI3K modulation (Carracedo and Pandolfi, 2008). PTEN has shown to regulate IRF-3 nuclear translocation, hence PTEN is inhibitory to IFNβ production (Li et al., 2016).

1.13 Cell cytoskeleton reorganisation by PI3K/Akt and its implications for budding virus morphogenesis

Although viral morphology is a genetic trait, factors like host cell type and cytoskeletal composition and spatial differences in the shape, structure and cell function referred to as cell polarity may greatly influence the morphogenesis of budding influenza virus. Most cell types exhibit cellular polarity enabling them to carry out specialized functions. Cellular polarity has been shown to influence the shape of budding influenza virus, particularly release of filamentous virion particles. Roberts and Compans (1998) observed extensive filament formation in epithelial polarized cell types like MDCK, MDBK, HEC-1 and Vero cells but not in BHK21 cells, which, although of kidney origin, are non-polar in nature. Influenza viruses released from polarized cells were filamentous in contrast to spherical viruses released from non-polarized cells. A functional link between

the presence of intact actin cytoskeleton and lipid raft domains in cell membrane and generation of filamentous virion particles was extensively studied by Simpson-Holley et al. (2002). Disruption of the actin cytoskeleton with specific actin inhibitors showed the aggregation of lipid raft domains into the annuli surrounding actin cores, which blocked the generation of filamentous virions. However, actin inhibition did not affect generation of spherical viruses mostly because of the need of much smaller domains for formation of spherical virion particles. These findings suggest crucial role of PI3K/Akt mediated cytoskeletal actin remodelling in virus morphogenesis. The role of PI3K/Akt in cytoskeletal actin remodelling and AIV morphogenesis are investigated in Chapter 4.

1.14 Importance of adopting species specific cell culture system for study of signalling pathways during AIV infections

Enhanced level of PI3K/Akt activity has been observed in many cancerous conditions (Wang et al., 2015). Activation has also been observed in influenza virus infection in many cell systems; however most of the studies have been done in established immortalised cell lines that are essentially cancerous in nature. In vitro assessments of host pathogen interactions display wide variability that could inherently result from cell lines used or from the infectious agent itself. The expression data so obtained from established cell lines may not always reflect true expression pattern of host cells as there could

be potential acquired differences, especially in the regulation of signalling cascades between primary cells and established cell lines. Distinct differences were observed in IAV replication kinetics and host response between primary and transformed continuous cells (Seng et al., 2014). Variations in cell type specificity in the regulation of cellular signalling cascades among mammalian and avian host species and evolution of low pathogenic virus to highly pathogenic virus in chickens warrants the need to fully understand the role of cellular signalling pathways in influenza virus pathogenesis in avian hosts. Hence, a species-specific primary cell culture system or in vitro organ culture studies may reveal near-correlative expression patterns that can be compared to in vivo systems in order to better understand the mechanisms underlying evolution of high pathogenic influenza viral strains in chicken hosts.

Activation of the innate immune response via TLRs triggers production of cytokines. However, it has been shown that prolonged and excessive stimulation of innate immunity could be harmful leading to fatality due to severe tissue damage (Ulevitch and Tobias, 1995). To mitigate such an undesirable outcome, the innate immune system may use PI3K/Akt as a strong 'gate keeping system' that ensures appropriate magnitude of response and overcomes the multiple waves of stimuli by influenza viruses. Recent research focusing on the role of PI3K pathway in innate immune response have

raised the possibility of it acting as a safety system to control the magnitude of immune stimuli (Kobayashi et al., 2002). The precise mechanisms underlying disparate AIV pathogenesis in chicken and ducks and PI3K contribution in AIV pathogenesis needs to be investigated in avian species. Hence this project is to investigate the regulation of host PI3K/Akt signalling pathway and its implications on virus replication for better understanding of the molecular mechanisms of AIV pathogenesis.

1.15 Study hypothesis

Differences in the outcome of avian influenza virus infection in chicken and ducks is driven by host-specific cellular responses.

1.15.1 Aims and objectives of the study

The overall aim was to study the regulation of the PI3K/Akt signalling pathway in avian influenza virus infected primary chicken and duck embryo cells. The aim was achieved by following objectives.

1) Establish activation of the PI3K/Akt pathway in avian influenza virus infected chicken and duck cells and its implications for virus replication.
2) Compare PI3K/Akt pathway specific transcriptomic expression data between chicken and duck cells and establish the role of PI3K/Akt in cytoskeletal actin remodelling and viral morphogenesis.
3) Study protein–protein interactions between AIV NS1 and PI3K p85β subunit by *in-silico* modelling for PI3K activation compatibility analysis.
4) Determine possible differences whether the AIV NS1 proteins of LPAI and HPAI viruses differ in activation of the PI3K pathway by using recombinant H5N1viruses with NS1 swaps.

Chapter 2. General Materials and Methods

2.1 Influenza viruses used in the study

The two low pathogenic avian origin influenza A viruses H2N3 (A/mallard duck/England/7277/06) and H6N1 (A/turkey/England/198/09) maintained in the laboratory were used in the present study.

2.1.1 Propagation of virus stocks in eggs

Both H2N3 and H6N1 viruses used in the present study were propagated in 10-day-old embryonated hen's eggs sourced from Dekalb white leg horn chickens (Henry Sewart & Co Ltd, UK). The fertile eggs were set in the egg incubator (Brinsea) at 37°C, humidified atmosphere as per the manufacturer's recommendations. The eggs were examined using an egg candler to ascertain the growth of embryo. All the unfertile and cracked shell eggs were discarded. The air sac area was marked with a pencil, and x mark was drawn on the allantoic cavity area as location guidance. All the selected eggs were replaced back in the egg incubator until the inoculum was prepared.

Virus diluting fluid (DF) was prepared by adding 2ml tryptose phosphate broth (Sigma) to 100 ml sterile PBS along with 1% antibiotics (100 U/ mL penicillin and 100 µg/ mL streptomycin, (Invitrogen). Inoculum was prepared by diluting seed virus stock to make a working concentration of 1:1000 DF for both viruses. The diluted virus inoculum was sterilised by passing through 0.22 µm

syringe filter (Millex, Millipore). Previously marked eggs were sterilised by mopping with 70% IMS (industrial methylated spirit) which was then allowed to evaporate. Holes were pierced in the eggshell, first at the air sac and then at the site of inoculation (x mark). With the help of 1ml insulin syringe and 25G needle, 0.1ml of diluted virus was inoculated per egg by piercing the needle through the egg shell approximately 2mm deep into the allantoic cavity. Once the inoculation completed, the holes on the eggs were sealed with molten paraffin wax and eggs labelled. Eggs were incubated for 72 hours with daily observations.

After 72 hours of incubation the eggs were removed from the incubator and the egg racks with eggs were wrapped in autoclave bags, sealed with tape and placed at 4°C overnight to kill the embryos and contract the blood vessels to reduce blood contamination of allantoic fluids while harvesting. Eggs were harvested in a Class II safety cabinet using sterile scissors. The egg was opened on the broader end by removing shell from air sac area. Allantoic fluid was collected with the help of a 10 ml syringe from each egg. The stock allantoic fluid was pooled from all the eggs in a 50 ml falcon tube with proper labelling of virus name. The pooled allantoic fluid was centrifuged at 2500 rpm for 5 min. Clear virus stock was aliquoted in 1 ml labelled cryotubes and stored at -80°C. An aliquot of harvested virus was used to perform haemagglutination assay (HA) by serial dilution of 50 µl virus in

sterile phosphate buffered saline (PBS) and addition of an equal volume of chicken erythrocytes (1% packed cell volume) in a V-bottomed microtiter plate to confirm the growth of virus.

2.1.2 Preparation and maintenance of chicken and duck primary embryo fibroblast cells

The chicken and duck embryo fibroblast (CEF and DEF) were prepared from 8–10 day old embryonated hen's eggs sourced from commercial lines of Dekalb white leg horn chickens evolved originally from light Sussex strains (Henry Sewart & Co Ltd, UK) or from 12 day old Pekin duck eggs (Fecanda foods Ltd). Upon receipt of eggs from the supplier the potential contaminants from fertile eggs were removed by mopping thoroughly with 70% IMS and allowed to dry before placing them in the egg incubator(Brinsea) as explained in 2.1.1. On the day of harvesting, the embryos were mopped wth 70% IMS to avoid possible contaminants and embryos were collected by breaking open the eggs at the broader end with sterile forceps in class II cabinet hoods. Chorio–allontoic membrane was disrupted and the embryo was located, The embryo was firmly held with sterile forceps and pulled out from the egg and placed in a petridish containing sterile PBS. The head was decapitated with sterile scissors, the limbs and visceral contents, were removed from rest of the tissue. The remaining embryo tissue was washed three times in sterile PBS. The embryo tissue was minced into small pieces with the help of sterile scissors. Tissue homogenate was then transferred

to a falcon tube containing approx 25-30 ml Dulbecco's modified eagle's medium (DMEM)-Glutamax (Gibco), 0.25% trypsin EDTA (Sigma) and 100 units/ ml penicillin and 100µg/ml streptomycin solution (invitrogen). The tissue homogenate suspended in trypsin solution was incubated in a shaking incubator unit (Thermo electron) at 37ºC for 30 minutes. The cell suspension was then filter sterilized through a 40µm Falcon cell strainer (BD Biosciences) and centrifuged (Thermo scientific) at 1200x*g* for 5 min. The supernatant was carefully discarded and the cell pellet was dispersed and re-suspended in 3 ml complete cell-culture medium (CCM) comprising of DMEM-Glutamax (Gibco) with 10% fetal calf serum (FCS) (Sigma) and 100 units/ml penicillin and 100 µg/ml streptomycin here in after referred as CCM, before diluting cell suspension further to seed in T75 canted neck tissue culture flasks (Corning) for propagation or for cryopreservation of cells for use in subsequent experimental chapters 3.3, 4.3.3,4.3.4 and 5.3.5. The CEFs and DEFs cells were cultured in CCM adopting standard cell culture protocol as outlined in 2.1.3

2.1.3 Standard protocol adopted for propagation of cells

The cell monolayer was washed twice with 1x PBS to remove any dead cells or other cellular debris. The monolayer was then trypsinized by adding 4ml of 0.05% trypsin EDTA (Invitrogen) in a T75 flask and incubated for 5 min at 37°C or until the monolayer was detached and disrupted. The flask was gently tapped to dislodge

any attached cells and trypsin was inactivated by adding 12 ml DMEM with 10% FCS to. The contents were then transferred to a 50 ml falcon tube (Costar) and centrifuged at 1200x*g* for 5 min. After carefully discarding the supernatant, the cell pellet was re-suspended in 1 ml CCM. The dead and live cells were enumerated by the trypan blue dye exclusion method using a Neubauer counting chamber. Briefly, the cell suspension was prepared by appropriately diluting in 0.4% trypan blue. One part cell suspension was mixed 1:1 with trypan blue in a eppendorf tube and mixed thoroughly. A 10µl suspension was charged on to the edge of the coverslip for uniform capillary spread of the suspension across the grid chamber. The live and dead cells were differentiated based on trypan blue dye exclusion method. The live cells appeared transparent without taking the dye into the cell while dead cells appeared blue round bodies because of trypan blue dye in the cells. The live and dead cells were enumerated in four large squares (top left, top right, bottom left, and bottom right) using the 10X objective lens under light microscope. The number of cells/ml was calculated from the average count of the four large squares multiplied by the dilution factor and 10^4. Based on the experimental needs in chapter 3, 4 and 5, the cells were seeded either in a T75 canted neck cell culture flasks (Corning) at a seeding density of 5000 to 6000 cells/cm^2 or at the rate of 10000 cells/well in 96 well plate (Costar) or $5X10^4$ in 24 well plate (Costar) or $2X10^5$ cells per well in 6 well plate (Costar) followed

for both CEF and DEFs and incubated at 37°C with 5% CO_2. Seeding density for MDCK cells was 8000 cells per well of 96 well plate.

2.1.4 Cryopreservation and revival of cells

Cells were trypsinised as in and were re–suspended with a cell density of $5X10^6$ per ml in freezing medium (FM) containing DMEM-Glutamax with 50% FCS and 10% cell culture grade dimethyl sulphoxide (DMSO, Sigma). The cell suspension was distributed into pre-chilled cryovials (Nunc) at the rate of 1 ml per vial and placed in an isopropanol-filled freezing container ("Mr. Frosty", Nalgene) and frozen at a controlled temperature reduction rate of 1°C/min overnight in a -70°C freezer. The cryovials containing cells were then transferred from -70°C freezer to -196°C liquid nitrogen storage facility on the following day for long–term storage. Two vials of frozen cells were brought up from liquid nitrogen and rapidly swirled in the water bath (37°C) until a small ice chip was left in the tube. The thawed cells were diluted in the 5ml pre-warmed CMM in a 15 ml falcon tube and centrifuged at 1200*g* for 5 minutes to obtain cell pellet for revival of cells. Further cells were seeded T75 tissue culture flasks as outlined in 2.1.3.

2.1.5 Titration of influenza viruses

All the viruses used in the study were diluted in serum free medium (SFM) comprising of DMEM (Gibco) supplemented with 20nM L-glutamine (Sigma), 100 units/ml penicillin, 100 µg/ml streptomycin and 500ng/ml tosyl phenylalanyl chloromethyl ketone

(TPCK) treated trypsin(Gibco). Multiplicity of infection (MOI) of virus stocks and virus titres in supernatants collected from infection experiments was determined on MDCK cells. Briefly, the MDCK cells were seeded in a 96 well plate as described in section 2.1.3 one day prior. When cells attained about 90% confluency, the cells were washed with 1X sterile PBS and inoculated with 100 µl per well of serially diluted stock H2N3 or H6N1 virus, or with 100 µl of supernatant derived from cell infection experiments for calculation of focus forming units (FFU) or for measuring virus titres in supernatants. 100 µl of PBS per well was inoculated as negative control in triplicate well format. After 2 hours' incubation at 37°C with 5% CO_2, virus inoculum was removed and cells were gently washed with 1X sterile PBS followed by addition of 100 µl fresh SFM to all the wells and the plate was incubated at 37°C with 5% CO_2 for further 4 hours before cells were washed twice with 1X PBS and fixed with ice cold acetone:methanol (1:1) for 10 min.

2.1.6 Immuno–cytochemical staining for detection of IAV NP protein in the infected cells

Initial standardisation for optimum concentration of primary antibody dilution to be used for probing the virus infected MDCK cells was performed by incubation of H2N3 virus infected (1MOI) MDCK cells with 50 µl of serially diluted primary mouse monoclonal antibody to influenza virus NP (Abcam). It was concluded that 50 µl solution containing diluted antibody in a ratio of 1:8000 would be

sufficient to stain nearly 100% the virus infected cells. Hence, the primary antibody was diluted to 1:8000 before use in all the virus titration assays in the chapter 3 and 5. The ice cold acetone: methanol fixed cells detailed in 2.1.5 were washed three times with 1X TBS to remove traces of acetone and methanol. The fixed cells were stained using EnVision+System-HRP (DAB) kit (Dako) following the manufacturer's instructions. Briefly, cells were blocked by incubating the cells with 50µl/well blocking reagent against endogenous peroxidase for 10 min, then washed twice with 1X tris buffered saline (TBS) and probed with 50 µl/well diluted primary mouse monoclonal antibody to influenza virus NP (Abcam) and incubated at room temperature for 1h. The cells were then rinsed thrice with TBS and incubated with 50 µl/well horseradish peroxidase (HRP)-labelled anti-mouse IgG (Dako) for 1h followed by three washes with TBS. Subsequently, cells were incubated with 50 µl/well of 3, 3'-diaminobenzidine (DAB)-chromogen solution diluted in substrate buffer (1 drop DAB-chromogen in 1 ml substrate buffer) for 3–10 min and washed carefully with distilled water. The virus infected cells stained brown while the uninfected cells remained unstained.

2.1.7 Determination of MOI and viral focus forming units

The highest dilution of stock virus that resulted in infection of 95–100% cells in a well of 96 well plate was considered as an MOI of 1 for use in cell infection experiments. For determination of FFU, a

representative and consistent systematic approach was adopted in capturing the images from the well of 96 well plate as shown in (Figure 2-1). Images from five different fields from a well were captured randomly at 10X low power magnification on light microscope (Leica). The infected NP stained positive cells in all five images were enumerated using ImageJ image analysis software and averaged. Calculation of FFU was based on the images captured at 100x microscopic magnification with an approximation that a confluent well of 96 well plate had 30000 MDCK cells and number of MDCK cells in one microscopic field as in captured image is approximately 1000 cells.

A = number of NP positive cells per captured field

X = µl of infectious supernatants

Therefore, ffu/µl = (30A)/X

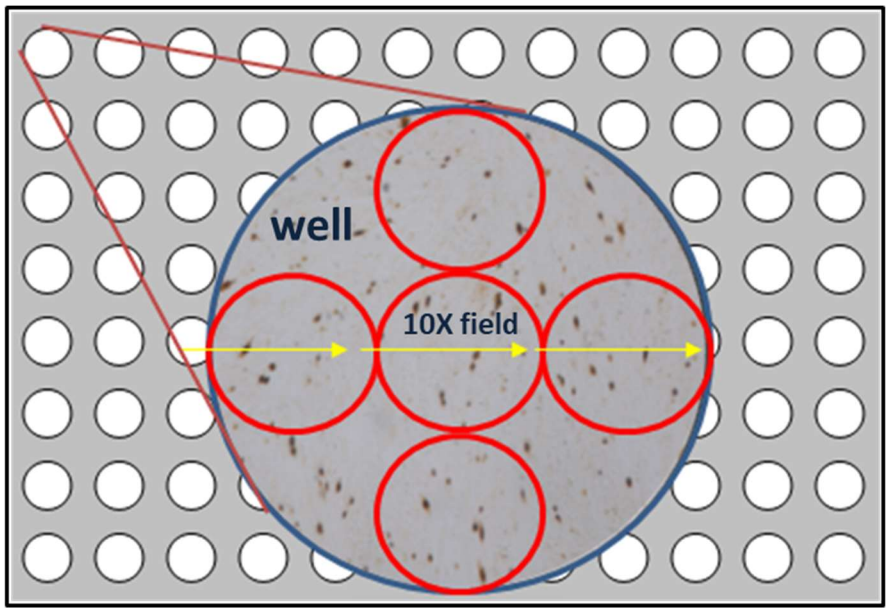


Figure 2-1: Representative imaging technique adopted for imaging 96 well plate for virus titration studies.

2.2 Experimental infection of cells IAVs

Chicken or duck fibroblast cells were cultured either in 6 or 24 well cell culture plates (Costar). The monolayers were gently washed 1x with sterile PBS and were infected with 1 or 0.1 MOI of influenza H2N3 or H6N1 virus diluted in SFM. Infected plates were incubated at 37°C with 5% CO_2 for 2 hours. The plates were removed from incubator and virus inoculum was washed with 1x PBS before any treatment or replenishing with required volume of fresh SFM as per experimental plan. Cells were further incubated at 37°C with 5% CO_2 at stated times as per experimental plan as explained in chapters 3.3.8 3.3.9 and 5.3. Upon completion of experiment the cell supernatants were harvested in 2 ml collection tubes and centrifuged at 1200*g* for 5 min to remove cellular debris and stored

at -80°C and infected on to MDCK cells for infectious virus titration as outlined in 2.1.7. The cell lysates were harvested either in RIPA (Santa cruz) for protein expression or in RLT plus buffer (Qiagen) for total RNA extraction and stored at -80°C for use in western blotting and gene expression analysis studies.

2.3 Statistical analysis of data

Statistical analysis where applicable in the present study was performed using GraphPad Prism V.7. The analysis of infectious virus output from H2N3 or H6N1 or recombinant H9N2 virus infected chicken or duck cells was performed using two-way ANOVA by multiple comparison of means in a grouped data set. The error bars indicate standard error of mean. The raw counts of NP stained cells originated from five low power (10X) images and such values are averaged from three different replicates. The Grey values or fluorescence intensity from immunofluorescence stained images were analysed from intensity values acquired from three independent images using two-way ANOVA by multiple comparison of means (Figure 4-12), While the unpaired data was analysed by unpaired t-test from intensity values acquired from three independent images (Figure 4-13). With respect to qPCR data, the standard curve for each gene was plotted based on the R^2 slope value calculated by linear regression analysis. The relative fold

change expression of individual genes in qPCR experiment was analysed by two-way ANOVA by multiple comparison of means.

Chapter 3. Regulation of phosphatidylinositol-3-kinase (PI3K/Akt) pathway in H2N3 or H6N1 virus-infected chicken and duck embryo fibroblast cells

3.1 Introduction

3.1.1 PI3K/Akt pathway in virus-induced pathogenesis

The viral hijacking of critical host cell signalling pathways like the phosphatidylinositol 3-kinase (PI3K), nuclear factor-κB (NF-κB), mitogen-activated protein kinase (MAPK) and TLR/RIG-I pathways for their transcriptional and translational needs, of these pathways, the PI3K/Akt pathway has received much recent attention due to its central role in the maintenance of cellular homeostasis (Ehrhardt and Ludwig, 2009, Gaur et al., 2011). The host PI3K/Akt pathway is an essential signalling cascade that mediates diverse intracellular functions of cell growth, proliferation and survival by regulatory control over apoptosis mechanism (Franke et al., 2003). Activation of the PI3K/Akt pathway is regarded as the prominent strategy employed by many viruses to promote cellular survival or to suppress cell death (Gaur et al., 2011). Many DNA and RNA viruses like Epstein-Barr virus, papillomavirus, Hepatitis B virus (Cooray, 2004) and Hepatitis C virus (Mannova and Beretta, 2005). Additionally, SARS coronavirus, poliovirus, flaviviruses and influenza A viruses have all shown to induce the PI3K signaling pathway for their replication advantage (Ehrhardt and Ludwig, 2009, Mizutani et al., 2004, Autret et al., 2008, Lee et al., 2005). A recent study also showed that Newcastle disease virus (NDV) infection in chicken

fibroblast cells transiently activates PI3K/Akt pathway, which promotes viral replication (Kang et al., 2017).

The cellular heterodimeric PI3Ks once activated produce a potent second messenger phosphatidylinositol-3,4,5-triphosphate (PIP3) molecule that in turn recruits PH domain-containing signalling proteins like Akt. The effector kinase Akt upon phosphorylation activation (on threonine 308 and serine 407residues) directly or indirectly mediates a wide array of PI3K-regulated responses like cell survival and proliferation (Figure 3-1).

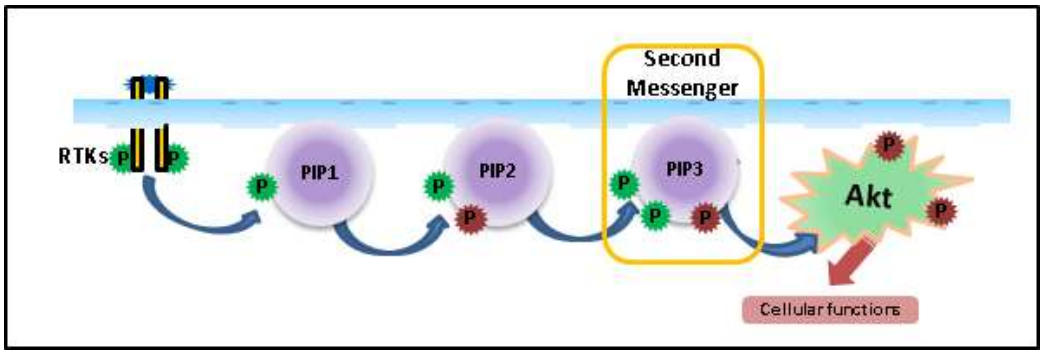


Figure 3-1 Formation of second messenger PIP3 molecule and recruitment of downstream effector kinase.
Sequential phosphorylation of phosphoinositides at 3'-OH (hydroxyl) position of inositol ring, leads to generation of phosphatidylinositol-3-monophosphate (PIP1), phosphatidylinositol-3,4-bisphosphate (PIP2) and finally second messenger molecule phosphatidylinositol-3,4,5-trisphosphate (PIP3) that recruits PH domain containing effector kinase AKT for cellular functions.

Litrature suggests activation of the PI3/Akt pathway at a specific stage of virus–host interactions that are beneficial for the virus. Studies using mammalian host systems report either an early/transient and/or late/sustained PI3K/Akt activation in PR8 virus infected cells. It is conceived that late activation of the pathway is mediated by viral proteins and hence is replication dependent,

while an early or a transient activation was observed upon initial viral binding to host cell surface facilitating virus internalisation (Ehrhardt and Ludwig, 2009). A transient induction of PI3K/Akt was reported in porcine circovirus-2 (PCV2) infected PK15 cells. Inhibition of the pathway in PCV2 infected cells resulted in a reduction in virus output and enhanced cellular apoptosis, suggesting activation of the pathway is essential for cell survival (Wei et al., 2012). Two medically essential pathogens of flavivirus group, Japanese encephalitis virus (JEV) and dengue viruses have shown transient activation of the PI3K pathway in neuronal cells. Chemical abrogation of PI3K activity resulted in enhanced flavivirus mediated characteristic cytopathic changes and early apoptosis induction in the infected cells (Lee et al., 2005). Inhibition of PI3K activity resulted in significant reduction in Ebola virus internalisation in early stages of infection (Saeed et al., 2008). The vaccinia and cowpox viruses hijack PI3K/Akt pathway to facilitate their endocytosis (Izmailyan et al., 2012). Infection of mouse embryonic fibroblast (MEF) cells with vaccinia and cowpox viruses revealed that the activation of PI3K/Akt pathway was essential for both viral replication and host cell survival (Soares et al., 2009). Porcine pseudorabies virus (PRV) elicited PI3K/Akt and NF-κB signalling to bring about anti-apoptotic activity leading to cell survival to facilitate virus replication, inhibition of the same pathway resulted in enhanced cell death (Chang et al., 2013). Similar observations were

made on involvement of host signalling cascades in the regulation of virus internalisation and apoptotic cell death in avian reo virus infected DF-1 cells (Lin et al., 2010) and bovine ephemeral fever virus infected MDBK and Vero cells (Chen et al., 2010) suggesting an absolute dependence on host signalling machinery for efficient virus replication through inhibition of apoptosis of infected cells.

3.1.2 PI3K/Akt pathway activation by influenza A virus and its implications on virus propagation

A biphasic diversity in PI3K/Akt pathway activation IAV infected cells was described, consequently leading to the activation of downstream effector kinase Akt at different stages of infection (Ehrhardt et al., 2006, Ehrhardt and Ludwig, 2009) (Figure 3-2). Interestingly, similar activation was not observed in influenza B virus-infected cells, making it a unique feature of IAVs (Ehrhardt et al., 2007a). Initial binding and cellular interaction of IAV with sialic acid receptors on the host cell membrane is regarded as the earliest point of PI3K/Akt pathway activation. The initial IAV interactions with the cell is likely to result in binding of the PI3K to autophosphorylated receptor tyrosine kinases (RTKs) leading to clustering of lipid rafts in the plasma membrane and subsequent phosphorylation of PIP2 and generation of PIP3 'second messenger' system and phosphorylation activation of Akt kinase (Eierhoff et al., 2010, Diehl and Schaal, 2013) (Figure 3-1). Glycogen synthase kinase 3β (GSK3β) dependent inhibition of influenza PR8 virus entry

was observed upon inhibition of Akt kinase activity in virus infected A549 cells (Hirata et al., 2014). Inhibition of PI3K interaction between Ras (Rat sarcoma) and PI3K has been shown to be indispensable in clathrin-independent influenza virus endocytosis in PR8 virus infected MEF cells (Fujioka et al., 2011). The PI3K upstream tyrosine kinase, focal adhesion kinase (FAK) has been shown to regulate cellular migration through PI3K dependent phosphorylation of growth factor receptor-bound protein 7 (GRB7) adaptor molecule (Han and Guan, 1999). Chemical inhibition of FAK led to the disruption of actin-network resulting in the sequestration of virus in the cell periphery and subsequent reduction in virus localisation in early endosomes leading to significantly reduced titres in PR8 H1N1 virus infected A549 cells (Elbahesh et al., 2014). A contrasting report to that from Ehrhardt et al. (2006) suggested no transient activation of PI3K/Akt pathway upon viral attachment and entry (Shin et al., 2007b). PI3K mediated Akt phosphorylation was observed only upon PR8 H1N1 virus infection at 6 hpi, as Akt phosphorylation was not observed in mock infected A459 cells, implying that late and sustained activation of PI3K/Akt pathway is virus replication dependent and may not be mediated by initial virus-host cell interactions. Treatment of PR8 H1N1 virus infected MDCK cells with LY294002 a specific PI3K inhibitor resulted in significant reduction of virus output suggesting altering disease outcome upon PI3K activation (Shin et al., 2007b).

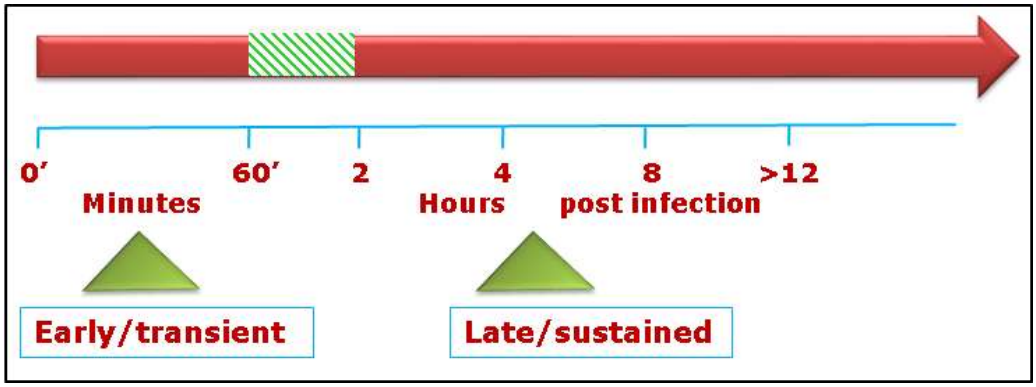


Figure 3-2: Time course activation of the PI3K pathway in influenza A virus infected MDCK, A549 or glial cells.

A transient activation of the pathway was observed shortly after virus infection, facilitating virus internalisation. A more sustained activation was observed later in the infection. Figure adapted from Ehrhardt and Ludwig (2009).

3.1.3 Importance of IAV induced PI3K/Akt activation for viral replication

The importance of PI3K/Akt kinase mediated cellular survival and death has been studied widely in the pathogenesis of degenerative diseases and cancer biology (Franke et al., 2003) and has immensely contributed towards better understanding the role of the PI3K/Akt pathway in infectious disease pathogenesis. A significant decrease in progeny virus production was observed upon inhibition of Akt kinase activity (Ehrhardt et al., 2006, Hirata et al., 2014) indicating the need for cellular PI3K/Akt phosphorylation events in progeny virus production. Inhibition of PI3K/Akt activity resulted in the inhibition of viral RNA and protein synthesis and subsequent cytoplasmic retention of viral RNP complex in PR8 virus infected A549 cells, suggesting significant involvement of the PI3K/Akt in the viral replication process (Shin et al., 2007b).

A broad range of cellular functions that support virus replication have been shown to be altered in later stages of virus mediated PI3K/Akt activation. PI3K is involved in inhibition of apoptotic cell death by phosphorylation inhibition of pro-apoptotic factors in normal cells. Initial studies have revealed that IAV infection results in inhibition of apoptotic process (Zhirnov et al., 2002). Later it was identified that the PI3K/Akt pathway is a key molecular regulator in the phosphorylation inhibition of pro-apoptotic factors like caspase-3/9 and GSK-3β that results in impeding apoptosis in IAV infected cells (Ehrhardt et al., 2007a, Shin et al., 2007b, Zhirnov and Klenk, 2007). IAV mediated apoptosis induction is closely related to disease severity in the infected cells (Iwai et al., 2013). Viral PB1-F2 protein is shown to localise at the mitochondrial membrane and make cells more susceptible to apoptosis (Zamarin et al., 2005). Early apoptotic induction was also observed in avian influenza H5N1 virus encompassing full-length PB1-F2 infected porcine alveolar macrophages resulting in limiting virus spread (Chang et al., 2015) besides, direct apoptotic effects mediated through Bcl2 (B-cell lymphoma 2) associated death (Bad) promoters in IAV infected A549 cells (Lu et al., 2010). The JNK (c-jun N-terminal kinase) mediated apoptotic regulation was observed in equine influenza virus infected cells (Lin et al., 2001b). It is potentially a strategy employed by influenza viruses to slow down cell death to prolong its replication by way of PI3K/Akt activation in mammalian cells (Ji and Liu, 2008).

3.1.4 Species specificity, a crucial factor to consider for studying host cellular signalling mechanism

Most of the research on the regulation of the PI3K/Akt pathway in IAV infections has been conducted in transformed, immortalised mammalian cells. The most commonly used ones are human alveolar basal epithelial cells (A549)(Chakrabarti et al., 2010) and Madin-Darby canine kidney (MDCK) cells (Youil et al., 2004), which are readily permissive to laboratory-adapted influenza virus strains. However, immortalised cells may exhibit altered virus susceptibility and may exhibit a broad range of differences especially in the regulation of signalling cascades as they no longer mimic their originator cells due to oncogenic transformation.

It has been shown previously that host antiviral pathways are greatly impaired due to cellular oncogenic transformation (Stojdl et al., 2000). Activation of the PI3K/Akt through multiple cellular signals in different cell types (Koyasu, 2003) suggests that the PI3Ks regulate under complex intracellular control in various hosts to mount an appropriate host response.

Several studies also revealed differences in the antiviral host response among IAV infected primary cells from different hosts. A comparative study of primary human and swine broncho-epithelial (HBE/SBE) cells showed that SBE cells exhibited relatively limited antiviral response compared to human cells when infected by a

range of human, swine and avian origin influenza virus subtypes (Hauser et al., 2013).

Among avian species, chicken and ducks display a wide array of differences in their response to influenza A virus infections. It has been shown that duck cells undergo rapid apoptosis and produce less infectious virus particles compared to chicken cells upon AIV infection (Kuchipudi et al., 2012a, Al-Mubarak et al., 2015). The exact reasons contributing to this disparate disease outcome between AIV infected chicken and ducks are not entirely understood. It is possible that the PI3K pathway, which plays a crucial role in regulation of several essential cellular functions may be involved in bringing about this differential disease outcome.

A paucity of knowledge exists concerning host signalling pathway regulation in avian species. Therefore, revealing PI3K pathway regulation in chicken and duck cells would aid in bridging the knowledge gap on the activation of the PI3K/Akt pathway in chickan and duck hosts in general and contribute further to better understanding the reasons for disparate disease outcome in IAV infected chicken and ducks in particular.

3.2 Aims and objectives

3.2.1 Aims

To establish and compare the role of the PI3K/Akt signalling pathway in avian influenza virus replication in chicken and duck cells.

3.2.2 Objectives

1. To determine the status of regulation of the PI3K/Akt pathway in primary chicken and duck embryo fibroblast cells.
2. To determine the effect of PI3K pathway activation on cell survival and IAV replication in primary chicken and duck embryo cells.
3. To determine PI3K regulation in an avian-origin macrophage (HD11) continuous cell line and in *ex vivo* chicken tracheal organ cultures (TOCs) infected with H2N3 virus.

3.3 Materials and Methods

The specific materials and methods used in this chapter are described here briefly.

3.3.1 Cell lysate preparation for protein expression

Cells from each well of a 6-well plate were washed twice with 1x sterile PBS and lysed by adding 115 µl of RIPA buffer (Santa Cruz) supplemented with 1% phenylmethylsulfonyl fluoride (PMSF), 1% inhibitor cocktail and 1% sodium orthovanadate (denoted as complete RIPA buffer in further text). Cell lysates were scraped with the help of a cell scraper and lysate collected in a microcentrifuge tube. The lysates were gently agitated and placed on ice for 30 min allowing complete cellular disruption. The lysates were then centrifuged at 14000xg for 15 min at 4°C. The supernatants were collected into fresh microcentrifuge tube discarding the pellet, aliquoted, labelled and stored in -80°C freezer for long term storage.

3.3.2 Total protein quantification

Five dilutions of known protein standards were prepared using bovine serum albumin (BSA, Sigma). The protein standard concentrations were 2, 1.0, 0.5, 0.25 and 0.125 mg/ml. The total protein concentration in the sample lysates was quantified by Bradford protein assay reagent (BIORAD) following the manufacturer's instructions in a 96 well plate. Briefly, the protein assay reagent was diluted in 1:5 ratio in MilliQ water before use.

Five µl protein lysate or protein standards were added in triplicate wells followed by 150 µl of diluted protein assay reagent to each well, and the plate was incubated for 5–10 minutes at room temperature (RT). Spectrophotometric absorbance was measured at 590–595nm using Fluostar Optima, (BMG Labtech) and protein concentration of samples was determined using a standard curve plotted with the BSA standards.

3.3.3 SDS-Polyacrylamide gel electrophoresis

A total of 10 µg protein lysate was mixed with 1.5 µl NuPAGE sample reducing agent and 3.5 µl NuPAGE lithium dodecyl sulphate (LDS) sample buffer, total volume was made up to 15 µl by adding nuclease-free water. The protein buffer mix was heated at 70°C for 10 min on a hotplate. The 12 well, 1mm thick precast NuPAGE® 4–12% Bis-Tris protein gel (Invitrogen) was assembled correctly and clamped in the gel tank slot. The 3-*N*-morpholino propane sulfonic acid (MOPS) gel running buffer was prepared by diluting 50ml 20X stock solution (Invitrogen) in 1000 ml purite water to make 1X concentration. Two hundred ml 1X running buffer was aliquoted, and 500µl antioxidant was mixed and poured into the inner core area of gel assembly tank. The surrounding area of the gel was filled with 600ml running buffer for the optimum running of the electrophoresis. The sample mix (15 µl) was loaded into individual wells. An amount of 10µl pre-stained protein marker ranging between 3–198 kDa (Invitrogen) was loaded in a separate lane and

electrophoresis was set to run at 200 volts for 45–55 min. All reagents and gel running tanks used in this experiment were from Invitrogen.

3.3.4 Protein transfer onto PVDF membrane and blocking

The 1X transfer buffer was prepared in 10% methanol by diluting 50ml 20X Nupage, transfer buffer (Invitrogen) stock in 850 ml purite water. The polyvinylidene fluoride (PVDF) membrane (Amersham) and filter paper (Whatmann) were prepared by cutting into appropriate dimensions matching to the size of gels. The PVDF membrane was charged by dipping in methanol for 30 seconds and soaked in purite water before clamping on to the gel. The membrane, filter papers and sponge pads were pre-soaked in the transfer buffer. The gel with resolved protein bands was disassembled from the cast module and sandwiched between PVDF membrane, filter paper and sponge pads were arranged in the following order for the efficient transfer of resolved proteins from gel to PVDF membrane; sponge/paper/gel/membrane/paper/sponge. The sandwich was clamped tightly in the transfer apparatus and submerged into the XCell II blot module (Invitrogen), 30 volts current was applied and allowed to run for 1h for the migration of resolved proteins from the gel onto the PVDF membrane.

Tris-buffered saline-Tween (0.1%) (TBST) was prepared by adding 1ml Tween–20 in 1 litre TBS. A 5% BSA solution was

prepared in TBST (2.5g BSA in 50 ml TBST) and used as blocking solution. After the protein transfer, blot/PVDF membrane was soaked in 10-15ml or sufficient volume of blocking solution to submerge the PVDF membrane and incubated at room temperature on a shaker for 1hour.

3.3.5 Incubation with primary and secondary antibodies

Once the blocking was done, the membrane was washed two times in TBST with 5 min each wash. The primary antibody for various target proteins like native Akt, Phospho Akt, IAV PB1 and beta-actin as a loading control were used for probing. The concentrations and incubation period for each primary and secondary antibody is shown in (Table 3-1). The membrane was incubated with primary antibody at 4°C overnight on a plate shaker. Following day the membrane was washed with TBST for 3–5 changes, each wash lasting for 5 min to remove any unbound primary antibodies. Subsequently, the membrane was probed with appropriate HRP conjugated secondary antibody and incubated at RT for 1–2 hrs on the shaker. After the incubation, the membrane was washed with TBS-T as explained above.

Table 3-1: Primary antibodies used in this study

Serial No	Primary Antibody (Ab)			HRP conjugated secondary Ab		Supplier
	Origin	Specificity	Dilution	Specificity	Dilution	
1	Rabbit	Native Akt	1:10000	Anti-rabbit Goat IgG	1:10000	CST
2	Rabbit	Phospho Akt	1:3000	Anti-rabbit Goat IgG	1:10000	CST
3	Rabbit	IAV PB1	1:20000	Anti-rabbit Goat IgG	1:10000	GeneTex
4	Rabbit	Beta-actin	1:10000	Anti-rabbit Goat IgG	1:10000	NeoMarkers

3.3.6 Chemiluminescent development

The Amersham ECL prime western blotting detection reagent (GE Healthcare) was prepared as per the manufacturer's instructions. Briefly, the membrane was laid on a clean, transparent cling film (Sarogold), about 300 µl of reagent A and 300 µl of reagent B of developing solution were mixed in an Eppendorf tube just before use and flooded on to the membrane and allowed for a uniform spread for 1-2 minutes. After which, the membrane was gently held vertically on the corner with the help of a fine tweezers to drain off the excess developing solution before wrapping in transparent cling film for chemiluminescence observation. The membrane was exposed to the photon counting (PhoTek) camera immediately for observing chemiluminescence development.

3.3.7 Determination of binding specificity of rabbit origin primary pAkt (Ser473) antibody for use in avian cells

The non-availability of avian/chicken-specific primary antibodies for detection of phosphorylated Akt was a major constraint in the present study. Commercially available rabbit

specific pAkt primary antibody (CST #9271) was used to determine the detection specificity of phosphorylated Akt in IAV infected chicken cells, by comparing alongside a known pAkt positive control cell lysate (CST #9902) derived from Calyculin A treated Jurkat cells. The antibody proved to be detecting pAkt protein of expected size in chicken cell lysates without any non-specific binding. After ascertaining specific detection of pAKT protein in chicken cells, AIV infected chicken cell lysate harvested at 9hpi was used as the positive control for detection of pAkt and also served as positive control for IAV PB1 protein detection as infection control. Canonical stimulation of PI3K/Akt pathway in DEF cells was performed by exposure of DEF cells with IGF-1(100ng/ml). Hence the IGF-1 treated duck cell lysate showing phosphorylated Akt was used as the positive control in duck western blot experiments in the present study.

3.3.8 Titration of LY294002 or Wortmannin dose for use in cell culture

The commercially available LY294002 (Sigma) or wortmannin (Sigma) were dissolved by adding required volume of cell culture grade DMSO (Sigma) to give a stock concentration of 1 mg/ml solutions as per the manufacturer's instructions. The effective concentration of LY294002 and wortmannin for complete abrogation of Akt phosphorylation was determined in the H2N3 virus (1MOI) infected CEF cells in 6 well plates. Increasing concentrations of

LY294002 (1, 2.5, 5, 10, 20, 40, 50 and 100 μM) or 1, 2.5, 5, 10, 20, 40, 50 and 100 nM wortmannin were prepared in 5 ml serum-free infection medium. Each well-containing virus infected CEF cells were exposed to different strengths of LY294002 or wortmannin for one hour and washed three times before supplementing with fresh infection medium for further incubation. After 9 hpi, the cells were washed thrice with sterile 1XPBS before lysate preparation in RIPA buffer. These cell lysates were subjected to western blotting to determine effective concentration of chemical inhibitor that is required for complete inhibition of PI3K/Akt activity.

3.3.9 Titration of infectious virus production in MDCK cells

The infectious virus output in supernatants was quantified by focus-forming assay (FFA) as described previously by Kuchipudi et al. (2012a). Briefly, MDCK cells were seeded in 96-well plate, when the cells were approximately 80-90% confluent, cells were washed and inoculated with 100 μl supernatants derived from infected cells or PBS as infection control in triplicate. After incubation cells were washed and fixed with ice cold acetone: methanol (1:1) for immunocytochemical staining as described in sections 2.1.5 and 2.1.6. Determination of infectious virus production was measured by measuring viral focus forming units (FFU) determined by enumerating the nucleoprotein (NP) positively stained cells under the microscope as described previously in section 2.1.7.

3.3.10 Measurement of cell metabolic activity

The dehydrogenase enzymes released by the metabolically active cells reduce tetrazolium compound 3-(4, 5-dimethylthiazol-2-yl)-2 5-diphenyltetrazolium bromide reduction (MTT) (Owen's reagent) into a coloured formazan product. The quantity of formazan formed can be measured by addition of CellTiter 96® AQueous One Solution (MTS assay, Promega) and is directly proportional to the number of living cells in culture medium. The metabolic activity of influenza H2N3 virus infected (1MOI) or uninfected chicken and primary duck cells was performed by addition of MTS assay reagent.

Primary CEF and DEF cells were seeded in to 96-well cell culture plates (Costar) at a seeding density of 10000 cells per well as described in 2.1.3. Following 24 hrs incubation at 37ºC, the medium was removed, and cells were gently washed thrice with sterile PBS (1X). The cells were then infected with 100 µl infection medium (IM) containing an avian H2N3 virus (1 or 0.1 MOI), in triplicate well format. An equal number of wells were sham-infected with IM without the virus. After incubation at 37ºC for two hrs, the virus was removed from the cells, and the cells were rinsed three times with PBS before adding IM with or without 20 µM LY294002 (PI3K inhibitor) or another potent irreversible PI3K inhibitor Wortmannin at a concentration of 10 nM was considered for use in the experiments involving recording observations beyond 24 hrs post exposure. The plates were further incubated for one hour before

washing and replenishing with 100 µl IM per well and incubated at 37ºC for appropriate time points and the metabolic activity of the cells was analysed using CellTiter 96® AQueous one solution cell proliferation assay (Promega) as per the manufacturer's instructions. Briefly, 20µl of assay reagent was added to each well of the 96-well assay plate containing 100 µl culture medium. The plates were incubated at 37ºC for 2 hrs in a humidified, 5% CO_2 atmosphere. After incubation, the absorbance was recorded at 490 nm wavelength using 96-well plate reader Fluostar optima (BMG Labtech) to measure the amount of soluble formazan produced by cellular reduction of MTT.

3.3.11 Measurement of activated caspase 3/7 activity

The members of the cysteine aspartic acid-specific protease (caspase) family play key effector roles in programmed cell death. Activated Caspase 3 and 7 levels in either influenza virus infected or control uninfected CEF and DEF cells was measured using luminescent Caspase-Glo 3/7 assay (Promega), according to the manufacturer's instructions. CEF or DEF cells were seeded into 96-well cell culture plates (Costar) at a seeding density of 10000 cells per well as described previously in 2.1.3. Following 24 hrs incubation, the cells were infected with 100 µl infection medium (IM) containing an avian H2N3 virus (1 or 0.1 MOI), in triplicate well format along with an equal number of sham-infected no virus control wells. Two hours post-infection, the cells were treated with 20 µM

LY294002 or 10 nM Wortmannin (PI3K inhibitor) or an equivalent volume of DMSO as described in section 3.3.12. The plates were further incubated for one hour before washing and replenishing with 100 µl IM per well and incubated at 37ºC for 24 or 48 hrs. Once the incubation was complete, 100 µl Caspase-Glo 3/7 reagent was added to all the wells containing cells and reagent blanks without cells. The contents were gently mixed on a plate shaker at 300–500 rpm for 30s and the plate was incubated at RT for 1 hr. After one hour the contents of each well was gently mixed and transferred to the white-walled 96-well plate (Costar). The luminescence intensity of each sample was measured as relative light units (RLU) per second with the help of Orion L micro plate luminometer (Berthold detection systems) and analysed using Simplicity software version 4.10.

3.3.12 Preparation of tracheal organ cultures

The experimental studies involving tracheal organ cultures (TOCs) was kindly performed by Dr.Holly Shelton at The pirbright institute. The transverse sections of the tracheal organ cultures was prepared from 18 day old chicken embryos sourced from SPF hen eggs following methods described previously (Maier et al., 2013, Hennion, 2015). Briefly, on a clean workbench or hood the embryonated eggs were sterilised by mopping the egg shell with 70% IMS. Using a sterile curved scissor the egg shell was gently removed and embryo was lifted from the egg and placed in a 150 mm Petri dish. With sterile scissors the embryos were decapitated;

the tracheae were carefully separated from surrounding tissue and placed in pre-warmed TOC culture medium containing minimum essential medium-Eagles along with antibiotics (Appendix-I). The extraneous tissue attached to the tracheal tube was cleared with the help of a scalpel blade and forceps. The cleared tracheal tube was then placed on sterile whatmann filter paper and each trachea were cut into approximately 0.6-mm-thick rings using sterile scissors and forceps. Few rings from both terminal ends were discarded and the rings from middle portion of the trachea were immersed in tube containing 0.6 ml of pre-warmed TOC culture medium (Appendix I).

Care was taken to add only one tracheal ring per 1 mL tube before incubating the tubes at 37°C in a rotating incubator at 8 rotations per minute speed. After 24 hours, the ciliary activity of the tracheal epithelium of each TOC was examined under a low power (100 x magnifications). The TOCs showing 100% ciliary activity were selected for virus infection experiments. TOCs were infected with H2N3 virus at an MOI of 1 or mock infected with PBS and incubated at 37 °C for 2 h, After incubation the virus inoculum was removed and the TOCs were washed with sterile PBS for three times. Following washing, the TOCs were supplemented with TOCs medium and further incubated at 37 °C on a rotator until 6, 9 and 24 hpi. After respective incubation times the supernatants were collected in 1.5 ml screw cap vial and stored at -80’C for virus titration. The

H2N3 virus infected tracheal rings were immersed in RIPA buffer for cell lysis and protein expression studies.

3.3.13 Propagation and infection with H2N3 virus of chicken macrophage (HD11) cells

The chicken macrophage cell line used in the present study were a kind gift from Dr. Stephen Dunham, School of Veterinary and Science, Sutton Bonington campus. University of Nottingham. The HD11 cells were propagated in cell culture medium supplemented with chicken serum (Appendix I) as described previously were cultured as previously described (Kaiser et al., 2000). The H2N3 virus infection studies involving HD11 cells was performed similar to that explained previously for CEF cells in2.1.2 and 2.1.3.

3.4 Results

3.4.1 CEF cells produce higher titres of IAV than DEF cells

Infectious virus production in H2N3 virus infected CEF and DEF cells has been previously studied and demonstrated that DEFs produce significantly less infectious virus particles than chicken fibroblast cells (Kuchipudi et al., 2012a, Al-Mubarak et al., 2015). In this study H2N3 virus infected (1MOI) CEF cells produced significantly ($P \leq 0.0001$) higher levels of infectious virus titres compared to DEF cells at 9 and 24 hpi (Figure 3-3), substantiating previous findings.

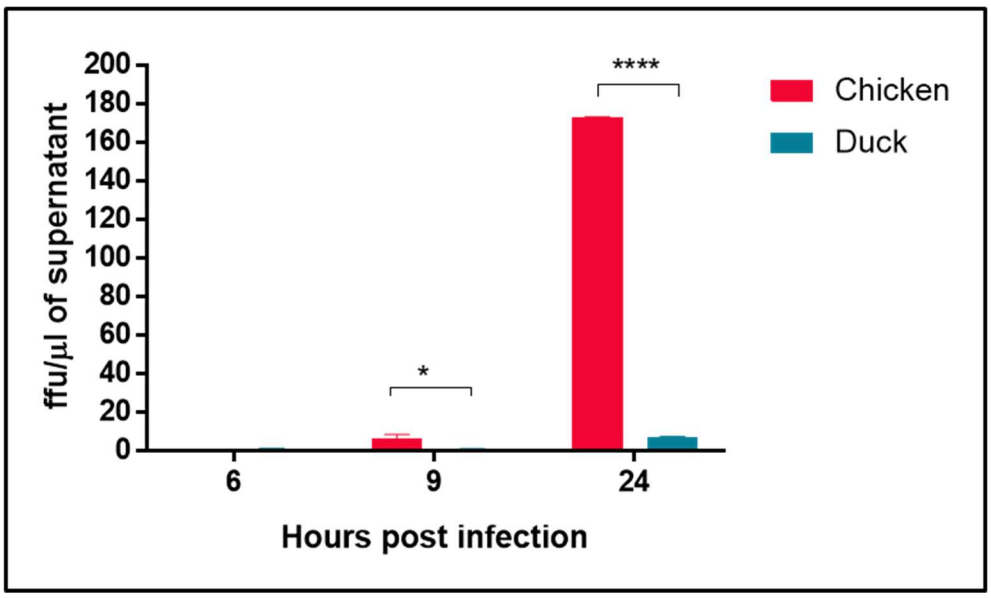


Figure 3-3: Infectious virus production in H2N3 virus infected chicken and duck fibroblast cell supernatants.

Supernatants from avian H2N3 virus (1MOI) infected CEF and DEF cells harvested at 6, 9 and 24 hrs post-infection. Infectious virus titre was measured in focus-forming unit per microlitre (ffu/µl) on Madin Darby canine kidney cells. Data shown represent the mean of triplicate wells with error bars showing standard error of the mean (SEM). Statistical analysis was performed using two way ANOVA by multiple comparison of means. Level of significance *=$p \leq 0.05$, ****=$P \leq 0.0001$.

3.4.2 AIV infection induces activation of the PI3K/Akt pathway in chicken embryo fibroblast cells

Activation of the PI3K/Akt pathway in CEF cells was determined by western blot analysis of lysates derived from either IAV-infected or uninfected cells, to detect phosphorylated Akt (pAkt). Akt phosphorylation was not observed in healthy uninfected CEF cells despite the presence of native Akt protein (Figure 3-4A). Akt phosphorylation was observed in cells infected with either LPAI H2N3 or LPAI H6N1 viruses, as evidenced by the presence of pAkt protein at 6 and 9hpi (Figure 3-4B & C). However, no evidence of Akt phosphorylation was observed at 2 and 24 hpi (Figure 3-4B & C). The presence of native Akt was observed at all time points 2 to 24 hpi in both infected and uninfected controls (Figure 3-4A, B & C). A time-dependent increase in the accumulation of influenza virus PB1 protein was observed in virus-infected CEF cells at 6, 9 and 24 hpi (Figure 3-4B & C).



Figure 3-4: Western blot analysis of uninfected or LPAI H2N3 or LPAI H6N1 virus infected CEF cells.

Western blot analysis of CEF cell lysates using antibodies against the viral PB1 protein, Akt, and phosphorylated Akt (Ser473). PC=Positive control-Calyculin A treated Jurkat cell lysate expressing pAkt (CST #9902). A) Uninfected cell lysates in duplicate (denoted as U). CEF cells were infected with B) LPAI H2N3 and C) LPAI H6N1 virus at an MOI of 1. Cell lysates were prepared at 2, 6, 9 and 24 hrs post-infection (hpi).

3.4.3 Titration of effective dose of LY294002 or wortmannin for PI3K/Akt inhibition and cytotoxicity assessment

Involvement of PI3K/Akt pathway activation in viral replication was determined by inhibition of the pathway with known PI3K/Akt chemical inhibitors LY294002 (Arrowsmith et al., 2015) or wortmannin (McNamara and Degterev, 2011). The effective dosage of chemical inhibitors for complete abrogation of Akt phosphorylation was titrated on H2N3 virus (1MOI) infected CEF cells with a range from 1-100 μM concenterations of chemical. Cells were exposed to inhibitors two hours post infection (hpi) before harvesting the supernatants and cell lysates at 9 hpi. Abrogation of PI3K/Akt activity was observed with increasing concentrations of PI3K chemical inhibitor. However complete abrogation was observed at 20 μM LY294002 concentration as evidenced by the total loss of pAkt formation (Figure 3-5A).

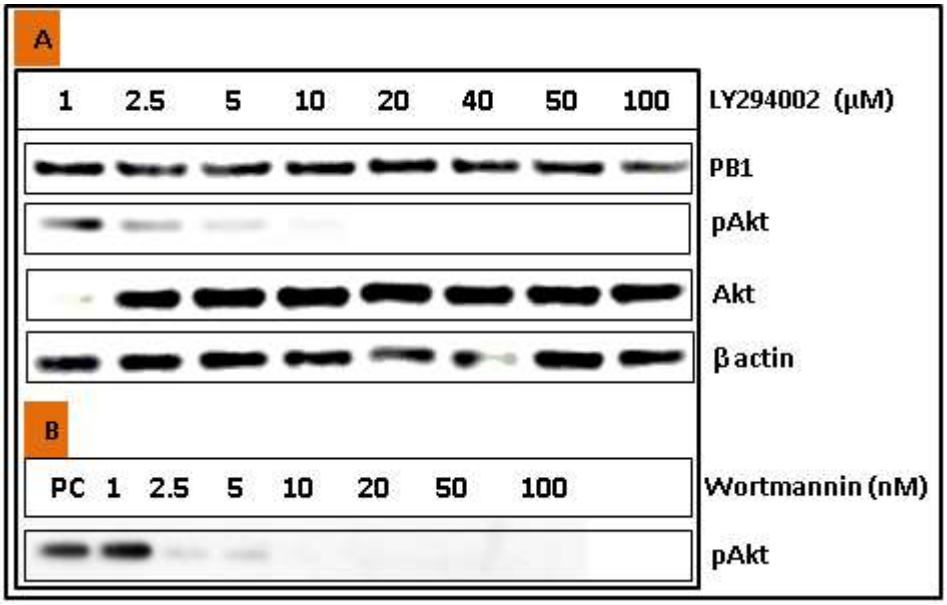


Figure 3-5: Titration of LY294002 and wortmannin dose for inhibition of the PI3K/Akt pathway.

Two hrs after infection with 1MOI of the H2N3 virus, CEFs were treated for 1 hour with (A) LY294002 at 1—100 μM or (B) wortmannin at 1—100 nM. Cell lysates were harvested at 9 hpi and analysed by western blot using antibodies against the viral PB1 protein, pAkt, Akt and beta-actin as a loading control.PC-H2N3 virus infected CEF cell lysate as a positive control.

Measurement of infectious virus output from supernatants obtained from representative inhibitor concentration (5-50 μM) treated cells revealed no significant differences in the infectious virus output between inhibitor and mock treated cells in 5 and 10 μM inhibitor concentrations (Figure 3-6). However, a significant ($P \leq 0.01$) reduction in virus output was observed in the supernatants originating from cells treated with 20–50 μM PI3K inhibitor concenterations compared to the mock treated cells (Figure 3-6).

Hence, the use of 20 μM dose of LY294002 as an effective dose for inhibition of PI3K activity pathway inhibition studies in the present chapter was decided based on the results of protein blotting that suggested a complete abrogation of PI3K activity at 20 μM

(Figure 3-5) and considering the results of virus titration assay that suggested 20 µM as the lowest concentration of LY294002 showing significant reduction in virus output (Figure 3-6) without deleterious cytotoxic effects on the cells. Wortmannin also showed similar inhibitory action but at further lower concentration of 10 nM (Figure 3-5B).

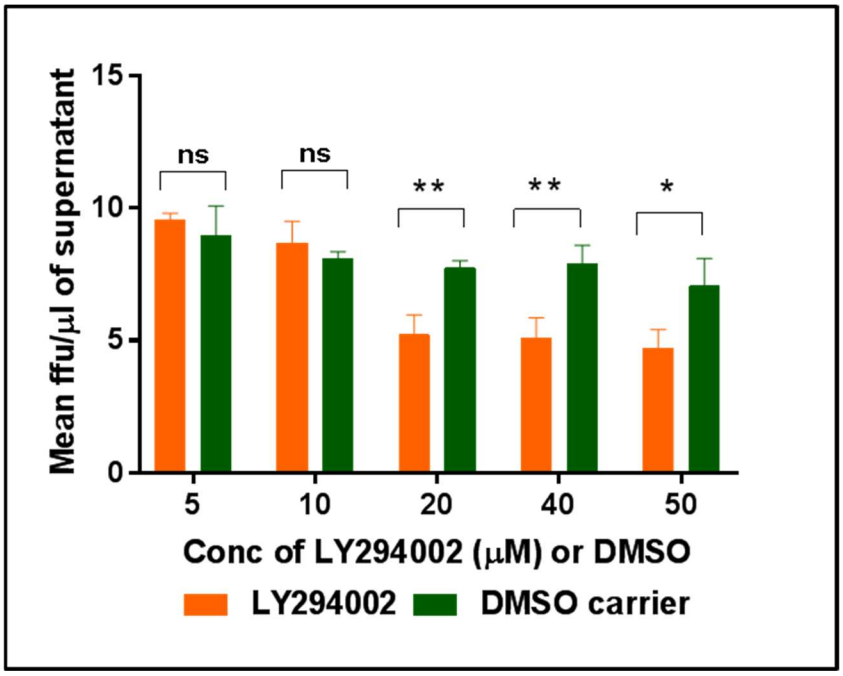


Figure 3-6: Titration of infectious virus output in supernatants derived from LY294002 treated CEF cells.
Confluent CEF cells were exposed to increasing concentrations of LY294002 for 1 hr, two hrs post-H2N3 virus infection at 1 MOI. Cell culture supernatants were harvested at 9 hrs post infection and titrated on MDCK cells. The mean focus-forming units per micro litre for triplicate wells are shown. Error bars indicate standard error of the mean (SEM). Statistical analysis was performed using two way ANOVA by multiple comparison of means. **=P ≤ 0.01.

The toxicity of LY294002 on CEF cells was measured by exposing the CEFs to the chemical inhibitor for one hour and measuring the metabolic activity of exposed cells by MTS assay (Promega) as per the manufacturer's protocol. The results of the MTS assay did not reveal any significant difference in mean

absorbance between 20uM LY294002 or vehicle-treated or the negative control cells at both 9 and 24 hrs post-treatment (Figure 3-7).

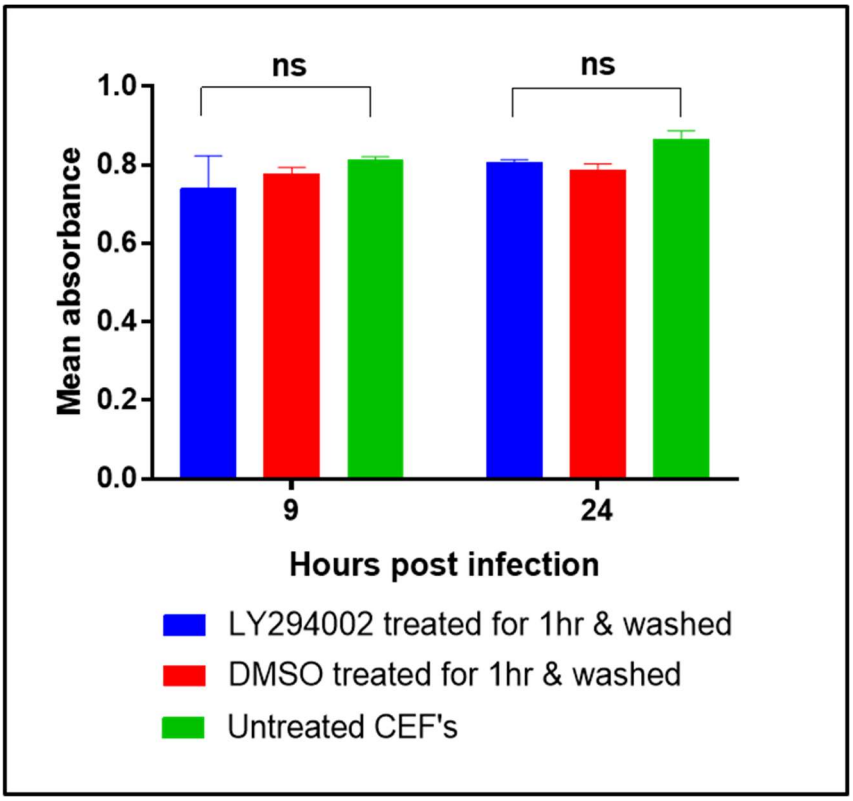


Figure 3-7: Measurement of cytotoxicity following treatment of CEF cells with 20 µM LY294002 chosen for inhibition of the PI3K/Akt pathway.

Confluent CEF monolayer cells were exposed to 20 µM LY294002 or an equivalent volume of DMSO carrier for one hour before washing three times with sterile 1X PBS and replenishing with fresh serum-free infection medium. MTS reagent was added at 9 or 24 hrs, and the absorbance was read at 490nm. Data derived is the mean absorbance of triplicate wells. Statistical analysis was performed using two way ANOVA by multiple comparison of means. Error bars indicate standard error of the mean (SEM). ns=non-significant.

3.4.4 Binding and entry of influenza A virus does not transiently activate the PI3K/Akt pathway

Transient activation of the PI3K/Akt pathway, facilitating virus entry in influenza virus infected cells, was determined by infection of CEFs with the H2N3 virus at 1MOI. Cell lysates were harvested at

10-min intervals for 60 min. Akt phosphorylation was not observed, despite the presence of native Akt protein (Figure 3-8).

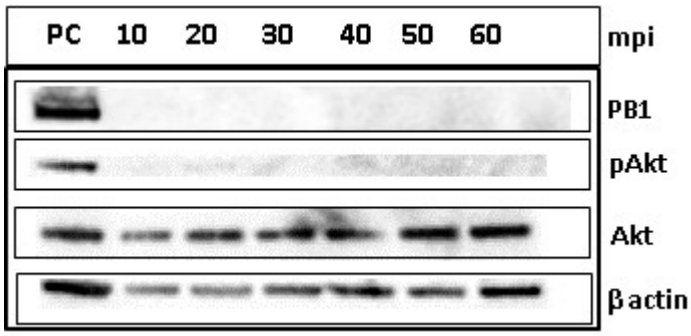


Figure 3-8: Protein expression profiling of LPAI H2N3 virus infected CEF cells up to 1 hour post-infection.
Western blot analysis of H2N3 virus infected (1MOI) CEF cell lysates harvested at every 10 minutes interval until 60 minutes post infection (mpi) and probed with rabbit primary and anti-rabbit secondary antibodies against the viral PB1 protein, Akt, and phosphorylated Akt (Ser473). β actin used as loading control. PC = positive control.

3.4.5 Influenza virus entry into cells is independent of PI3K activity

Involvement of PI3K pathway in virus entry into the host cell was determined by treatment of CEFs with 20 μM LY294002 one hour before H2N3 virus (1MOI) infection. Immunocytochemical staining of infected and fixed CEF cells was undertaken targeting influenza virus NP protein. Microscopy of immune stained cells revealed no evident differences in virus infectivity between inhibitor and carrier treated, infected cells. Based on visual impression, an equal and uniform distribution of influenza viral nucleoprotein stained (suggesting virus infection) cells was observed in inhibitor and carrier treated, infected cells at both 4 and 6 hpi (Figure 3-9). Virus titration from supernatants collected at 6 hpi on MDCK cells showed no significant differences in virus output between the LY294002 and DMSO (carrier treated) groups (Figure 3-10).

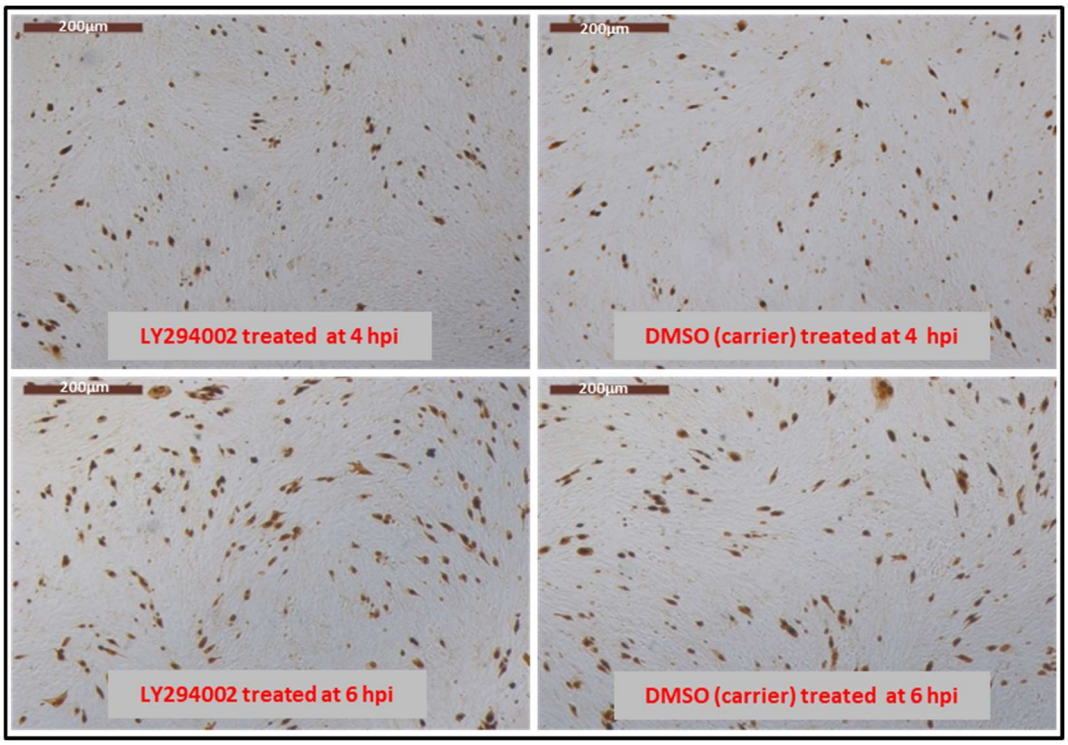


Figure 3-9: Immunocytochemical staining of CEF cells treated with LY294002 for one hour before H2N3 virus infection depicting comparable virus infectivity.

Confluent CEF cells were treated for 1h with either 20 µM LY294002 or an equivalent volume of DMSO then infected with the H2N3 virus at 1MOI1. The cells were incubated at 4 or 6hpi before fixing and probing with primary antibody against influenza A virus nucleoprotein (NP) and subsequent development with Dako kit (Dako). Images captured at 10X magnification and processed on Leica application suite.

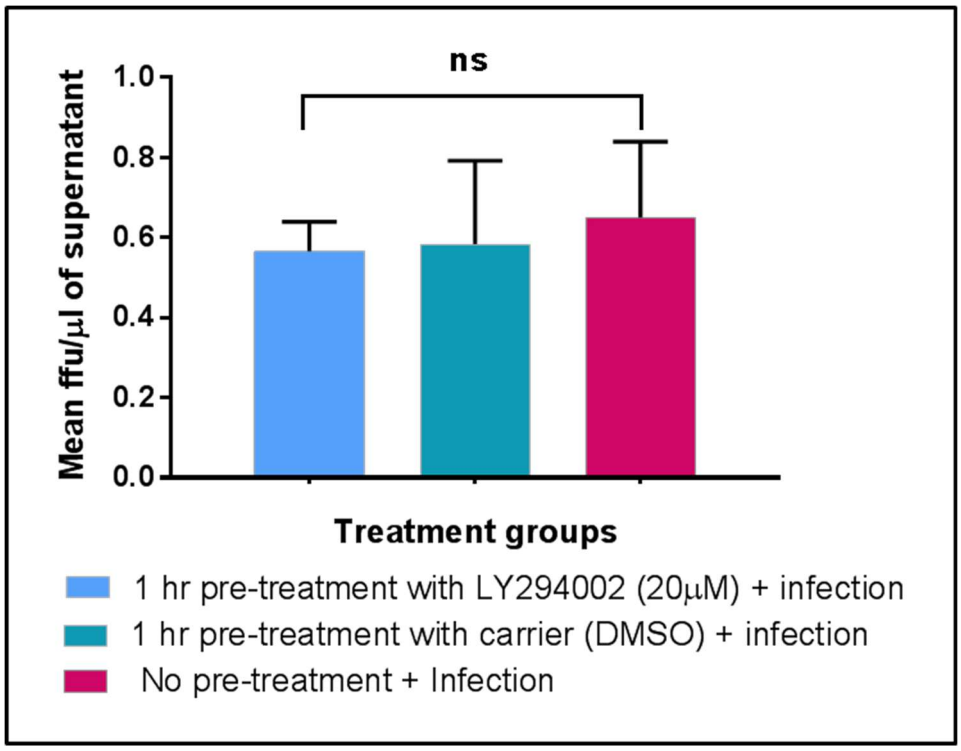


Figure 3-10: Titration of infectious virus in supernatants derived from CEF cells treated with LY294002 before H2N3 virus infection.
Chicken fibroblast cells were treated for 1h with either 20 µM LY294002 or an equivalent volume of DMSO or untreated then infected with the H2N3 virus at 1MOI. Supernatants were collected at six hpi and titrated on MDCK cells. The mean ffu per µl was derived from triplicate wells. Error bars indicate the standard error of the mean (SEM), ns= non-significant. Statistical analysis was performed using two way ANOVA by multiple comparison of means.

3.4.6 Post-infection inhibition of the PI3K/Akt pathway results in a significant reduction in infectious virus output in CEF cells

The effect of post-infection PI3K/Akt pathway inhibition on influenza H2N3 virus replication was determined by infecting CEF cells at 1MOI and titration of cell culture supernatants in MDCK cells. A time-dependent reduction in virus output was observed in the inhibitor-treated CEF cells. Pathway inhibition resulted in a reduction of virus output at 6, 9 and 24 hpi when compared to control groups. This decrease was significant at 6 ($P \leq 0.05$), 9 ($P \leq 0.0001$) and 24 ($P \leq 0.0001$) hpi (Figure 3-11).

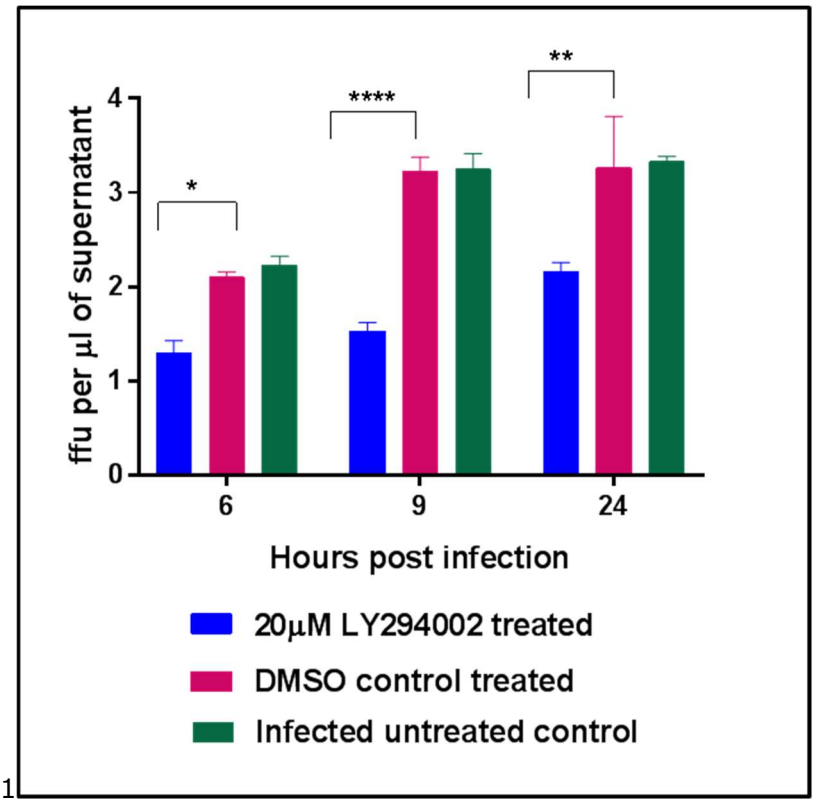


Figure 3-11

Figure 3-11: Effect of inhibition of the PI3K/Akt pathway on infectious virus output from infected CEFs.
Confluent CEF cells were infected with the H2N3 virus at 1MOI. Two hrs post-infection, cells were treated with 20 µM LY294002. Supernatants were collected at 6, 9 and 24 hrs post-infection and were titrated on MDCK cells. The mean focus-forming units per µl were derived from triplicate wells. Error bars indicate the standard error of the mean (SEM). Statistical analysis was performed using two way ANOVA by multiple comparison of means. *=P≤0.05, **=P ≤ 0.01,****=P ≤ 0.0001.

3.4.7 Influenza A virus infection does not induce the PI3K/Akt signalling pathway in DEF cells

The regulation of PI3K/Akt in DEF cells was established by protein expression profiling of lysates derived from either uninfected or H2N3 virus infected (1MOI) cells. Western blot results revealed the absence of phosphorylated Akt in both virus-infected and uninfected control cells at all four- time points observed. However, native Akt protein was detected in both infected and uninfected cells at all time points (Figure 3-12A & B). A time course dependent

increase in the accumulation of IAV PB1 protein was observed in infected cells (Figure 3-12B), confirming progressive infection of the cells (Figure 3-12B). Canonical stimulation of duck fibroblast cells with either 10 or 100 ng/mL IGF1 (insulin-like growth factor-1), resulted in activation of PI3K pathway as evidenced by phosphorylation of native Akt protein (Figure 3-12C)

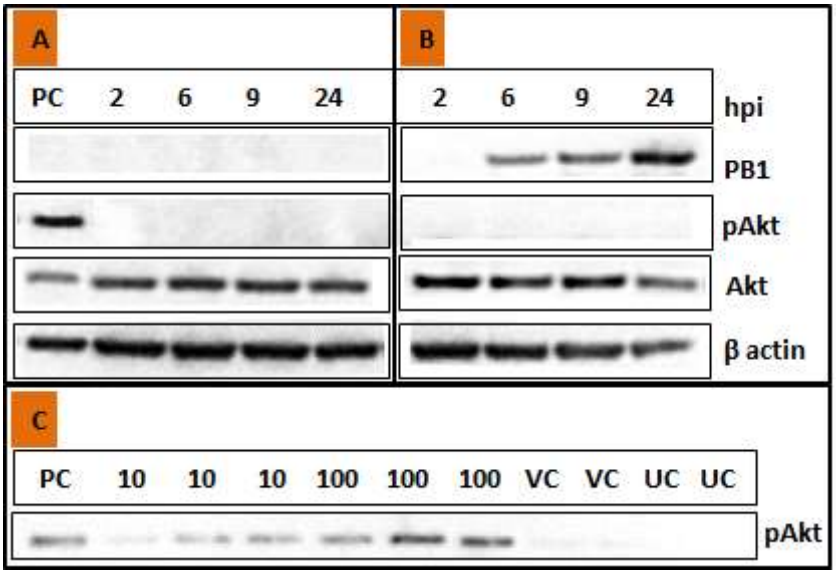


Figure 3-12: Western blotting to determine PI3K/Akt pathway regulation in DEF cells.
DEF cell lysates were subjected to western blot analysis probing with antibodies against the viral PB1, native Akt, and phosphorylated Akt (Ser473) proteins. A) Uninfected cells. B) Cells infected with LPAI H2N3 virus at 1MOI. C) DEF cells treated with IGF1 at 10 & 100 ng/ml in triplicate. VC=virus control, i.e. cells infected with the 1MOI H2N3 virus, UC= uninfected and untreated cells, both in duplicate. PC = positive control IGF1 stimulated DEF cell lysates expressing phosphorylated Akt (pAkt) protein.

3.4.8 PI3K/Akt inhibition leads to enhanced caspase-mediated apoptosis in H2N3 virus infected CEFs

Activated caspase-3/7 activity was measured following H2N3 virus infection with or without PI3K/Akt inhibitor (wortmannin) at different time intervals to determine whether apoptosis was regulated by PI3K in both chicken and duck fibroblast cells. Basal caspase activity in uninfected duck cells was significantly

(P<0.0001) higher compared to uninfected chicken cells notably at 48 hrs time point. Treatment of H2N3 virus infected (1 and 0.1 MOI) CEFs with wortmannin resulted in significantly ($P \leq 0.0001$) higher apoptosis induction compared to DMSO carrier treated and infected group at both 24 and 48 hpi (Figure 3-13A, B, C & D). On the other hand, H2N3 virus (1 and 0.1 MOI) infected DEF cells were completely unaffected by inhibitor treatment and showed a comparable apoptosis induction pattern with that of DMSO carrier treated cells at both 24 and 48 hpi (Figure 3-13A, B, C & D). Comparatively, H2N3 virus (1MOI) infected and inhibitor or DMSO carrier treated DEFs exhibited more pronounced apoptosis than infected and treated CEFs at both 24 and 48 hrs post-infection (Figure 3-13A&B). A comparable trend was also observed in H2N3 virus (0.1 MOI) infected cells (Figure 3-13C & D).

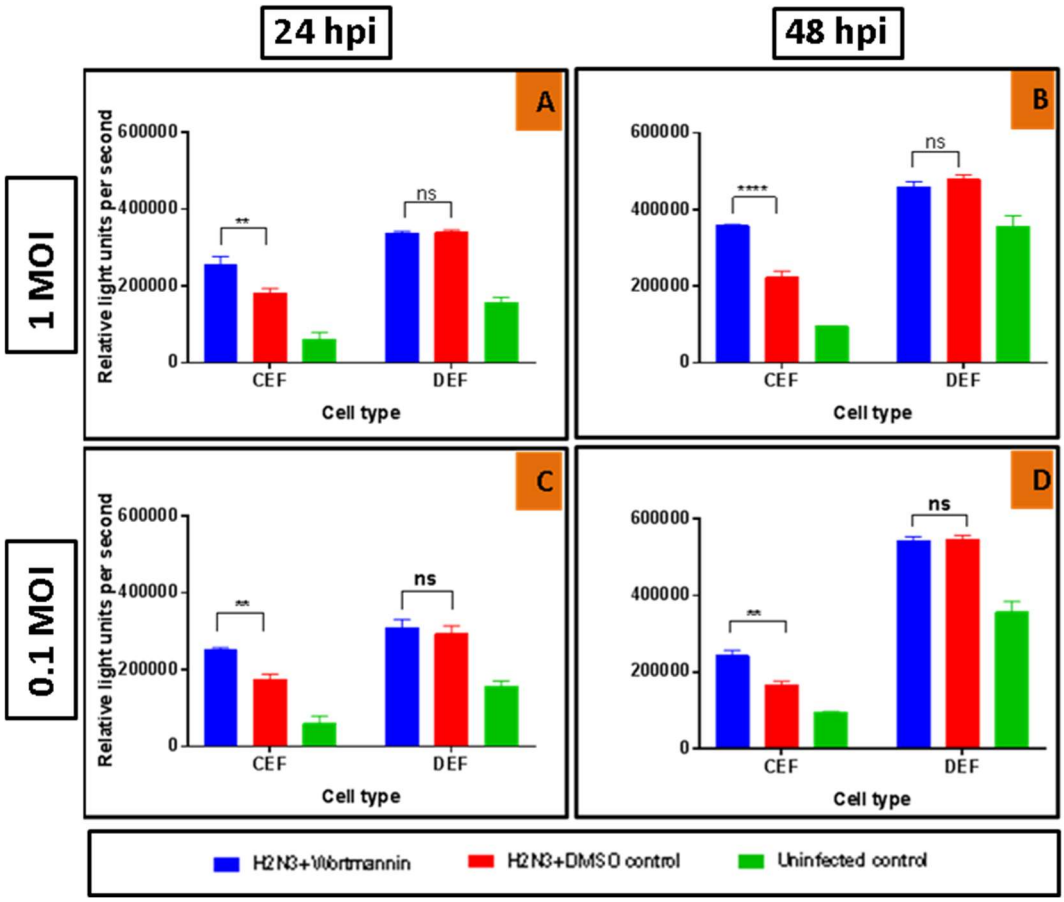


Figure 3-13: Measurement of activated caspase 3/7 activity in H2N3 virus infected or uninfected and PI3K inhibitor or carrier treated chicken and duck embryo fibroblast cells at 24 and 48 hpi.

The CEF and DEF cells were infected with H2N3 virus (1 & 0.1MOI) or uninfected and inhibitor (Wortmannin 10 nM) or carrier (DMSO, equivalent volume) treated before measuring activated caspase 3/7 activity (Caspase-Glo® 3/7 Assay, Promega). The data derived is the mean of triplicate wells. Error bars indicate the standard error of the mean (SEM). **-p ≤ 0.01,****-P ≤ 0.0001, ns=non-significant. Statistical analysis was performed using two way ANOVA by multiple comparison of means.

3.4.9 Chemical inhibition of PI3K activity leads to reduced cellular metabolic activity in H2N3 virus infected chicken embryo fibroblast cells

The cell proliferation or the metabolic activity of the H2N3 virus infected or uninfected CEFs and DEFs, with or without PI3K/Akt inhibitor (10nM wortmannin) was studied by addition of CellTiter 96® AQueous One Solution assay reagent after 24 or 48 hpi before recording the absorbance at 490nm with a 96-well plate reader. The

assay results suggested a marginal reduction in basal metabolic activity in uninfected CEF cells at 48-hour time point, compared to 24 hrs. While no apparent differences were observed in the metabolic activity of uninfected duck cells at both 24 and 48 hr time points. However, a comparison between uninfected CEF and DEF cells revealed significantly ($P<0.0001$) greater metabolic activity in duck cells over chicken cells at 48 hrs, while no obvious difference was observed at 24 hrs time point. A significantly ($P \leq 0.01$) reduced metabolic activity in H2N3 virus infected (1MOI), and inhibitor-treated CEFs was observed compared to DMSO carrier treated cells (Figure 3-14A and B). A similar trend of reduction in metabolic activity was evident following 0.1 MOI H2N3 virus infection and wortmannin treatment in chicken cells at both 24 and 48 hpi (Figure 3-14C & D).

Although the virus-infected DEF cells showed significantly reduced metabolic activity, compared to uninfected cells, there were no significant differences between H2N3 virus (1MOI) infected and inhibitor or carrier treated cells at both 24 and 48 hpi (Figure 3-14A & B). Duck cells infected with 0.1 MOI H2N3 virus also showed a similar trend as in 1MOI infected cells, irrespective of treatment type at both 24 and 48 hrs post-infection (Figure 3-14C & D).

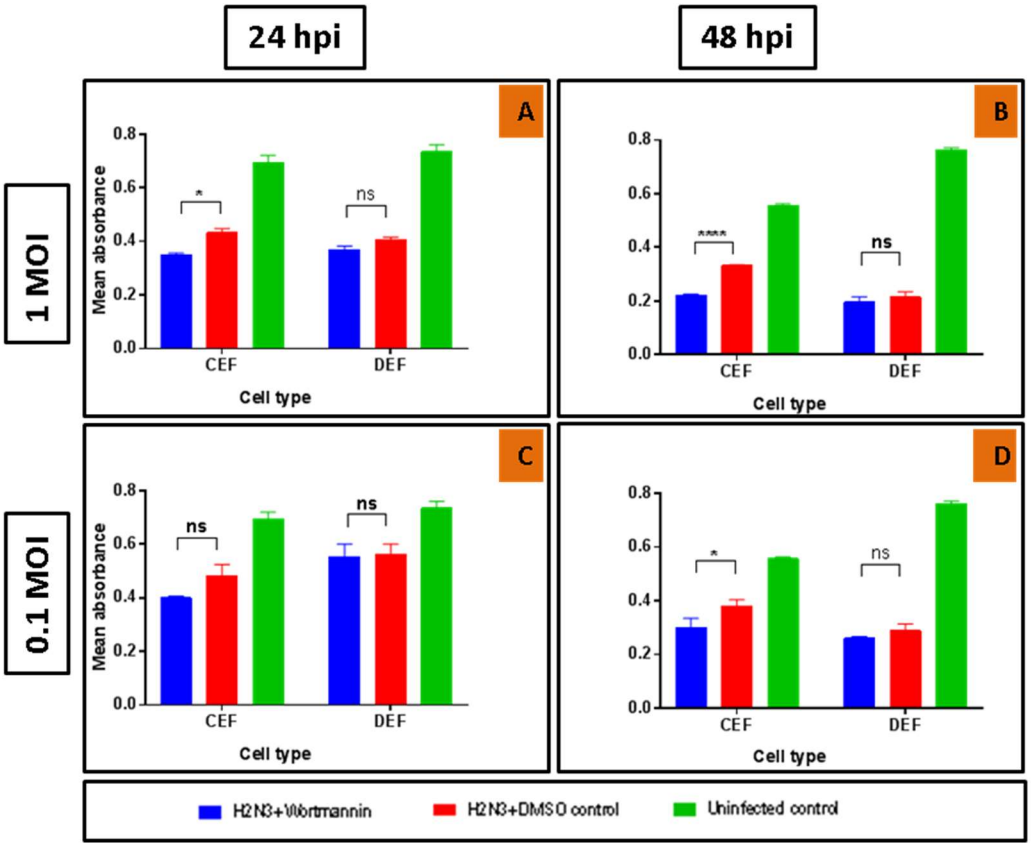


Figure 3-14: Measurement of cell metabolic activity in H2N3 virus infected or uninfected and PI3K inhibitor or carrier treated CEF and DEFs at 24 and 48 hpi.

The CEF and DEF cells were infected with H2N3 virus (1 & 0.1MOI) or uninfected and inhibitor (Wortmannin 10 nM) or carrier (DMSO, equivalent volume) treated before measuring cell metabolic activity (CellTiter 96® AQueous One Solution Assay, (Promega). The data derived is the mean of triplicate wells. Error bars indicate the standard error of the mean (SEM). *-p ≤ 0.05,****-P ≤ 0.0001, ns=non-significant. Statistical analysis was performed using two way ANOVA by multiple comparison of means.

3.4.10 Activation of the PI3K/Akt pathway was not observed in HD11 (chicken macrophage) cell line despite virus infection

The chicken macrophage (HD11) cell line was explored as an alternative model to CEF cells for the study of PI3K/Akt signalling pathway regulation. Protein expression profiling of healthy uninfected or H2N3 virus infected (1MOI) HD11 cell lysates harvested at 9 hpi, targeting Ser473 phosphorylated Akt protein was undertaken. Western blot results revealed the absence of

phosphorylated Akt in both virus-infected and uninfected control HD11 cell lysates. Although, native Akt protein was detected in both infected and uninfected control cells (Figure 3-15) the intensity of Akt protein was moderately reduced in H2N3 virus infected cells (Figure 3-15). IAV PB1 protein was detected in infected HD11 cells (Figure 3-15), confirming infection of the cells.



Figure 3-15: Western blot analysis of cell lysates derived from H2N3 virus infected or uninfected HD11 cells.
Western blot analysis of LPAI H2N3 virus infected (1MOI) or uninfected HD11 cell lysates (in triplicate) harvested in RIPA lysis buffer (Santa Cruz) at 9 hrs post infection (hpi), and probing with antibodies against the viral PB1, native Akt, and phosphorylated Akt (Ser473) proteins. PC = Cell lysate derived from H2N3 virus infected cells harvested at 9 hpi expressing phosphorylated Akt (pAkt) protein used as positive control.

3.4.11 The PI3K/Akt pathway is actively regulated in chicken tracheal organ cultures (TOCs)

The PI3K/Akt pathway regulation in the *ex-vivo* model was determined by using tracheal organ cultures (TOCs) harvested from 18 day-old chick embryos. The tracheal rings were infected with LPAI H2N3 virus at 1MOI or sham-infected with sterile PBS and incubated for specified time points before harvesting the protein lysates for western blot analysis targeting Ser473 phosphorylated Akt protein. Western blot results revealed the phosphorylation of Akt in both virus-infected and uninfected TOCs lysates as evidenced by detection of pAkt protein in the lysates (Figure 3-16). However,

slight reduction in the intensity of pAkt was observed in H2N3 virus infected cells compared to uninfected cells (Figure 3-16). IAV PB1 protein was detected at 9 and 24 hpi in infected cells (Figure 3-16), confirming active virus infection of the cells.

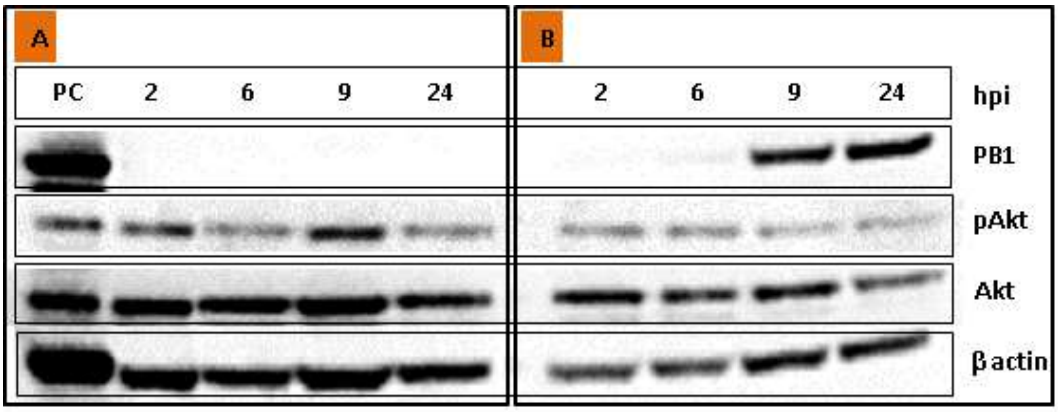


Figure 3-16: Western blot analysis of H2N3 virus or uninfected chick embryo tracheal organ cultures.
Western blot analysis of H2N3 virus infected (1MOI) or uninfected TOCs lysates harvested at 2, 6, 9 and 24 hpi in RIPA lysis buffer and probed with antibodies against the viral PB1, native Akt, and phosphorylated Akt (Ser473) proteins. (A) Uninfected TOCs samples, (B) H2N3 virus (1MOI) infected TOCs lysates collected at different time points as indicated. β actin is shown as the loading control. PC = positive control.

3.5 Discussion

3.5.1 Activation of the PI3K/Akt in CEF and DEF cells

The PI3K dependent downstream effector kinases influence diverse cellular functions upon activation (Vanhaesebroeck et al., 1997a). The present study demonstrated the activation of the PI3K/Akt pathway in AIV infected CEF cells as evidenced by the Akt phosphorylation at serine 473 (Ser473) site that is essential for full activation of Akt and is strictly PI3K mediated (Alessi et al., 1996). H2N3 or H6N1 virus mediated PI3K/Akt pathway activation is in cognisance with the previous studies that observed IAV mediated pathway activation in mammalian cells (Ehrhardt et al., 2006, Hale et al., 2006, Shin et al., 2007c, Zhirnov and Klenk, 2007). These observations suggest a possible similarity in PI3K/Akt pathway activation kinetics in IAV infected mammalian and chicken cells. However, a solitary observation by Ehrhardt et al. (2006) revealed transient activation of the PI3K/Akt pathway in PR8 virus infected MDCK and A549 cells soon after infection potentially facilitating PI3K mediated virus internalisation through lipid raft formation (Eierhoff et al., 2010). In sharp contrast, this study found no evidence of transient activation in AIV infected chicken cells. One potential explanation for this difference could be inherent differences in the pathway activation kinetics between mammalian and avian cells. Another potential reason could be the differences in the shapes of

IAVs used in the two studies. Mammalian origin IAVs like PR8 virus an highly lab adapted strain used by Eierhoff et al. (2010) tend to be more spherical in architecture and may need PI3K activation for clathrin-mediated endocytosis, while avian-origin viruses like the H2N3 virus used in the present study are moderatly spherical and may enter the host cell through PI3K independent micropinocytosis. The multiplicity of infection is a good measure of infectivity ratio between the virus and the infecting host cells a crucial factor for establishing infection. Several studies indicated the use of 1:1 ratio between virus and cells as used in this study. The findings in the present study are similar to that of Shin et al. (2007b) who also used similar MOI as in the present study. The amount of virus used for cell infection varied considerably between present study (1MOI) and Ehrhardt et al. (2006) who used a higher dose of virus (5 MOI) and concluded biphasic PI3K activation that was not observed in the present study.

3.5.2 Effect of PI3K/Akt activation on virus propagation

The present study observed significantly higher infectious virus output from infected CEF cells compared to duck cells, a consistent feature that was observed previously by Kuchipudi et al. (2012a) and Al-Mubarak et al. (2015). Since the PI3K/Akt pathway activation was observed only late in IAV infection cycle, it was assumed that the activation was virus replication dependent. The contributions of the PI3K/Akt pathway was studied by chemical

inhibition with either LY294002 or Wortmannin. A final concentration of 20 μM LY294002 or 10 nM Wortmannin used in the present study was similar to that employed in previous studies to achieve similar inhibitory effect hence the inhibitor dose titration was in accordance with previous findings (Hui and Nayak, 2002, Shin et al., 2007b). However, Zhirnov and Klenk (2007) evidenced slightly lower dose of 10 μM for treating MDCK cells to study effect on PI3K mediated apoptosis regulation. Chemical inhibition of PI3K/Akt pathway resulted in significant reduction in progeny virus output from IAV infected chicken cells. A similar trend that is observed and consistent with studies in mammalian cells (Ehrhardt et al., 2006, Hale et al., 2006, Shin et al., 2007b, Zhirnov and Klenk, 2007). The results of the present study indicate a clear evidence towards the "pro-viral" behaviour of the PI3K/Akt pathway in CEF cells and complement similar observations from mammalian experiments.

3.5.3 IAV infected duck cells exhibited no evidence of PI3K/Akt activation

In contrast to the observations made in chicken cells, protein expression profiling of duck fibroblast cells revealed no signs of PI3K/Akt induction, despite similar virus output in both infected chicken and duck cells at 6 and 9 hpi. However, IGF-1 mediated induction demonstrates physiological induction of the pathway. Although not much literature is available, present results may be compared to a similar study that showed PI3K/Akt activation in

follistatin treated duck myoblast cells (Li et al., 2014). This suggests intrinsic activation of the pathway upon specific stimuli, but influenza A viruses fail to induce activation. Hence, results of this study demonstrate differential regulation of the PI3K/Akt pathway in influenza A virus infected chicken and duck primary fibroblast cells.

3.5.4 Apoptosis regulation in IAV infected CEF and DEF cells

The results of present study indicate virus mediated PI3K induction and inhibition of same resulted in significant reduction in the virus titre in CEF cells. It is crucial to know the cellular function/s affected by PI3K/Akt inhibition in chicken cells that are of consequence to IAV replication. Recent studies have suggested that influenza viruses avert apoptosis leading to prolonged cellular survival and higher virus propagation in mammalian cells (Ehrhardt and Ludwig, 2009). Rapid apoptosis induction was observed in AIV infected duck cells compared to chicken cells (Kuchipudi et al., 2012a). The results of the present study reveal significantly higher caspase activity upon inhibition of PI3K/Akt in IAV infected chicken cells compared to control groups, suggesting a critical role of activated PI3K/Akt in controlling cellular apoptosis that helps in cell survival and possibly results in higher virus output. These findings are in agreement with similar observations made in IAV infected MDCK or A549 cells, which exhibited progression of cell cycle upon PI3K activation hence limiting apoptotic activity (Ehrhardt et al., 2007a, Aguirre et al., 2007, Zhirnov and Klenk, 2007, Ji and Liu,

2008, Ehrhardt and Ludwig, 2009, Lu et al., 2010). In contrast, the duck cells showed no difference in the caspase activity between PI3K inhibitor-treated or control groups possibly because of the absence of PI3K/Akt activity. Results of the present study suggested duck cells manifested robust apoptotic cell death compared to chicken cells, a finding that complements observations by Kuchipudi et al. (2012a). A corresponding time and virus dose-dependent reduction in cellular metabolic activity was observed in IAV infected chicken cells. In summary, the results of caspase assay suggest that activation of PI3K/Akt tightly regulates caspase-mediated apoptosis in IAV infected chicken cells. A possible lack of upstream regulatory control mechanism could be the reason for observing higher caspase activity in AIV infected duck cells.

A higher basal metabolic activity and apoptotic cell death were observed in uninfected duck cells compared to uninfected chicken cells. The comparable results obtained from two independent batches infected with 0.1 and 1MOI H2N3 virus, suggested the existence of a more rapid cellular turn over in duck cells than chicken cells, as evidenced by pronounced caspase activity that is compensated by increased proliferation rate. Albeit this observation contradicts with the findings of Kuchipudi et al. (2012a) who observed near similar caspase activity in both uninfected CEFs and DEFs. A simple batch to batch variations in the primary chicken and duck cells may also be responsible for this difference.

3.5.5 Evaluation of continuous cells and ex-vivo organ culture models for study of PI3K/Akt activation

Primary cells, although they have advantages over transformed continuous cell lines as they mimic near similar cellular characteristics from which they are derived, also pose several growth challenges and are at times difficult to grow and work with. Hence, chicken macrophage (HD11) cell line was examined to explain the activation of the PI3K/Akt pathway as an alternative as they are more convenient to use in further studies to explore IAV interaction studies. The results demonstrated lack of PI3K activity despite H2N3 virus infection in HD11 cells. An earlier study by Bhat et al. (2010) observed activation of the pathway in CpG ODN (CpG oligodeoxynucleotides) treated HD11 cells. It is likely that CpG ODN treatment induces PI3K/Akt activation in HD11 cells, while IAV infection may not induce pathway activation. A similar study with swine-origin influenza H3N2 virus also failed to activate PI3K/Akt in porcine alveolar macrophages (Delgado-Ortega et al., 2014). These observations suggest cell type specific differences in the regulation of PI3K/Akt, a potential prospective future work.

Tracheal organ cultures (TOCs) have long been used in the study of virus pathogenesis and vaccine research as these were considered as the most relevant *ex-vivo* models especially for the study of respiratory viruses. TOC cultures were employed in the identification of single-nucleotide polymorphisms (SNPs) following

in-vitro TOCs infection with live infectious bronchitis vaccine (IBV) virus (Ball et al., 2016) or *in-vivo* in broiler chickens (Ball et al., 2017). Equine TOCs were used as a tool to study equine influenza viruses (Lin et al., 2001a). Protein expression profiling targeting pAkt in H2N3 virus infected TOC cultures derived from 18-day old chick embryos in the present study revealed activation of the PI3K/Akt in both virus infected and uninfected control groups. A logical explanation for pan PI3K activated status in TOCs may be due to the involvement of the PI3K in a wide array of crucial cellular developmental functions like differentiation and proliferation in rapidly developing embryonic tissues. A sheer mechanical damage during the preparation of TOCs may also have been a trigger point for regenerative or tissue repair oriented PI3K activation. However there is no literature that supports this hypothesis.

3.5.6 Conclusions

The present study revealed a conclusive evidence for AIV dependent PI3K/Akt pathway activation in virus infected CEF but not in DEF cells, potentially suggesting a differential PI3K/Akt pathway regulation between chicken and duck cells. Inhibition of PI3K/Akt pathway in infected chicken cells resulted in significant reduction in progeny virus titres signifying a "pro-viral" role. PI3K/Akt phosphorylation inhibition of pro-apoptotic factors like caspases and beclin-2 associated death promotors (BAD) by PI3K mediated activated effector kinase Akt could potentially be the underlying

mechanism for progression of cellular survivability leading to higher infectious virus production in infected chicken cells. In contrast, lack of PI3K/Akt activity may compel early induction of apoptosis in IAV infected duck cells leading to confinement of cellular virus spread.

Although a fair understanding of PI3K/Akt activity in chicken and duck cells was achieved in the present study, identifying the crucial host factors that are responsible for activation of the PI3K/Akt pathway in IAV infected chicken cells and the possible reasons for differential regulation of pathway between chicken and duck cells need further investigation. A possible rational approach would be to undertake a PI3K/Akt regulatory specific comparative transcriptomic expression analysis that may shed some light on the basis for differential PI3K/Akt regulation in chicken and duck cells.

Albeit, a transcriptional analysis for study of PI3K/Akt signalling pathway is an approach of lowered preference. However, advantage of availability of a large scale transcriptional expression data originated from equivalent cell types and involving similar viruses (in the present scenario, chicken or duck primary lung cells infected with H2N3 virus) may well be considered as a preferred approach for species wide comparative analysis to gain deeper transcriptional level understanding that may help in speculating and identifying distinct phenotypic dissimilarities observed. In the present study, it was opined to undertake CEF and DEF comparative transcriptional analysis to gain insights into identify probable

reasons for differential PI3K/Akt pathway activation between chicken and duck cells.

Chapter 4. Transcriptomic insights into the interplay of PI3K/Akt pathway, actin remodelling and AIV morphogenesis

4.1 Introduction

4.1.1 Deciphering functional genomics knowledge from transcriptome data of IAV infected avian lung cells

Synchronous measurement of expression abundance of thousands of genes or a cluster of genes provides novel insights that can describe the relationship between changes to the host transcriptome and its phenotypical behaviour. Use of publicly available gene expression data can be a quick and effective way to understand the PI3K/Akt pathway regulation dynamics. A comparative analysis of transcriptome data from five different breast cancer cell lines was used to identify the gene expression pattern upon ribosomal protein S6 kinase beta-1 (p70S6K) suppression or PI3K/Akt pathway inhibition (Heinonen et al., 2008), suggesting transcriptome data analysis as a valid approach for large scale PI3K/Akt pathway specific gene expression analysis. Transcriptional profiling of infectious bursal disease virus (IBDV) infected DT40 cells (chicken B cell line) was recently carried out to identify the underlying molecular mechanisms of immunosuppressive IBDV pathogenesis (Quan et al., 2017).

The objective of the present study was to investigate the underlying molecular mechanisms for differential PI3K/Akt activation in IAV infected chicken and duck cells, and to evaluate the influence of PI3K/Akt related gene cluster expression on cytoskeletal actin

remodelling and IAV morphogenesis. To this end, a customised analysis of previously published microarray expression data from avian influenza virus infected chicken and duck cells from Kuchipudi et al. (2015) was performed. Influenza A virus morphogenesis in chicken and duck fibroblast cells was studied by Al-Mubarak et al. (2015); the findings revealed budding of elongated virion particles from duck cells while chicken cells produced roughly spherical particles. Gene segment sequence analysis revealed no differences in any of the viral segments produced from both chicken and duck cells. Cytoskeletal actin was initially thought to be responsible for this morphological difference. However, chemical disruption of actin revealed no morphological changes in the budding virus. Therefore, it was speculated that host cellular factors other than actin responsible for differences in the morphology of budding virus in chicken and duck cells.

4.1.2 High throughput gene expression profiling

Modern high throughput gene expression techniques like DNA microarray and Next Generation Sequencing (NGS) allow simultaneous screening of the entire transcriptome regulation. The fundamental principle of the microarray is DNA hybridisation, two strands of DNA hybridise if they are complementary to each other, a standard Watson–Crick model (Knudsen, 2004). In a microarray, thousands of small strings of gene-specific DNA (probes) are attached to an inert surface to form an array. The reverse

transcribed mRNA from cells or tissues is usually labelled with a fluorescent dye and hybridised on to the array. Laser induced-fluorescent imaging quantifies the amount of fluorescence generated. The amount of fluorescence generated at each specific location on the array directly corresponds to the amount of matching complementary mRNA sequence in the sample analysed and is taken as the level of expression of a particular gene (Knudsen, 2004). High throughput gene expression technologies are frequently used in clinical research for comparing the pattern of gene expression among different subjects or between specific clinical conditions. Comparative gene expression analyses have more recently been employed in dissecting the molecular mechanisms involved in health and disease (Aguan et al., 2000). For example functional gene expression analysis of glioma stem cells and glioblastoma samples revealed overexpression of PI3K/Akt pathway-related genes (Vastrad et al., 2017).

4.1.3 Avian specific transcriptomic studies

Completion of the chicken genome project (International Chicken Genome Sequencing, 2004) showed considerable differences in the genetic constitution between birds and other vertebrates. Ducks, which harbour most IAVs as the primary reservoir, diverged from chickens and other gallinaceous species nearly 90–100 million years ago (Hackett et al., 2008). The first avian-specific functional genomic microarray was developed by Keeler et al. (2007), which

predominantly included genes related to innate immune pathways. Infection of tracheal epithelial cells (TECs) with two H5N1 virus subtypes revealed differential transcriptomic expression of innate immune-related genes between chicken and duck TECs as early as 6 hours post-infection. Although both chicken and duck TECs supported virus replication, differences in virus replication kinetics was observed between the two species. Chicken TECs produced higher titres of infectious virus than duck TECs (Sarmento et al., 2008). A study by Crowley et al. (2009) validated the use of a chicken-specific microarray for the study of gene expression profiles in other avian species by cross-species hybridisation. Huang et al. (2013) have undertaken a detailed transcriptomic expression analysis of H5N1 virus infected duck lung tissues and proposed that increased expression of β-defensin and butyrophilin-like repertoires could explain the basis of influenza virus resistance in ducks. Gene expression following IAV infection could be different based on the virus subtype and the host species involved. For example, infection of Pekin ducks with chicken, turkey or duck origin low pathogenicity H7 virus subtypes resulted in unique host response signatures against each virus. In contrast, 12 core genes associated with immune-related pathways (RIG-I, NOD, TLR) were differentially expressed in AIV infected ducks compared to chicken and turkey irrespective of species of origin of influenza H7 subtype viruses (Maughan et al., 2013). Microarray global gene expression analysis

showed that the viral PA-X protein dampens the host response by downregulating inflammatory and cell death associated genes to H5N1 infection in mice, chicken and ducks (Hu et al., 2015). A global gene expression of influenza virus infected chicken and duck primary lung cells revealed higher induction of immune-related genes in two HPAI H5N1 and LPAI H2N3 virus infected chicken compared to duck cells (Figure 4-1). Key genes were shown to be downregulated in chickens while they were unaffected in duck cells (Kuchipudi et al., 2014, Kuchipudi et al., 2015).

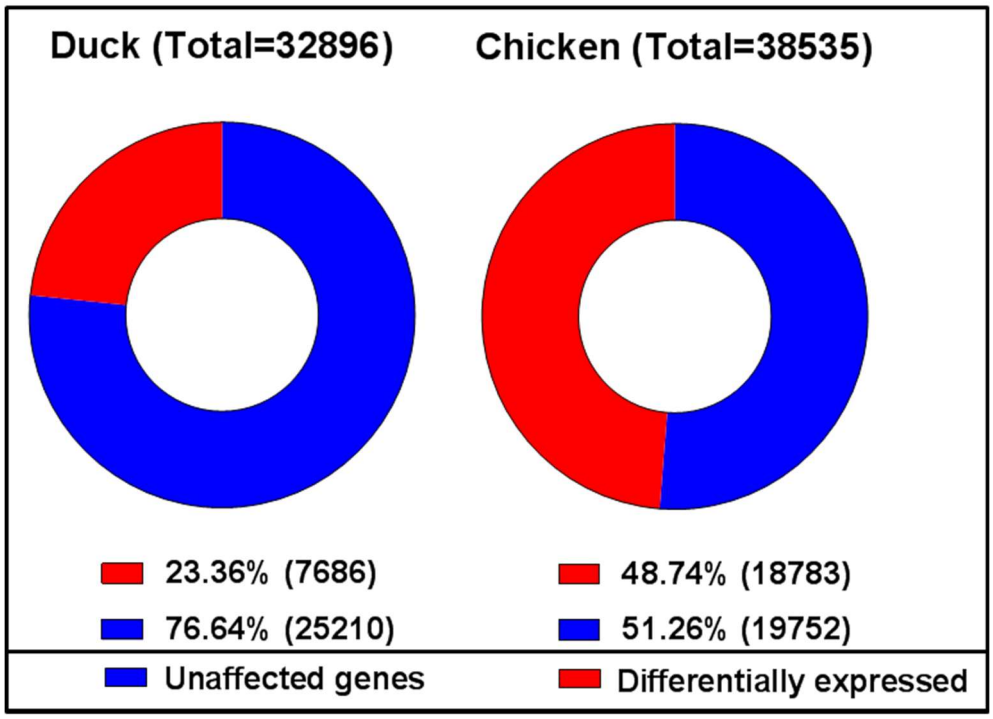


Figure 4-1: Combined global gene expression pattern in IAV infected primary chicken and duck lung cells.

Infection of chicken and duck lung cells with two HPAI H5N1 (H5N1-tyEng91 and H5N1 tyTR05) and an LPAI H2N3 virus subtypes demonstrated significant ($P < 0.05$) differential expression among transcripts. Chicken lung cells showed upregulation 48.74% (18783 of 38535) of genes compared to duck lung cells with only 23.36% (7686 of 32 896) at 24 hpi. The pie (doughnut) diagrams were generated using data points from Kuchipudi et al. (2014).

4.1.4 IAV mediated PI3K/Akt activation and apoptosis

PI3K/Akt are a significant class of enzymes predominantly stimulated by insulin and insulin-like growth factor receptors (GFRs) such as fibroblast growth factor receptor 1 (FGFR1), insulin-like growth factor 1 receptor (IGF1R) and epidermal factor receptors (EGFRs) (Ma et al., 2015) resulting in the activation of pathway. IGF1 stimulation of salivary acinar cells (C5) resulted in PI3K/Akt dependent apoptosis suppression. Further IGF1 and EGF treatment synergised PI3K/Akt mediated anti-apoptotic activity (Limesand et al., 2003), suggesting a significant contribution of growth factors and their associated members in PI3K/Akt pathway mediated apoptosis regulation. Influenza A viruses have been shown to activate PI3K/Akt as a strategy to slow down apoptotic cell death (Figure 4-2), increasing cellular survivability probably resulting in enhanced virus replication (Ji and Liu, 2008). Infection of A549 cells with PR8 virus resulted in virus mediated induction of PI3K/Akt which inhibited Bax (bcl-2-like protein X), a cytoplasmic pro-apoptotic factor, to help efficient virus replication (Lu et al., 2010). We hypothesised that duck cells exhibit inherent passive apoptosis activation by negative regulation of PI3K/Akt resulting in rapid apoptosis induction, however this needs to be elucidated.

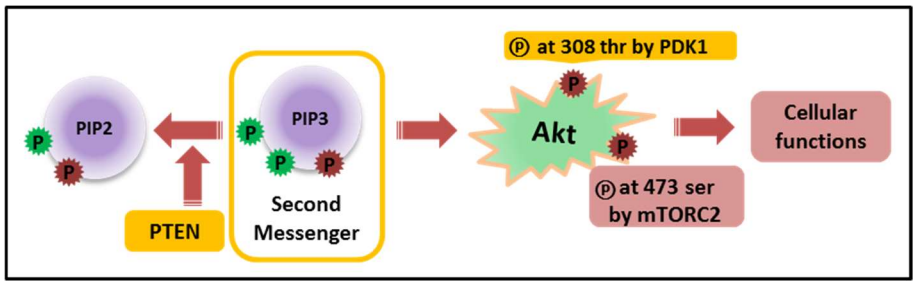


Figure 4-2: Regulation of PI3K activation by PTEN and PDK1.

Activation of the PI3-kinase involves formation of phosphoinositide (3,4,5) trisphosphate (PI(3,4,5)P3) a second messenger molecule that activates Akt by phosphorylation at threonine 308 (Thr308) in the activation loop by the protein kinase PDK1, and at serine 473 (Ser473) in the C-terminal hydrophobic motif by the mTORC2 complex. The whole cascade of activation can be dysregulated at multiple steps, by PTEN by dephosphorylating PIP3 to PIP2 and by lowered expression of PDK1 there by abolishing Akt phosphorylation.

4.1.5 PI3K/Akt role in cytoskeletal actin remodelling

PI3K/Akt is an important cytoskeletal actin remodelling regulator, aiding in cellular polarity and mobility through actin filament polymerisation (Cain and Ridley, 2009). The discrete actin fibres assist cells in adhesion to the substratum, maintaining the shape and generating the contractile force required for pseudopodial mobility (Hall, 1998). Inhibition of PI3K/Akt showed abolition of insulin-induced actin remodelling resulting in membrane ruffle formation (Tsakiridis et al., 1999, Khayat et al., 2000). The litrature suggests importance of insulin-induced small Rho GTPases Cdc42 (Cell division control protein 42 homologs) and RAC1 (Ras-related C3 botulinum toxin substrate 1) in actin remodelling through PI3K/Akt mediated activation (Defilippi et al., 1999, Tsakiridis et al., 1999). The PI3K/Akt dependent actin remodelling was demonstrated in healthy chicken fibroblast cells by Qian et al. (2004). It was shown

that influenza viruses directly interact and suppress RAC1 expression facilitating virus replication (Jiang et al., 2016). Endocytosis of adenovirus was shown to be dependent on cytoskeletal actin reorganisation through activation of Rho GTPases (Li et al., 1998). Latent membrane protein 1 (LMP1) of Epstein-Barr virus induces actin filament reorganisation through PI3K/Akt activation (Dawson et al., 2003). Cytoplasmic trafficking of viral segments from the nucleus is mediated through CRM1 (chromosome region maintenance one protein) dependent nuclear pore complex (NPC). Inhibition of CRM1 has been shown to affect trafficking efficiency, resulting in nuclear retention of vRNP in infected cells (Elton et al., 2001). PI3K mediated Ran-binding protein 3 (RanBP3) is a Ran-interacting protein that is a cofactor for CRM1. Hence, inhibition of RanBP3 also has been shown to affect influenza A viral segment trafficking resulting in nuclear retention of vRNP (Predicala and Zhou, 2013), impling the significance of CRM1-Ran proteins in viral cargo trafficking in IAV infected A549 cells.

The role of FAK (focal adhesion kinase) a non-receptor cytoplasmic tyrosine kinase in influenza virus entry was studied by Elbahesh et al. (2014) who observed localisation of the virus at the cell periphery, and at later stages disrupted viral RNA replication leading to significant reduction in virus output upon FAK inhibition, suggesting a novel role of FAK as a central link between receptor-mediated PI3K activation and actin remodelling in IAV infected cells.

It is evident based on the existing literature that PI3k/Akt is an important regulator of cytoskeletal actin reorganisation. Since there are striking differences in the PI3K/Akt pathway activation between chicken and duck cells observed in the present study. It is important to investigate the underlying molecular basis for the differential PI3/Akt activation through functional clustering and comparative analysis of large-scale microarray expression data.

4.2 Aims and objectives

4.2.1 Aims

To evaluate expression of PI3K/Akt pathway related genes in H2N3 virus infected chicken and duck lung cells and their functional relevance in actin remodelling and virus morphogenesis.

4.2.2 Objectives

1. To analyse publicly available DNA microarray expression data (accession# GSE 33389) to investigate the transcriptional pattern of genes associated with the activation and effector function of PI3K/Akt pathway.

2. To analyse the transcriptional regulation of genes associated with cytoskeletal actin remodelling in H2N3 virus infected chicken and duck lung primary cells.

3. To determine the effect of PI3K/Akt pathway inhibition on cytoskeletal actin-remodelling in H2N3 virus infected chicken and duck cells by immunofluorescence (IF) and to study virus morphogenesis by electron microscopy (EM).

4.3 Materials and Methods

4.3.1 Microarray experimental design and data processing

The complete laboratory experiments involving cell preparation, virus infection and preparation of samples for microarray experiment, the acquisition of microarray expression data and submission of the microarray data to the public domain National Center for Biotechnology information (NCBI) was carried out by Suresh V Kuchipudi at the School of Veterinary Medicine and Science, University of Nottingham as outlined in Kuchipudi et al. (2015) in a study titled 'DNA microarray global gene expression analysis of influenza virus-infected chicken and duck cells'. However, for the ease of reference, excerpt of experimental protocols from Kuchipudi et al. (2015) have been outlined here briefly, primary lung cells were infected or mock infected with avian LPAI H2N3 (A/mallard/duck/England/7277/06) virus at multiplicity of infection (MOI) of one or with sterile PBS, respectively. Cells from both infected and mock infected wells were lysed using RLT plus buffer (Qiagen) for total RNA extraction at 24 hpi following the manufacturer's instructions. The transcriptomic data generated was submitted to NCBI gene expression omnibus (GEO) data repository and is publicly available with accession number GSE33389 (https://www.ncbi.nlm.nih.gov/geo/query/acc.cgi?acc=GSE33389).

4.3.2 Transcriptomic data analysis and interpretation

In the present study, the microarray expression data with accession number GSE33389, freely available from public domain NCBS GEO was downloaded and analysed based on the set objectives of the present study. My profound thanks to my supervisor for sending me to Earlham Institute, Norwich to obtain training on the basic bioinformatics skills and knowledge that helped me to plan and execute microarray data analysis in the present chapter. I am also indebted for the kind support from Tania Dottorini, Assistant Professor in Bioinformatics, Faculty of Medicine & Health Sciences, University of Nottingham and Sankalp Arya, bioinformatics PhD student, School of Biosciences University of Nottingham, in writing and execution of R scripts for analysis of microarray data. The microarray expression data was analysed using 'R' (build 3.3.1) Bioconductor (V3.4) The core Bioconductor algorithms including necessary library packages essential for the analysis of raw transcriptomic data, these library packages were installed locally before execution. The data analytical command line scripts were run through R studio (1.1.383), an integrated development environment interface (IDE) for R. The Robust Multichip Averaging (RMA) probe summarisation algorithm described previously (Irizarry et al., 2003a, Irizarry et al., 2003b) allowed for background correction and normalisation of the data.

Comprehensive annotation of normalised data yielded log expression values of over 33000 transcripts.

Generation of Heat maps for visual interpretation; The normalised, annotated log expression values were exported to an excel sheet for selection of PI3K/Akt specific genes and clustering of these selected genes based on their Akt upstream or downstream effector functions according to the objectives of the study. The mean log expressions from duplicate samples of each pre-identified genes (partly based on extensive literature search and partly from gene listings from commercial assay kits (Hers et al., 2011, Ehrlich, 2017) were plotted for generation of heat maps for visual interpretation of expression pattern. The fold change expression was calculated relative to the expression of particular gene in the mock infected samples. The complete working script for downloading microarray .cel files pertaining to accession number GSE33389 from GEO domain, normalisation, and annotation and exporting the data file onto the local directory is detailed in appendix-II.

4.3.3 Immunofluorescence staining of CEFs and DEFs for actin-staining and H2N3 viral morphogenesis

Cells, viruses and experimental layout; Chicken and duck embryo fibroblast cells were propagated on 13 mm diameter glass coverslips placed in 24 well plates with a seeding rate of $5X10^3$ cells per well. The cells were infected with avian influenza H2N3 virus (A/mallard/duck/England/7277/06) at MOI of 1.0 when the cells

were 80–90% confluent. Infected cells were treated with LY294002 or carrier or untreated for 1 hr before incubating until 6 hpi and fixing with 4% paraformaldehyde (PFA).

Fixation, permeabilization and blocking of cells; After removing the the medium, the cells were washed twice with 1X PBS and fixed by adding 4% PFA 100 µl/well (or volume sufficient to cover the cells) and incubated at room temperature (RT) for 20 min before washing three times with 1X PBS 5 min each time. The fixed cells were either permeabilised or were submerged in 200 µl PBS and stored at 4^{o}C. The fixed cell monolayer was permeabilised by overlaying 200 µl of freshly prepared 0.1% triton X-100 (Fisher bioreagents, Belgium) per well for 30 min before washing with PBS. Blocking of permeabilised cells was performed by overlaying 200 µl of 2% BSA (Fisher, USA) per well for 45 minutes at RT. The blocking buffer was carefully removed, and the cell monolayer was incubated with 200 µl of primary antibody for one hour at RT (chicken H2N3 antiserum diluted 1:1000 in 1% BSA, a kind gift from Dr Stephen Dunham, School of Veterinary medicine and science, Sutton Bonington campus, University of Nottingham).

The cell monolayer was gently washed thrice in PBS for 5 min each time and was incubated with 200 µl of diluted Alexa Fluor® 488 labelled goat anti-chicken IgG secondary antibody (Invitrogen) (antibodies were diluted in 1% BSA as 1:500 v/v) and incubated in the dark for one hour at RT. After washing three times with PBS,

cells were further incubated with 200 µl of Alexa Fluor® 546 Phalloidin (Invitrogen) for actin staining in the dark for one hour. Cells were gently washed, the coverslips were carefully removed from wells with the help of a curved end long needle and a pair of fine tweezers. The coverslips with the cells were placed facing up, on the absorbent paper towel for drying. A small drop of 10 µl of Prolong® Gold AntiFade Reagent with 4',6–diamidino–2–phenylindole DAPI (Life Technologies) was placed in the centre of a clean glass slide, the coverslip was placed with the cells facing down onto the prolong-gold mountant. The circular coverslip border was sealed with clear nail polish to prevent drying and movement of coverslips over time. The fluorescently stained cells were stored at 4°C overnight for stabilisation before imaging. The photomicrographs were obtained by imaging slides on Leica DM 5000B epifluorescence imaging system.

Measurement of grey value from IF stained images; The grey value or the image intensity from an immunofluresently stained image or the specific area in the immunofluorescent stained H2N3 virus infected cells was measured using ImageJ image analysis application. Briefly, specific image from virus infected cell either HA stained or DAPI stained image is opened in ImageJ. A straight line is drawn across the long axis of the cell from one end to the other, in such way that the line approximately divides the whole cell including the nucleus in the centre. Once the straight line is drawn,

image is processed for calculation of the pixel intensity across the line. A mean pixel intensity across the line is calculated from several computer generated data points. For measurement of image intensity of particular colour like green (H2) in the cytoplasmic area and nuclear area, the image intensity is measured twice one from the long axis of the cell and another from only the nuclear area, the mean intensity of nuclear area is then deducted from the mean intensity of long axis that gives the intensity of only cytoplasmic area. At least three randomly chosen images were used for measurement of the grey value. Finally, a mean grey value is calculated by pooling the means of all three cell images and plotted on to graph for visual interpretation. Two calculate the cytoplasmic intensity alone, the mean nuclear intensity is subtracted from long axis mean. Similar measurement protocol is applied for Phalloidin stained actin (red) intensity. A representative diagram is shown in Figure 4-3.

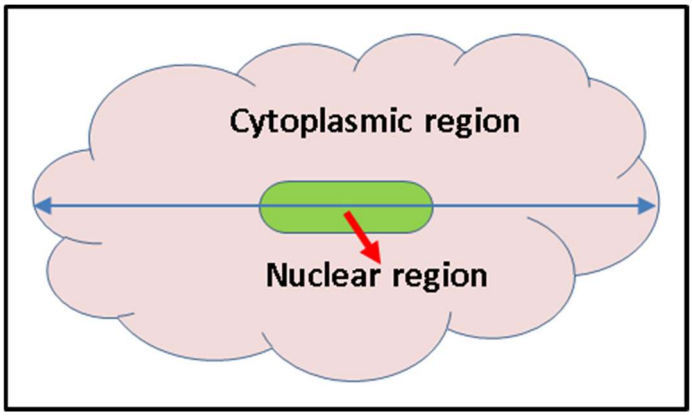


Figure 4-3: Pictorial depiction showing measurement of grey value from H2N3 virus infected CEF or DEF cells

4.3.4 Electron microscopy of H2N3 virus infected CEF cells

CEF cells were propagated on 13 mm Thermanox Plastic Coverslips (Nunc) in 24–well plates with a seeding density of $5X10^3$ cells per well. H2N3 virus infection (1MOI) and inhibitor treatment were carried out as described in section 4.3.3. The cells were fixed after set time points using 3% glutaraldehyde in 0.1M cacodylate buffer at RT for 10 min. Post-fixation washing was done with cacodylate buffer, and the cell monolayer was overlaid with 100 µl of cacodylate buffer to prevent drying of cells and stored at 4°C until further processing.

4.3.5 Preparation of samples for transmission electron microscopy

The resin mix preparation, sample dehydration and section cutting from resin blocks was as per the protocol described previously by Al-Mubarak et al. (2015). Briefly, resin used for embedding and blocking the cell samples was prepared by mixing the chemicals listed in Table 4-1 in a tri-pour beaker. After adding all the components and vigorous mixing, the beaker was covered with aluminium foil and incubated at 60°C for 20 min in a hot air oven for eliminating any air bubbles that may have formed during mixing.

Table 4-1: Preparation of resin solvent mix

Chemical component	Volume (ml)
Araldite CY212 resin	25
Agar 100 resin	15
Dodecenylsuccinic anhydride (DDSA)	55
The mixture was stirred well before adding	
Dibutyl phthalate	2
DMP–30	1.5

The glutaraldehyde-fixed cells were osmicated with 1% aqueous osmium tetroxide for 30 min, followed by washing with distilled water five times leaving each wash for at least 1 min. Dehydration of samples was performed by submerging the coverslip in a series of graded ethanol concentrations. The standard time and concentration combination used were; 50% ethanol for 2X 5 min each wash, 70% ethanol for 2X 5 min each wash, 90% ethanol for 2X 5 min each wash and finally with 100% ethanol for 3X 10 min each wash. The coverslips were then transferred to ceramic cups and infiltrated with 100% propylene oxide for 2 x 5 min. The dehydrated cells were infiltrated with a range of resin: propylene oxide combinations in three sequential steps: first infiltration with 1:3 resin: propylene oxide mix for 1 hour. Second, with 1:1 resin: propylene oxide mix for 1 hour, and finally with pure resin for 3 x 1 hr duration. The coverslips were then transferred and pressed deep into the bottom of the resin filled polyvinyl capsule with the cells facing upwards. The capsules were incubated in the hot air oven at

60°C for 72 hrs allowing polymerisation of the resin. When the incubation was complete, the polymerised blocks were removed from the capsule by pressing on the bottom of capsule and coverslips were gently pulled out, leaving the cells attached to the surface of the block.

The block was trimmed finely with a manual saw to remove excess resin while conserving the surface containing the cells. Roughly rectangular discs were prepared to contain cells on one of the surfaces. The discs were securely fitted on to the EM UC6 ultramicrotome (Leica). Microscopic sectioning of resin discs was performed by trimming several times carefully to obtain uniformly thin tissue sections. The sections so obtained were carefully floated on a small water-filled boat. Presence of cells on the sections was ascertained by staining a representative section on a 3–aminopropyl triethoxysilane (APES)-coated slide. The section was placed on a hotplate to flatten and to dry, after which a few drops of 1% toluidine blue-O in 1% sodium borate were added. The slide was dried again on the hotplate for 1 min, rinsed and dried and observed under a light microscope for the presence of cells.

Once the presence of cells on was assessed, the knife holder was replaced by a flat holder. The block was then gently trimmed using a single-edged blade and sectioned as described above to a thickness of 90 nm with a diamond knife. Attachment of two or more sections were avoided by gently separating them with a fine eyelash

and sections were flattened by exposing to chloroform vapours. Using fine tweezers, the sections were mounted on the rough surface of copper grids (FC200Cu, Formvar/Carbon film on Copper 200, EM resolutions). Grids were stained with ethanolic uranyl acetate followed by lead acetate, air dried and placed in a petri dish laid with filter paper and labelled appropriately with the details of the sample on the grid and stored at room temperature until imaged. Sample grids were photomicrographed on Tecnai biotin G212 digital transmission electron microscope system run on 100-kilovoltage power. Images were captured on various resolutions from different points across a vertical section of the sample and saved as .TIFF format.

4.4 Results

4.4.1 H2N3 virus infected chicken and duck lung cells display equivalent PI3K/Akt stimulatory gene cluster expression

PI3K/Akt stimulatory gene cluster transcriptomic analysis revealed similar expression pattern in H2N3 virus or mock infected chicken and duck lung cells. The expression range measured as fluorescence probe intensity ranged between 0 and 10. Among a cluster of genes (or transcript variants denoted by similar name) only HRAS (HRas or transforming protein p21) a small GTPase in the Ras subfamily, and MAP2K1 (dual specificity mitogen-activated protein kinase kinase 1) were noticeably expressed in both H2N3 virus infected or mock infected chicken compared to duck lung cells. CSNK2A1 (casein kinase 2, alpha 1), SRF (serum response factor) and IGF1R showed mild expression across all samples. No expression of the transcript variants of son of sevenless homolog 1 (SOS1) and GRB2-related adapter protein 2 (GRAP2) and a minimal expression of Fos Proto-Oncogene (FOS), insulin-like growth factor 1(IGF1), insulin receptor substrate 1(IRS1), SHC-transforming protein 1(SHC1), proto-oncogene c-RAF 1(RAF1), tyrosine-protein phosphatase non-receptor type 1 (PTPN1) and mitogen activated protein kinase 8 (MAPK8) was found in both chicken and duck lung cells. Slightly higher expression of insulin-like growth factor 1 receptor (IGF1R) was observed in duck compared to chicken lung

cells. Overall, the gene expression pattern in both virus and mock infected chicken and duck lung cells was comparable (Figure 4-4).

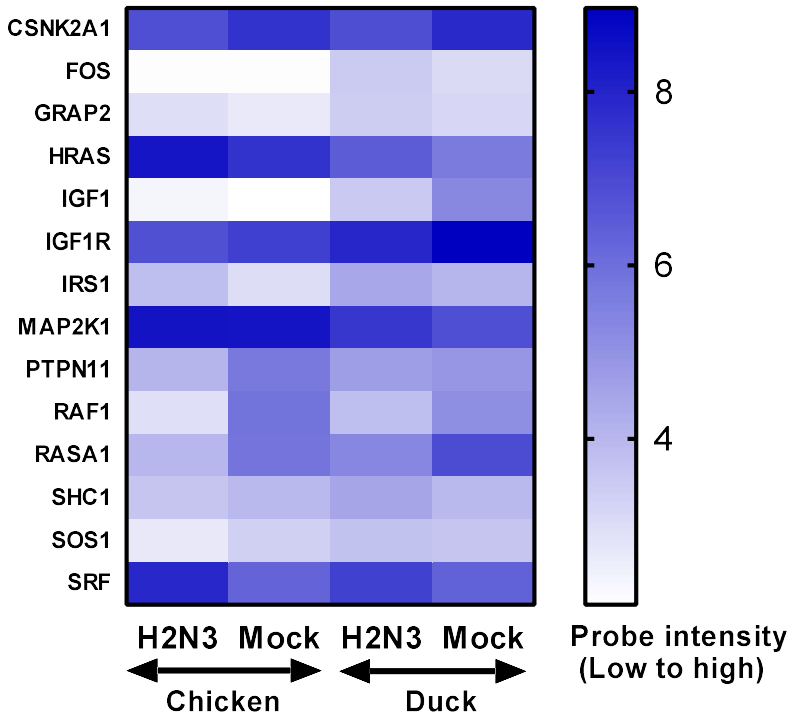


Figure 4-4: IGF-1 signalling (PI3K activation initiator) gene cluster expression.
The mean fluorescence probe intensity corresponding to the mean log expression pattern of the particular gene or the transcript variants denoted by similar name is depicted and are coloured from light (low) to blue (high) on a scale of 0 – 10. Rows correspond to gene name and columns indicate H2N3 virus infected or mock infected chicken and duck lung cells.

4.4.2 Host anti-apoptosis gene cluster expression revealed higher basal expression of adaptor protein Growth factor receptor-bound protein 2 (GRB2)

Growth factor receptor-bound protein 2 expression was down-regulated in virus infected chicken compared to mock infected lung cells. Whereas the expression of GRB2 gene was not significantly affected between virus and mock infected duck cells (Figure 4-5). GRB2 functions as an adaptor protein and mediate cell to cell signal transduction through epidermal growth factor receptor binding.

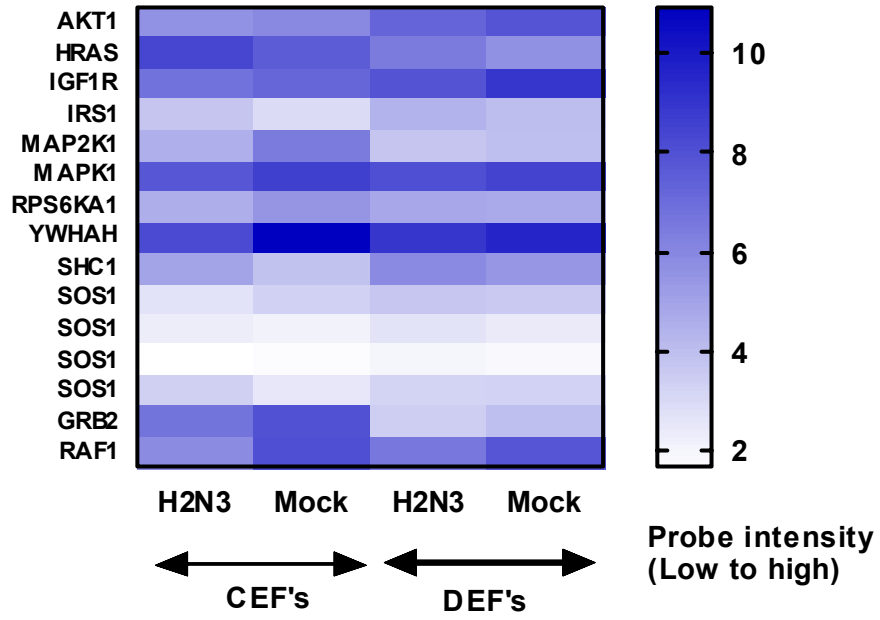


Figure 4-5: Beclin-2 associated death (BAD) promoter phosphorylation and associated host anti-apoptotic response.
The mean fluorescence probe intensity corresponding to the mean log expression pattern of the particular gene or the transcript variants denoted by similar name is depicted and are coloured from light (low) to blue (high) on a scale of 0 – 12. Rows correspond to gene name and columns indicate H2N3 virus infected or mock infected chicken and duck lung cells.

4.4.3 PI3K/Akt negative regulator phosphatase and tensin homolog (PTEN) was constitutively over expressed in duck compared to chicken cells

Expression of PTEN dependent apoptosis regulatory genes revealed differences between chicken and duck species. The Fas ligand (FASLG) a transmembrane protein that forms death-inducing complex upon ligand binding and activation and FOXO3 (Forkhead Box O3) a member of forkhead transcription factor family that serve as the trigger for apoptosis showed fairly lower expression trend in both cells. A moderate expression of PTK2 (protein tyrosine kinase 2) associated with tyrosine kinase-mediated cellular adhesion functions, MAPK1 (mitogen activated protein kinase 1) and RBL2

(Retinoblastoma-like protein 2) genes were observed in both species. Few genes like ITGB1 (integrin beta 1) and MAPK1 that are involved in skeletal muscle remodelling were equally well expressed in both chicken and duck cels. Integrin-linked kinases (ILK) essential in integrin-mediated signal transduction was highly expressed in chicken compared to duck lung cells.

The most striking difference observed was in the expression of PDK1 (phosphoinositide-dependent protein kinase-1) and PTEN genes, which were inversely expressed in duck to that in chicken lung cells (Figure 4-6). Considerably higher PDK1 expression was observed in chicken cells compared to duck cells, while duck cells exhibited very low expression pattern. The expression of PTEN was noticeably higher in duck compared to chicken lung cells. SHC1 (SHC-transforming protein 1) involved in the cell cycle arrest and apoptosis regulation have shown similar expression pattern in both chicken and duck cells.

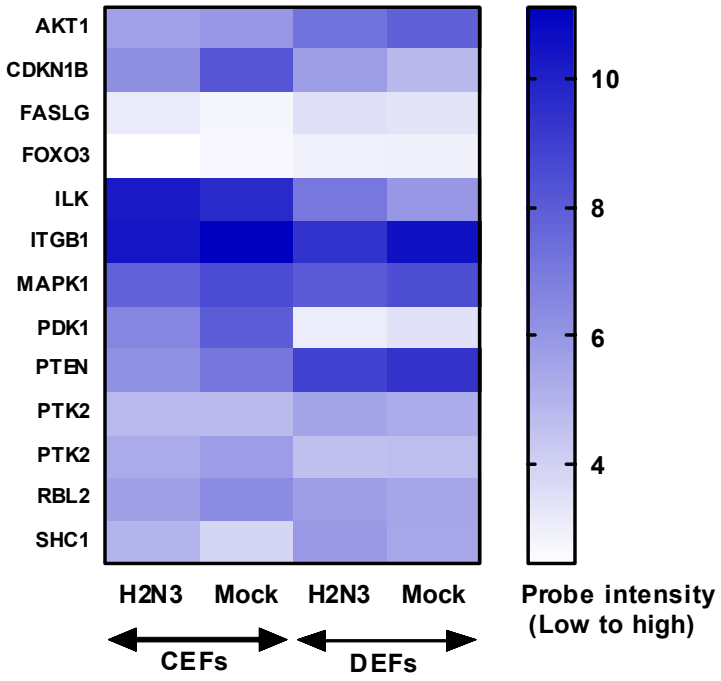


Figure 4-6: PTEN-dependent cell cycle arrest and apoptosis.
The mean fluorescence probe intensity corresponding to the mean log expression pattern of the particular gene or the transcript variants denoted by similar name is depicted and are coloured from light (low) to blue (high) on a scale of 0 – 12. Rows correspond to gene name and columns indicate H2N3 virus infected or mock infected chicken and duck lung cells.
.

4.4.4 Higher expression of cell division control protein 42 homolog (Cdc42) and Ras-related C3 botulinum toxin substrate 1(RAC1) observed in chicken but not in duck cells

Expression analysis of a set of eight PI3K/Akt dependent cytoskeletal re-organisation related genes revealed distinct differences in the expression of Rho family members Cdc42 and RAC1. A marginal higher expression of RhoA was observed in duck compared to chicken cells. While expression of Cdc42 and RAC1 was appreciably higher in chicken compared to duck cells. PAK1 (p21 activated kinase 1) that interact with Rho family members Cdc42 and RAC1 were upregulated slightly in chicken over duck cells (Figure 4-7). However, the expression levels between infected and

mock-infected chicken cells were nearly similar. Mock-infected duck cells showed relatively lower expression PAK1 compared to chicken cells and were further suppressed in virus infected duck cells in both virus infected chicken and duck cells. Although, a reasonable down-regulation of PDGFRA (platelet-derived growth factor receptor A) was observed in H2N3 virus infected chicken cells than mock infected cells but the level of expression was comparable in both cell types. The WASL (Wiskott-Aldrich syndrome-like) was slightly upregulated in duck cells compared to chicken cells.

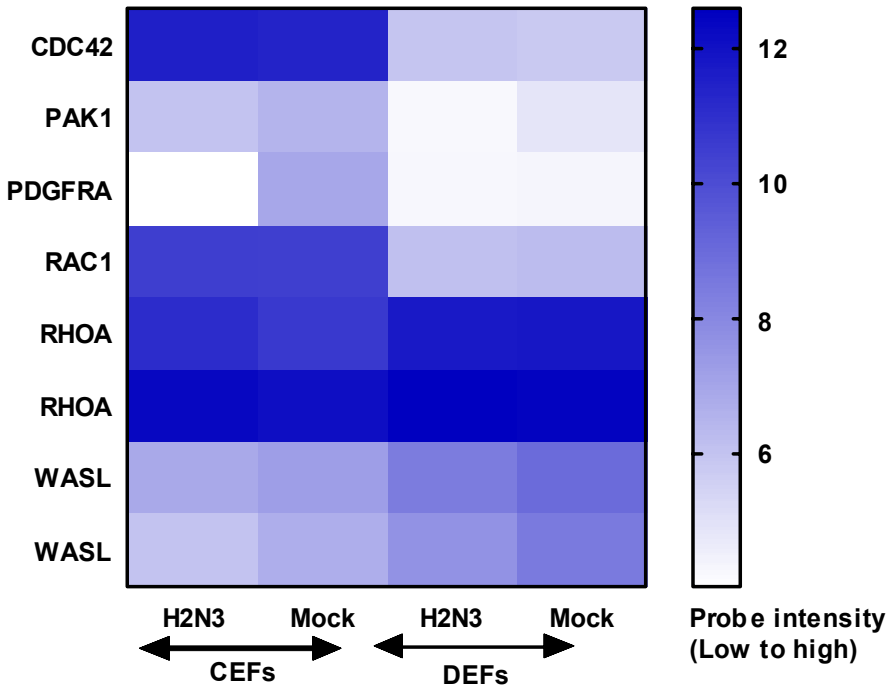


Figure 4-7: Expression of small GTPases involved in actin remodelling and cytoskeletal regulation in chicken and duck lung cells.

The mean fluorescence probe intensity corresponding to the mean log expression pattern of the particular gene or the transcript variants denoted by similar name is depicted and are coloured from light (low) to blue (high) on a scale of 0 – 12. Rows correspond to gene name and columns indicate H2N3 virus infected or mock infected chicken and duck lung cells.

4.4.5 Five key PI3K/Akt associated genes differentially expressed in chicken and duck lung cells

Overall, analysis of microarray data revealed differences in the expression pattern of of three important SH2 domain containing PI3K/Akt pathway-specific genes GRB2, PDK1 and PTEN that are essential pre-requisites in recruitment and phosphorylation activation of effector Akt kinase. Approximately a twofold lower mean fluorescence intensity of GRB2 and PDK1 was observed in H2N3 virus infected duck cells compared to chicken cells. Similarly, a fold higher mean fluorescence intensity of PTEN was observed in H2N3 virus infected duck cells compared to infected chicken cells. The expression pattern of these one anti and two pro-PI3K genes probably suggests a complementing activity for multi-level control of PI3K/Akt activation in duck cells. Lower mean fluorescence intensity of Cdc42 and RAC1 genes that participate in cytoskeletal actin remodelling was observed in H2N3 virus infected duck cells compared to chicken cells. Table 4-2 highlights a comparative summary of PI3K/Akt pathway mediated differentially expressed genes between H2N3 virus infected chicken and duck lung cells.

Table 4-2: Summary of differentially expressed genes in both cells

(Mean fluorescence intensity values in parenthesis)

Gene Name	Duck	Chicken
Grb2	↓ (3.7)	↑ (7.4)
PDK1	↓ (3.3)	↑ (7.3)
PTEN	↑ (9.1)	↓ (6.6)
Cdc42	↓ (6.1)	↑ (11.5)
RAC1	↓ (6.2)	↑ (10.5)
Expression pattern	↓ Downregulation	↑ Upregulation

4.4.6 PI3K/Akt inhibition resulted in cytoskeletal actin disruption and cytosolic viral cargo retention in CEFs

The implications of PI3K/Akt activation on the regulation of cytoskeletal actin remodelling and conservation of actin integrity was studied by immunofluorescence staining of H2N3 virus infected CEF and DEF cells upon PI3K/Akt inhibition. Phalloidin-stained cytoskeleton actin appeared red-orange, and DAPI stained nucleus appeared blue in the merged images giving distinct cellular architecture in uninfected CEFs and DEFs (Figure 4-8F, Figure 4-10F). Visible absence of green fluorescence in mock-infected CEF and DEF cells served as negative control (Figure 4-8E,Figure 4-10E). A characteristic green fluorescence was evident in H2N3 virus infected CEFs and DEFs suggesting the distribution viral HA antigen in the infected cells (Figure 4-8B,Figure 4-10B). Inhibition of PI3K/Akt in H2N3 virus infected CEF cells resulted in visible actin deformation as evidenced by irregular and disorganised actin distribution leading to the membrane ruffle formation compared to

infected carrier treated or uninfected control cells. Intracellular retention of viral cargo upon PI3K/Akt inhibition as evidenced by significantly higher cytosolic green fluorescence was observed in virus infected CEFs (Figure 4-9B) compared to uninhibited CEF cells (Figure 4-9E and Figure 4-12). In contrast, green fluorescence density although was less but was uniformly distributed in the cell cytosol in both virus infected and pathway inhibited (Figure 4-11B) or uninhibited (Figure 4-11E and Figure 4-12) DEF cells.

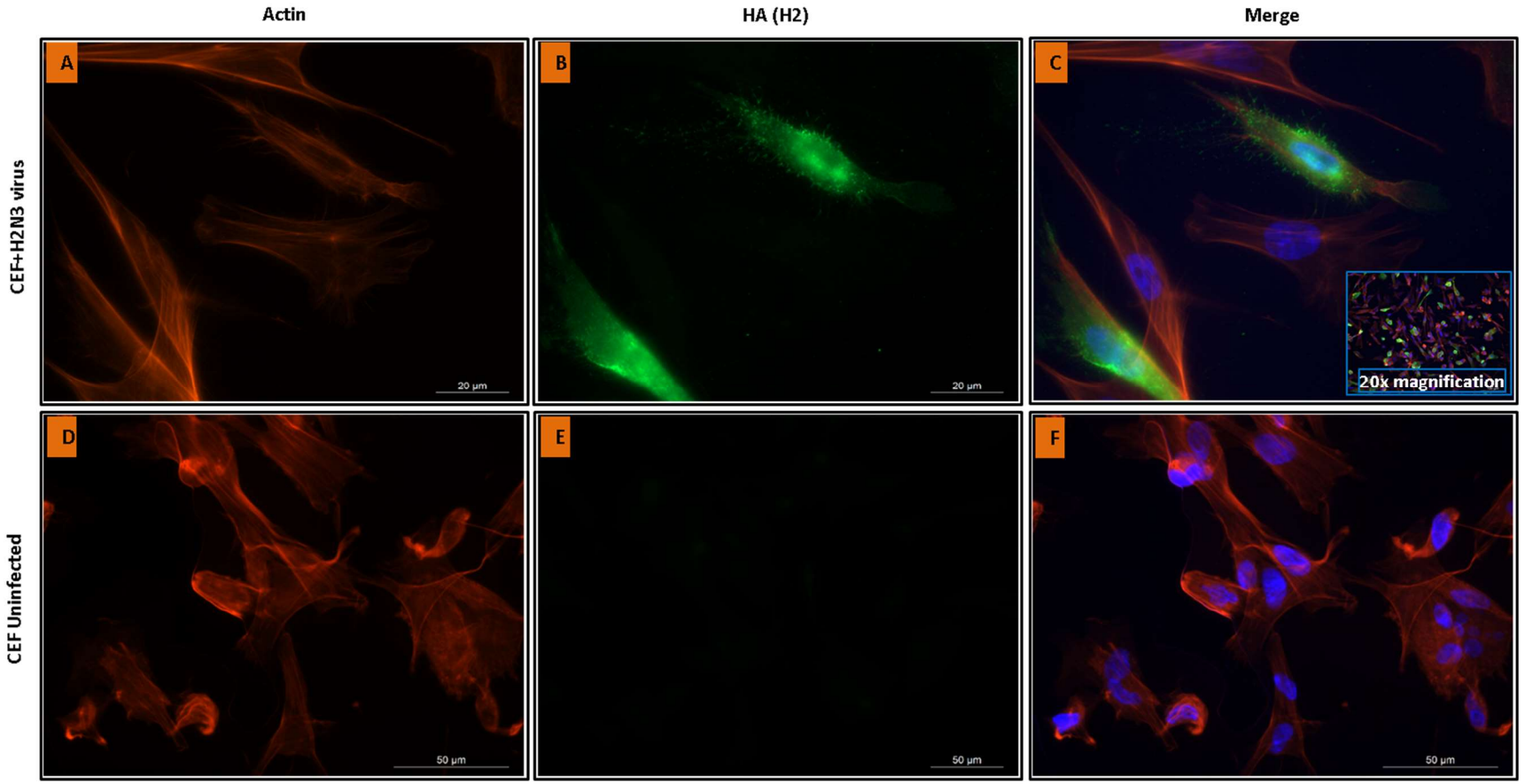


Figure 4-8: H2N3 virus infected (1MOI) or uninfected control CEF cells.

The CEF cells infected or uninfected with H2N3 virus (1MOI). Photomicrographs depict: A/D- Phalloidin stained (red) actin fibre network, B-HA green fluorescence, E-uninfected cells C/F –Actin +DAPI stained blue nucleus. Images were captured on Leica fluorescent microscopy and processed in Leica image processing software package.

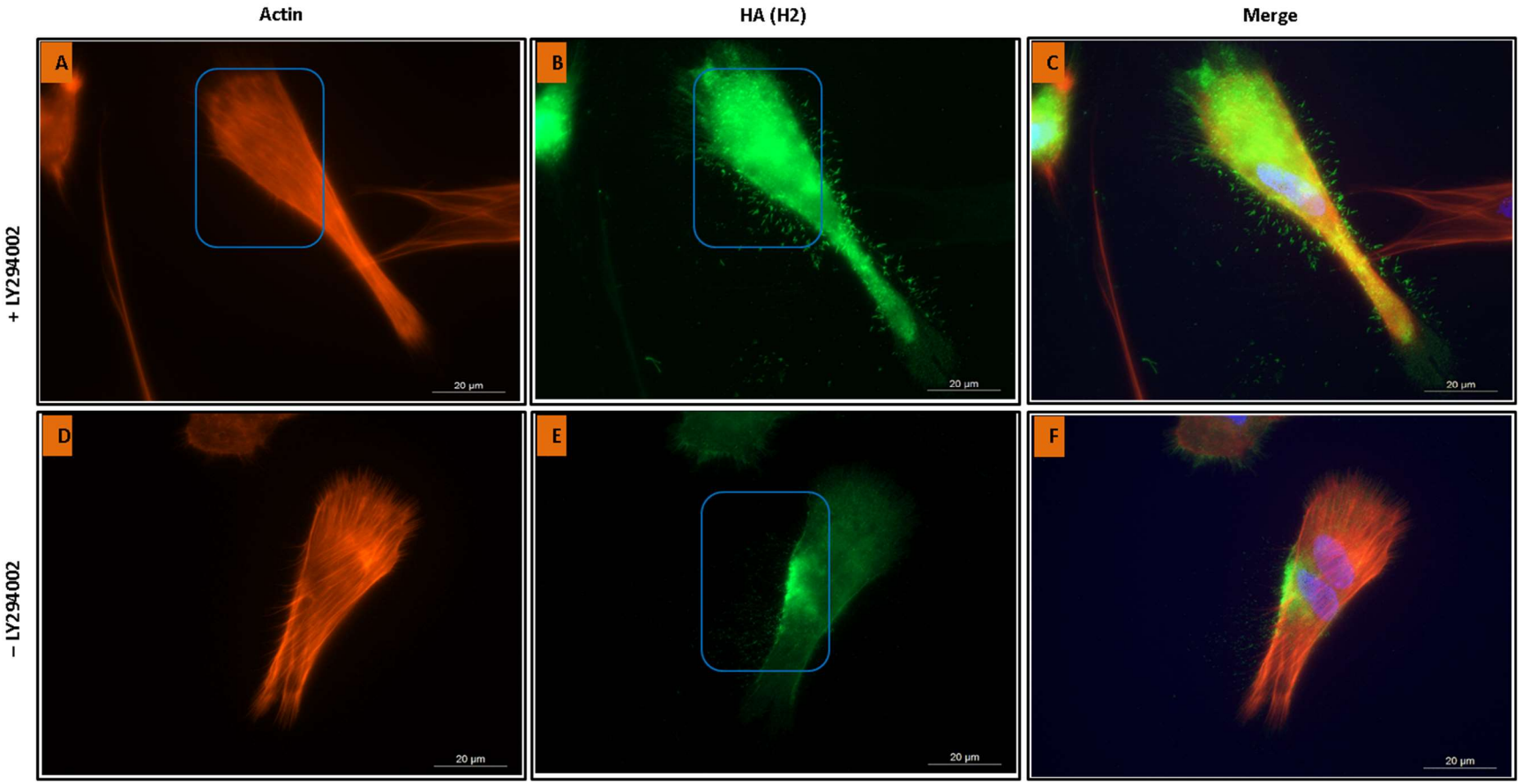


Figure 4-9: CEF cells infected with H2N3 virus (1MOI) and LY294002 treated or mock treated 2 hpi.
The CEF cells infected with H2N3 virus (1MOI) and LY294002 treated cells (top row) or mock-treated cells (bottom row) and stained for surface HA (green), actin (red-orange), and nuclear DNA (blue). Photomicrographs depict: A-disintegrated actin fibre network (boxed),B/E-HA green fluorescence, C/F – Actin +DAPI stained nucleus. Images were captured on Leica fluorescent microscopy and processed in Leica image processing software package.

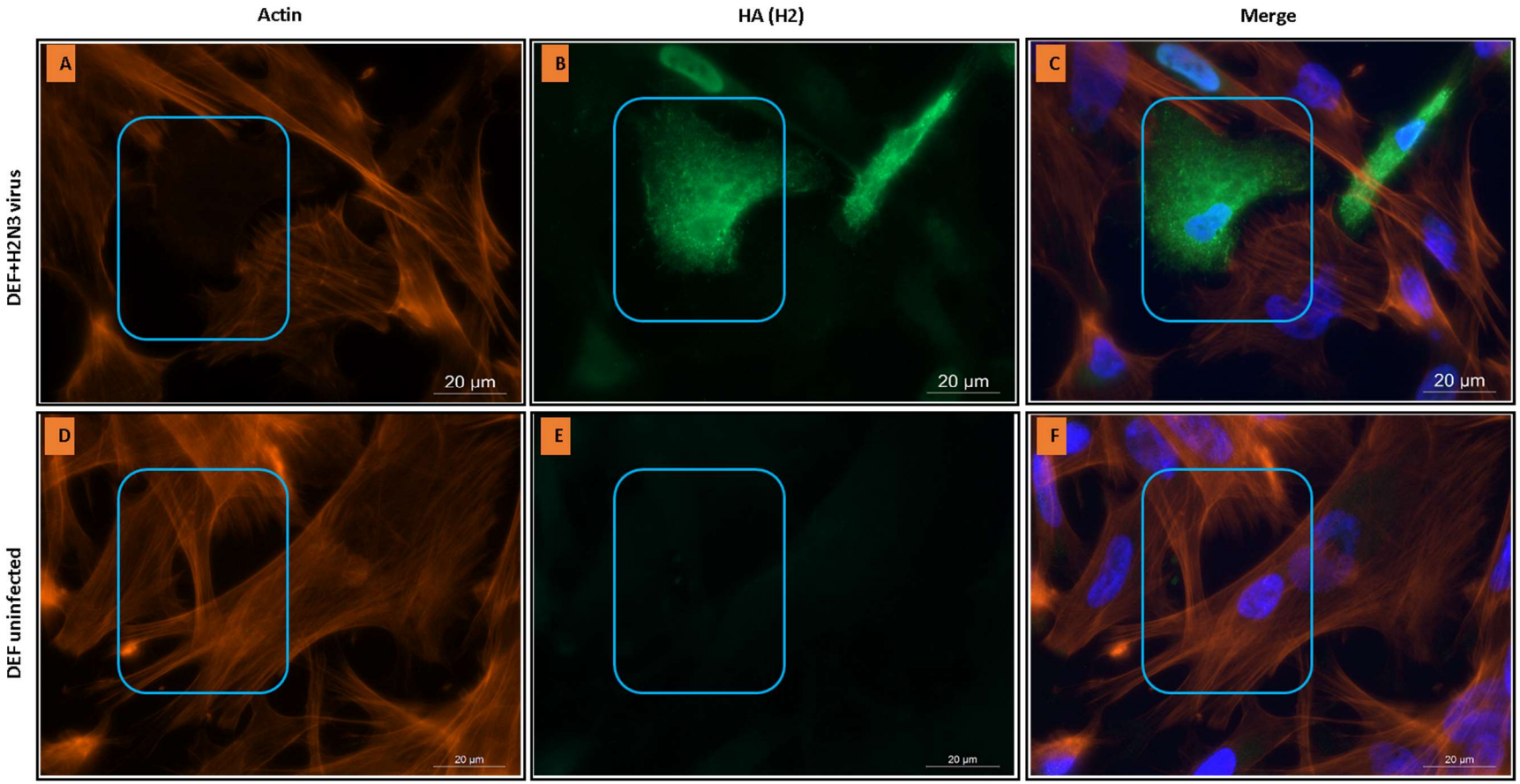


Figure 4-10: H2N3 virus infected (1MOI) or uninfected control DEF cells.

The DEF cells were infected or mock infected with H2N3 virus (1MOI) and incubated for 7 hrs and stained for surface HA (green), actin (red-orange), and nuclear DNA (blue). Photomicrographs depict: A-Complete loss of actin fibre network (boxed), B –HA green fluorescence, C/F actin +DAPI stained nucleus. Images were captured on Leica fluorescent microscopy and processed in Leica image processing software package.

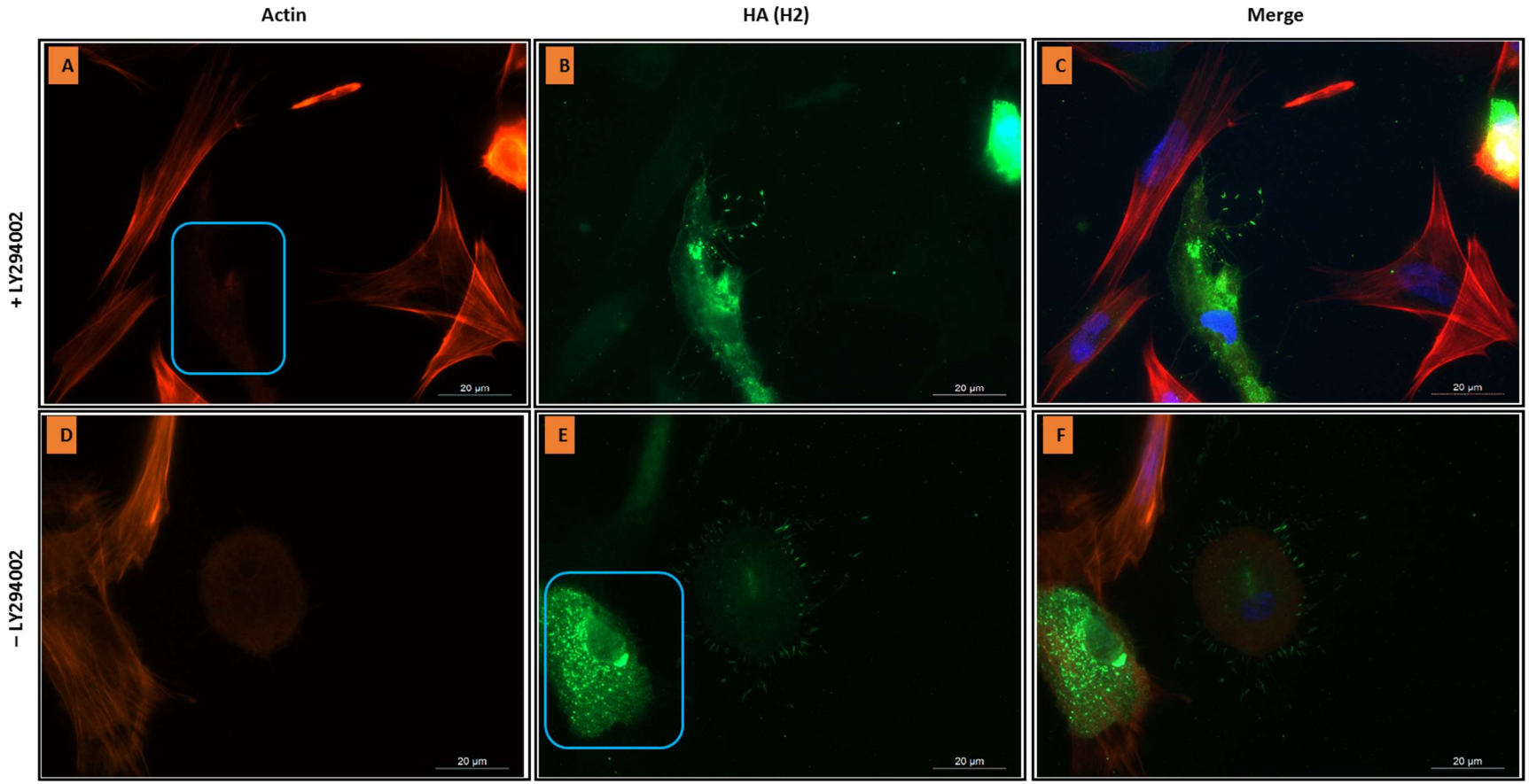


Figure 4-11: DEF cells infected with H2N3 virus (1MOI) and LY294002 treated or mock treated 2 hpi.

The DEF cells infected or mock infected with H2N3 virus (1MOI) and LY294002 treated cells (top row) Infected and mock-treated cells (bottom row) and stained for surface HA (green), actin (red-orange), and nuclear DNA (blue). Photomicrographs depict: A-Actin fibre network, B/F – uniformly distributed HA green fluorescence, C/F actin +DAPI stained nucleus. Images were captured on Leica fluorescent microscopy and processed in Leica image processing software package.

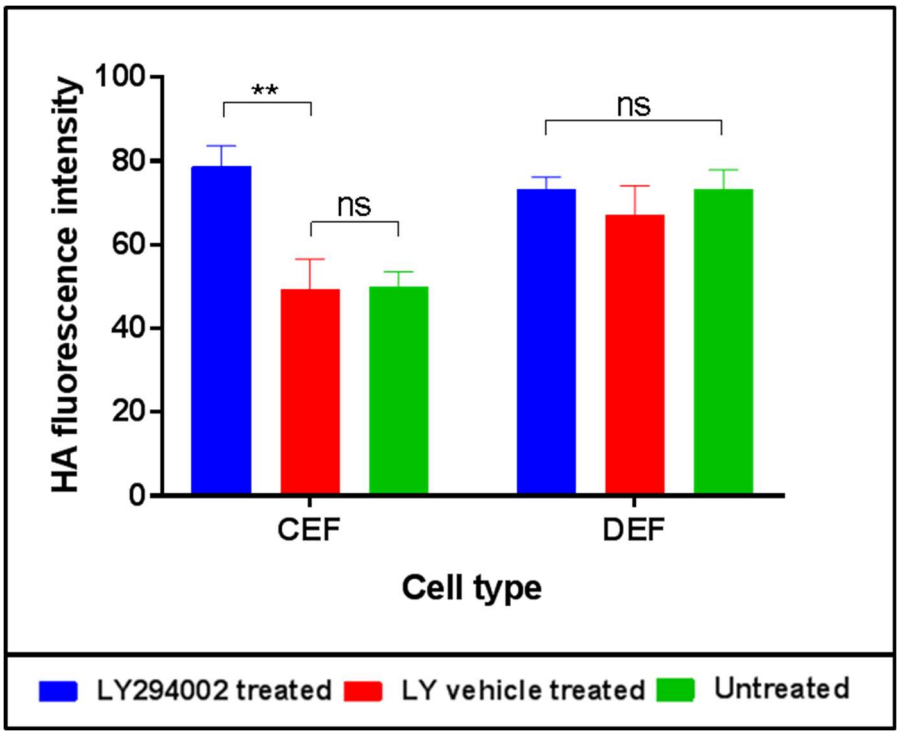


Figure 4-12: Comparative cytosolic retention of HA (H2) antigen in H2N3 virus infected CEF and DEF cells.
The HA intensity (Gray value) from the fluorescent stained image was quantified using ImageJ software. The bars represent mean cytosolic HA intensity values acquired from three independent images. Error bars indicate SEM, **- P ≤ 0.01 significance level, ns=statistically non-significant.

4.4.7 Complete loss of actin integrity observed in H2N3 virus infected duck fibroblast cells

The H2N3 virus infected (1MOI) duck primary fibroblast cells revealed a significant ($p<0.05$) loss of cellular actin architecture in in all three treatment groups (Figure 4-13). The pattern of actin disruption was restricted to only virus infected cells but not in healthy DEF cells (Figure 4-10A/D). The actin filaments appeared intact and regular in unaffected healthy adjacent cells (Figure 4-10D/F).

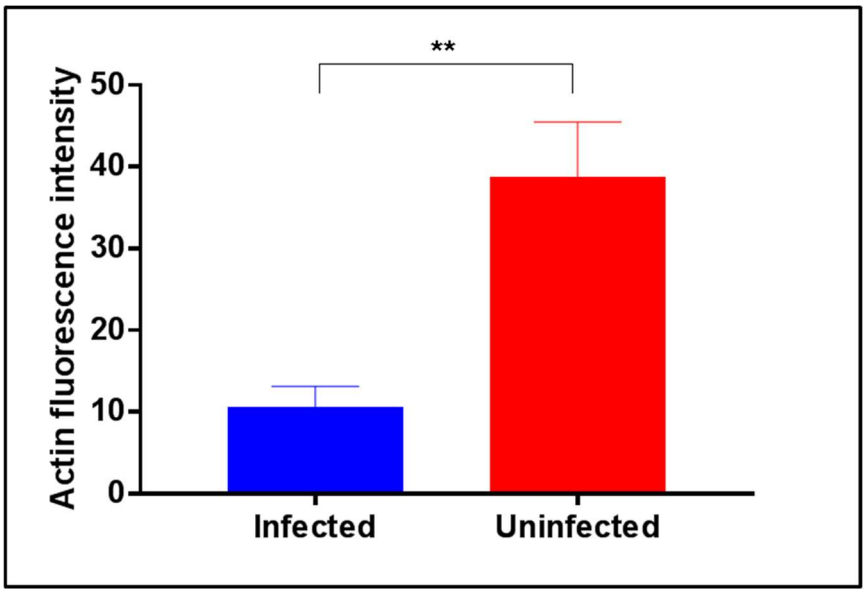


Figure 4-13: Comparative mean fluorescence intensity of actin from H2N3 virus infected and uninfected DEF cells.
Actin fluorescence intensity (Gray value) from fluorescent stained images was quantified using ImageJ software. The bars represent mean actin stained Phalloidin (red-orange) intensity values acquired from three independent images. Bar diagram using unpaired t-test. Error bars indicate SEM, **- $P < 0.05$ significance level.

4.4.8 PI3K/Akt inhibition influenced budding virus morphology in chicken cells

The impact of PI3K/Akt cascade abrogation on budding virion morphogenesis was studied by immunofluorescence staining and confirmatory electron microscopy. The results revealed that the progeny viruses budding from PI3K/Akt inhibitor untreated chicken fibroblasts resembled although spherical but appeared more elliptical or bullet shaped. Transmission electron microscopy (TEM) substantiated the immunofluorescence observations. While the progeny viruses from PI3K/Akt inhibitor (LY294002) treated chicken cells mostly appeared spherical in immunofluorescence staining while TEM imaging of the same confirmed budding of perfectly spherical virion particles from the infected CEF cells (Figure 4-14F).

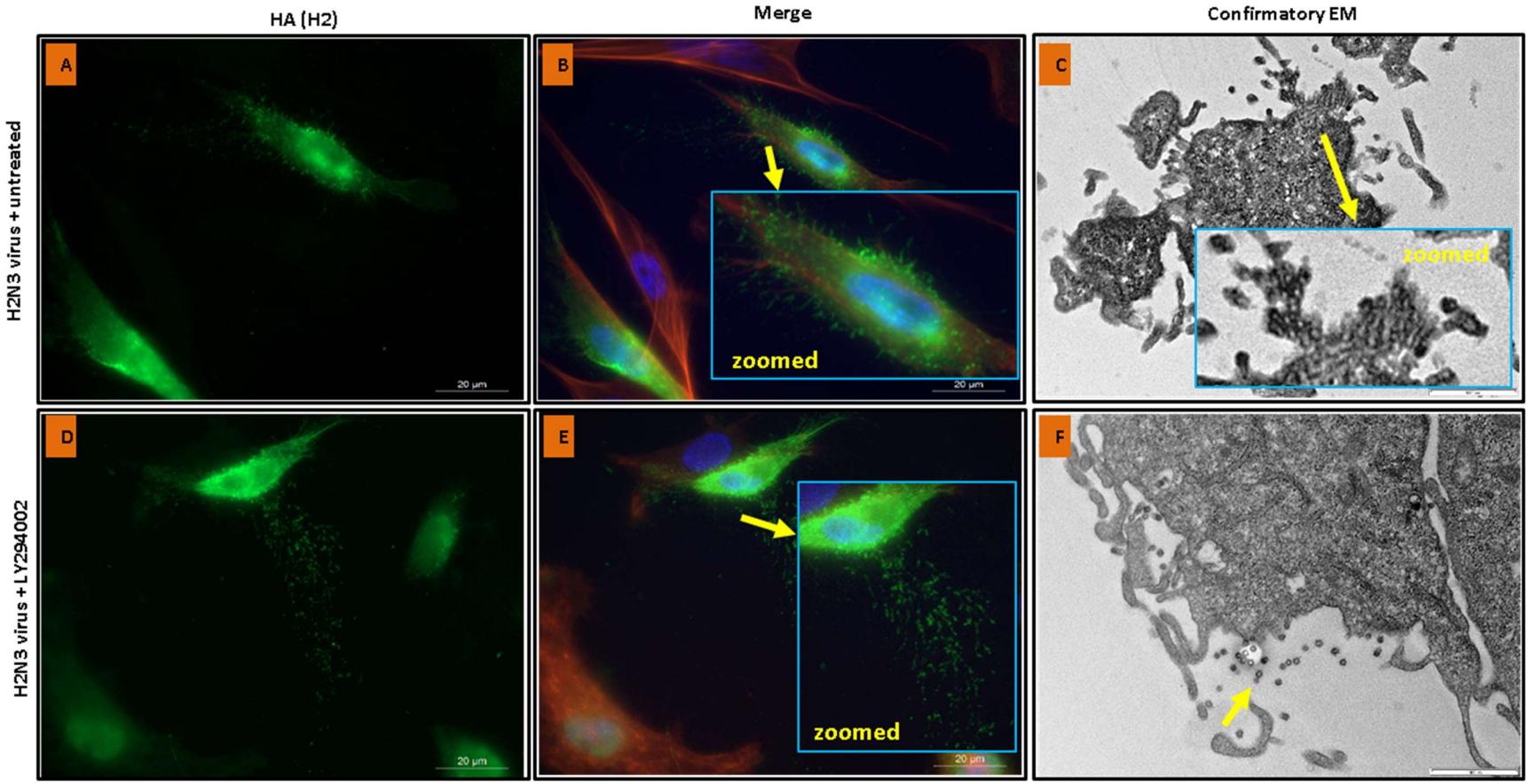


Figure 4-14: Morphogenesis of H2N3 virus in PI3K/Akt inhibitor treated chicken fibroblast cells.

The CEF cells were infected with H2N3 virus (1MOI), and untreated (top row) or PI3K/Akt inhibitor (LY294002) treated cells (bottom row). Stained for surface HA (green), actin (red-orange), and nuclear DNA (blue). The LY294002 treated cells showed perfectly spherical budding virus (D/F) compared to untreated cells that showed slightly elongated morphology (A/C). Fluorescent images were captured on Leica fluorescent microscopy and processed in Leica image processing software package.

4.5 Discussion

The transcriptomic data from IAV infected or mock-infected chicken and duck primary lung cells (Kuchipudi et al., 2015) was analysed to gain insights into the transcriptional regulation of PI3K/Akt pathway associated genes. Expression profiles revealed presence of salient differences in the expression of functionally important PI3K/Akt mediated GRB2, PTEN and PDK1 genes, possibly suggesting potential functional contribution of these in the host response to IAV infection. GRB2 is shown to be crucial in key cellular functions like signal transduction, cell cycle progression and actin-dependent cell motility and acts as linker of epidermal growth factor receptor tyrosine kinase to RAS and downstream kinase Akt (Tari and Lopez-Berestein, 2001). Targeted functional disruption of Grb2 results in impaired cell proliferation and lethal to mice during embryonic development (Jia et al., 2012).

The PI3K/Akt activation involves phosphorylation of Akt at threonine 308 position by PDK1 and at serine at position 473 for activation (Ding et al., 2010). Failure to phosphorylate at one of these sites could lead to failure of activation of the whole signalling cascade. Studies have shown PTEN as the predominant negative regulator of PI3K signalling by dephosphorylating PIP3 back to PIP2, leading to suppression of PIP3 'second messenger' molecule that is essential for phosphorylation activation of Akt effector kinase

(Carracedo and Pandolfi, 2008). PTEN promotes cellular apoptosis, by downregulating the PI3K/AKT Pathway (Lu et al., 2016). As PI3K/AKT activation is a multi-step process, it is highly likely that downregulation of crucial genes (GRB2, PDK1) and higher PTEN expression in duck cells could contribute at least in part for the previously described higher apoptosis (Kuchipudi et al., 2012a) to IAV infection compared to chicken cells.

The functional contribution of PI3K/Akt dependent Rho proteins like Cdc42 and RAC1 in the regulation of cytoskeletal actin reorganisation has been studied in mammalian cell culture systems (Hall, 1998, Tsakiridis et al., 1999, Taylor et al., 2011) and in CEF cells (Qian et al., 2004). This study found actin disruption in H2N3 virus infected and PI3K/Akt inhibited chicken cells in accordance with previous reports of PI3K/Akt dependent mediation of cytoskeletal actin reorganisation. A previous study by Jiang et al. (2016) demonstrated the importance of PI3K mediated RAC1 expression in actin filament remodelling. In contrast to chicken cells, an acute cytoskeletal actin loss in H2N3 virus infected duck fibroblast cells was found in this study as evidenced by immunofluorescence staining. This observation along with the downregulation of RAC1 and Cdc42 genes in duck lung cell transcriptome highlight a key mechanism of dysregulation of cytoskeletal actin in IAV infected duck cells. However, present study did not investigate the expression of these genes in IAV infected duck fibroblasts, and as

such warrant further studies to establish functional association between loss of actin and RAC1 and Cdc42. Significantly higher cytosolic accumulation of H2N3 viral HA protein was evidenced in PI3K/Akt inhibited chicken cells compared to duck cells. Retention of HA suggested a potential interference in the post-translational translocation of viral components in the cytosolic environment in PI3K/Akt inhibited cells. This could also be a potential explanation for the significant reduction in virus titres in PI3K/Akt inhibited chicken cells observed in the present study.

The results of the present study confirmed previous observations by Al-Mubarak et al. (2015) that duck cells produced elongated while chicken cells produced moderately spherical viruses. However, chemical inhibition of PI3K/Akt in chicken cells resulted in budding of perfectly spherical virion particles as evidenced by electron microscopy, suggesting potential contribution of PI3K/Akt in the regulation of viral morphogenesis in chicken cells. In contrast, PI3K inhibition had no influence on virion morphology in duck cells and still produced elongated virion particles. The results suggest that PI3K activity is not directly connected to the differential virus morphology observed between chicken and duck cells. Other actin regulatory proteins like Rab11 and Rab11-family interacting protein 3 (FIP3) were shown to be essential for elongated virion morphology in mammalian cells (Bruce et al., 2010). Hence, generation of elongated avian influenza viruses from infected duck cells suggest

involvement of host factors other than PI3K/Akt which need further investigation.

In summary, the present study identified key genes associated with PI3K/Akt pathway activation in influenza virus infected chicken and duck fibroblast cells. Further investigation of the functional association of these genes could provide valuable insights into the molecular basis for influenza virus susceptibility and resistance in chickens and ducks.

Chapter 5. Innate response to avian influenza viruses and importance of NS1–p85β interactions in PI3K/Akt activation in chicken cells

5.1. Introduction

5.1.1 Innate immune response to avian influenza virus

Avian influenza viruses cause a range of disease outcomes in chickens. Low pathogenicity avian influenza viruses (LPAIV) induce mild to self-limiting disease, whilst high pathogenicity avian influenza viruses (HPAIV) elicit an intense host response that is reflected in disease severity. HPAI viruses have been shown to replicate rapidly, reaching high titres compared to LPAI viruses in the infected chicken cells (Kuchipudi et al., 2012a). As soon as the virus is internalised, the host innate response is activated. Pattern recognition receptors (PRRs) act as the first responders to AIV infection by sensing pathogen-associated molecular patterns (PAMPS) or damage associated molecular patterns (DAMPs). Cytoplasmic PRRs RIG-I, MDA5 and LGP2 participate in cytosolic AIV viral nucleic acid recognition. A very important family of PRRs are the Toll-like receptors (TLRs). TLR3, TLR7, TLR8 and TLR9 localise in the endosome and participate in the recognition of AIV viral nucleic acids (Ramos and Fernandez-Sesma, 2015). Sensing of viral PAMPs or DAMPs by PRRs leads to a sequence of events that eventually activates multiple signalling cascades, culminating in interferon (IFN) induction, accomplishing the antiviral response (Iwasaki and Pillai, 2014).

Recent investigations into the pathogenesis of AIV infections have suggested that HPAIV infection results in higher immune and cytokine response compared to LPAIV infection in chicken cells (Kuchipudi et al., 2014). A low pro-inflammatory response was observed among pigs and mice contributing to a reduced cellular damage in H5N1 virus infections (Lipatov et al., 2005, Nelli et al., 2012). These findings indicate that dysregulation of the host pro-inflammatory response to infection is a key contributor to the morbidity and mortality of virulent avian influenza virus infections.

5.1.2 IAV NS1 in host innate response and PI3K activation

Viruses have evolved to evade the host innate immune barriers enabling infection to be established. The IAV NS1, a 230 amino acid short protein, is described as the multitasking virulence factor. NS1 antagonises host innate response and operate as a "pro-viral" component in the infected cells as reviewed by (Ayllon and Garcia-Sastre, 2015). The NS1 is thought to play role in the regulation of viral RNA and protein synthesis while disrupting host cell homeostasis, hence it is a potent contributor to influenza pathogenesis and disease outcome (Ayllon and Garcia-Sastre, 2015). Upon sensing of virus intrusion by PRRs, the host cells mount a type-I interferon response leading to the production of IFNα and IFNβ, resulting in the expression of an array of interferon-stimulated genes (ISGs) bringing about an effective antiviral state (Schneider et al., 2014). However, NS1 impedes host innate immune

capabilities by repressing type-I IFN induction at different stages in the interferon-signalling pathway (Ayllon and Garcia-Sastre, 2015). Recognition of intermediary dsRNA species with 5'-triphosphates by cytosolic RNA helicases, RIG-I or MDA5 in chickens that lack RIG-I, results in a series of events eventually leading to phosphorylation and nuclear translocation of IRF-3 and NF-kB transcription factors that results in type-I IFN production (McWhirter et al., 2005). The cleavage and polyadenylation specificity factor 30 (CPSF30), which recognises conserved AAUAAA sequence and catalyse host pre-mRNA formation by addition of a poly A tail to nascent mRNA (Wahle and Keller, 1996). The AIV NS1 protein is shown to complex with RIG-I (Mibayashi et al., 2007) and CPSF30 (Nemeroff et al., 1998) resulting in the pre-transcriptional suppression of IRF3 and NFkB (Talon et al., 2000, Wang et al., 2000). Interferon-stimulated genes are critical in bringing about the antiviral state in AIV infected cells. The first ISG to be identified to confer resistance to AIV was Mx1 (Horisberger et al., 1983). The RNA binding serine/threonine kinase PKR is activated upon sensing dsRNA in the virus infected host cell, leading to activation of different signal transduction cascades to counteract intruding viruses (Garcia et al., 2006). It has been postulated that NS1 hinders crucial conformational modification resulting in suppression of PKR activation and subsequent antiviral effects (Li et al., 2006). Influenza viral NS1 has been attributed for suppression of PKR mediated antiviral response, further the study

demonstrated suppression of PKR through use of PR8 virus with deltaNS1 suggesting NS1 as the key contributor for suppression of PKR mediated antiviral response (Bergmann et al., 2000). AIV NS1 is suggested to inhibit 2'-5' oligo (A) synthetase (OAS) an RNase L activator and suppressor of viral RNA predominantly by degradation of viral products. Silencing of RNase L activity has shown enhanced virus replication in recombinant A/Udorn/72 (H3N2) virus infected cells (Min and Krug, 2006).

While antagonising the host antiviral response, AIV NS1 promotes potent "pro-viral" functionalities by over-riding the host cellular machinery. AIV NS1 is known to interact with multiple host proteins resulting in the activation of host signalling pathways. Literature from mammalian studies shows NS1 interaction with PI3K p85β, resulting in pathway activation through phosphorylation of downstream effector kinase Akt (Hale et al., 2006, Shin et al., 2007c). PI3K is well characterised as an anti-apoptotic factor; activation by AIV NS1 is believed to prolong cell survival aiding higher viral replication (Zhirnov et al., 2002). Recombinant PR8 virus lacking NS1 effector domain (deltaNS1 ED) showed impaired surface glycoprotein HA mRNA levels, suggesting a role for NS1 in viral RNA synthesis (Maamary et al., 2012). Laboratory studies revealed efficient hijacking of cellular protein synthesis by influenza viruses and NS1 is believed to be the contributor to preferential viral protein

translation by shutting off host gene expression (Ayllon and Garcia-Sastre, 2015).

High throughput sequence screening coupled with bioinformatics tools have identified a PDZ domain-binding motif (PDM) at the C-terminal of IAV NS1 with a conserved sequence RSKV/RSEV in human isolates and ESEV/EPEV in avian influenza virus isolates (Obenauer et al., 2006). PDZ domains are critical in cytoskeletal receptor protein anchorage and play a role in the regulation of signalling pathways (Harris and Lim, 2001). The PI3K signalling pathway is ascribed as the checkpoint in the regulation of cellular homeostasis hence is tightly regulated. Recent studies have suggested the occurrence of mutations at two important positions in HPAI H5N1 virus NS1, one at PDM ESEV to ESKV and the second at F138Y. These two sites are suggested to play role in the interaction of PDM with cellular PDZ domain proteins and PI3K induction (Fan et al., 2013). A mouse infection study with A/duck/Hunan/69/2004 (H5N1) virus carrying NS1 PDM ESEV and 138F proved fatal. While H5N1 virus carrying NS1-PDM ESKV and 138Y resulted in the confinement of infection to respiratory tract in the infected mice, possibly suggesting a synergistic interplay between PDZ domains and NS1 PDM in AIV virulence and virus mediated PI3K activation (Fan et al., 2013).

5.1.3 The p85β-NS1 interaction and its significance in PI3K activation

The functional interaction of IAV NS1 with host proteins modulates many host cellular processes contributing significantly to disease pathogenesis as described previously. Infection of cells with a mutant virus with deltaNS1, showed reduced Akt phosphorylation, suggesting the importance of NS1 in PI3K/Akt activation (Ehrhardt et al., 2006). It was demonstrated that direct interaction of IAV NS1 with p85β inter SH2 (iSH2) region as the novel mechanism for the activation of the pathway in virus infected cells (Hale et al., 2006, Li et al., 2008, Hale et al., 2008). The molecular determinants that facilitated the PI3K activation in AIV infected cells were elucidated based on the fact that the class-I PI3K p85α and p85β regulatory subunits consists of two SH2, one SH3 and other protein interacting domains (Figure 5-1A) (Okkenhaug and Vanhaesebroeck, 2001). The SH2 domains are considered as the primary readers of phosphotyrosine and mostly recognise phosphotyrosine motifs embedded in a specific YXXM consensus format enabling p85 binding (Songyang et al., 1993, Pawson, 2004). The AIV NS1 also has a YXXXM motif at amino acid (aa) 89–93 position, that is similar to the p85 SH2-binding motif YXXM.

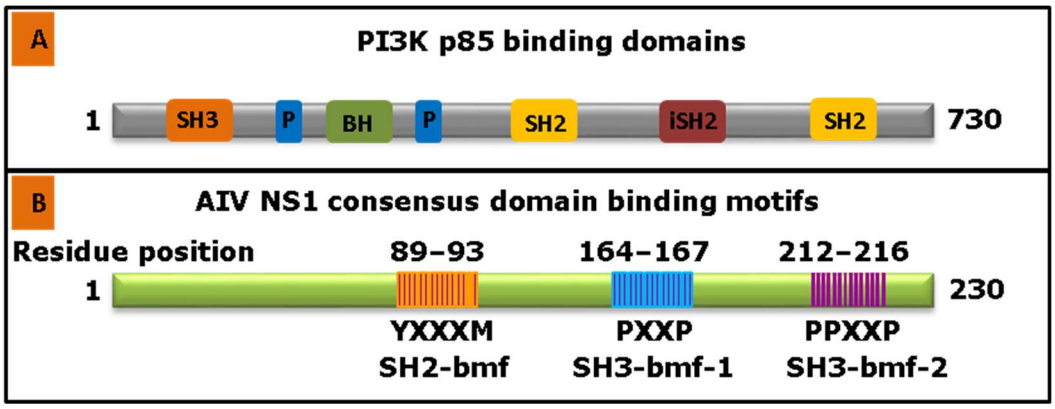


Figure 5-1: Distribution of domains and binding motifs.

A) PI3K-p85, hosts N terminal SH3 domain, BH domain located between two proline-rich regions. The iSH2 is tethered between N and C-terminal SH2 domains. **B)** AIV NS1 domain architecture showing the position of two SH3 domain binding motifs-1 and 2 and an SH2 domain binding motif positioned at Y89.

A study in HEP2 cells constitutively expressing PR8 virus NS1 effector domain confirmed the indispensable role of a tyrosine residue at position 89 for direct interaction of AIV NS1 with p85β-iSH2, resulting in the phosphorylation activation of PI3K downstream kinase Akt (Figure 5-2) (Hale et al., 2006). In the inactive state, the p85β regulatory subunit stabilises the catalytic subunit (p110) and exerts an inhibitory action on PI3K lipid kinase activity. The p110 inhibitory effect is relieved by binding of NS1 phosphotyrosine motif to the N-terminal SH2 domain in the p85β (Yu et al., 1998).

Recent studies have demonstrated the presence of two proline-rich motifs within the AIV NS1 sequence, carrying consensus sequence PXXP at aa 164–167 and at 213–216 positions with PPXXP proposed as SH3 binding motif-1 (SH3-bmf-1) and SH3-bmf-2 respectively (Figure 5-1B) (Shin et al., 2007c). Binding domains of such proline-rich motifs were found within host signalling proteins

like PI3K-p85 subunit (Pawson, 1995). Mutational analysis of NS1 revealed contribution of SH3-bmf-1 in PI3K activation over SH3-bmf-2 (Shin et al., 2007a). Over expression of p85β SH3 in MDCK cells as an antiviral strategy resulted in reduced Akt phosphorylation and consequently reduced viral replication, however the effect observed was virus strain dependent (Zhang et al., 2010).

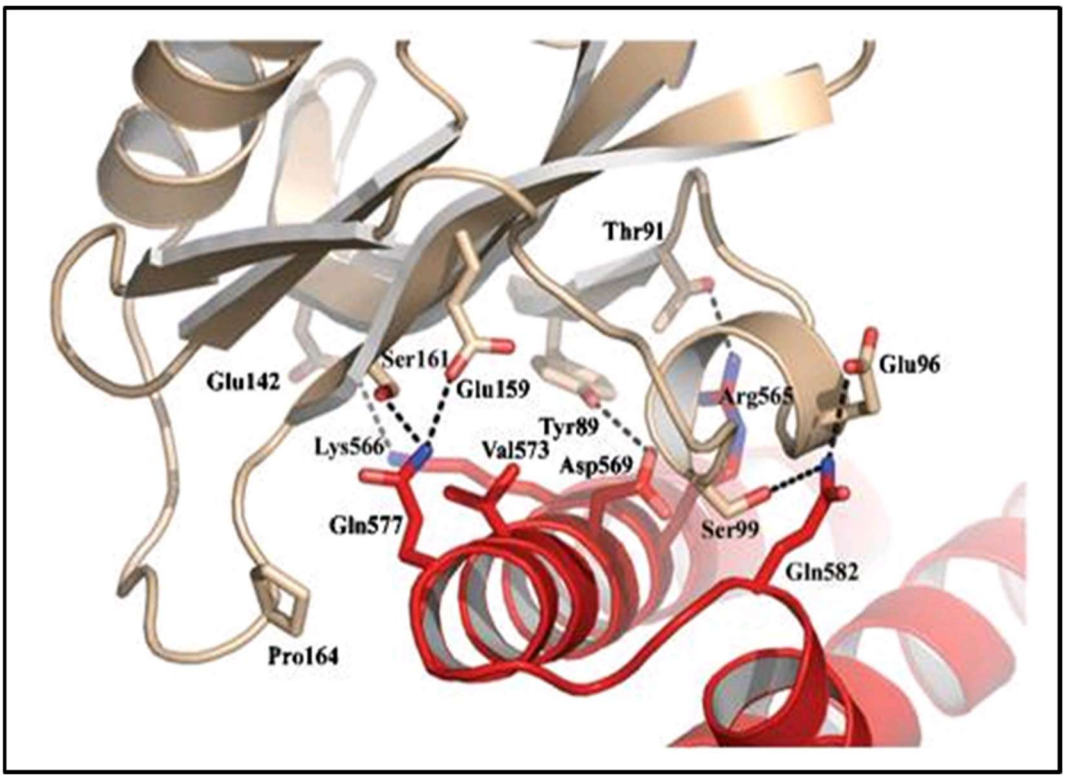


Figure 5-2: p85β-iSH2 protein-protein interaction interface showing the amino acid residues involved in the complex formation.

NS1 is labelled in gold colour and p85-iSH2 is shown in red. Interacting amino acid residues are represented as sticks and potential hydrogen bond formation are indicated by dotted lines in black. NS1-Tyrosine at position 89 is shown to interact with aspartic acid residue at position 569. Image graphics modified from (Hale et al., 2010).

5.2 Aims and objectives

5.2.1 Aim

To study the innate host response to LPAI and HPAI viruses and evaluate the role of influenza A virus NS1 in PI3K/Akt activation.

5.2.2 Objectives

1. To profile host innate response to LPAI and HPAI viruses in chicken cells
2. To profile and compare PI3K activation in recombinant LPAI H9N2 and HPAI H5N1 virus-infected chicken cells
3. To generate recombinant influenza viruses with NS1 swaps from HPAI virus to investigate the role of AIV NS1 in PI3K activation.
4. *In-silico* AIV NS1–PI3K p85 protein-protein interaction modelling to decipher potential virus and host-specific sites that drive PI3K activation.

5.3 Materials and Methods

5.3.1 Infection of chicken fibroblast cells and collection of cell lysates

The chicken fibroblast cells grown in 6 well plate format were infected with either H2N3 or H6N1 virus at an MOI of 1 following the protocol described in 2.2. The virus inoculum was washed two hours post infection and 2ml fresh infection medium was dispensed in each well before incubating the plates at 37°C at 5% CO_2 level. The cell lysates from H2N3 or H6N1 virus infected cells were prepared in RLT plus buffer (Qiagen) for RNA extraction at 9 and 24 hpi. The Work involving HPAI H5N1 (50-92) virus infections, and RNA isolation from these infected samples, was carried out at APHA Weybridge with kind support from Sharon M. Brookes and Ian H. Brown, These RNA samples were transported to school of veterinary medicine and science Sutton bonington campus, University of Nottingham for cDNA conversion and gene expression analysis. The cDNA samples from H5N1 virus infected cells were kindly provided by Kuchipudi et al. (2014) to carry out gene expression studies in the present work.

5.3.2 RNA extraction, cDNA conversion and gene expression studies.

The relative quantification of host innate immune-related gene expression was performed from virus infected or uninfected control cells using SYBR green chemistry on a LightCycler® 96 machine

(Roche) by reverse transcription-quantitative polymerase chain reaction (RT-qPCR). Total RNA was extracted from H2N3 or H6N1 virus infected or mock infected cells using the RNeasy mini kit (Qiagen) according to the manufacturer's protocol. Briefly, cells were lysed by adding RLT buffer, and the lysates were homogenized by QIAshredder (Qiagen) and centrifuged at 8000 *g* for 2 min. The flow-through was transferred to a gDNA eliminator spin column placed in a 2 ml collection tube and centrifuged at 8000 *g* for 30 s. A volume of 500 µl, 70% ethanol was added to the flow through and mixed well by pipetting. The mixture was then transferred to an RNeasy spin column placed in a 2 ml collection tube and centrifuged at 8000 *g* for 15 s. The flow-through was discarded and 500 µl of RPE buffer was added to the RNeasy spin column and centrifuged at 8000 *g* for 2 min. After discarding the flow-through, the spin column was placed in a new collection tube and centrifuged at 8000 *g* for 1 min. The spin column was placed in a 1.5 ml centrifuge tube and 30 µl RNeasy-free water added. Subsequently, the spin column was centrifuged at 8000 *g* for 1 min to elute RNA. The quality and concentration of extracted total RNA was determined by Nanodrop ND1000 spectrophotometer (Thermo Scientific) according to the manufacturer's instructions.

Complementary DNA (cDNA) was synthesized from 1 µg of total RNA sample using Superscript III First Strand synthesis kit (Invitrogen) following the manufacturer's instructions. Briefly, 1 µl

of random hexamers, 1 µl of 10 mM dNTPs (Invitrogen) and 1 µg of total RNA were mixed together and made up to 13 µl with diethylpyrocarbonate (DEPC)-treated water. The mix was incubated at 65°C for 5 min before placing on ice for at least 1 min, and 7 µl cDNA synthesis mix comprising 4 µl of 5x RT buffer, 1 µl of 0.1 M DTT, (Invitrogen) 1 µl of RNase OUT (Invitrogen) and 1 µl of SuperScript III reverse transcriptase enzyme (Invitrogen) was added to all the tubes. The total reaction mix of 20 µl was incubated at 25°C for 5 min, followed by incubation at 50°C for 1 h. The reaction was terminated by heating at 70°C for 5 min. cDNA was stored at -20°C.

Normalisation of RT-qPCR reactions and relative gene expression quantification by standard curve method

Normalisation of quantification cycle (Cq) values was performed using *18S* rRNA; 18S has been shown to be an appropriate normalisation gene for chicken cells infected with influenza virus (Kuchipudi et al., 2012b). The standard curve for each gene was plotted based on Cq value and log concentration of five 2-fold-serial dilutions of a pool of all cDNA samples. The R^2 slope value was calculated by linear regression analysis. The relative expression of the target gene was determined by the concentration of target gene divided by the concentration of *18S* rRNA.

5.3.3 Host immune related gene expression analysis

The response to AIV in CEF cells was studied by gene expression analysis by RT–qPCR using cycling profile as in Table 5-1. The data were analysed using LightCycler® 480 SW 1.5 software (Roche). Primer sequence for chicken 18S rRNA, was as previously described (Kuchipudi et al., 2012a, Barber et al., 2010). Oligonucleotide primers for rest of the genes listed in Table 5-2 were designed from published sequences using Primer Express software version 3.0.1 (Applied Biosystems). All primers were synthesised by Sigma Aldrich. The statistical analysis of data was done using GraphPad Prism statistical analysis package.

Table 5-1: SYBR green-based RT-qPCR cycling profile

Steps		Cycling temp (°C)	Time (S)	Cycles
Initial denaturation		95	300	1
Melting	Denature	95	10	45
	Annealing	55	30	
	Extension	72	20	
Melting	Denature	95	5	1
	Annealing	65	60	
	Extension	72	1	
Cooling		4	Hold	1

Table 5-2: List of primers used in the study

Gene Name	Primer	Sequence (5'-3')*	Accession No/ Source
Interferon-α (IFN-α)	Forward	CTTCCTCCAAGACAACGATTACAG	NC 006127
	Reverse	AGGAACCAGGCACGAGCTT	
Interferon-β (IFN- β)	Forward	TCCAACACCTCTTCAACATGCT	NC 006127
	Reverse	TGGCGTGTGCGGTCAAT	
TLR-3	Forward	GCAATTTCTCCTTCACCTTTTCA	NC 006091
	Reverse	CCTTTATGTTTGCTATGTTGTTATTGCT	
TLR-7	Forward	GAATTCAAGAGGTTCAGGAACATGA	NC 006088
	Reverse	TTAGGGCAGGGAGTACAAGGATAT	
Interleukin-1β (IL-1 β)	Forward	TGCTGGTTTCCATCTCGTATGT	NC 006109
	Reverse	CCCAGAGCGGCTATTCCA	
IL-6	Forward	CACGATCCGGCAGATGGT	NC 006089
	Reverse	TGGGCGGCCGAGTCT	
IL-8	Forward	CCCTCGCCACAGAACCAA	NC 006091
	Reverse	CAGCCTTGCCCATCATCTTT	
IL-18	Forward	GGCAGTGGAATGTACTTCGACAT	NC 006111
	Reverse	ACCTGGACGCTGAATGCAA	
Melanoma differentiation-associated protein-5 (MDA-5)	Forward	AGGAGGACGACCACGATCTCT	NC 006094
	Reverse	CCACCTGTCTGGTCTGCATGT	
Oligoadenylate synthetase (2',5'-OAS)	Forward	GGTGCTCTTCATCAACTGCTT	NC 006099
	Reverse	CTCGATGATGGCGAGGAT	
LITAF	Forward	CCCTTCTGAGGCATTTGGAA	AY765397
	Reverse	CAGCCTGCAAATTTTGTCTTCTT	

5.3.4 Recombinant influenza virus rescue

The recombinant(r) viruses with specific genetic constellations were rescued using reverse genetics (RG). Reverse genetics tool allows generation of a 'recombinant infectious virus clone' from full-length viral genome cDNA copy integrated into a plasmid DNA. AIV RG includes co-transfection of cells with eight transcription plasmids carrying eight viral RNA segments together with four (NP, PA, PB1, and PB2) protein expression plasmids or eight bidirectional plasmids representing viral segments. After incubation for 48 hrs, cell supernatants are harvested and subjected to a haemagglutination assay for detection of infectious virus particles (Neumann et al., 1999) (Figure 5-3).

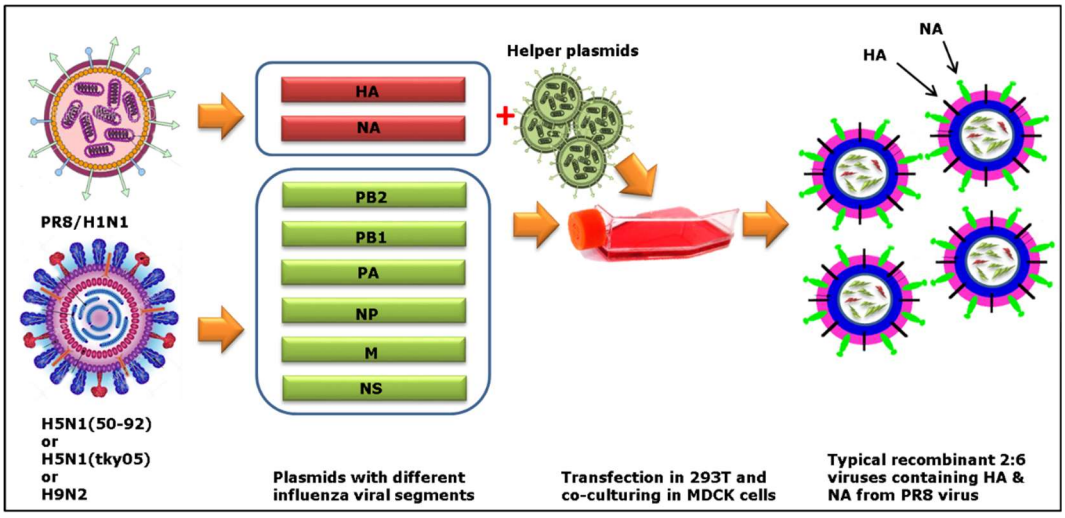


Figure 5-3: Illustration of recombinant virus rescue.

Individual plasmid DNAs incorporating viral gene segments along with four helper plasmids were co-transfected in 293T cells in the presence of lipofectamine 2000. After four hrs, the transfected 293T cells were re-suspended and co-cultured with MDCK cells for optimum virus replication.

5.3.5 Recombinant viruses used in the present study

Both H5N1 (tky05) and H5N1 (50-92) exhibit marked phenotypic differences when infected to chicken and ducks. Infection with H5N1 (tky05) results in higher mortality and show greater transmissibility in ducks compared to chickens. However, 100% fatal in chickens when compared to ducks. While H5N1 (50-92) infection in chickens is more sever causing greater mortality, but, non-infectious to ducks. These virus subtype specific factors that contribute to the differences in disparate disease outcome can be better understood by generation of recombinant(r) viruses with specific genetic constellations. In the present study 2:6 H5N1 (50–92), or H5N1 (Tky05) or rH9N2 viruses were generated using two membrane glycoproteins (HA and NA) derived from the mouse-adapted PR8 strain A/Puerto Rico/8/1934 (H1N1). The remaining six internal genes were derived from various AIV subtypes as indicated in Table 5-4. The recombinant viruses were rescued by co-transfection of the 12-plasmid system: 8 pol I plasmids and 4 helper expression plasmids encoding A/Victoria/3/75 (VIC) polymerase components and NP expressed by the pCAGGS vector. The 2:6 viruses were generated at The Pirbright Institute, UK (Munir et al., 2013, James et al., 2016, Long et al., 2016). The plasmid constructs for individual viral segments used for generation of recombinant viruses with segment eight swaps in the present study were kind gift from Dr Holly Shelton, The Pirbright Institute, UK.

Virus rescue with segment eight (NS) swaps was generated in the present study by transfection of 293T cells. Briefly, the transfection mix was prepared by mixing 1 µg of required plasmid DNA (Table 5-3) in 100 µl of OptiMEM (Gibco) in a 1.5 ml centrifuge tube and incubated for 5 minutes. While in incubation, OptiMEM and lipofectamine 2000 (Invitrogen) mix was prepared by adding 3.5 µl lipofectamine to 100 µl of OptiMEM in a separate 1.5ml tube by gentle mixing. The OptiMEM-lipofectamine and DNA mix were combined into a single tube and mixed gently and incubated for 15 min at RT. Meanwhile, the requisite number of wells of a 12-well plate containing 293T cells were labelled, gently washed twice with OptiMEM. After incubation, all 200 µl transfection mix containing DNA was pipetted and added on to 293T cells drop by drop. An additional media supplementation was done by adding 300 µl OptiMEM media per well containing 2% FCS without antibiotics. Once the whole process was complete, the cells were incubated for 4 hrs. After 4 hrs incubation, the transfection medium was gently removed and disposed of in 1% Virkon (Dupont). The cells were then supplemented with 1ml growth medium (DMEM+10% FCS) and incubated overnight at 37°C with 5% CO2.

Table 5-3: Details of plasmids used and the concentrations.

Virus subtype	Plasmid with viral gene	DNA conc ng/ul
PR8/H1N1	PB2	2368
	PB1	1323
	PA	1284
	HA	1204
	NP	1262
	NA	1259
	M	673.5
	NS	1097.7
UDL H9N2	PB2	1094
	PB1	635
	PA	1700
	NP	1012
	M	938.58
	NS	845
H5N1 (50-92)	PB2	1145
	PB1	472
	PA	1051
	NP	1319
	M	1336
	NS	1150

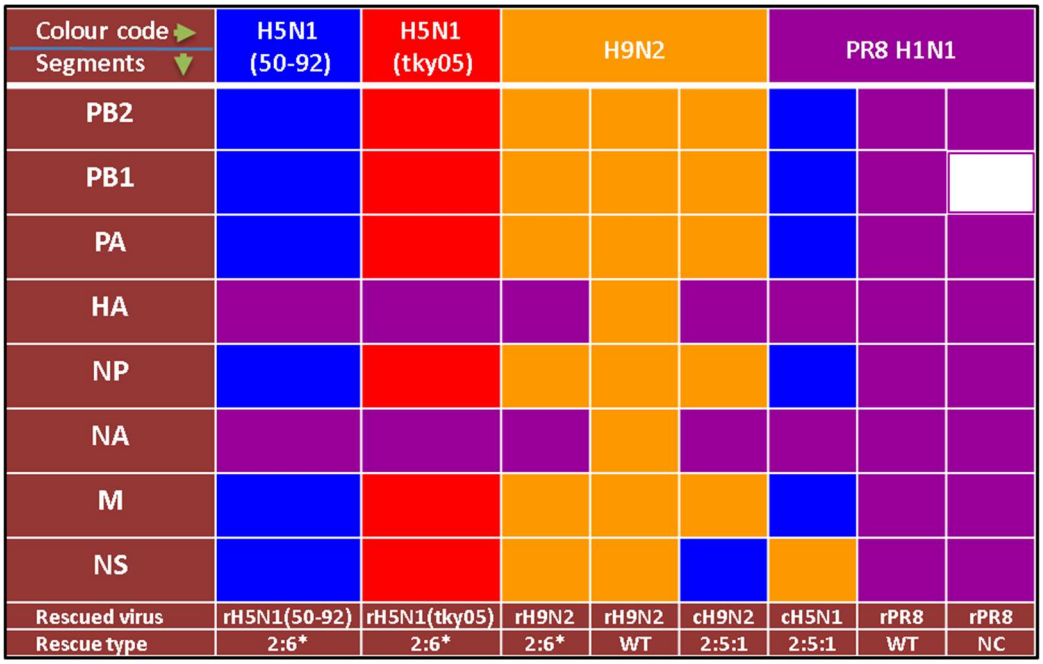
On the following day, confluent MDCK cells grown in a T75 flask were trypsinized, pelleted, re-suspended and distributed into fresh T25 flasks at the rate of 4 ml per flask. The transfection medium from 12-well plate was removed and the 293T cells were gently dislodged and re-suspended by pipetting 1 ml fresh growth medium per well. Once the cells were completely suspended, the whole content was mixed into a T25 flask containing 4 ml MDCK cells for co-culturing and incubated for 2 hrs. Once the cells attached to the flask, the medium was removed and the cells were washed with OptiMEM once

before adding 5 ml virus growth medium (DMEM+2mg/ml TPCK trypsin). The flasks were incubated for 3 days at 37°C with 5% CO_2 before observing 50% cytopathic effect (CPE). After 72 hrs incubation, supernatants from all the wells were collected separately and centrifuged at 1200 rpm for 5 min at 4°C. Although, attempted for four different combinations of virus rescue (rH9N2WT, rH9N2 (2:5:1) with NS from H5N1 (50-92), rH5N1 (2:5:1 with NS from H9N2 and PR8 (WT), only two types, rH9N2 (2:5:1) with NS from H5N1 (50-92) and PR8 (WT)) have been successfully rescued. Haemagglutination assay (HA) was performed to titrate the virus using the supernatant. All the viruses showing positive HA test were propagated in 10-day-old embryonated hen's eggs and allantoic fluid was harvested at 72 hours post inoculation. Allantoic fluid containing infectious virus was aliquoted and stored at -80°C.

All the combinations of recombinant viruses generated or attempted for rescue are as indicated in Table 5-4. The PB1 deficient rPR8 virus served as the negative control in the rescue process. For ease of identification the triple reassortant H9N2 carrying NS segment from H5N1 (50-92) is referred as chimeric H9N2 (cH9N2) whilst all other reassortants are prefixed with 'r' implying recombinant rescued virus subtype, throughout the chapter. Rescue of cH5N1 carrying NS segment from the H9N2 virus was unsuccessful. Recombinant virus rescue work was carried out at the Pirbright institute in accordance with Health and Safety Executive

approvals at biosafety level 2 laboratory facility at The Pirbright Institute, United Kingdom.

Table 5-4: The details of virus rescue combinations study



Virus rescue combinations generated or used in the present study are indicated above. Colour coding indicates the segment derived from. * indicates 2:6 viruses rescued at the Pirbright institute as mentioned in 5.3.5

5.3.6 PI3K–p85β and AIV NS1 sequence analysis.

In silico protein sequence analysis was performed using freely available bioinformatics tools. The viral NS1 and PI3K p85β amino acid sequences from specific species were aligned using MUSCLE (multiple sequence comparison by log-expectation) an accurate multiple sequence alignment (MSA) tool for medium length protein sequences (www.ebi.ac.uk/Tools/msa/muscle/). Alignment results from MUSCLE were further processed on Expasy Boxshade for similarity dependent colour coding and generation of consensus sequences (https://www.ch.embnet.org/software/BOX_form.html). Functional analysis of protein sequences and classification into

families and predicting domains and important sites was performed on InterPro (www.ebi.ac.uk/interpro/). Amino acid residue based protein binding region identification of viral and host protein sequences were executed on PredictProtein www.predictprotein.org/) a service that predicts sequence based protein functional structures (Ofran and Rost, 2007). Protein 3D structural analysis highlighting functional sites and ligands of p85 β–NS1 complex was retrieved and generated in Proteopedia http://en.wikipedia.org/wiki/Proteopedia. Most of the 'in-silico' bioinformatics analysis in the present section is the original work performed by the student along with kind support from Tania Dottorini, Assistant Professor in Bioinformatics, Faculty of Medicine & Health Sciences, University of Nottingham.

5.4 Results

5.4.1 TLR expression was significantly higher compared RLR and NLR responses

Chicken embryo fibroblast cells were infected with either LPAI or HPAI viruses as described in section 2.2 to evaluate the host innate response to AIV infection. The H2N3 virus induced about eight-fold higher ($P \leq 0.0001$) TLR3 expression at 9 hpi compared to H6N1 virus or uninfected control, however, about two fold down regulation was observed in both LPAIs at 24hpi. Notably, expression levels in H6N1 virus infected cells were no longer significantly higher than uninfected controls at 24 hpi. However, TLR3 expression increased from three-fold higher than uninfected controls at 9 hpi to over ten-fold higher ($P \leq 0.0001$) at 24 hpi in H5N1 virus infected cells (Figure 5-4A). The TLR7 expression at 9 hpi in both LPAI infected cells was non-significant, rising to five-fold increase ($P \leq 0.0001$) at 24 hpi. However, H5N1 virus infected cells showed a fivefold higher TLR7 levels than uninfected controls ($P \leq 0.0001$) that increased from 9 to 24hpi (Figure 5-4B). Melanoma differentiation-associated protein 5 (MDA5) expression was a fold ($P \leq 0.01$) upregulated at 9 hpi while significantly downregulated ($P \leq 0.0001$) in H2N3 virus infected cells at 24 hpi. Both H6N1 and H5N1 viruses showed significant ($P \leq 0.0001$) down regulation of MDA5 than uninfected cells at 9 hpi however, the suppression was only

observed in H5N1 infected cells at 24 hpi while the expression from H6N1 virus infected cells at 24 hpi was nearly equivalent to uninfected control cells (Figure 5-4C). Induction of laboratory of genetics and physiology 2 (LGP2) at both 9 and 24 hpi was non-significant in H6N1 virus infected cells while a three fold ($P \leq 0.001$) upregulation was observed in H2N3 virus infected cells at 24 hpi. Initial downregulation of LGP2 in H5N1 virus ($P \leq 0.05$) at 9hpi was observed, however, was non-significant at 24 hrs post infection. NOD-like receptor family, pyrin domain containing 3 (NLRP3) was significantly ($P \leq 0.0001$) downregulated across all three virus subtypes. The overall expression pattern suggested lowered expression of cytosolic viral recognition receptors RLRs (MDA5 and LGP2) and NLRs (NLRP3) (Figure 5-4C, D and E) compared to TLRs (TLR3 and TLR7) (Figure 5-4A and B).

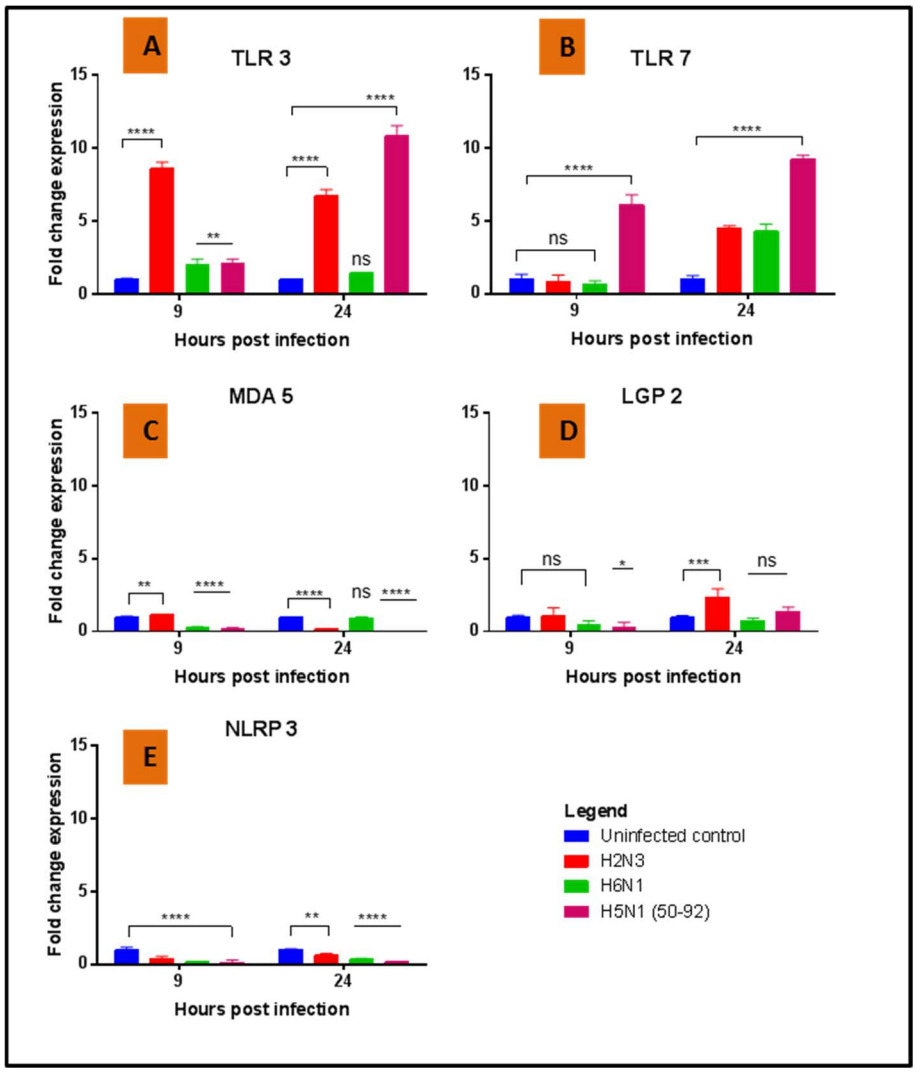


Figure 5-4: Expression of innate immune sensors of viral nucleic acids in AIV infected chicken cells.

(A) TLR3, (B) TRL7, (C) MDA5, (D) LGP2 and NLRP3 mRNA expression levels from H2N3 or H6N1 or HPAI H5N1 virus infected CEFs normalized to 18S RNA. The values indicate fold change expression levels compared to the uninfected controls at 9 and 24 hpi. Statistical analysis performed using two way ANOVA by multiple comparisons of means. Data points represent the mean and standard error of the mean (SEM) from three repeat experiments. Asterisk suggests level of significance *=0.05, **=0.01, ***=0.001 and ****=0.0001.

5.4.2 LPAI viruses induced more potent Mx1 and OAS response than an H5N1 virus.

The results of gene expression by CEFs infected with two LPAI viruses H2N3 and H6N1 or an HPAI H5N1 (50-92) virus revealed that H5N1 virus-induced early (9 hpi) and higher type-I response compared to the two LPAI viruses. A significant ($P \leq 0.0001$)

seventy-fold increase in IFNβ levels compared to uninfected controls was observed upon H5N1 infection at 9 hpi and moderately downregulated by 24hpi. Both H2N3 and H6N1 virus upregulated IFNβ and evidenced an upward trend from 12- and 6-fold ($P \leq 0.0001$) at 9 hpi to 30- and 10-fold ($P \leq 0.0001$) at 24 hpi, respectively (Figure 5-5B). H2N3 virus induced significantly higher ($P \leq 0.0001$) Mx1 expression of 230-fold at 9 hpi increasing to 326-fold at 24 hpi. Similarly, around 80-fold increase at 9 hpi and 60-fold increase at 24 hpi was observed in H6N1 virus infected cells (Figure 5-5C). Evidently, H2N3 and H5N1 virus infection resulted in about 80-fold ($P \leq 0.0001$) upregulation of OAS at 9 hpi whiel a 10 fold decrease at 24 hpi was observed. However, H6N1 virus only slightly but stably induced OAS at 20-fold difference compared controls at both time points (Figure 5-5D).

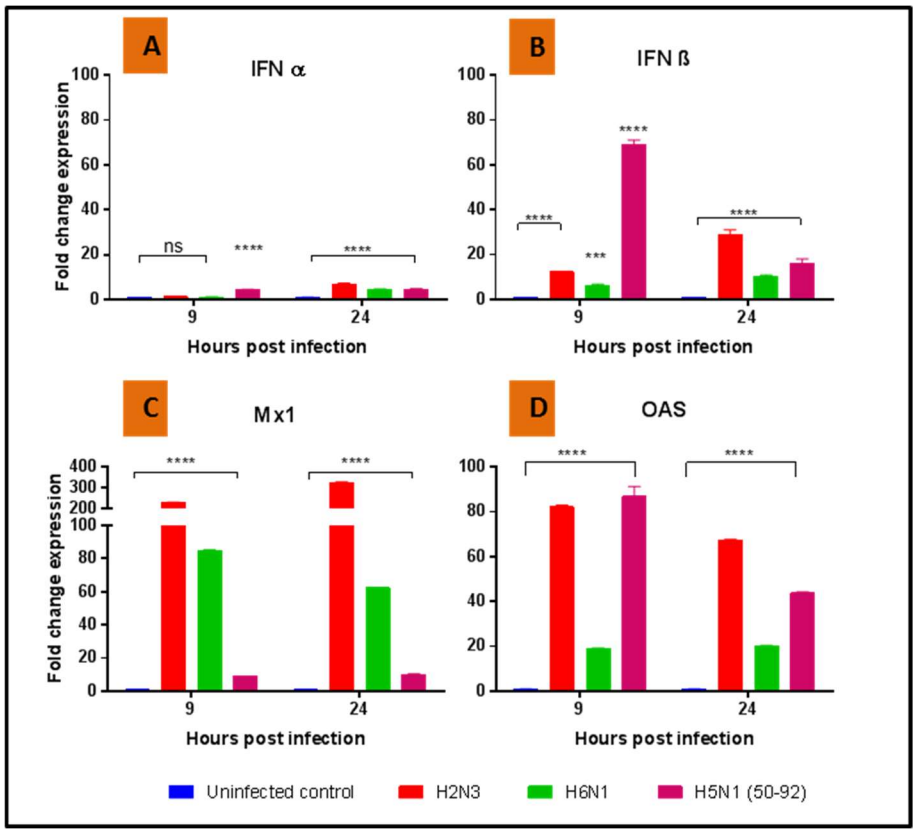


Figure 5-5: Induction of type-I interferon (IFN) response to HPAI H5N1 and LPAI virus infection.

(A)IFN-α, (B) IFN-β, (C) Mx1 and (D) OAS mRNA expression levels from H2N3 or H6N1 or HPAI H5N1 (50-92) virus infected CEFs normalized to 18S RNA. The values indicate fold change expression levels compared to the uninfected controls at 9 and 24 hpi. Statistical analysis performed using two way ANOVA by multiple comparisons of means. Data points represent the mean and standard error of the mean (SEM) from three repeat experiments. Asterisk suggests level of significance *=0.05, **=0.01, ***=0.001 and ****=0.0001.

5.4.3 LPAI and HPAI viruses differentially induce pro-inflammatory cytokine response in infected CEFs.

The results of transcriptional evaluation of pro-inflammatory cytokine response revealed an eight-fold higher ($P \leq 0.0001$) induction of IL1β at 24 hpi compared to an insignificant level at 9hpi by both LPAI viruses. H5N1 virus infection, although induced significant ($P \leq 0.0001$) levels of IL1β at both 9 and 24 hpi, the expression levels were moderately lower compared to both LPAI's at 24 hpi (Figure 5-6A). A pronounced ($P \leq 0.0001$) elevation of IL6

was observed in H5N1 virus infected cells at 9 hpi, with a reduction in levels during the progression of infection at 24 hpi. Similarly, there was the early moderate induction of IL6 by both LPAI viruses, with marked downregulation at 24hpi (Figure 5-6B). A ten-fold ($P \leq 0.0001$) induction at 9 hpi leading to a fifty-fold ($P \leq 0.0001$) increase in the levels of IL8 at 24 hpi was observed in cells infected with both LPAI viruses. While H5N1 induced nearly the same levels as LPAI viruses at 9 hpi and was severely downregulated compared to LPAI viruses at 24 hpi (Figure 5-6C). H5N1 (50-92) virus significantly ($P \leq 0.0001$) downregulated IL18 induction at both 9 and 24 hpi was significantly down-regulated in H6N1($P \leq 0.01$) and virus infected cells at both 9 and 24 hpi but the downregulation was comparatively more pronounced in H5N1 infected cells at both time points (Figure 5-6D). Both H2N3 and H6N1 viruses induced significantly ($P \leq 0.0001$) higher levels of LITAF, but the comparative level of expression was much higher in H2N3 virus infected cells at 9 and 24 hpi. A steady level of induction was observed in H6N1 virus infected cells at both 9 and 24 hpi (Figure 5-6E). Data points for H5N1 (50-92) not shown due to limited sample.

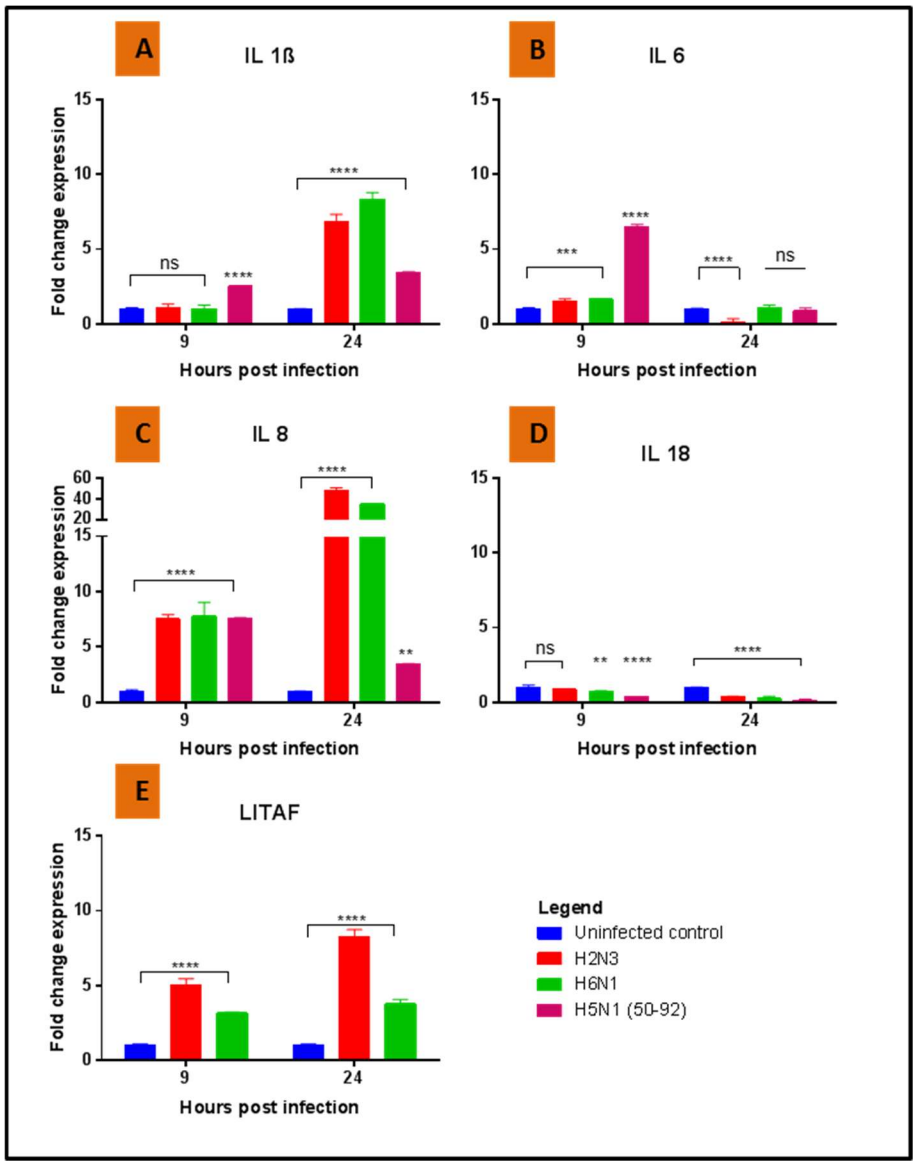


Figure 5-6: Pro-inflammatory cytokine expression in LPAI and HPAI virus infected chicken cells.

(A)IL1β, (B) IL6,(C) IL8, (D) IL18 and (D) LITAF mRNA expression levels from H2N3 or H6N1 or HPAI H5N1 (50-92) virus infected CEFs normalized to 18S RNA. The values indicate fold change expression levels compared to the uninfected controls at 9 and 24 hpi. Statistical analysis performed using two way ANOVA by multiple comparisons of means. Data points represent the mean and standard error of the mean (SEM) from three repeat experiments. Asterisk suggests level of significance *=0.05, **=0.01, ***=0.001 and ****=0.0001.

5.4.4 Recombinant H5N1 and rH9N2 viruses differentially activate PI3K/Akt pathway

Protein blotting results revealed inherent differences in the PI3K activation by HPAI and LPAI viruses as evidenced by the differences in Akt phosphorylation. Akt phosphorylation was not observed at 2

hpi in any of the virus infected cells. However, infection of CEFs with either rH5N1 (50-92) or rH5N1 (Tky05) resulted in prolonged Akt phosphorylation from 6 to 24 hpi (Figure 5-7A & B). Although activation of the PI3K pathway in rH9N2 infected cells followed a similar pattern to that of rH5N1 virus infected cells, activation was no longer apparent at 24 hpi (Figure 5-7C). The time-dependent increasing intensity of AIV PB1 protein from 6 to 24 hpi suggested an active viral infection across virus subtypes (Figure 5-7A, B and C). Non-phosphorylated native Akt protein was observed at four-time points in all the cell lysates irrespective of virus subtypes. Beta-actin was blotted as the loading control; that suggested uniform sample distribution (Figure 5-7A, B and C).

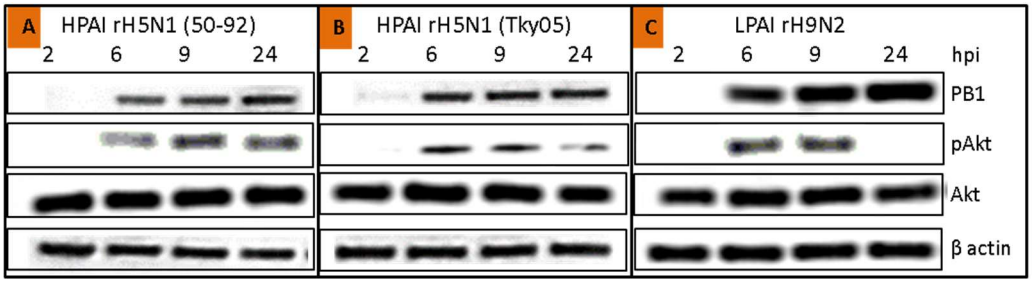


Figure 5-7: Akt phosphorylation in recombinant virus infected CEF cells.

Protein expression of CEF cell lysates infected with (A) rH5N1 (50-92); (B) rH5N1 (Tky05) or (C) LPAI rH9N2 virus, targeting antibodies against the viral PB1, Akt, and phosphorylated Akt (Ser473) proteins. A) and B) showing phosphorylation of Akt at 6, 9 and 24 hpi as indicated by the presence of pAkt protein. C) pAkt observed only at 6 and 9 hpi but not at 24 hpi. pAkt protein not observed in all three virus infected cells at 2hpi. Native Akt protein present at all four-time points in all three virus infected cells. A time-dependent increase in viral PB1 represents active virus infection. Presence of uniform β actin served as the internal loading control.

5.4.5 H5N1 NS1 is responsible for prolonged PI3K activation.

The role of AIV NS1 in PI3K activation was determined by generation of recombinant viruses with segment eight swaps. Protein expression profiling of cell lysates derived from recombinant

virus infected chicken cells revealed differences in the Akt phosphorylation. Both rPR8 (WT) and rH9N2 (2:6) viruses carrying PR8 surface glycoproteins (HA and NA) showed pAkt protein at only 6 and 9 hpi (Figure 5-8 B and C). Whilst, chimeric H9N2 virus encompassing NS segment from H5N1 (50-92) virus showed a prolonged pAkt protein expression from 6 to 24 hpi (Figure 5-8A), a distinct difference compared to those of rPR8 (WT) and rH9N2 viruses and is in line with the initial results obtained with rH5N1 shown in Figure 5-7. These observations clearly rule out the involvement of surface glycoproteins (HA and NA) in the regulation of PI3K activity, as all three (r)viruses had the same PR8 HA NA backbone (Table 5-3) hence confirms the significance of segment eight in Akt phosphorylation and PI3K activation. Presence of native Akt protein at all-time points suggests the uniform availability of precursor Akt protein (Figure 5-8) confirming variation observed in Akt phosphorylation is not due to the variation in Akt itself. A time-dependent increase in the accumulation of AIV PB1 protein at 6, 9 and 24 hpi indicated an ongoing active infection in the cells. Uniform distribution of beta-actin in all the samples proved as the internal loading control (Figure 5-8).

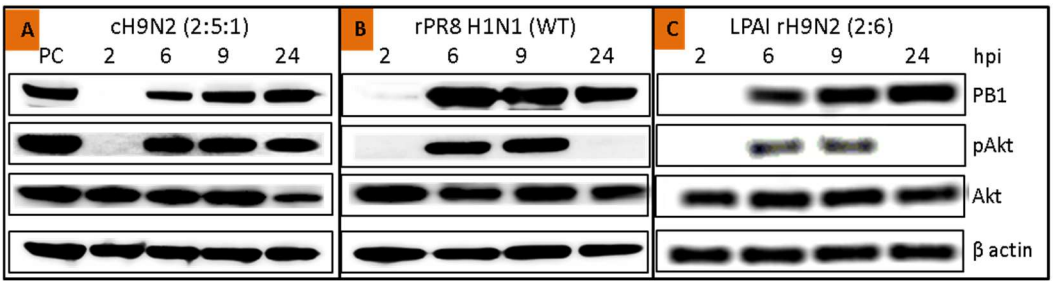


Figure 5-8: Prolonged activation of PI3K as evidenced by the presence of pAKT at 24 hpi in PR8 TRIG infected CEF's.

Representative protein blots from CEF cell lysates infected with (A) cH9N2 (2:5:1); (B) rPR8 H1N1 or (C) LPAI rH9N2 (2:6) virus, probed against the viral PB1, Akt, and phosphorylated Akt (Ser473) proteins. A) Showing phosphorylation of Akt at 6, 9 and 24 hpi as indicated by the presence of pAkt protein. B) and C) pAkt observed only at 6 and 9 hpi but not at 24 hpi. A, B and C) pAkt protein not observed in all three virus infected cells at 2hpi. Native Akt protein present at all four-time points in all three virus infected cells. A time-dependent increase in viral PB1 represents active virus infection. Presence of uniform β actin served as the internal loading control.

5.4.6 Infectious virus production was significantly reduced in PI3K/Akt inhibited cH9N2 virus infected CEF cells.

The implications of PI3K/Akt inhibition on cH9N2 infectious virus production in the infected chicken cells was determined by titration of supernatants harvested from infected chicken cells on MDCK cells. Titration results revealed an initial slower virus production until 9hpi and were non-significant across PI3K inhibited or carrier treated or untreated groups. A steep increase in virus titre was evidenced at 24 hpi in both carrier and untreated cells. However, the virus titre was significantly ($P \leq 0.0001$) reduced in PI3K inhibitor-treated cells (Figure 5-9).

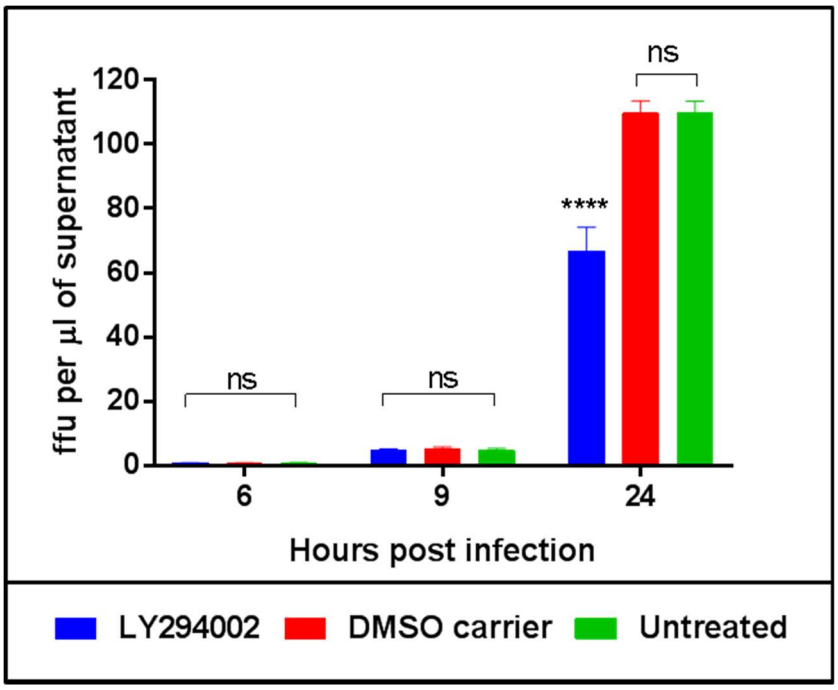


Figure 5-9: Significant reduction in virus titre in PI3K/Akt inhibitor-treated cells compared to the untreated cell.

Confluent CEF cells were infected with cH9N2 (2:5:1) virus at 1MOI. Two hrs post-infection, cells were treated with 20 µM LY294002 PI3K inhibitor. Supernatants were collected at 6, 9 and 24 hrs post-infection and were titrated on MDCK cells. The mean focus-forming units per µl were derived from triplicate wells. Error bars indicate the standard error of the mean (SEM). Statistical analysis was performed using two way ANOVA by multiple comparison of means. ****=P ≤ 0.0001, ns-non-significant.

5.4.7 AIV NS1 sequence analysis revealed variations in genetic constitution between HPAI and LPAI viruses.

Alignment of NS1 protein sequences from HPAI H5N1 (50-92) H5N1(tky05) and three other viruses H9N2, H6N1 and H2N3 virus used in the present study revealed variations in the amino acid (aa) residues at more than one position (Figure 5-10). The significance of a tyrosine (Y) residue at position 89 for PI3K-p85β binding was previously described (Hale et al., 2006) and is conserved across subtypes studied (Figure 5-10, highlighted in light red). However, three additional tyrosine residue modifications at positions Y14, Y103 and Y221 were exclusive to H5N1 (50-92) compared to other

four viruses, observed in the present study. The Y at positions 14 and 103 were substituted by phenylalanine (F) in all four viruses, and the Y at position 221 was replaced by lysine (K) in the H5N1 (tky05), H2N3 and H6N1 viruses, and arginine (R) in the H9N2 virus (Figure 5-10, highlighted in light green). Unlike most HPAI viruses, deletion of five aa residues from the 80-84 position was not observed in HPAI H5N1 (50-92), while the same was observed in H5N1 (tky05) virus NS1 sequence. Surprisingly, H5N1 (tky05) sequence closely matched sequences from UDL-01 H9N2 and two LPAI viruses used in the study except two specific modifications replacing serine at position 58 to asparagine (S58N) and F138Y compared to H5N1 (50-92) sequence.

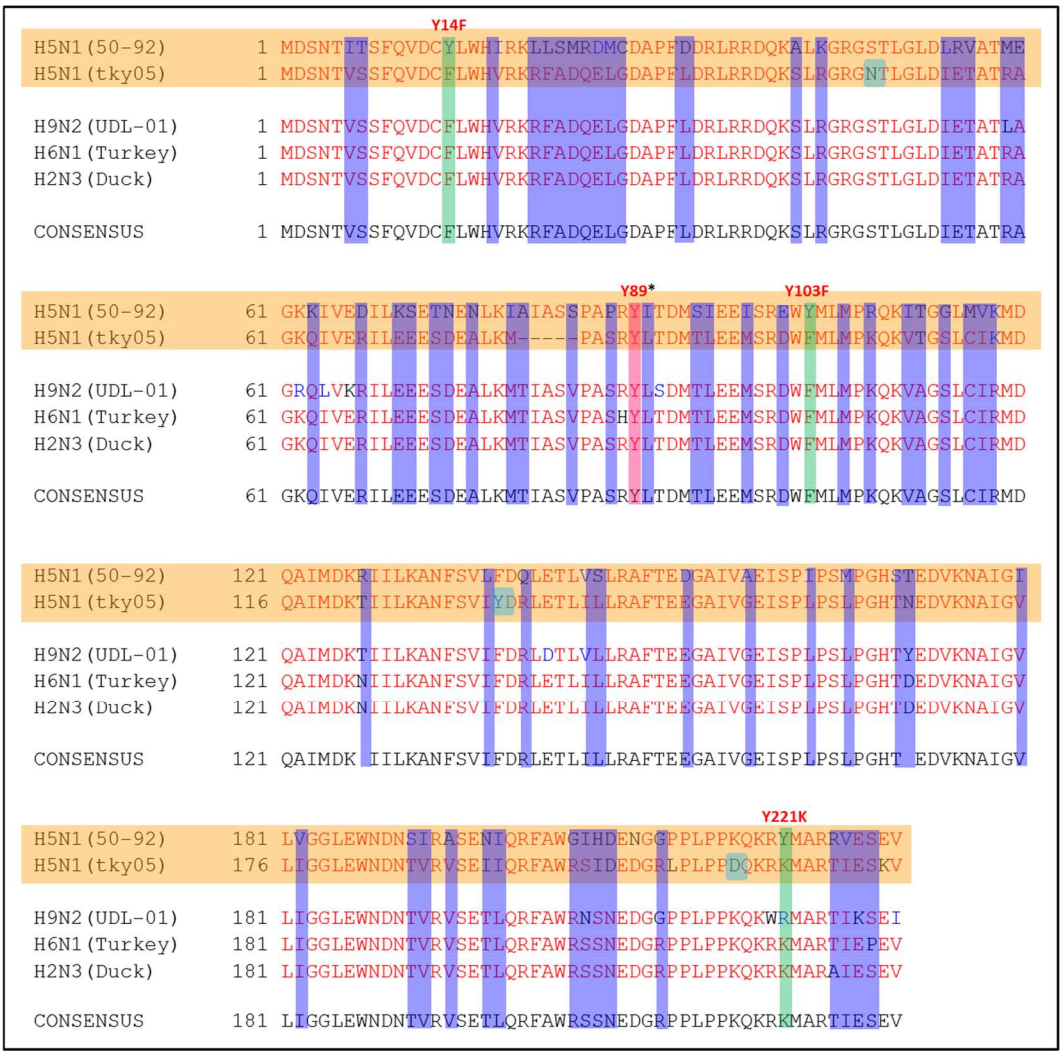


Figure 5-10: HP and LPAI NS1 sequence homology analysis reveal three tyrosine residue modifications.

Protein sequences of H5N1 (50-92) (AAC40503.1), H5N1(tky05) (ABQ58905.1) H9N2 (ACP50713.1) and the H2N3 (duck) and H6N1 (Turkey) virus NS1 gene sequenced at (source biosciences Nottingham, UK) during the present study were aligned using MUSCLE tool, colour coding of the alignment was performed using the Boxshade tool. The regions highlighted in light blue indicates the positions of aa substitutions. *Conserved tyrosine residue at position 89 across all five viruses, highlighted in light red. Three other specific tyrosine residue modifications were observed at Y14F, Y103F and Y221K highlighted in light green.

5.4.8 Presence of an additional SH3 binding motif 1 (SH3 bmf1) may contribute for prolonged PI3K/Akt activation in rH5N1 infected cells.

The presence of inherent differences in the NS1 protein sequences between H5N1 (50-92) and H2N3 viruses observed in (Figure 5-10), prompted to speculate if these differences influence the host protein binding affinity that results in differential PI3K

activation. Results of the protein binding site prediction showed the presence of more protein binding regions in H5N1 (50-92) NS1 compared to the H2N3 virus used in present study. Detailed analysis of the protein binding sites revealed presence of a polynucleotide binding site and protein binding sites at residues 20, 23-29, 46, 55, 59-60 and 62 in the RNA-binding domain (1-74 aa, RBD) and at positions 84, 152, 164-167, 197, 203, 209-213, 220-221 and 223-226 in the effector domain of H5N1 (50-92) (Figure 5-11 A). The binding sites observed in the H2N3 virus were at positions 4, 20, 24-27, 29, 35 and 59 positions in the RBD and at 76, 152, 197, 203, 209-213, 220 and 224-225 in the effector domain of the H2N3 virus (Figure 5-11B). The comparative evaluation revealed the presence of an additional SH3-binding motif-1 at position 164-167 in the H5N1 (50-92) virus (Figure 5-11 A), while SH3-bmf1 was absent in the H2N3 virus sequence (Figure 5-11B). Two amino acid residues at position 220-221 and three at 223-226 were involved in the formation of a binding region in H5N1 (50-92) virus (Figure 5-11 A) while only one at 220 and two at 224-225 positions form the binding site in H2N3 virus (Figure 5-11B).

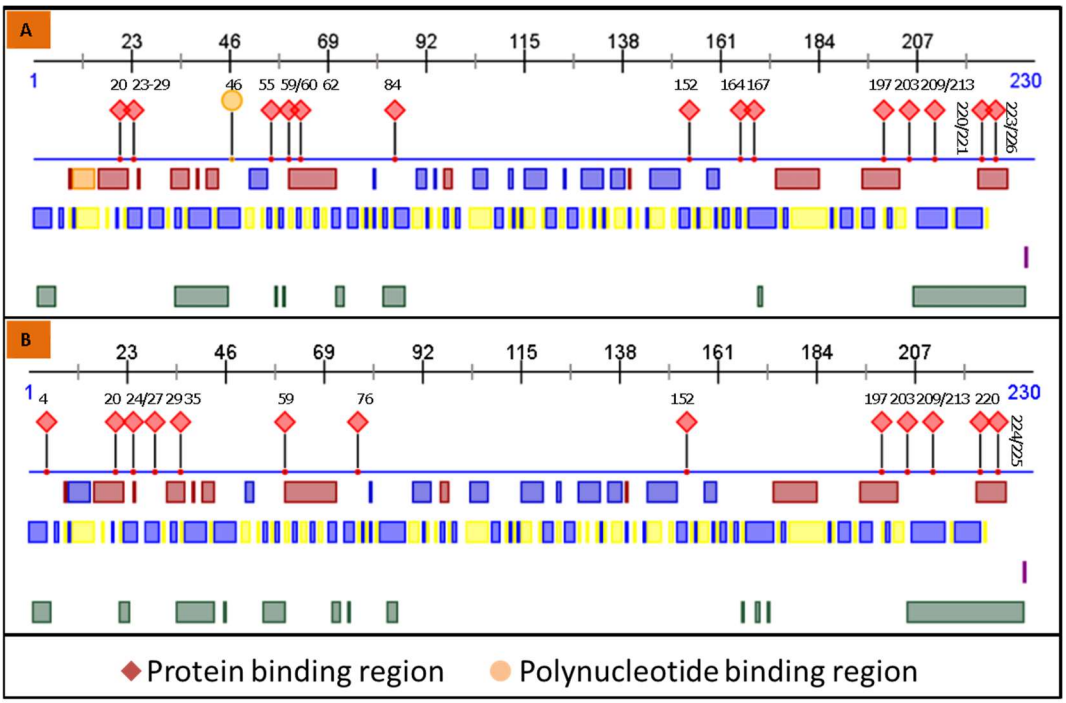


Figure 5-11: Positions of protein binding regions between HPAI H5N1 (50-92) and H2N3 virus NS1.

AIV NS1 sequence-based protein binding site identification performed on PredictProtein software (A) HPAI H5N1 (50-92) and (B) H2N3 virus. Coloured squares in the image represent Top line: Pink box=helix, Blue= Strand. Centre line: Blue=exposed residues, Yellow=buried residues. Bottom line: Grey box= disordered regions.

5.4.9 Duck PI3K-p85β subunit exhibits sequence diversity compared to chicken.

The inability of duck cells to activate the PI3K pathway despite AIV infection observed in the present study prompted further evaluation of PI3K-p85β regulatory subunit protein sequence. Analysis of the protein sequence in InterPro© revealed the presence of an equal number of domains in both chicken and ducks. Both chicken (Figure 5-12A) and duck (Figure 5-12B) p85β consisted of an SH3 domain followed by Rho-activating protein domain and two SH2 domains, divided into nSH2 (N-terminal SH2) and cSH2 (C-terminal SH2 by an inter-SH2 region (iSH2). Literature suggests the iSH2 region is indispensable for PI3K/Akt pathway activation.

Detailed mammalian and avian p85β sequence alignment and diversity analysis from selected species (Appendix-II) confirmed the presence of mammalian or avian specific aa residue substitutions in the sequence (Appendix III). Alignment of iSH2 sequences revealed a conserved amino acid glutamic acid (E) residue at position 475 (numbering based on duck sequence) across both mammalian and avian species (Figure 5-12 C and D). However, conserved E475 residue in chicken, was substituted by a non-polar valine (V) (E475V) in ducks (Figure 5-12D). Highly acidic glutamic acid residue with side chains may have potential role in post translational modification of p85β subunit that may have implications on AIV viral NS1-p85β interactions.

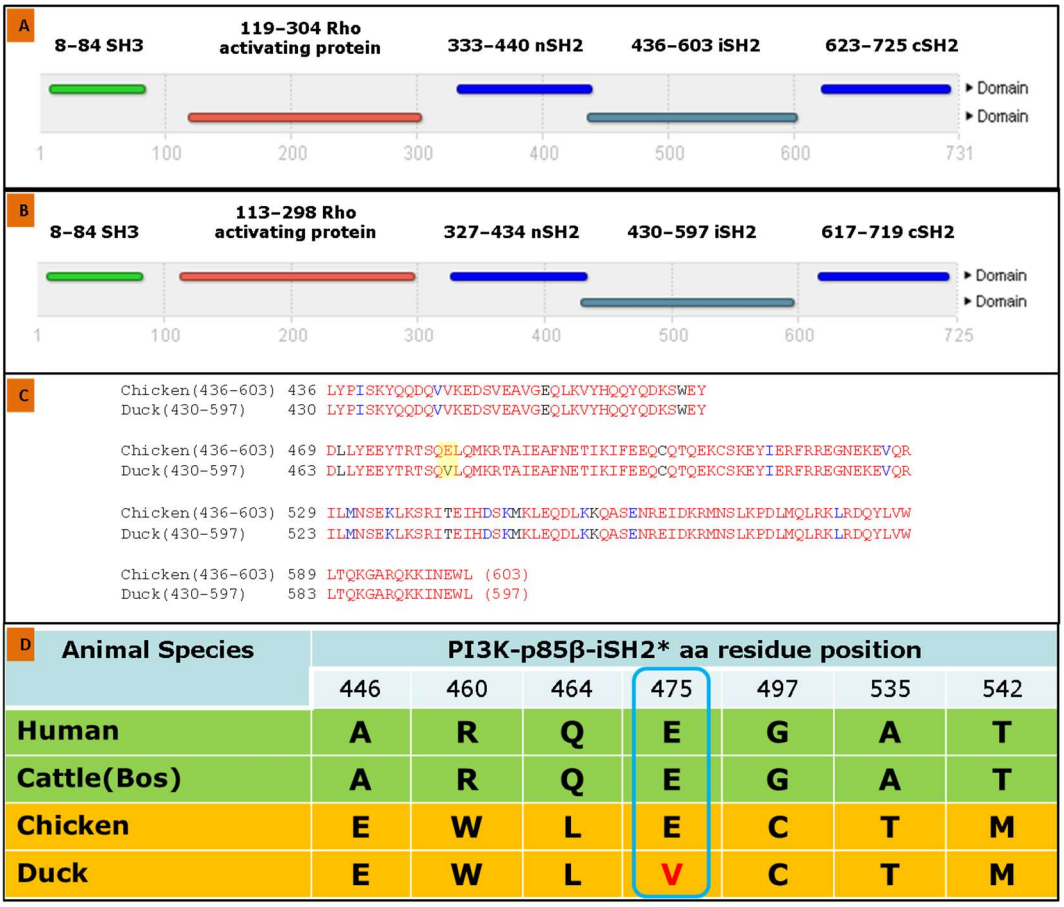


Figure 5-12: PI3K-p85β sequence analysis reveals a conserved Glutamic acid (E475) residue replaced by non-polar valine (E475V) in ducks.

Chicken and duck PI3K-p85β regulatory subunit sequence analysis and alignment summary. A) Chicken and B) duck p85β sequence-based domain identification performed on Interpro© protein functional analysis and classification tool. C) Chicken and duck p85β iSH2 domain sequence alignment. D) Important residue positions in the iSH2 domain depicting conserved residues within the mammalian or avian species. At position 475 (as per duck sequence) residue E is conserved across species except for duck where E is replaced by non-polar valine residue.

5.4.10 Protein structural modelling suggested E475V is bound on the helix outside the P85β–NS1 interaction site

Structural orientation of species-wide conserved glutamic acid (E) residue was determined using p85β, 3D protein structure (PDB id 2V1Y). The p85β (2V1Y) structure comprised of two SH2 domain and a coiled-coil iSH2 domain (depicted as yellow) tightly bound to an adaptor binding domain (ABD) of the catalytic unit (p110) (shown in blue colour (Figure 5-13A). A 3D model of 2V1Y depicting iSH2

(light green) along with adapter binding domain (grey colour) was generated showing the exact orientation of 475 amino acid residue, using Proteopedia residue identification tool (Figure 5-13B). The generated protein structure revealed the location of glutamic acid residue on the helix, indicated by yellow colour in the dorsal view (Figure 5-13B).

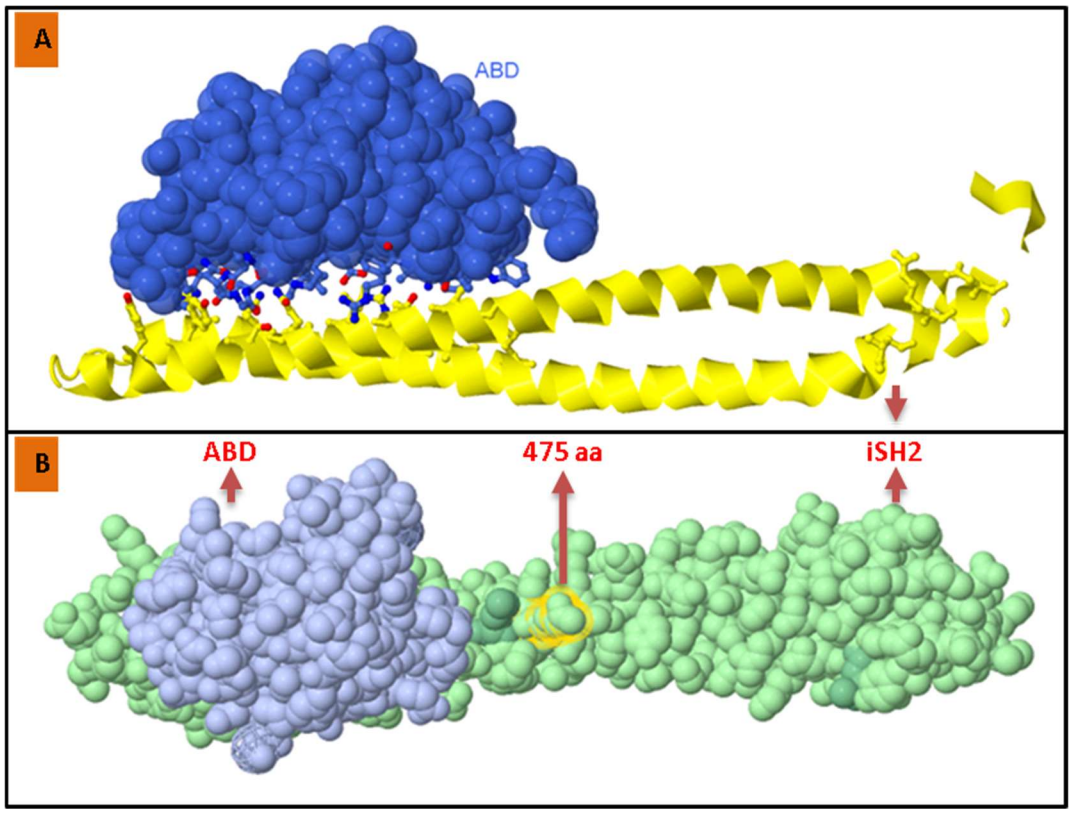


Figure 5-13: PI3K p85β-NS1 protein-protein interaction model.
Summary of P85β subunit structure. A) 3D structure of p85β showing iSH2 domain (Yellow) tightly bound to the catalytic domain through adapter binding protein (blue). B) Protein structure generated using Proteopedia showing the orientation of the glutamic acid residue (E475V) on the helix of iSH2 (Yellow). ABD is depicted in grey and iSH2 in light green colour.

5.4.11 In silico analysis revealed role of chicken p85β E475 residue in conferring protein binding sites on iSH2 domain

For better understanding the possible role of E475 residue in determining protein-protein interactions, chicken and duck p85β sequences were analysed for the formation of protein binding region

(PBR). Binding site prediction results showed a total of 10 binding sites in the original chicken sequence with 'E' at position 475 of which six sites were noted only in the iSH2 domain (436–603aa) (Figure 5-14A). Single aa residue substitution from E475V resulted in dramatic reduction in binding sites to only six and none were located in the iSH2 region. Additionally, a polynucleotide binding region (PnBR) region was introduced (Figure 5-14B). The original duck sequence with valine at position 475 resulted in only four binding sites and one PnBR, however, none were located on the iSH2 domain (430–597aa) (Figure 5-14C). Notably, replacement of V with E (V475E) in the duck sequence resulted in the prediction of a total of nine binding sites along with one PnBR and one protein binding site was located within the iSH2 domain (Figure 5-14D). Interestingly, replacement of E with V residue at position 475 in the chicken sequence resulted in the distribution of binding sites similar to that of duck original (V475) sequence (Figure 5-14B & C).

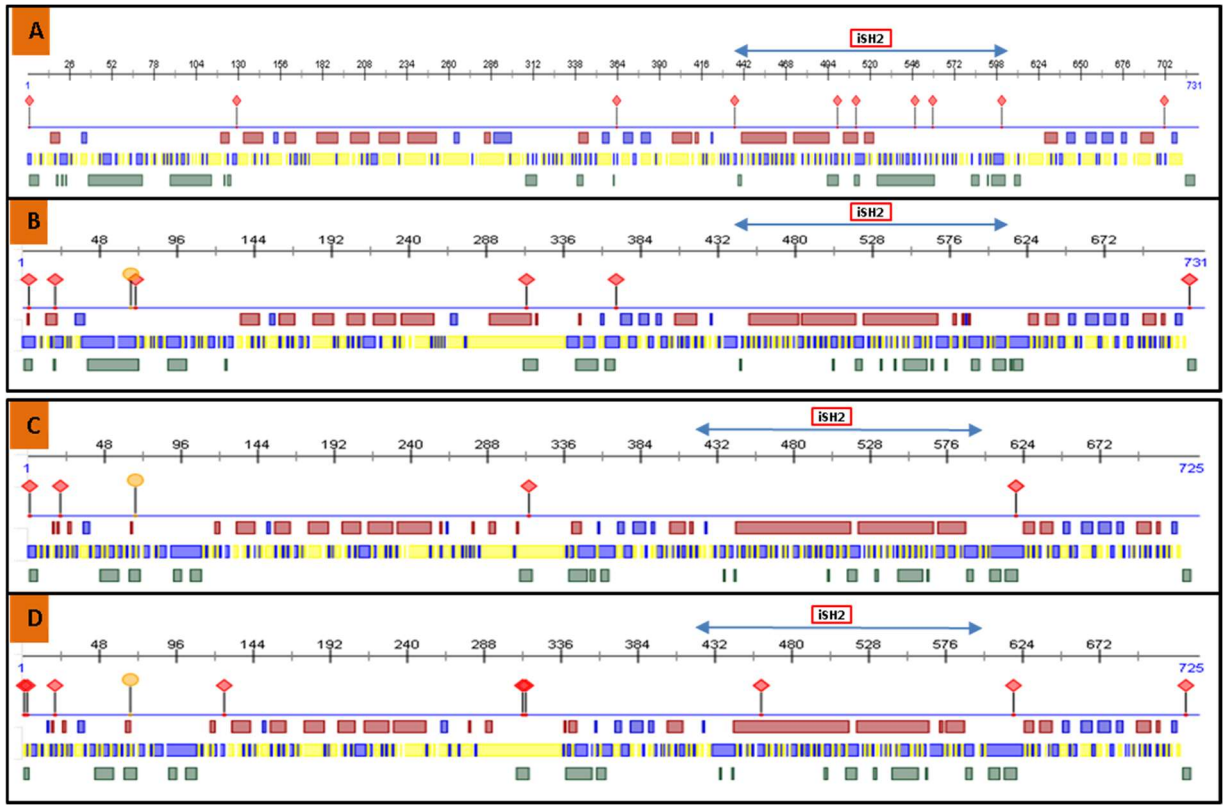


Figure 5-14: PI3K-p85β sequence-based protein binding site prediction

Chicken (A and B) and duck (C and D) PI3K-p85β sequence-based protein binding region detection. A) The original sequence with 'E' at 475 positions showing the concentrated distribution of protein binding regions in iSH2 region. B) Replacement of E475V residue resulted in a pronounced reduction (six) in binding sites and none were located on iSH2 region. C) Original duck sequence revealed very less number of binding sites (4) along with a polynucleotide binding region. D) Substitution of V475E in the duck sequence resulted in a reciprocal gain of the function showing nine active binding regions along with a polynucleotide binding site. Sequence-based protein binding site prediction was performed using PredictProtein software. Coloured squares in the image represent Top line: Pink box=helix, Blue= Strand. Centre line: Blue=exposed residues, Yellow= buried residues. Bottom line: Grey box= Disordered regions. ◆ PBR, ● PnBR.

5.5 Discussion

5.5.1 Host cytokine response to influenza virus infection

Present study revealed significantly higher expression of TLRs in H5N1 compared to LPAI virus infected cells, possibly suggesting the importance of TLRs for robust interferon response and cytokine storm. These findings are in agreement with previous observations (Le Goffic et al., 2006, Iwasaki and Pillai, 2014, Kuchipudi et al., 2014). A reduced IFNβ response at 24 hpi in H5N1 virus infected CEFs compared to 9 hpi is likely due to significant suppression of MDA5 at similar time point. The results showed pronounced early induction of IFN β in H5N1 virus infected cells. Higher expression of IFNβ than IFNα may be due to the fact that fibroblast cells preferentially express IFNβ. Potent induction of interferon-inducible genes, Mx1 and OAS by H2N3 and H6N1 viruses compared to H5N1 virus at 9 hpi suggested important role of Mx1 and OAS in conferring antiviral response especially in early stages of LPAI infections.

The rapid induction of pro-inflammatory markers to significantly higher level in H5N1 virus infected cells at 9hpi, probably suggests augmented host response against efficiently replicating virus. These observations correlate with previous observations of Kuchipudi et al. (2014) who also speculated increased pro-inflammatory response as the reason for the severity of the disease. Robust pro-inflammatory response in H5N1 virus

infected cells at 9 hpi may possibly leading to increased apoptotic death resulting in reduced pro-inflammatory response in advanced stages of infection. However, LPAI viruses induced significantly higher levels of pro-inflammatory markers IL1β, IL8 and LITAF at 24 hpi probably suggesting better host cellular response. As the immune system constantly needs to optimize the levels of activation and inhibition of immune response to prevent immune-mediated detrimental effects, TLR signalling might be tightly regulated by negative feedback mechanisms by activation of the PI3K pathway (Liew et al., 2005). (Ni et al., 2012) et al. (2012) have shown the involvement of the B-cell adaptor for PI3K (BCAP) in negative regulation of TLR response by activation of the PI3K pathway. However, there is a gap in the literature suggesting the existence of similar mechanisms in chicken cells and the possible role of influenza viral proteins like NS1 in mediating the PI3K response.

5.5.2 Differences in the rH5N1 and LPAI mediated PI3K/Akt activation and AIV NS1 contributions.

Comparative evaluation of PI3K/Akt activation between rH5N1 and rH9N2 or rPR8 H1N1 virus infected chicken cells revealed prolonged pathway activation in rH5N1 virus infected cells. cH9N2 virus carrying NS1 from HPAI H5N1 (50-92) confirmed the contribution of AIV segment eight in prolonged pathway activation possibly conferring cellular survival by exerting an anti-apoptotic effect to enhance progeny virus output. NS1 dependent PI3K/Akt

activation observed in present study substantiates similar observations in mammalian cells (Ehrhardt et al., 2006, Shin et al., 2007a, Shin et al., 2007b) as PR8 virus lacking NS1 (deltaNS1) failed to activate pathway (Ehrhardt et al., 2006). A significant reduction in progeny virus production in cH9N2 virus infected cells, observed in the present study as a consequence to chemical inhibition of PI3K/Akt pathway are in line with the previous observations in the mammalian cells (Ehrhardt et al., 2006, Hale et al., 2006, Shin et al., 2007b, Zhirnov and Klenk, 2007). Reduced virus output in cH9N2 virus infected cells upon PI3K/Akt inhibition is similar to that observed in LPAI virus infection experiments in the present study, these observations collectively suggest strong viral dependence on the host PI3K/Akt signalling for its replication needs. Hence we hypothesize "pro-viral" role of PI3K/Akt in AIV infected cells.

5.5.3 Differences in the genetic constellation of AIV NS1 and PI3K activation.

Analysis of NS1 sequences of all the five viruses used in the present study revealed differences in the amino acid constitutions. These changes in the NS1 sequences may possibly explain differences in PI3K activation between LPAI or rH9N2 and rH5N1 virus infected chicken cells, observed in the present study. Amino acid residues 1-73 forms the RNA binding domain (RBD), while the rest of the protein is identified as the effector domain (ED). RBD antagonises type-I IFN production while ED hosts essential host

protein binding motifs besides carrying nuclear import and export signals (Krug et al., 2003). Detection of highly conserved tyrosine residue at position 89 in all the viruses used in the present study is in agreement with Hale et al. (2006) who suggested the importance of Y89 residue in p85 iSH2 interaction and activation of PI3K/Akt. Besides Y89, three additional tyrosine residues at positions Y14, Y103 and Y221 were exclusively observed in H5N1 (50-92) NS1 sequences compared to other four viruses used in the present study. The tyrosine residue at positions Y14 and Y103 were substituted by phenylalanine (Y14F and Y103F) in all three viruses. While Y221K in the H2N3 and H6N1 viruses, and Y221R substitution was observed in the H9N2 virus. A similar study by Shin et al. (2007c) suggested the importance of both conserved Y89 and M93 residues in a consensus YXXXM format that serves as SH2-binding motif (SH2-bmf) for p85 binding. Observations in the present study also revealed presence of YXXXM consensus SH2-bmf in AIV NS1 and hence is in agreement with Shin et al. (2007c). Additionally, the presence of two proline-rich SH3 binding motifs, SH3-bmf-1 (PXXP) and SH3-bmf-2 (PPXXP) have been identified in AIV NS1; a mutational study revealed that only SH3-bmf-1 is involved in p85 binding and activation of PI3K (Shin et al., 2007a). In silico analysis of AIV NS1 sequences in the present study strikingly revealed the presence of SH3-bmf-1 in H5N1 (50-92) virus NS1 sequence while absent in other four viruses studied. NS1 SH3-bmf-1 together with

SH2-bmf mediate p85 interaction, leading to the removal of inhibitory action on p110 subunit. It is likely that SH3-bmf-1 in H5N1 (50-92) virus may potentially strengthen the p85-NS1 anchorage leading to the prolonged activation of PI3K/Akt in H5N1 (50-92) virus infected chicken cells observed in the present study. However, this may not be true for all H5N1 virus subtypes, as another rH5N1 (tky05) although did not possess additional SH3-bmf-1 but still activated PI3K/Akt for a period equivalent to that observed in H5N1 (50-92) virus infected cells. Collectively, these observations hint presence of variations among AIV virus subtypes in PI3K/Akt activation and warrants further investigation.

5.5.4 Diversity in duck PI3K-p85 may potentially hinder pathway activation

Present study revealed absence of PI3K activity despite viral infection in duck fibroblast cells. Upon similarity check of p85-iSH2 sequences from important avian and mammalian species, avian or mammalian group amino acid specific residue modifications were observed at several locations. However, these residues were uniquely conserved within avian or mammalian species. Surprisingly, a specific glutamic acid (E) residue at position 475 was conserved across all species irrespective of avian or mammalian group. However, in ducks this conserved acidic residue E475 was replaced by a non-polar valine (V) residue (E475V). In silico protein-protein interaction modelling confirmed the exact orientation of

V475 residue on the helix outside of the NS1-iSH2 binding interface, suggesting no direct involvement in p85-NS1 interaction. In silico protein binding site prediction by substitution of non-polar V with acidic E (V475E) residue in the duck and *vice versa* in chicken, resulted in duck sequence regaining nearly equivalent number of binding sites as that of chicken sequence with E475 residue. Similarly, replacement of E with V (E475V) in the chicken sequence resuted in extensive reduction in protein binding sites. These protein interaction studies potentially suggest an important contribution of E475 residue in post-translational modification (PTM) of p85-iSH2 region. A comparison study of human and bovine p85β-iSH2 in multiple conformations revealed that the coiled-coil iSH2 domain exhibits 'conformational plasticity' in the inter-helical turn region (Schauder et al., 2010). It is likely that the residue E475 located on the iSH2 helical region might take part in bringing about conformational flexibility and PTM of p85-iSH2. However, functional significance of present findings can be validated by performing pulldown assays with cells constitutively expressing E475V mutant protein as described in Hale et al. (2006).

Chapter 6. General Discussion

6.1 General discussion

The reasons for differences in the host response to IAV infection between chicken and ducks may be multifactorial. Both virus and the host may equally contribute to these contrasting disease outcomes in chicken and ducks. Influenza A viruses (IAV) have been shown to interact with multiple intracellular pathways either to antagonise host antiviral response or to utilise host cellular machinery for viral advantage as reviewed by Gaur et al. (2011). It has been shown that influenza A virus mediated PI3K/Akt activation helps efficient virus propagation. However, regulation and the significance of the PI3K/Akt signalling pathway in avian influenza virus replication and its contribution towards disease pathogenesis in chickens that are highly susceptible and ducks, which are reservoir hosts, is yet to be elucidated. The aim of the present study was to elucidate the regulation of PI3K/Akt and its implications on viral replication, morphogenesis and pathogenesis in AIV infected chicken and duck cells. Chicken and duck primary fibroblast cells were used in the present study over established cell lines as these cells represent host species, and both have been shown equally susceptible to AIV infection (Kuchipudi, 2010). Cell lines are essentially cancerous that may have altered cellular integrity hence may exert differences especially in signal transduction pathways. The activation of PI3K/Akt kinase is rather complex and is mediated

by diverse mechanisms. Activated effector kinase regulates many important functions in the living cells. The first report originated from mammalian cell culture models that revealed IAV mediated PI3K/Akt activation in a biphasic pattern; an early induction at viral entry and later during replication (Ehrhardt et al., 2006) by interacting with PI3K p85β regulatory subunit (Hale et al., 2006).

Results from the present study (3.4) revealed only late phase activation hence slightly deviated from previous biphasic activation observed (Ehrhardt et al., 2006, Elbahesh et al., 2014). Activation of the PI3K/Akt later in the infection cycle observed in the present study is thought to be viral replication dependent and is in agreement with previous observations (Shin et al., 2007b, Zhirnov and Klenk, 2007). Viral replication dependent PI3K/Akt activation was confirmed with a recombinant PR8/H1N1 virus with delta NS1 that failed to activate PI3K/Akt pathway (Ehrhardt et al., 2006). Chemical inhibition of PI3K/Akt resulted in significant reduction in infectious virus production in infected CEFs, confirming viral replication dependency on host PI3K/Akt in the present study. The absence of phosphorylated Akt suggested PI3K/Akt is no longer activated at 24 hpi in LPAI H2N3 virus infected CEF cells. A possible explanation for this phenomenon could be the reduction in intracellular viral titre because of the effective host antiviral response that might have led to the inactivation of pathway due to

lack of stimuli as this pathway is not basally activated in CEF cells as observed in the present study.

Influenza A virus NS1 has been shown to interact with PI3K-p85β subunit resulting in PI3K/Akt activation (Hale et al., 2006, Ehrhardt et al., 2007b, Shin et al., 2007c, Hale et al., 2008). The contribution of AIV NS1 in PI3K/Akt activation was elucidated by Ehrhardt et al. (2006) who infected MDCK cells with recombinant PR8/H1N1 virus lacking NS1 (delta NS1) in MDCK cells, which failed to activate the pathway. Possible differences in the pattern of PI3K/Akt activation in infected CEF cells was studied by comparative analysis of PhosphoAkt protein expression in two WT LPAIs or rH9N2 and two rescued recombinant H5N1 viruses. The experimental data revealed a prolonged PI3K/Akt activation even at 24 hpi in rH5N1 virus infected cells compared to LPAIs or rH9N2, which showed similar trend in the expression of phosphoAkt protein from 6 until 9 hpi. Importance of NS1-SH3 binding motif-1 and 2 (SH3-bmf-1 and 2) for PI3/Akt activation was determined by insertion of specific mutations in these binding site motifs, which revealed that SH3-bmf-1 is crucial for pathway activation but not SH3-bmf-2 (Shin et al., 2007a). Sequence similarity check of NS1 from LPAIs and rH5N1 viruses used in the present study (5.4.9) revealed presence of an additional SH3-bmf-1 in rH5N1 (50-92) NS1. Therefore, It is hypothesised that presence of an additional SH3-bmf-1 in rH5N1 NS1 may facilitate stable tethering of NS1-p85 complex resulting in

prolonged PI3K/Akt activation in rH5N1 virus infections. The contribution of AIV segment 8 (NS) in prolonged PI3K/Akt activation was experimentally confirmed in the present study by generating a chimeric H9N2 virus (cH9N2) carrying segment 8 from HPAI H5N1 (50-92) virus. Hence present study reports differential PI3K/Akt activation between LPAI and rH5N1 virus subtypes.

Significantly higher apoptotic cell death was observed in H2N3 virus infected and PI3K/Akt inhibited CEF cells compared to carrier treated or untreated control cells as measured by caspase 3/7 activity (3.4.8). These results correlated with previous observations of (Zhirnov and Klenk, 2007, Ehrhardt et al., 2007b, Lu et al., 2010) who showed PI3K/Akt mediated anti-apoptotic activity in influenza A virus infected MDCK cells. Together the results suggested that the PI3K/Akt activation mediated apoptosis inhibition may potentially favour longer cellular survival rate allowing availability cellular environment for virus replication in AIV infected cells. Prolonged PI3K/Akt activation in rH5N1 virus infected cells as observed in the present study may exhibit potent anti-apoptotic activity leading to enhanced infectious virus production culminating in rapid intracellular spread of virus to adjacent cells and higher virus replication consequently possibly leading to higher pathogenesis and pronounced disease severity.

A comparative PI3K/Akt activation study in LPAI H2N3 virus infected duck fibroblast cells revealed contrasting findings in the

present study. Surprisingly, PI3K/Akt pathway was not activated despite H2N3 virus infection in duck cells. However, the existence of the PI3K/Akt pathway was ascertained by canonical IGF-1 stimulation of DEF cells, which resulted in Akt phosphorylation suggesting PI3K/Akt activity (3.4.7). These observations indirectly confirm the inability of AIV H2N3 virus to activate PI3K/Akt pathway in duck cells. However, H2N3 virus infected DEFs showed rapid onset of apoptotic cell death in both PI3K/Akt inhibited or uninhibited groups. Possibly suggesting inherent lack of PI3K/Akt activity that is potent upstream regulator of caspase mediated apoptosis may result in the onset of rapid apoptosis in H2N3 virus infected duck cells. The observations of rapid apoptotic cell death in H2N3 virus infected DEF cells coincide with the observations of Kuchipudi et al. (2012a) who reported similar outcome in AIV infected duck cells. Based on the observations in the present study, it may be speculated that trigger of rapid apoptosis in virus infected DEF cells may restrict virus with loss of cellular environment for further replication and spread to adjacent cells hence conferring disease resistance. Measurement of caspase activity with or without PI3K/Akt inhibitor treatment of H2N3 virus infected duck cells revealed no influence of inhibitor treatment hence the level of caspase activity in both PI3K/Akt inhibitor treated and mock treated were comparable, strongly implying inherent lack of PI3K activity in the infected cells (3.4.8). It was observed that the basal level of apoptotic activity in duck cells

was far greater compared to chicken cells. Hence, it was hypothesed that lack of upstream caspase regulatory PI3K/Akt activity probably is the reason for elevated apoptosis process. Rapid onset of apoptosis also means complete shutdown of host antiviral response in the virus infected cells, a potential host mechanism for low profiled host antiviral response, possibly aiding the host to serve as the reservoir of virus

The binding and interaction of AIV NS1 with p85β-iSH2 region was identified as the mechanism for virus-mediated PI3K/Akt activation in infected cells (Hale et al., 2006, Hale et al., 2008). Sequence alignment and similarity check of p85β-iSH2 region from important avian and mammalian species, was carried out to find out a plausible answer for absence of PI3K/Akt activity in duck cells observed in the present study. The results of the sequence alignment and similarity check revealed presence of conserved amino acid residues within mammalian and avian classes. However, a specific highly acidic glutamic acid (E) residue at position 475 (E475) (numbered based on duck sequence) was conserved across both avian and mammalian sequences, but the same was substituted by, a non-polar valine (V) residue (V475) in ducks (5.4.9). Protein-protein interaction modelling revealed that the acidic residue lies on the helix outside the iSH2-NS1 binding interface. However, sequence based protein binding site prediction revealed replacement of 'V' with 'E' (V475E) in duck sequence

regained chicken comparable number of binding sites especially in the iSH2 region. Comparison of human and bovine p85β structures revealed 'conformational plasticity' in the coiled-coil iSH2 region (Schauder et al., 2010). Because of the position of the E475 residue located on the iSH2 helical region, it may be hypothesised that E475 residue may have important contribution in conferring conformational plasticity during potential post-translational modification that confers protein binding sites for AIV NS1 attachment leading to PI3K activation in chickens. While presence of non-polar valine at 475 may hinder post-translational modification of iSH2 helix that prevents AIV NS1 interaction, also higher expression of PTEN a key negative regulator of PI3K may complement in the inhibition of PI3K/Akt activation (4.4.5), resulting in absence of AIV virus mediated PI3K/Akt activation in duck cells.

Regulation of cytoskeletal actin filament dynamics is critical for controlling cellular polarity, morphology, adhesion and motility. PI3K/Akt kinases are shown to regulate cytoskeletal rearrangement by interacting with multiple RhoGTPases that regulate actin dynamics (Ridley et al., 2003, Cain and Ridley, 2009). Extensive studies on virus morphogenesis with or without actin disruption by Al-Mubarak et al. (2015) revealed that CEFs produce spherical while DEFs produced elongated virion particles and observed no differences in any genes of chicken and duck cell derived viruses

hence, a potential role of host factors in determining the budding virus morphology was speculated.

Results from the present study revealed disruption of actin fibre integrity leading to formation of ruffled membrane upon PI3K/Akt inhibition in H2N3 virus infected CEF cells (4.4.6). The loss of cytoskeletal actin integrity in virus infected and PI3K/Akt inhibited CEFs suggested a definitive control of cytoskeletal actin reorganisation by PI3K/Akt in chicken cells. PI3K/Akt dependent actin reorganisation observed in the present study are in agreement with previous observations of Qian et al. (2004) who reported similar findings in chicken fibroblast cells and Tsakiridis et al. (1999) who observed membrane ruffling upon inhibition of PI3K/Akt in muscle and adipose cells. A comparative investigation in duck cells revealed a complete loss of actin architecture in the virus-infected cells (4.4.7), however, the exact mechanism behind this observation couldn't be determined in the present study hence a scope for future investigations. Immunofluorescence studies revealed that CEF cells produced moderately spherical while DEFs produced elongated virion particles these observations are in agreement with Al-Mubarak et al. (2015). However the present study revealed that CEF cells produced perfectly spherical virion particles upon PI3K inhibition as evidenced by electron microscopy (4.4.8). Above observations suggested potential involvement of PI3K/Akt on cytoskeletal actin remodelling

and may possibly influence budding virus morphology in chicken cells.

6.2 Summary and future scope of the study

In summary, the present study demonstrated AIV-mediated PI3K/Akt pathway activation in chicken but not in duck fibroblast cells. Infection of CEF cells with LPAI or rH9N2 viruses led to brief PI3K/Akt activation, while recombinant H5N1 viruses activated the pathway for a prolonged period. In silico NS1 gene sequence analysis from LPAI and HPAI viruses used in the present study suggested specific changes in the NS1 and cH9N2 virus carrying NS from H5N1 (50-92) virus generated in the present study suggested NS1 as responsible for prolonged pathway activation. However, a detailed study with residue substitutions at specific locations in the AIV NS1 as speculated in the present study may pin point the contributions of specific amino acid residues for PI3K/Akt activation.

Despite virus infection, PI3K/Akt activation was not observed in duck fibroblast cells. Sequence analysis of p85-iSH2 region revealed substitution of a highly acidic glutamic acid residue with a non-polar valine residue at 475 position in duck iSH2 region. Noteworthy to mention that aa residue E475 was conserved across major avian and mammalian influenza virus susceptible hosts analysed (Appendix II) in the present study. Functional contribution of V475 residue in averting p85β-NS1 interactions and subsequent

PI3K/Akt activation observed in ducks may be confirmed by pulled-down assay by generating constructs with aa residue substitutions at position 475 and subsequent expression of these constructs in cell cultures followed by affinity isolation and immunoblot analysis using relevant antibodies as described by Hale et al. (2008).

Higher transcriptomic expression of cytoskeletal actin reorganisation related genes and PI3K/Akt negative regulator PTEN was observed in chicken and duck primary lung cells respectively. However, functional relationship between these gene expression pattern and their contribution in actin remodelling may be studied extensively in the future. Implications of PI3K/Akt activation on host innate response and cross-talks between host innate response and PI3K/Akt signalling loop and their contributions may be an area to explore in the future. The present study provides a basal understanding of PI3K/Akt signalling pathway regulation in two important avian hosts which may form the basis for studies involving PI3K-p85 manipulations as an antiviral strategy against influenza A viruses.

Appendices

APPENDIX-I
Reagent and media formulation
(Chapter 3)

Cell culture medium

DMEM+GlutaMax……500 mL

Fetal calf serum (FCS)……50 mL

Penicillin-streptomycin (Penstrep)……5 mL

Infection medium (IM)

DMEM+GlutaMax……50 mL

Penstrep……500 µl

TPCK trypsin……1 mL

Media for egg embryo inoculation

Phosphate buffered saline (PBS)……47 mL

Tryptose phosphate broth……2 mL

Penstrep……1 mL

Tris Acetate EDTA (TAE) 50X

Tris Base……242 g

Glacial acetic acid……57.1 mL

0.5 M EDTA (pH 8.0)……100 mL

Make up the volume to 1 litre with MilliQ ultrapure water. TAE can be stored at room temperature for long time.

Tris buffered saline (TBS) 10X

Sodium chloride (NaCl)……87.66 g

Tris (Trzma) base……60.55 g

0.5 M EDTA (pH 8.0)……100 mL

Dissolve the contents in 800 mL ultrapure water and adjust the pH to 7.4 with 0.1M Hcl and make up the volume to one litre with ultrapure water.

Tris buffered saline with Tween 20 (TBS-T) 1X

TBS (10X)……100 mL

Tween 20……1 mL

Ultrapure water……899 mL

TOC culture medium

10x Minimum Essential Medium-Eagles ……100 mL

7.5% sodium bicarbonate ……20 mL

Sterile distilled water ……900 mL

Penicillin-streptomycin solution ……4 mL

Culture medium for HD11 cells

RPMI 1640 Minimum……500 mL

L-glutamine (20 mM) ……5 mL

Chicken serum ……12.5 mL

Foetal bovine serum ……12.5 mL

Tryptose phosphate broth ……10 mL

Penicillin-streptomycin solution ……5 mL

APPENDIX-II R script
(Chapter 4)

```
#install the requisite core bioconductor packages, (if not already installed)
source("http://bioconductor.org/biocLite.R")
biocLite()

# install additional bioconductor libraries, (if not already installed)

biocLite("GEOquery")
biocLite("simpleaffy")
biocLite("affy")
biocLite("gcrma")
biocLite("genefilter")
biocLite("hugene10stv1cdf")
biocLite("hugene10stv1probe")
biocLite("hugene10stprobeset.db")
biocLite("hugene10sttranscriptcluster.db")
biocLite(c("GenomicFeatures", "AnnotationDbi"))
biocLite("oligo")

Package directory in the home drive :
C:\Users\svxst1\AppData\Local\Temp\Rtmp5jiGCN\downloaded_packages

#Load the necessary libraries
library(GEOquery)
library(simpleaffy)
library(affy)
library(gcrma)
library("genefilter")
library(hugene10stv1cdf)
library(hugene10stv1probe)
library(hugene10stprobeset.db)
library(hugene10sttranscriptcluster.db)
library(GenomicFeatures)
library(AnnotationDbi)
library("oligo")

#Set working directory for download
setwd("R:\\Daly-Virology-Group\\Sanjeev\\Microarray\\working dircectory R")

#Download the CEL file package for this dataset (by GSE - Geo series id)
getGEOSuppFiles("GSE33389")

#Unpack the CEL files
setwd("R:\\Daly-Virology-Group\\Sanjeev\\Microarray\\working dircectory
R\\GSE33389")
untar("GSE33389_RAW.tar", exdir="data")
```

```
cels = list.files("data/", pattern = "CEL")

setwd("R:\\Daly-Virology-Group\\Sanjeev\\Microarray\\working dircectory
R\\GSE33389\\data")
raw.data=ReadAffy(verbose=TRUE, filenames=cels, cdfname="hugene10stv1")


#perform RMA normalization
data.rma.norm=rma(raw.data)

#Read CEL files
celFiles <- list.celfiles()
affyRaw <- read.celfiles(celFiles)

#Package pd.chicken install
library(pd.chicken)

#RMA
eset <- rma(affyRaw)

#Write output file
write.exprs(eset,file="Sanjeev_Chicken.txt")

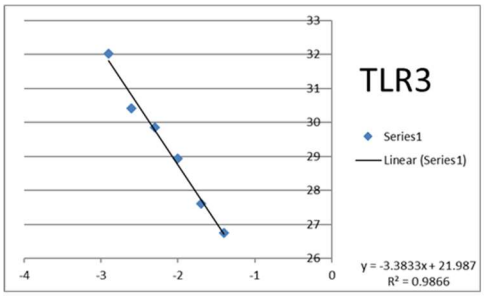
#annotation Library
biocLite("chicken.db")
library(chicken.db)

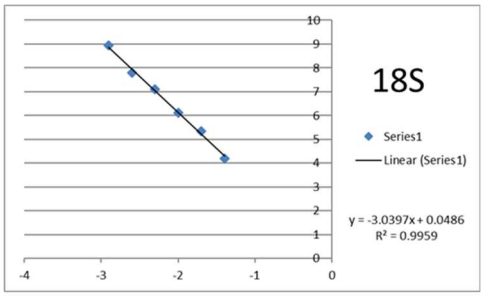
#run chicken() to see the available information

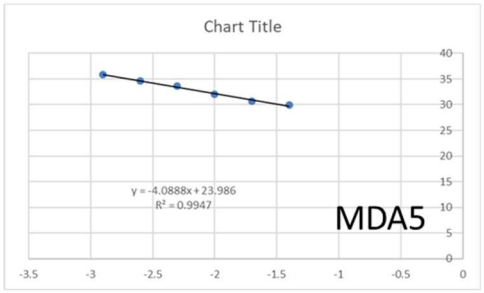
#create frame and add annotation data
my_frame <- data.frame(exprs(eset))
Annot <- data.frame(ACCNUM=sapply(contents(chickenACCNUM), paste,
collapse=", "), SYMBOL=sapply(contents(chickenSYMBOL), paste, collapse=", "),
DESC=sapply(contents(chickenGENENAME), paste, collapse=", "))

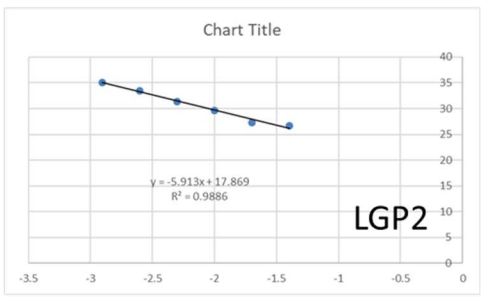
#merge the two frames and write file
all <- merge(Annot, my_frame, by.x=0, by.y=0, all=T)
write.table(all,file="data.ann.txt",sep="\t")
```

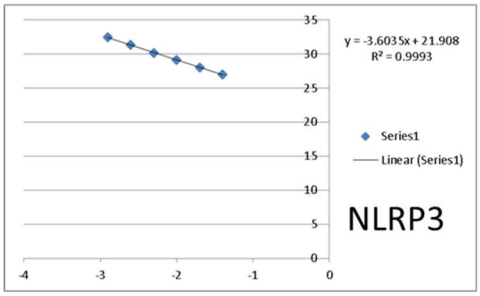
APPENDIX-III
RT-qPCR standard curve and Melting curve
(Chapter 5)

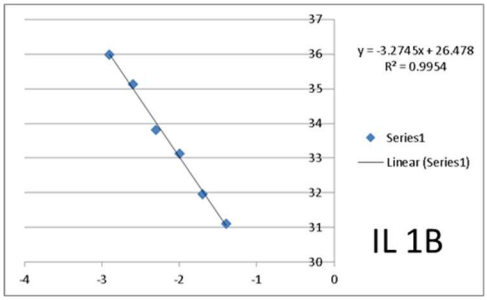


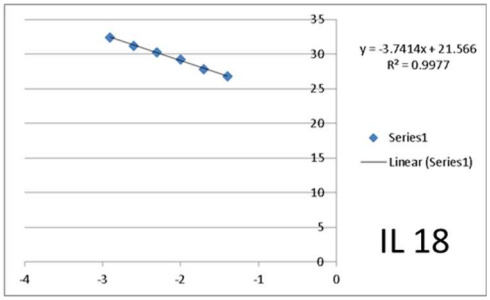


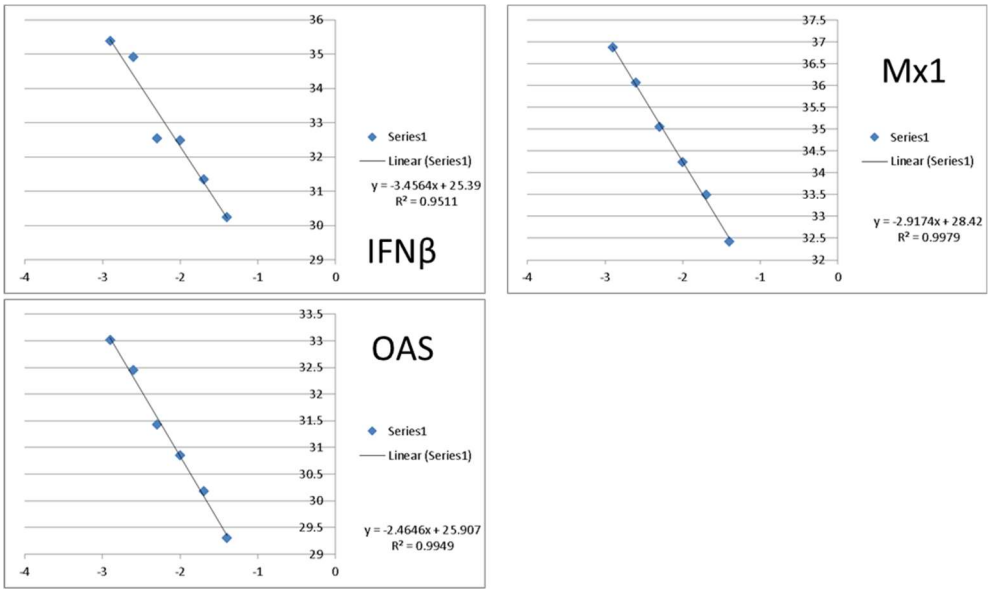


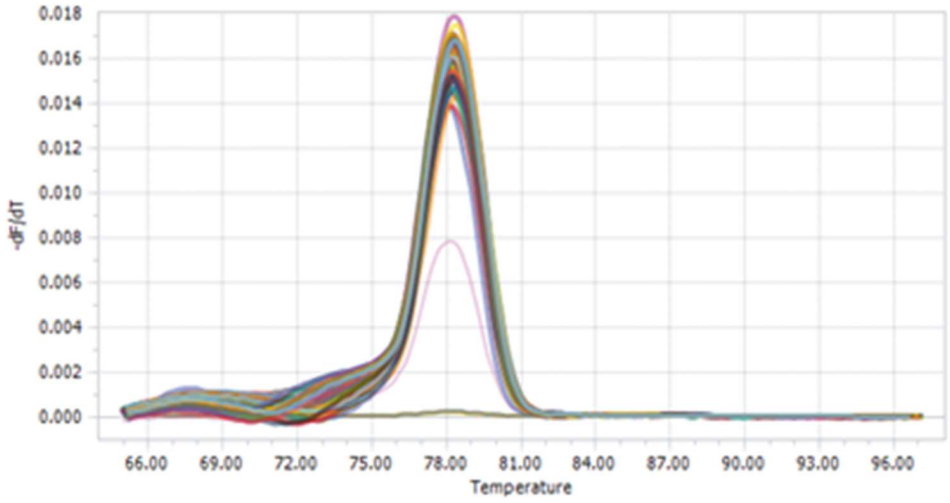












Representative melting curve obtained from TLR3 RT-qPCR showing the specificity of the primer

APPENDIX-IV PI3K-p85β
(Chapter 5)

PI3K-p85β sequence alignment for diversity analysis

```
HUMAN/1-728          1 ----MAGPEGFQYRALYPFRRERPEDLELLPGDVLVVSRAALQALGVAEGGERCPQSVGW
Cattle(Bos)/1-7      1 ----MAGPEGFQYRALYPFRRERPEDLELLPGDVLVVSRAALQALGVAEGNERCPQSVGW
Chicken/1-731        1 MAERMGSTDGFQYRALYPYRKEREEDIDLVPGDILVVSKGALQALGFKDGDEQNPNQIGW
Duck/1-725           1 MAERMGSTDGFQYRALYPYRKEREEDIDLLPGDILVVSKGALQALGFKDGDEQNPNQIGW
consensus            1 MAERMA  EGFQYRALYPFRRER EDLELLPGDVLVVSRAALQALG  EGDE  PQ VGW

HUMAN/1-728         57 MPGLNERTRQRGDFPGTYVEFLGPVALARPGPRPRGPRPLPARPRDG------APEPGLT
Cattle(Bos)/1-7     57 MPGLNERTRQRGDFPGTYVEFLGPVALARPGPRPRGPRPLPARPRDG------PPEPGLT
Chicken/1-731       61 ILGVNERTKQKGDFPGTYVEYVGPVKISVPSHRPRVQRPLPATPGASGCRLQEALEQGSP
Duck/1-725          61 ILGVNERTKQKGDFPGTYVEYVGPVKISVPSHRPRGPIPLSAASSLS------PSSPGSP
consensus           61 M GLNERTRQRGDFPGTYVEFLGPV L  P  RPRGPRPLPARPRD        PEPG

HUMAN/1-728        111 LPDLPEQFSPPDVAPPLLVKLVEAIERTGLDSESHYRPE----LPAPRTDWSLSDVDQWD
Cattle(Bos)/1-7    111 LPDLPEQFSPPDVAPPILVKLVEAIERTGLDS---YRPE----PPAVRTDWSLSDVEQWD
Chicken/1-731      121 LPDLQEQFSPPEVAPPLLVKLVEAIEKKGLDSEMLYRTSGSELRQALRTDWSLGDLEPFD
Duck/1-725         115 LPDLQEQFSPPEIAPPLLVKLVEAIEKKGLDSEMLYRTSGSELRQALRTDWSLGDLEPFD
consensus          121 LPDL EQFSPPDVAPPLLVKLVEAIER GLDSEMLYR  GSELR ALRTDWSL DVE WD

HUMAN/1-728        167 TAALADGIKSFLLALPAPLVTPEASAEARRALREAAGPVGP------ALEPPTLPLHRAL
Cattle(Bos)/1-7    164 AAALSDGVKGFLLALPAPLVTPEAAAEAHRALREAAGPVGP------ALEPPTLPLHHAL
Chicken/1-731      181 VHSLSEALRGYLQDLPSPVVPVSVHGDILRILQEIPQPENCRKQLLLALESPAIPLQNTL
Duck/1-725         175 VHSLGEALRGYLQDLPSPVVPVAVHGDILRVLQEVPQPENCRKQLLLALESPAVPLQNTL
consensus          181 V  LSDGLKGFL  LP PLV  E HAE LRAL EA  P   RKQLLLALE P LPL N L

HUMAN/1-728        221 TLRFLLQHLGRVASRAPALGPAVRALGATFGPLLLRAPPPPSSPPPGGAPDGSEPSPDFP
Cattle(Bos)/1-7    218 TLRFLLQHLGRVAGRAPAPGPAVRALGATFGPLLLRAPPPP-SPPPGGAPDGTEPTPDFP
Chicken/1-731      241 TLQFLLRHLGKVSQQAESNSLHPQALGEIFGPLLLRLP--------GASP---ELSPDFS
Duck/1-725         235 TLQFLLRHLGKVSQQAESNNLHPRALGEIFGPLLLRLP--------GASP---ELSPDFS
consensus          241 TL FLL HLGRV Q A  NG   RALG  FGPLLLR PPPP SPPPGG PDGSE SPDF

HUMAN/1-728        281 ALLVEKLLQEHLEEQEVAPPALPPKPPKAKPASTVLANGGSPPSLQDAEWYWGDISREEV
Cattle(Bos)/1-7    277 ALLVEKLLQEHLEEQEVAPPALPPKPPKTKPAPTGLANGGSPPSLQDAEWYWGDISREEV
Chicken/1-731      290 VLFLEMLLQTKELEPEQLPPALPPKPPKPKPSAASLANGNSVP-LQDAEWYWGDISREEV
Duck/1-725         284 VLFLEMLLQLKELEPEQLPPALPPKPPKPKPSAASLANGNSVP-LQDAEWYWGDISREEV
consensus          301  L VE LLQEH  E E  PPALPPKPPKPKP A SLANG S PSLQDAEWYWGDISREEV

HUMAN/1-728        341 NEKLRDTPDGTFLVRDASSKIQGEYTLTLRKGGNNKLIKVFHRDGHYGFSEPLTFCSVVD
Cattle(Bos)/1-7    337 NEKLRDTPDGTFLVRDASSKIQGEYTLTLRKGGNNKLIKVFHRDGHYGFSEPLTFCSVVD
Chicken/1-731      349 NEKLRDTPDGTFLVRDASSKIQGEYTLTLRKGGNNKLIKIFHREGKYGFSEPLTFGSVVE
Duck/1-725         343 NEKLRDTPDGTFLVRDASSKIQGEYTLTLRKGGNNKLIKIFHREGKYGFSEPLTFGSVVE
consensus          361 NEKLRDTPDGTFLVRDASSKIQGEYTLTLRKGGNNKLIKVFHRDGHYGFSEPLTF SVVD

HUMAN/1-728        401 LINHYRHESLAQYNAKLDTRLLYPVSKYQQDQIVKEDSVEAVGAQLKVYHQQYQDKSREY
Cattle(Bos)/1-7    397 LITHYRHESLAQYNAKLDTRLLYPVSKYQQDQIVKEDSVEAVGAQLKVYHQQYQDKSREY
Chicken/1-731      409 LITHYRHESLAQYNAKLDTRLLYPISKYQQDQVVKEDSVEAVGEQLKVYHQQYQDKSWEY
Duck/1-725         403 LITHYRHESLAQYNAKLDTRLLYPISKYQQDQVVKEDSVEAVGEQLKVYHQQYQDKSWEY
consensus          421 LITHYRHESLAQYNAKLDTRLLYPVSKYQQDQIVKEDSVEAVG QLKVYHQQYQDKS EY
```

References

ABDELWHAB EL, S. M., VEITS, J. & METTENLEITER, T. C. 2013. Genetic changes that accompanied shifts of low pathogenic avian influenza viruses toward higher pathogenicity in poultry. *Virulence,* 4**,** 441-52.

ADAMS, S. & SANDROCK, C. 2010. Avian influenza: update. *Med Princ Pract,* 19**,** 421-32.

ADAMS, S. C., XING, Z., LI, J. & CARDONA, C. J. 2009. Immune-related gene expression in response to H11N9 low pathogenic avian influenza virus infection in chicken and Pekin duck peripheral blood mononuclear cells. *Mol Immunol,* 46**,** 1744-9.

AGUAN, K., CARVAJAL, J. A., THOMPSON, L. P. & WEINER, C. P. 2000. Application of a functional genomics approach to identify differentially expressed genes in human myometrium during pregnancy and labour. *Mol Hum Reprod,* 6**,** 1141-5.

AGUIRRE, A. A., KEEFE, T. J., REIF, J. S., KASHINSKY, L., YOCHEM, P. K., SALIKI, J. T., STOTT, J. L., GOLDSTEIN, T., DUBEY, J. P., BRAUN, R. & ANTONELIS, G. 2007. Infectious disease monitoring of the endangered Hawaiian monk seal. *J Wildl Dis,* 43**,** 229-41.

AL-MUBARAK, F., DALY, J., CHRISTIE, D., FOUNTAIN, D. & DUNHAM, S. P. 2015. Identification of morphological differences between avian influenza A viruses grown in chicken and duck cells. *Virus Res,* 199**,** 9-19.

ALESSI, D. R., ANDJELKOVIC, M., CAUDWELL, B., CRON, P., MORRICE, N., COHEN, P. & HEMMINGS, B. A. 1996. Mechanism of activation of protein kinase B by insulin and IGF-1. *EMBO J,* 15**,** 6541-51.

ARROWSMITH, C. H., AUDIA, J. E., AUSTIN, C., BAELL, J., BENNETT, J., BLAGG, J., BOUNTRA, C., BRENNAN, P. E., BROWN, P. J., BUNNAGE, M. E., BUSER-DOEPNER, C., CAMPBELL, R. M., CARTER, A. J., COHEN, P., COPELAND, R. A., CRAVATT, B., DAHLIN, J. L., DHANAK, D., EDWARDS, A. M., FREDERIKSEN, M., FRYE, S. V., GRAY, N., GRIMSHAW, C. E., HEPWORTH, D., HOWE, T., HUBER, K. V., JIN, J., KNAPP, S., KOTZ, J. D., KRUGER, R. G., LOWE, D., MADER, M. M., MARSDEN, B., MUELLER-FAHRNOW, A., MULLER, S., O'HAGAN, R. C.,

OVERINGTON, J. P., OWEN, D. R., ROSENBERG, S. H., ROTH, B., ROSS, R., SCHAPIRA, M., SCHREIBER, S. L., SHOICHET, B., SUNDSTROM, M., SUPERTI-FURGA, G., TAUNTON, J., TOLEDO-SHERMAN, L., WALPOLE, C., WALTERS, M. A., WILLSON, T. M., WORKMAN, P., YOUNG, R. N. & ZUERCHER, W. J. 2015. The promise and peril of chemical probes. *Nat Chem Biol,* 11**,** 536-41.

AUTRET, A., MARTIN-LATIL, S., BRISAC, C., MOUSSON, L., COLBERE-GARAPIN, F. & BLONDEL, B. 2008. Early phosphatidylinositol 3-kinase/Akt pathway activation limits poliovirus-induced JNK-mediated cell death. *J Virol,* 82**,** 3796-802.

AYLLON, J. & GARCIA-SASTRE, A. 2015. The NS1 protein: a multitasking virulence factor. *Curr Top Microbiol Immunol,* 386**,** 73-107.

BAE, S. H., CHEONG, H. K., LEE, J. H., CHEONG, C., KAINOSHO, M. & CHOI, B. S. 2001. Structural features of an influenza virus promoter and their implications for viral RNA synthesis. *Proc Natl Acad Sci U S A,* 98**,** 10602-7.

BALL, C., AWAD, F., HUTTON, S., FORRESTER, A., BAYLIS, M. & GANAPATHY, K. 2017. Infectious bronchitis vaccine virus detection and part-S1 genetic variation following single or dual inoculation in broiler chicks. *Avian Pathol,* 46**,** 309-318.

BALL, C., BENNETT, S., FORRESTER, A. & GANAPATHY, K. 2016. Genetic mutations in live infectious bronchitis vaccine viruses following single or dual in vitro infection of tracheal organ cultures. *J Gen Virol,* 97**,** 3232-3237.

BARBER, M. R., ALDRIDGE, J. R., JR., WEBSTER, R. G. & MAGOR, K. E. 2010. Association of RIG-I with innate immunity of ducks to influenza. *Proc Natl Acad Sci U S A,* 107**,** 5913-8.

BERGMANN, M., GARCIA-SASTRE, A., CARNERO, E., PEHAMBERGER, H., WOLFF, K., PALESE, P. & MUSTER, T. 2000. Influenza virus NS1 protein counteracts PKR-mediated inhibition of replication. *J Virol,* 74**,** 6203-6.

BHAT, A., GOMIS, S., POTTER, A. & TIKOO, S. K. 2010. Role of Hsp90 in CpG ODN mediated immunostimulation in avian macrophages. *Mol Immunol,* 47**,** 1337-46.

BOUVIER, N. M. & PALESE, P. 2008. The biology of influenza viruses. *Vaccine,* 26 Suppl 4**,** D49-53.

BRACIALE, T. J., SUN, J. & KIM, T. S. 2012. Regulating the adaptive immune response to respiratory virus infection. *Nat Rev Immunol,* 12**,** 295-305.

BRAZIL, D. P., YANG, Z. Z. & HEMMINGS, B. A. 2004. Advances in protein kinase B signalling: AKTion on multiple fronts. *Trends Biochem Sci,* 29**,** 233-42.

BRUCE, E. A., DIGARD, P. & STUART, A. D. 2010. The Rab11 pathway is required for influenza A virus budding and filament formation. *J Virol,* 84**,** 5848-59.

CABEZAS, J. A. 1991. [Studies on sialidase and esterase in influenza viruses]. *Ann Pharm Fr,* 49**,** 57-66.

CAIN, R. J. & RIDLEY, A. J. 2009. Phosphoinositide 3-kinases in cell migration. *Biol Cell,* 101**,** 13-29.

CAPUA, I. & ALEXANDER, D. J. 2009. Avian influenza infection in birds: a challenge and opportunity for the poultry veterinarian. *Poult Sci,* 88**,** 842-6.

CARRACEDO, A. & PANDOLFI, P. P. 2008. The PTEN-PI3K pathway: of feedbacks and cross-talks. *Oncogene,* 27**,** 5527-41.

CHAKRABARTI, A. K., VIPAT, V. C., MUKHERJEE, S., SINGH, R., PAWAR, S. D. & MISHRA, A. C. 2010. Host gene expression profiling in influenza A virus-infected lung epithelial (A549) cells: a comparative analysis between highly pathogenic and modified H5N1 viruses. *Virol J,* 7**,** 219.

CHANG, C. D., LIN, P. Y., LIAO, M. H., CHANG, C. I., HSU, J. L., YU, F. L., WU, H. Y. & SHIH, W. L. 2013. Suppression of apoptosis by pseudorabies virus Us3 protein kinase through the activation of PI3-K/Akt and NF-kappaB pathways. *Res Vet Sci,* 95**,** 764-74.

CHANG, P., KUCHIPUDI, S. V., MELLITS, K. H., SEBASTIAN, S., JAMES, J., LIU, J., SHELTON, H. & CHANG, K. C. 2015. Early apoptosis of porcine alveolar macrophages limits avian influenza virus replication and pro-inflammatory dysregulation. *Sci Rep,* 5**,** 17999.

CHEN, C. Y., CHANG, C. Y., LIU, H. J., LIAO, M. H., CHANG, C. I., HSU, J. L. & SHIH, W. L. 2010. Apoptosis induction in BEFV-

infected Vero and MDBK cells through Src-dependent JNK activation regulates caspase-3 and mitochondria pathways. *Vet Res,* 41**,** 15.

CHEN, S., CHENG, A. & WANG, M. 2013. Innate sensing of viruses by pattern recognition receptors in birds. *Vet Res,* 44**,** 82.

CHEN, W., CALVO, P. A., MALIDE, D., GIBBS, J., SCHUBERT, U., BACIK, I., BASTA, S., O'NEILL, R., SCHICKLI, J., PALESE, P., HENKLEIN, P., BENNINK, J. R. & YEWDELL, J. W. 2001. A novel influenza A virus mitochondrial protein that induces cell death. *Nat Med,* 7**,** 1306-12.

CHEUNG, C. Y., POON, L. L., LAU, A. S., LUK, W., LAU, Y. L., SHORTRIDGE, K. F., GORDON, S., GUAN, Y. & PEIRIS, J. S. 2002. Induction of proinflammatory cytokines in human macrophages by influenza A (H5N1) viruses: a mechanism for the unusual severity of human disease? *Lancet,* 360**,** 1831-7.

CHEUNG, T. K. & POON, L. L. 2007. Biology of influenza a virus. *Ann N Y Acad Sci,* 1102**,** 1-25.

CHIAPPONI, C., FACCINI, S., DE MATTIA, A., BAIONI, L., BARBIERI, I., ROSIGNOLI, C., NIGRELLI, A. & FONI, E. 2016. Detection of Influenza D Virus among Swine and Cattle, Italy. *Emerg Infect Dis,* 22**,** 352-4.

COLMAN, P. M., GOUGH, K. H., LILLEY, G. G., BLAGROVE, R. J., WEBSTER, R. G. & LAVER, W. G. 1981. Crystalline monoclonal fab fragment with specificity towards an influenza virus neuraminidase. *J Mol Biol,* 152**,** 609-14.

COLOMA, R., VALPUESTA, J. M., ARRANZ, R., CARRASCOSA, J. L., ORTIN, J. & MARTIN-BENITO, J. 2009. The structure of a biologically active influenza virus ribonucleoprotein complex. *PLoS Pathog,* 5**,** e1000491.

CONNOR, R. J., KAWAOKA, Y., WEBSTER, R. G. & PAULSON, J. C. 1994. Receptor specificity in human, avian, and equine H2 and H3 influenza virus isolates. *Virology,* 205**,** 17-23.

COORAY, S. 2004. The pivotal role of phosphatidylinositol 3-kinase-Akt signal transduction in virus survival. *J Gen Virol,* 85**,** 1065-76.

CROS, J. F. & PALESE, P. 2003. Trafficking of viral genomic RNA into and out of the nucleus: influenza, Thogoto and Borna disease viruses. *Virus Res,* 95**,** 3-12.

CROWLEY, T. M., HARING, V. R., BURGGRAAF, S. & MOORE, R. J. 2009. Application of chicken microarrays for gene expression analysis in other avian species. *BMC Genomics,* 10 Suppl 2**,** S3.

DAI, X., ZHANG, L. & HONG, T. 2011. Host cellular signaling induced by influenza virus. *Sci China Life Sci,* 54**,** 68-74.

DALY, J. M., MACRAE, S., NEWTON, J. R., WATTRANG, E. & ELTON, D. M. 2011. Equine influenza: a review of an unpredictable virus. *Vet J,* 189**,** 7-14.

DAWSON, C. W., TRAMOUNTANIS, G., ELIOPOULOS, A. G. & YOUNG, L. S. 2003. Epstein-Barr virus latent membrane protein 1 (LMP1) activates the phosphatidylinositol 3-kinase/Akt pathway to promote cell survival and induce actin filament remodeling. *J Biol Chem,* 278**,** 3694-704.

DE GRAAF, M. & FOUCHIER, R. A. 2014. Role of receptor binding specificity in influenza A virus transmission and pathogenesis. *EMBO J,* 33**,** 823-41.

DEFILIPPI, P., OLIVO, C., VENTURINO, M., DOLCE, L., SILENGO, L. & TARONE, G. 1999. Actin cytoskeleton organization in response to integrin-mediated adhesion. *Microsc Res Tech,* 47**,** 67-78.

DELGADO-ORTEGA, M., MELO, S., PUNYADARSANIYA, D., RAME, C., OLIVIER, M., SOUBIEUX, D., MARC, D., SIMON, G., HERRLER, G., BERRI, M., DUPONT, J. & MEURENS, F. 2014. Innate immune response to a H3N2 subtype swine influenza virus in newborn porcine trachea cells, alveolar macrophages, and precision-cut lung slices. *Vet Res,* 45**,** 42.

DHAND, R., HILES, I., PANAYOTOU, G., ROCHE, S., FRY, M. J., GOUT, I., TOTTY, N. F., TRUONG, O., VICENDO, P., YONEZAWA, K. & ET AL. 1994. PI 3-kinase is a dual specificity enzyme: autoregulation by an intrinsic protein-serine kinase activity. *EMBO J,* 13**,** 522-33.

DIEHL, N. & SCHAAL, H. 2013. Make yourself at home: viral hijacking of the PI3K/Akt signaling pathway. *Viruses,* 5**,** 3192-212.

DIGARD, P., ELTON, D., BISHOP, K., MEDCALF, E., WEEDS, A. & POPE, B. 1999. Modulation of nuclear localization of the

influenza virus nucleoprotein through interaction with actin filaments. *J Virol,* 73**,** 2222-31.

DING, Z., LIANG, J., LI, J., LU, Y., ARIYARATNA, V., LU, Z., DAVIES, M. A., WESTWICK, J. K. & MILLS, G. B. 2010. Physical association of PDK1 with AKT1 is sufficient for pathway activation independent of membrane localization and phosphatidylinositol 3 kinase. *PLoS One,* 5**,** e9910.

DONG, C., DAVIS, R. J. & FLAVELL, R. A. 2002. MAP kinases in the immune response. *Annu Rev Immunol,* 20**,** 55-72.

EHRHARDT, C. & LUDWIG, S. 2009. A new player in a deadly game: influenza viruses and the PI3K/Akt signalling pathway. *Cell Microbiol,* 11**,** 863-71.

EHRHARDT, C., MARJUKI, H., WOLFF, T., NURNBERG, B., PLANZ, O., PLESCHKA, S. & LUDWIG, S. 2006. Bivalent role of the phosphatidylinositol-3-kinase (PI3K) during influenza virus infection and host cell defence. *Cell Microbiol,* 8**,** 1336-48.

EHRHARDT, C., WOLFF, T. & LUDWIG, S. 2007a. Activation of phosphatidylinositol 3-kinase signaling by the nonstructural NS1 protein is not conserved among type A and B influenza viruses. *J Virol,* 81**,** 12097-100.

EHRHARDT, C., WOLFF, T., PLESCHKA, S., PLANZ, O., BEERMANN, W., BODE, J. G., SCHMOLKE, M. & LUDWIG, S. 2007b. Influenza A virus NS1 protein activates the PI3K/Akt pathway to mediate antiapoptotic signaling responses. *J Virol,* 81**,** 3058-67.

EHRLICH, E. 2017. *Regulation of BAX mediated apoptosis by BCL2 family members* [Online]. Available: https://www.qiagen.com/gb/spotlight-pages/newsletters-and-magazines/articles/reviews-online-apoptosis/ [Accessed 2017].

EIERHOFF, T., HRINCIUS, E. R., RESCHER, U., LUDWIG, S. & EHRHARDT, C. 2010. The epidermal growth factor receptor (EGFR) promotes uptake of influenza A viruses (IAV) into host cells. *PLoS Pathog,* 6**,** e1001099.

ELBAHESH, H., CLINE, T., BARANOVICH, T., GOVORKOVA, E. A., SCHULTZ-CHERRY, S. & RUSSELL, C. J. 2014. Novel roles of focal adhesion kinase in cytoplasmic entry and replication of influenza A viruses. *J Virol,* 88**,** 6714-28.

ELTON, D., SIMPSON-HOLLEY, M., ARCHER, K., MEDCALF, L., HALLAM, R., MCCAULEY, J. & DIGARD, P. 2001. Interaction of the influenza virus nucleoprotein with the cellular CRM1-mediated nuclear export pathway. *J Virol,* 75**,** 408-19.

FAN, S., MACKEN, C. A., LI, C., OZAWA, M., GOTO, H., ISWAHYUDI, N. F., NIDOM, C. A., CHEN, H., NEUMANN, G. & KAWAOKA, Y. 2013. Synergistic effect of the PDZ and p85beta-binding domains of the NS1 protein on virulence of an avian H5N1 influenza A virus. *J Virol,* 87**,** 4861-71.

FOUCHIER, R. A., MUNSTER, V., WALLENSTEN, A., BESTEBROER, T. M., HERFST, S., SMITH, D., RIMMELZWAAN, G. F., OLSEN, B. & OSTERHAUS, A. D. 2005. Characterization of a novel influenza A virus hemagglutinin subtype (H16) obtained from black-headed gulls. *J Virol,* 79**,** 2814-22.

FRANKE, T. F., HORNIK, C. P., SEGEV, L., SHOSTAK, G. A. & SUGIMOTO, C. 2003. PI3K/Akt and apoptosis: size matters. *Oncogene,* 22**,** 8983-98.

FUJII, Y., WATANABE, T., HORIMOTO, T. & KAWAOKA, Y. 2003. [The enigma of influenza virus genome packaging revealed]. *Tanpakushitsu Kakusan Koso,* 48**,** 1357-63.

FUJIOKA, Y., TSUDA, M., HATTORI, T., SASAKI, J., SASAKI, T., MIYAZAKI, T. & OHBA, Y. 2011. The Ras-PI3K signaling pathway is involved in clathrin-independent endocytosis and the internalization of influenza viruses. *PLoS One,* 6**,** e16324.

GARCIA, M. A., GIL, J., VENTOSO, I., GUERRA, S., DOMINGO, E., RIVAS, C. & ESTEBAN, M. 2006. Impact of protein kinase PKR in cell biology: from antiviral to antiproliferative action. *Microbiol Mol Biol Rev,* 70**,** 1032-60.

GAUR, P., MUNJHAL, A. & LAL, S. K. 2011. Influenza virus and cell signaling pathways. *Med Sci Monit,* 17**,** RA148-54.

GREENSPAN, D., PALESE, P. & KRYSTAL, M. 1988. Two nuclear location signals in the influenza virus NS1 nonstructural protein. *J Virol,* 62**,** 3020-6.

GUAN, J., FU, Q., CHAN, M. & SPENCER, J. L. 2013. Aerosol transmission of an avian influenza H9N2 virus with a tropism for the respiratory tract of chickens. *Avian Dis,* 57**,** 645-9.

GUO, Y. J., JIN, F. G., WANG, P., WANG, M. & ZHU, J. M. 1983. Isolation of influenza C virus from pigs and experimental infection of pigs with influenza C virus. *J Gen Virol,* 64 (Pt 1)**,** 177-82.

HACKETT, S. J., KIMBALL, R. T., REDDY, S., BOWIE, R. C., BRAUN, E. L., BRAUN, M. J., CHOJNOWSKI, J. L., COX, W. A., HAN, K. L., HARSHMAN, J., HUDDLESTON, C. J., MARKS, B. D., MIGLIA, K. J., MOORE, W. S., SHELDON, F. H., STEADMAN, D. W., WITT, C. C. & YURI, T. 2008. A phylogenomic study of birds reveals their evolutionary history. *Science,* 320**,** 1763-8.

HALE, B. G., BATTY, I. H., DOWNES, C. P. & RANDALL, R. E. 2008. Binding of influenza A virus NS1 protein to the inter-SH2 domain of p85 suggests a novel mechanism for phosphoinositide 3-kinase activation. *J Biol Chem,* 283**,** 1372-80.

HALE, B. G., JACKSON, D., CHEN, Y. H., LAMB, R. A. & RANDALL, R. E. 2006. Influenza A virus NS1 protein binds p85beta and activates phosphatidylinositol-3-kinase signaling. *Proc Natl Acad Sci U S A,* 103**,** 14194-9.

HALE, B. G., KERRY, P. S., JACKSON, D., PRECIOUS, B. L., GRAY, A., KILLIP, M. J., RANDALL, R. E. & RUSSELL, R. J. 2010. Structural insights into phosphoinositide 3-kinase activation by the influenza A virus NS1 protein. *Proc Natl Acad Sci U S A,* 107**,** 1954-9.

HALL, A. 1998. Rho GTPases and the actin cytoskeleton. *Science,* 279**,** 509-14.

HAN, D. C. & GUAN, J. L. 1999. Association of focal adhesion kinase with Grb7 and its role in cell migration. *J Biol Chem,* 274**,** 24425-30.

HARRIS, B. Z. & LIM, W. A. 2001. Mechanism and role of PDZ domains in signaling complex assembly. *J Cell Sci,* 114**,** 3219-31.

HASS, J., MATUSZEWSKI, S., CIESLIK, D. & HAASE, M. 2011. The role of swine as "mixing vessel" for interspecies transmission of the influenza A subtype H1N1: a simultaneous Bayesian inference of phylogeny and ancestral hosts. *Infect Genet Evol,* 11**,** 437-41.

HAUSE, B. M., DUCATEZ, M., COLLIN, E. A., RAN, Z., LIU, R., SHENG, Z., ARMIEN, A., KAPLAN, B., CHAKRAVARTY, S., HOPPE, A. D., WEBBY, R. J., SIMONSON, R. R. & LI, F. 2013. Isolation of a novel swine influenza virus from Oklahoma in 2011 which is distantly related to human influenza C viruses. *PLoS Pathog,* 9**,** e1003176.

HAUSER, M. J., DLUGOLENSKI, D., CULHANE, M. R., WENTWORTH, D. E., TOMPKINS, S. M. & TRIPP, R. A. 2013. Antiviral responses by Swine primary bronchoepithelial cells are limited compared to human bronchoepithelial cells following influenza virus infection. *PLoS One,* 8**,** e70251.

HAYASHI, T., MACDONALD, L. A. & TAKIMOTO, T. 2015. Influenza A Virus Protein PA-X Contributes to Viral Growth and Suppression of the Host Antiviral and Immune Responses. *J Virol,* 89**,** 6442-52.

HAYASHI, T., WATANABE, C., SUZUKI, Y., TANIKAWA, T., UCHIDA, Y. & SAITO, T. 2014. Chicken MDA5 senses short double-stranded RNA with implications for antiviral response against avian influenza viruses in chicken. *J Innate Immun,* 6**,** 58-71.

HEINONEN, H., NIEMINEN, A., SAARELA, M., KALLIONIEMI, A., KLEFSTROM, J., HAUTANIEMI, S. & MONNI, O. 2008. Deciphering downstream gene targets of PI3K/mTOR/p70S6K pathway in breast cancer. *BMC Genomics,* 9**,** 348.

HENNION, R. M. 2015. The preparation of chicken tracheal organ cultures for virus isolation, propagation, and titration. *Methods Mol Biol,* 1282**,** 51-6.

HERFST, S., SCHRAUWEN, E. J., LINSTER, M., CHUTINIMITKUL, S., DE WIT, E., MUNSTER, V. J., SORRELL, E. M., BESTEBROER, T. M., BURKE, D. F., SMITH, D. J., RIMMELZWAAN, G. F., OSTERHAUS, A. D. & FOUCHIER, R. A. 2012. Airborne transmission of influenza A/H5N1 virus between ferrets. *Science,* 336**,** 1534-41.

HERS, I., VINCENT, E. E. & TAVARE, J. M. 2011. Akt signalling in health and disease. *Cell Signal,* 23**,** 1515-27.

HIRATA, N., SUIZU, F., MATSUDA-LENNIKOV, M., EDAMURA, T., BALA, J. & NOGUCHI, M. 2014. Inhibition of Akt kinase activity suppresses entry and replication of influenza virus. *Biochem Biophys Res Commun,* 450**,** 891-8.

HOFFMANN, E., STECH, J., GUAN, Y., WEBSTER, R. G. & PEREZ, D. R. 2001. Universal primer set for the full-length amplification of all influenza A viruses. *Arch Virol,* 146**,** 2275-89.

HOLTENIUS, J. & GILLMAN, A. 2014. The Spanish flu in Uppsala, clinical and epidemiological impact of the influenza pandemic 1918-1919 on a Swedish county. *Infect Ecol Epidemiol,* 4.

HORISBERGER, M. A., STAEHELI, P. & HALLER, O. 1983. Interferon induces a unique protein in mouse cells bearing a gene for resistance to influenza virus. *Proc Natl Acad Sci U S A,* 80**,** 1910-4.

HU, J., MO, Y., WANG, X., GU, M., HU, Z., ZHONG, L., WU, Q., HAO, X., HU, S., LIU, W., LIU, H., LIU, X. & LIU, X. 2015. PA-X decreases the pathogenicity of highly pathogenic H5N1 influenza A virus in avian species by inhibiting virus replication and host response. *J Virol,* 89**,** 4126-42.

HUANG, Y., LI, Y., BURT, D. W., CHEN, H., ZHANG, Y., QIAN, W., KIM, H., GAN, S., ZHAO, Y., LI, J., YI, K., FENG, H., ZHU, P., LI, B., LIU, Q., FAIRLEY, S., MAGOR, K. E., DU, Z., HU, X., GOODMAN, L., TAFER, H., VIGNAL, A., LEE, T., KIM, K. W., SHENG, Z., AN, Y., SEARLE, S., HERRERO, J., GROENEN, M. A., CROOIJMANS, R. P., FARAUT, T., CAI, Q., WEBSTER, R. G., ALDRIDGE, J. R., WARREN, W. C., BARTSCHAT, S., KEHR, S., MARZ, M., STADLER, P. F., SMITH, J., KRAUS, R. H., ZHAO, Y., REN, L., FEI, J., MORISSON, M., KAISER, P., GRIFFIN, D. K., RAO, M., PITEL, F., WANG, J. & LI, N. 2013. The duck genome and transcriptome provide insight into an avian influenza virus reservoir species. *Nat Genet,* 45**,** 776-83.

HUI, E. K. & NAYAK, D. P. 2002. Role of G protein and protein kinase signalling in influenza virus budding in MDCK cells. *J Gen Virol,* 83**,** 3055-66.

HUTCHINSON, E. C., VON KIRCHBACH, J. C., GOG, J. R. & DIGARD, P. 2010. Genome packaging in influenza A virus. *J Gen Virol,* 91**,** 313-28.

INOUE, E., WANG, X., OSAWA, Y. & OKAZAKI, K. 2010. Full genomic amplification and subtyping of influenza A virus using a single set of universal primers. *Microbiol Immunol,* 54**,** 129-34.

INTERNATIONAL CHICKEN GENOME SEQUENCING, C. 2004. Sequence and comparative analysis of the chicken genome

provide unique perspectives on vertebrate evolution. *Nature,* 432**,** 695-716.

IRIZARRY, R. A., BOLSTAD, B. M., COLLIN, F., COPE, L. M., HOBBS, B. & SPEED, T. P. 2003a. Summaries of Affymetrix GeneChip probe level data. *Nucleic Acids Res,* 31**,** e15.

IRIZARRY, R. A., HOBBS, B., COLLIN, F., BEAZER-BARCLAY, Y. D., ANTONELLIS, K. J., SCHERF, U. & SPEED, T. P. 2003b. Exploration, normalization, and summaries of high density oligonucleotide array probe level data. *Biostatistics,* 4**,** 249-64.

IWAI, A., SHIOZAKI, T. & MIYAZAKI, T. 2013. Relevance of signaling molecules for apoptosis induction on influenza A virus replication. *Biochem Biophys Res Commun,* 441**,** 531-7.

IWASAKI, A. & PILLAI, P. S. 2014. Innate immunity to influenza virus infection. *Nat Rev Immunol,* 14**,** 315-28.

IZMAILYAN, R., HSAO, J. C., CHUNG, C. S., CHEN, C. H., HSU, P. W., LIAO, C. L. & CHANG, W. 2012. Integrin beta1 mediates vaccinia virus entry through activation of PI3K/Akt signaling. *J Virol,* 86**,** 6677-87.

JACKSON, D., KILLIP, M. J., GALLOWAY, C. S., RUSSELL, R. J. & RANDALL, R. E. 2010. Loss of function of the influenza A virus NS1 protein promotes apoptosis but this is not due to a failure to activate phosphatidylinositol 3-kinase (PI3K). *Virology,* 396**,** 94-105.

JAGGER, B. W., WISE, H. M., KASH, J. C., WALTERS, K. A., WILLS, N. M., XIAO, Y. L., DUNFEE, R. L., SCHWARTZMAN, L. M., OZINSKY, A., BELL, G. L., DALTON, R. M., LO, A., EFSTATHIOU, S., ATKINS, J. F., FIRTH, A. E., TAUBENBERGER, J. K. & DIGARD, P. 2012. An overlapping protein-coding region in influenza A virus segment 3 modulates the host response. *Science,* 337**,** 199-204.

JAMES, J., HOWARD, W., IQBAL, M., NAIR, V. K., BARCLAY, W. S. & SHELTON, H. 2016. Influenza A virus PB1-F2 protein prolongs viral shedding in chickens lengthening the transmission window. *J Gen Virol,* 97**,** 2516-2527.

JI, W. T. & LIU, H. J. 2008. PI3K-Akt signaling and viral infection. *Recent Pat Biotechnol,* 2**,** 218-26.

JIA, Y., VISWAKARMA, N., CRAWFORD, S. E., SARKAR, J., SAMBASIVA RAO, M., KARPUS, W. J., KANWAR, Y. S., ZHU, Y. J. & REDDY, J. K. 2012. Early embryonic lethality of mice with disrupted transcription cofactor PIMT/NCOA6IP/Tgs1 gene. *Mech Dev,* 129**,** 193-207.

JIANG, W., SHENG, C., GU, X., LIU, D., YAO, C., GAO, S., CHEN, S., HUANG, Y., HUANG, W. & FANG, M. 2016. Suppression of Rac1 Signaling by Influenza A Virus NS1 Facilitates Viral Replication. *Sci Rep,* 6**,** 35041.

KAISER, P. 2010. Advances in avian immunology--prospects for disease control: a review. *Avian Pathol,* 39**,** 309-24.

KAISER, P., ROTHWELL, L., GALYOV, E. E., BARROW, P. A., BURNSIDE, J. & WIGLEY, P. 2000. Differential cytokine expression in avian cells in response to invasion by Salmonella typhimurium, Salmonella enteritidis and Salmonella gallinarum. *Microbiology,* 146 Pt 12**,** 3217-26.

KAMAL, R. P., KATZ, J. M. & YORK, I. A. 2014. Molecular determinants of influenza virus pathogenesis in mice. *Curr Top Microbiol Immunol,* 385**,** 243-74.

KANG, Y., YUAN, R., ZHAO, X., XIANG, B., GAO, S., GAO, P., DAI, X., FENG, M., LI, Y., XIE, P., LI, Y., GAO, X. & REN, T. 2017. Transient activation of the PI3K/Akt pathway promotes Newcastle disease virus replication and enhances anti-apoptotic signaling responses. *Oncotarget,* 8**,** 23551-23563.

KAREL ANTONI SCHAT, B. K., PETE KAISER 2014. *Avian Immunology*.

KARIN, M. & BEN-NERIAH, Y. 2000. Phosphorylation meets ubiquitination: the control of NF-[kappa]B activity. *Annu Rev Immunol,* 18**,** 621-63.

KAWAGUCHI, A., NAITO, T. & NAGATA, K. 2005. Involvement of influenza virus PA subunit in assembly of functional RNA polymerase complexes. *J Virol,* 79**,** 732-44.

KEELER, C. L., JR., BLISS, T. W., LAVRIC, M. & MAUGHAN, M. N. 2007. A functional genomics approach to the study of avian innate immunity. *Cytogenet Genome Res,* 117**,** 139-45.

KHALIQ, Z., LEIJON, M., BELAK, S. & KOMOROWSKI, J. 2015. A complete map of potential pathogenicity markers of avian

influenza virus subtype H5 predicted from 11 expressed proteins. *BMC Microbiol,* 15**,** 128.

KHAYAT, Z. A., TONG, P., YAWORSKY, K., BLOCH, R. J. & KLIP, A. 2000. Insulin-induced actin filament remodeling colocalizes actin with phosphatidylinositol 3-kinase and GLUT4 in L6 myotubes. *J Cell Sci,* 113 Pt 2**,** 279-90.

KNIPEE, D. M. & M.HOWLEY, P. 2013. *Fields Virology,* Philadalphia, Lippincott Williams & Wilkins.

KNUDSEN, S. 2004. *Guide to analysis of DNA microarray data*.

KOBAYASHI, K., HERNANDEZ, L. D., GALAN, J. E., JANEWAY, C. A., JR., MEDZHITOV, R. & FLAVELL, R. A. 2002. IRAK-M is a negative regulator of Toll-like receptor signaling. *Cell,* 110**,** 191-202.

KOYASU, S. 2003. The role of PI3K in immune cells. *Nat Immunol,* 4**,** 313-9.

KRAUSS, S. & WEBSTER, R. G. 2010. Avian influenza virus surveillance and wild birds: past and present. *Avian Dis,* 54**,** 394-8.

KREIJTZ, J. H., FOUCHIER, R. A. & RIMMELZWAAN, G. F. 2011. Immune responses to influenza virus infection. *Virus Res,* 162**,** 19-30.

KRUG, R. M. 1981. Priming of influenza viral RNA transcription by capped heterologous RNAs. *Curr Top Microbiol Immunol,* 93**,** 125-49.

KRUG, R. M., YUAN, W., NOAH, D. L. & LATHAM, A. G. 2003. Intracellular warfare between human influenza viruses and human cells: the roles of the viral NS1 protein. *Virology,* 309**,** 181-9.

KUCHIPUDI, S. V. 2010. *Studies on the cellular and molecular mechanisms of innate host susceptibility and resistance to influenza A viruses in chicken and ducks.* PhD, University of Glasgow.

KUCHIPUDI, S. V., DUNHAM, S. P. & CHANG, K. C. 2015. DNA microarray global gene expression analysis of influenza virus-infected chicken and duck cells. *Genom Data,* 4**,** 60-4.

KUCHIPUDI, S. V., DUNHAM, S. P., NELLI, R., WHITE, G. A., COWARD, V. J., SLOMKA, M. J., BROWN, I. H. & CHANG, K. C. 2012a. Rapid death of duck cells infected with influenza: a potential mechanism for host resistance to H5N1. *Immunol Cell Biol,* 90**,** 116-23.

KUCHIPUDI, S. V., NELLI, R., WHITE, G. A., BAIN, M., CHANG, K. C. & DUNHAM, S. 2009. Differences in influenza virus receptors in chickens and ducks: Implications for interspecies transmission. *J Mol Genet Med,* 3**,** 143-51.

KUCHIPUDI, S. V., TELLABATI, M., NELLI, R. K., WHITE, G. A., PEREZ, B. B., SEBASTIAN, S., SLOMKA, M. J., BROOKES, S. M., BROWN, I. H., DUNHAM, S. P. & CHANG, K. C. 2012b. 18S rRNA is a reliable normalisation gene for real time PCR based on influenza virus infected cells. *Virol J,* 9**,** 230.

KUCHIPUDI, S. V., TELLABATI, M., SEBASTIAN, S., LONDT, B. Z., JANSEN, C., VERVELDE, L., BROOKES, S. M., BROWN, I. H., DUNHAM, S. P. & CHANG, K. C. 2014. Highly pathogenic avian influenza virus infection in chickens but not ducks is associated with elevated host immune and pro-inflammatory responses. *Vet Res,* 45**,** 118.

LE GOFFIC, R., BALLOY, V., LAGRANDERIE, M., ALEXOPOULOU, L., ESCRIOU, N., FLAVELL, R., CHIGNARD, M. & SI-TAHAR, M. 2006. Detrimental contribution of the Toll-like receptor (TLR)3 to influenza A virus-induced acute pneumonia. *PLoS Pathog,* 2**,** e53.

LEE, C. J., LIAO, C. L. & LIN, Y. L. 2005. Flavivirus activates phosphatidylinositol 3-kinase signaling to block caspase-dependent apoptotic cell death at the early stage of virus infection. *J Virol,* 79**,** 8388-99.

LESLIE, N. R. & DOWNES, C. P. 2004. PTEN function: how normal cells control it and tumour cells lose it. *Biochem J,* 382**,** 1-11.

LI, E., STUPACK, D., BOKOCH, G. M. & NEMEROW, G. R. 1998. Adenovirus endocytosis requires actin cytoskeleton reorganization mediated by Rho family GTPases. *J Virol,* 72**,** 8806-12.

LI, S., MIN, J. Y., KRUG, R. M. & SEN, G. C. 2006. Binding of the influenza A virus NS1 protein to PKR mediates the inhibition of

its activation by either PACT or double-stranded RNA. *Virology,* 349**,** 13-21.

LI, S., ZHU, M., PAN, R., FANG, T., CAO, Y. Y., CHEN, S., ZHAO, X., LEI, C. Q., GUO, L., CHEN, Y., LI, C. M., JOKITALO, E., YIN, Y., SHU, H. B. & GUO, D. 2016. The tumor suppressor PTEN has a critical role in antiviral innate immunity. *Nat Immunol,* 17**,** 241-9.

LI, X., LIU, H., WANG, H., SUN, L., DING, F., SUN, W., HAN, C. & WANG, J. 2014. Follistatin could promote the proliferation of duck primary myoblasts by activating PI3K/Akt/mTOR signalling. *Biosci Rep,* 34.

LI, X. & PALESE, P. 1994. Characterization of the polyadenylation signal of influenza virus RNA. *J Virol,* 68**,** 1245-9.

LI, Y., ANDERSON, D. H., LIU, Q. & ZHOU, Y. 2008. Mechanism of influenza A virus NS1 protein interaction with the p85beta, but not the p85alpha, subunit of phosphatidylinositol 3-kinase (PI3K) and up-regulation of PI3K activity. *J Biol Chem,* 283**,** 23397-409.

LIANG, Q. L., LUO, J., ZHOU, K., DONG, J. X. & HE, H. X. 2011. Immune-related gene expression in response to H5N1 avian influenza virus infection in chicken and duck embryonic fibroblasts. *Mol Immunol,* 48**,** 924-30.

LIEW, F. Y., XU, D., BRINT, E. K. & O'NEILL, L. A. 2005. Negative regulation of toll-like receptor-mediated immune responses. *Nat Rev Immunol,* 5**,** 446-58.

LIMESAND, K. H., BARZEN, K. A., QUISSELL, D. O. & ANDERSON, S. M. 2003. Synergistic suppression of apoptosis in salivary acinar cells by IGF1 and EGF. *Cell Death Differ,* 10**,** 345-55.

LIN, C., HOLLAND, R. E., JR., WILLIAMS, N. M. & CHAMBERS, T. M. 2001a. Cultures of equine respiratory epithelial cells and organ explants as tools for the study of equine influenza virus infection. *Arch Virol,* 146**,** 2239-47.

LIN, C., ZIMMER, S. G., LU, Z., HOLLAND, R. E., JR., DONG, Q. & CHAMBERS, T. M. 2001b. The involvement of a stress-activated pathway in equine influenza virus-mediated apoptosis. *Virology,* 287**,** 202-13.

LIN, P. Y., LIU, H. J., LIAO, M. H., CHANG, C. D., CHANG, C. I., CHENG, H. L., LEE, J. W. & SHIH, W. L. 2010. Activation of PI 3-kinase/Akt/NF-kappaB and Stat3 signaling by avian reovirus S1133 in the early stages of infection results in an inflammatory response and delayed apoptosis. *Virology,* 400**,** 104-14.

LINIGER, M., SUMMERFIELD, A., ZIMMER, G., MCCULLOUGH, K. C. & RUGGLI, N. 2012. Chicken cells sense influenza A virus infection through MDA5 and CARDIF signaling involving LGP2. *J Virol,* 86**,** 705-17.

LIPATOV, A. S., ANDREANSKY, S., WEBBY, R. J., HULSE, D. J., REHG, J. E., KRAUSS, S., PEREZ, D. R., DOHERTY, P. C., WEBSTER, R. G. & SANGSTER, M. Y. 2005. Pathogenesis of Hong Kong H5N1 influenza virus NS gene reassortants in mice: the role of cytokines and B- and T-cell responses. *J Gen Virol,* 86**,** 1121-30.

LONG, J. S., GIOTIS, E. S., MONCORGE, O., FRISE, R., MISTRY, B., JAMES, J., MORISSON, M., IQBAL, M., VIGNAL, A., SKINNER, M. A. & BARCLAY, W. S. 2016. Species difference in ANP32A underlies influenza A virus polymerase host restriction. *Nature,* 529**,** 101-4.

LU, X., MASIC, A., LI, Y., SHIN, Y., LIU, Q. & ZHOU, Y. 2010. The PI3K/Akt pathway inhibits influenza A virus-induced Bax-mediated apoptosis by negatively regulating the JNK pathway via ASK1. *J Gen Virol,* 91**,** 1439-49.

LU, X. X., CAO, L. Y., CHEN, X., XIAO, J., ZOU, Y. & CHEN, Q. 2016. PTEN Inhibits Cell Proliferation, Promotes Cell Apoptosis, and Induces Cell Cycle Arrest via Downregulating the PI3K/AKT/hTERT Pathway in Lung Adenocarcinoma A549 Cells. *Biomed Res Int,* 2016**,** 2476842.

MA, C. X., REINERT, T., CHMIELEWSKA, I. & ELLIS, M. J. 2015. Mechanisms of aromatase inhibitor resistance. *Nat Rev Cancer,* 15**,** 261-75.

MA, W., KAHN, R. E. & RICHT, J. A. 2008. The pig as a mixing vessel for influenza viruses: Human and veterinary implications. *J Mol Genet Med,* 3**,** 158-66.

MAAMARY, J., PICA, N., BELICHA-VILLANUEVA, A., CHOU, Y. Y., KRAMMER, F., GAO, Q., GARCIA-SASTRE, A. & PALESE, P.

2012. Attenuated influenza virus construct with enhanced hemagglutinin protein expression. *J Virol,* 86**,** 5782-90.

MAIER, H. J., HAWES, P. C., COTTAM, E. M., MANTELL, J., VERKADE, P., MONAGHAN, P., WILEMAN, T. & BRITTON, P. 2013. Infectious bronchitis virus generates spherules from zippered endoplasmic reticulum membranes. *MBio,* 4**,** e00801-13.

MANNOVA, P. & BERETTA, L. 2005. Activation of the N-Ras-PI3K-Akt-mTOR pathway by hepatitis C virus: control of cell survival and viral replication. *J Virol,* 79**,** 8742-9.

MARTIN, K. & HELENIUS, A. 1991a. Nuclear transport of influenza virus ribonucleoproteins: the viral matrix protein (M1) promotes export and inhibits import. *Cell,* 67**,** 117-30.

MARTIN, K. & HELENIUS, A. 1991b. Transport of incoming influenza virus nucleocapsids into the nucleus. *J Virol,* 65**,** 232-44.

MATSUZAKI, Y., KATSUSHIMA, N., NAGAI, Y., SHOJI, M., ITAGAKI, T., SAKAMOTO, M., KITAOKA, S., MIZUTA, K. & NISHIMURA, H. 2006. Clinical features of influenza C virus infection in children. *J Infect Dis,* 193**,** 1229-35.

MATSUZAKI, Y., SUGAWARA, K., MIZUTA, K., TSUCHIYA, E., MURAKI, Y., HONGO, S., SUZUKI, H. & NAKAMURA, K. 2002. Antigenic and genetic characterization of influenza C viruses which caused two outbreaks in Yamagata City, Japan, in 1996 and 1998. *J Clin Microbiol,* 40**,** 422-9.

MAUGHAN, M. N., DOUGHERTY, L. S., PRESKENIS, L. A., LADMAN, B. S., GELB, J., JR., SPACKMAN, E. V. & KEELER, C. L., JR. 2013. Transcriptional analysis of the innate immune response of ducks to different species-of-origin low pathogenic H7 avian influenza viruses. *Virol J,* 10**,** 94.

MCNAMARA, C. R. & DEGTEREV, A. 2011. Small-molecule inhibitors of the PI3K signaling network. *Future Med Chem,* 3**,** 549-65.

MCWHIRTER, S. M., TENOEVER, B. R. & MANIATIS, T. 2005. Connecting mitochondria and innate immunity. *Cell,* 122**,** 645-7.

MIBAYASHI, M., MARTINEZ-SOBRIDO, L., LOO, Y. M., CARDENAS, W. B., GALE, M., JR. & GARCIA-SASTRE, A. 2007. Inhibition of retinoic acid-inducible gene I-mediated induction of beta

interferon by the NS1 protein of influenza A virus. *J Virol,* 81**,** 514-24.

MIN, J. Y. & KRUG, R. M. 2006. The primary function of RNA binding by the influenza A virus NS1 protein in infected cells: Inhibiting the 2'-5' oligo (A) synthetase/RNase L pathway. *Proc Natl Acad Sci U S A,* 103**,** 7100-5.

MIZUTANI, T., FUKUSHI, S., SAIJO, M., KURANE, I. & MORIKAWA, S. 2004. Importance of Akt signaling pathway for apoptosis in SARS-CoV-infected Vero E6 cells. *Virology,* 327**,** 169-74.

MONNE, I., FUSARO, A., NELSON, M. I., BONFANTI, L., MULATTI, P., HUGHES, J., MURCIA, P. R., SCHIVO, A., VALASTRO, V., MORENO, A., HOLMES, E. C. & CATTOLI, G. 2014. Emergence of a highly pathogenic avian influenza virus from a low-pathogenic progenitor. *J Virol,* 88**,** 4375-88.

MUNDT, E., GAY, L., JONES, L., SAAVEDRA, G., TOMPKINS, S. M. & TRIPP, R. A. 2009. Replication and pathogenesis associated with H5N1, H5N2, and H5N3 low-pathogenic avian influenza virus infection in chickens and ducks. *Arch Virol,* 154**,** 1241-8.

MUNIR, M., ZOHARI, S., IQBAL, M., ABBAS, M., PEREZ, D. R. & BERG, M. 2013. The non-structural (NS) gene segment of H9N2 influenza virus isolated from backyard poultry in Pakistan reveals strong genetic and functional similarities to the NS gene of highly pathogenic H5N1. *Virulence,* 4**,** 612-23.

MURANAKA, M., YAMANAKA, T., KATAYAMA, Y., HIDARI, K., KANAZAWA, H., SUZUKI, T., OKU, K. & OYAMADA, T. 2011. Distribution of influenza virus sialoreceptors on upper and lower respiratory tract in horses and dogs. *J Vet Med Sci,* 73**,** 125-7.

NELLI, R. K., DUNHAM, S. P., KUCHIPUDI, S. V., WHITE, G. A., BAQUERO-PEREZ, B., CHANG, P., GHAEMMAGHAMI, A., BROOKES, S. M., BROWN, I. H. & CHANG, K. C. 2012. Mammalian innate resistance to highly pathogenic avian influenza H5N1 virus infection is mediated through reduced proinflammation and infectious virus release. *J Virol,* 86**,** 9201-10.

NELLI, R. K., KUCHIPUDI, S. V., WHITE, G. A., PEREZ, B. B., DUNHAM, S. P. & CHANG, K. C. 2010. Comparative distribution of human and avian type sialic acid influenza receptors in the pig. *BMC Vet Res,* 6**,** 4.

NEMEROFF, M. E., BARABINO, S. M., LI, Y., KELLER, W. & KRUG, R. M. 1998. Influenza virus NS1 protein interacts with the cellular 30 kDa subunit of CPSF and inhibits 3'end formation of cellular pre-mRNAs. *Mol Cell,* 1**,** 991-1000.

NEUMANN, G., NODA, T. & KAWAOKA, Y. 2009. Emergence and pandemic potential of swine-origin H1N1 influenza virus. *Nature,* 459**,** 931-9.

NEUMANN, G., WATANABE, T., ITO, H., WATANABE, S., GOTO, H., GAO, P., HUGHES, M., PEREZ, D. R., DONIS, R., HOFFMANN, E., HOBOM, G. & KAWAOKA, Y. 1999. Generation of influenza A viruses entirely from cloned cDNAs. *Proc Natl Acad Sci U S A,* 96**,** 9345-50.

NI, M., MACFARLANE, A. W. T., TOFT, M., LOWELL, C. A., CAMPBELL, K. S. & HAMERMAN, J. A. 2012. B-cell adaptor for PI3K (BCAP) negatively regulates Toll-like receptor signaling through activation of PI3K. *Proc Natl Acad Sci U S A,* 109**,** 267-72.

NODA, T. 2015. Genome Packaging Mechanism of Influenza A Virus. *Yakugaku Zasshi,* 135**,** 1011-3.

NODA, T. & KAWAOKA, Y. 2010. Structure of influenza virus ribonucleoprotein complexes and their packaging into virions. *Rev Med Virol,* 20**,** 380-91.

O'NEILL, R. E., TALON, J. & PALESE, P. 1998. The influenza virus NEP (NS2 protein) mediates the nuclear export of viral ribonucleoproteins. *EMBO J,* 17**,** 288-96.

OBENAUER, J. C., DENSON, J., MEHTA, P. K., SU, X., MUKATIRA, S., FINKELSTEIN, D. B., XU, X., WANG, J., MA, J., FAN, Y., RAKESTRAW, K. M., WEBSTER, R. G., HOFFMANN, E., KRAUSS, S., ZHENG, J., ZHANG, Z. & NAEVE, C. W. 2006. Large-scale sequence analysis of avian influenza isolates. *Science,* 311**,** 1576-80.

OFRAN, Y. & ROST, B. 2007. ISIS: interaction sites identified from sequence. *Bioinformatics,* 23**,** e13-6.

OKKENHAUG, K. & VANHAESEBROECK, B. 2001. New responsibilities for the PI3K regulatory subunit p85 alpha. *Sci STKE,* 2001**,** pe1.

OSTERHAUS, A. D., RIMMELZWAAN, G. F., MARTINA, B. E., BESTEBROER, T. M. & FOUCHIER, R. A. 2000. Influenza B virus in seals. *Science,* 288**,** 1051-3.

OTSU, M., HILES, I., GOUT, I., FRY, M. J., RUIZ-LARREA, F., PANAYOTOU, G., THOMPSON, A., DHAND, R., HSUAN, J., TOTTY, N. & ET AL. 1991. Characterization of two 85 kd proteins that associate with receptor tyrosine kinases, middle-T/pp60c-src complexes, and PI3-kinase. *Cell,* 65**,** 91-104.

PARRISH, C. R., MURCIA, P. R. & HOLMES, E. C. 2015. Influenza virus reservoirs and intermediate hosts: dogs, horses, and new possibilities for influenza virus exposure of humans. *J Virol,* 89**,** 2990-4.

PASARE, C. & MEDZHITOV, R. 2005. Toll-like receptors: linking innate and adaptive immunity. *Adv Exp Med Biol,* 560**,** 11-8.

PAWSON, T. 1995. Protein modules and signalling networks. *Nature,* 373**,** 573-80.

PAWSON, T. 2004. Specificity in signal transduction: from phosphotyrosine-SH2 domain interactions to complex cellular systems. *Cell,* 116**,** 191-203.

PORTELA, A. & DIGARD, P. 2002. The influenza virus nucleoprotein: a multifunctional RNA-binding protein pivotal to virus replication. *J Gen Virol,* 83**,** 723-34.

POTTER, C. W. 2001. A history of influenza. *J Appl Microbiol,* 91**,** 572-9.

PREDICALA, R. & ZHOU, Y. 2013. The role of Ran-binding protein 3 during influenza A virus replication. *J Gen Virol,* 94**,** 977-84.

PRESTI, R. M., ZHAO, G., BEATTY, W. L., MIHINDUKULASURIYA, K. A., DA ROSA, A. P., POPOV, V. L., TESH, R. B., VIRGIN, H. W. & WANG, D. 2009. Quaranfil, Johnston Atoll, and Lake Chad viruses are novel members of the family Orthomyxoviridae. *J Virol,* 83**,** 11599-606.

QIAN, Y., CORUM, L., MENG, Q., BLENIS, J., ZHENG, J. Z., SHI, X., FLYNN, D. C. & JIANG, B. H. 2004. PI3K induced actin filament remodeling through Akt and p70S6K1: implication of essential role in cell migration. *Am J Physiol Cell Physiol,* 286**,** C153-63.

QUAN, R., ZHU, S., WEI, L., WANG, J., YAN, X., LI, Z. & LIU, J. 2017. Transcriptional profiles in bursal B-lymphoid DT40 cells infected with very virulent infectious bursal disease virus. *Virol J,* 14**,** 7.

QUAST, M., SREENIVASAN, C., SEXTON, G., NEDLAND, H., SINGREY, A., FAWCETT, L., MILLER, G., LAUER, D., VOSS, S., POLLOCK,

S., CUNHA, C. W., CHRISTOPHER-HENNINGS, J., NELSON, E. & LI, F. 2015. Serological evidence for the presence of influenza D virus in small ruminants. *Vet Microbiol*.

RAMOS, I. & FERNANDEZ-SESMA, A. 2015. Modulating the Innate Immune Response to Influenza A Virus: Potential Therapeutic Use of Anti-Inflammatory Drugs. *Front Immunol,* 6**,** 361.

REBEL, J. M., PEETERS, B., FIJTEN, H., POST, J., CORNELISSEN, J. & VERVELDE, L. 2011. Highly pathogenic or low pathogenic avian influenza virus subtype H7N1 infection in chicken lungs: small differences in general acute responses. *Vet Res,* 42**,** 10.

RIDLEY, A. J., SCHWARTZ, M. A., BURRIDGE, K., FIRTEL, R. A., GINSBERG, M. H., BORISY, G., PARSONS, J. T. & HORWITZ, A. R. 2003. Cell migration: integrating signals from front to back. *Science,* 302**,** 1704-9.

ROBERTS, P. C. & COMPANS, R. W. 1998. Host cell dependence of viral morphology. *Proc Natl Acad Sci U S A,* 95**,** 5746-51.

SAEED, M. F., KOLOKOLTSOV, A. A., FREIBERG, A. N., HOLBROOK, M. R. & DAVEY, R. A. 2008. Phosphoinositide-3 kinase-Akt pathway controls cellular entry of Ebola virus. *PLoS Pathog,* 4**,** e1000141.

SAMJI, T. 2009. Influenza A: understanding the viral life cycle. *Yale J Biol Med,* 82**,** 153-9.

SARBASSOV, D. D., GUERTIN, D. A., ALI, S. M. & SABATINI, D. M. 2005. Phosphorylation and regulation of Akt/PKB by the rictor-mTOR complex. *Science,* 307**,** 1098-101.

SARKAR, S. N., PETERS, K. L., ELCO, C. P., SAKAMOTO, S., PAL, S. & SEN, G. C. 2004. Novel roles of TLR3 tyrosine phosphorylation and PI3 kinase in double-stranded RNA signaling. *Nat Struct Mol Biol,* 11**,** 1060-7.

SARMENTO, L., PANTIN-JACKWOOD, M., KAPCZYNSKI, D. R., SWAYNE, D. E. & AFONSO, C. L. 2008. Immediate early responses of avian tracheal epithelial cells to infection with highly pathogenic avian influenza virus. *Dev Biol (Basel),* 132**,** 175-83.

SCHÄFER, W. 1955. Vergleichender sero-immunologische Untersuchungen über die Viren der Influenza und klassischen Geflügelpest. *Z Naturf* 10b**,** 81-91.

SCHAUDER, C., MA, L. C., KRUG, R. M., MONTELIONE, G. T. & GUAN, R. 2010. Structure of the iSH2 domain of human phosphatidylinositol 3-kinase p85beta subunit reveals conformational plasticity in the interhelical turn region. *Acta Crystallogr Sect F Struct Biol Cryst Commun,* 66**,** 1567-71.

SCHNEIDER, W. M., CHEVILLOTTE, M. D. & RICE, C. M. 2014. Interferon-stimulated genes: a complex web of host defenses. *Annu Rev Immunol,* 32**,** 513-45.

SCHRAUWEN, E. J. & FOUCHIER, R. A. 2014. Host adaptation and transmission of influenza A viruses in mammals. *Emerg Microbes Infect,* 3**,** e9.

SENG, L. G., DALY, J., CHANG, K. C. & KUCHIPUDI, S. V. 2014. High basal expression of interferon-stimulated genes in human bronchial epithelial (BEAS-2B) cells contributes to influenza A virus resistance. *PLoS One,* 9**,** e109023.

SHAW, M. L., STONE, K. L., COLANGELO, C. M., GULCICEK, E. E. & PALESE, P. 2008. Cellular proteins in influenza virus particles. *PLoS Pathog,* 4**,** e1000085.

SHIN, Y. K., LI, Y., LIU, Q., ANDERSON, D. H., BABIUK, L. A. & ZHOU, Y. 2007a. SH3 binding motif 1 in influenza A virus NS1 protein is essential for PI3K/Akt signaling pathway activation. *J Virol,* 81**,** 12730-9.

SHIN, Y. K., LIU, Q., TIKOO, S. K., BABIUK, L. A. & ZHOU, Y. 2007b. Effect of the phosphatidylinositol 3-kinase/Akt pathway on influenza A virus propagation. *J Gen Virol,* 88**,** 942-50.

SHIN, Y. K., LIU, Q., TIKOO, S. K., BABIUK, L. A. & ZHOU, Y. 2007c. Influenza A virus NS1 protein activates the phosphatidylinositol 3-kinase (PI3K)/Akt pathway by direct interaction with the p85 subunit of PI3K. *J Gen Virol,* 88**,** 13-8.

SIECZKARSKI, S. B. & WHITTAKER, G. R. 2002. Dissecting virus entry via endocytosis. *J Gen Virol,* 83**,** 1535-45.

SIMMS, L. & JEGGO, M. 2014. Avian influenza from an ecohealth perspective. *Ecohealth,* 11**,** 4-14.

SIMPSON-HOLLEY, M., ELLIS, D., FISHER, D., ELTON, D., MCCAULEY, J. & DIGARD, P. 2002. A functional link between the actin cytoskeleton and lipid rafts during budding of filamentous influenza virions. *Virology,* 301**,** 212-25.

SKEHEL, J. J., BAYLEY, P. M., BROWN, E. B., MARTIN, S. R., WATERFIELD, M. D., WHITE, J. M., WILSON, I. A. & WILEY, D. C. 1982. Changes in the conformation of influenza virus hemagglutinin at the pH optimum of virus-mediated membrane fusion. *Proc Natl Acad Sci U S A,* 79**,** 968-72.

SMITH, J., SMITH, N., YU, L., PATON, I. R., GUTOWSKA, M. W., FORREST, H. L., DANNER, A. F., SEILER, J. P., DIGARD, P., WEBSTER, R. G. & BURT, D. W. 2015. A comparative analysis of host responses to avian influenza infection in ducks and chickens highlights a role for the interferon-induced transmembrane proteins in viral resistance. *BMC Genomics,* 16**,** 574.

SOARES, J. A., LEITE, F. G., ANDRADE, L. G., TORRES, A. A., DE SOUSA, L. P., BARCELOS, L. S., TEIXEIRA, M. M., FERREIRA, P. C., KROON, E. G., SOUTO-PADRON, T. & BONJARDIM, C. A. 2009. Activation of the PI3K/Akt pathway early during vaccinia and cowpox virus infections is required for both host survival and viral replication. *J Virol,* 83**,** 6883-99.

SONGYANG, Z., SHOELSON, S. E., CHAUDHURI, M., GISH, G., PAWSON, T., HASER, W. G., KING, F., ROBERTS, T., RATNOFSKY, S., LECHLEIDER, R. J. & ET AL. 1993. SH2 domains recognize specific phosphopeptide sequences. *Cell,* 72**,** 767-78.

SONNBERG, S., WEBBY, R. J. & WEBSTER, R. G. 2013. Natural history of highly pathogenic avian influenza H5N1. *Virus Res,* 178**,** 63-77.

SPACKMAN, E. 2008. A brief introduction to the avian influenza virus. *Methods Mol Biol,* 436**,** 1-6.

SRIWILAIJAROEN, N. & SUZUKI, Y. 2012. Molecular basis of the structure and function of H1 hemagglutinin of influenza virus. *Proc Jpn Acad Ser B Phys Biol Sci,* 88**,** 226-49.

STALLKNECHT, D. E. & BROWN, J. D. 2009. Tenacity of avian influenza viruses. *Rev Sci Tech,* 28**,** 59-67.

STECH, O., VEITS, J., WEBER, S., DECKERS, D., SCHROER, D., VAHLENKAMP, T. W., BREITHAUPT, A., TEIFKE, J., METTENLEITER, T. C. & STECH, J. 2009. Acquisition of a polybasic hemagglutinin cleavage site by a low-pathogenic avian influenza virus is not sufficient for immediate

transformation into a highly pathogenic strain. *J Virol,* 83**,** 5864-8.

STEGMANN, T. 2000. Membrane fusion mechanisms: the influenza hemagglutinin paradigm and its implications for intracellular fusion. *Traffic,* 1**,** 598-604.

STOJDL, D. F., LICHTY, B., KNOWLES, S., MARIUS, R., ATKINS, H., SONENBERG, N. & BELL, J. C. 2000. Exploiting tumor-specific defects in the interferon pathway with a previously unknown oncolytic virus. *Nat Med,* 6**,** 821-5.

SUIRE, S., COADWELL, J., FERGUSON, G. J., DAVIDSON, K., HAWKINS, P. & STEPHENS, L. 2005. p84, a new Gbetagamma-activated regulatory subunit of the type IB phosphoinositide 3-kinase p110gamma. *Curr Biol,* 15**,** 566-70.

SZEWCZYK, B., BIENKOWSKA-SZEWCZYK, K. & KROL, E. 2014. Introduction to molecular biology of influenza a viruses. *Acta Biochim Pol,* 61**,** 397-401.

TAKEUCHI, K. & LAMB, R. A. 1994. Influenza virus M2 protein ion channel activity stabilizes the native form of fowl plague virus hemagglutinin during intracellular transport. *J Virol,* 68**,** 911-9.

TALON, J., HORVATH, C. M., POLLEY, R., BASLER, C. F., MUSTER, T., PALESE, P. & GARCIA-SASTRE, A. 2000. Activation of interferon regulatory factor 3 is inhibited by the influenza A virus NS1 protein. *J Virol,* 74**,** 7989-96.

TARI, A. M. & LOPEZ-BERESTEIN, G. 2001. GRB2: a pivotal protein in signal transduction. *Semin Oncol,* 28**,** 142-7.

TAYLOR, M. P., KOYUNCU, O. O. & ENQUIST, L. W. 2011. Subversion of the actin cytoskeleton during viral infection. *Nat Rev Microbiol,* 9**,** 427-39.

TELLIER, R. 2006. Review of aerosol transmission of influenza A virus. *Emerg Infect Dis,* 12**,** 1657-62.

TELLIER, R. 2009. Aerosol transmission of influenza A virus: a review of new studies. *J R Soc Interface,* 6 Suppl 6**,** S783-90.

THORPE, L. M., YUZUGULLU, H. & ZHAO, J. J. 2015. PI3K in cancer: divergent roles of isoforms, modes of activation and therapeutic targeting. *Nat Rev Cancer,* 15**,** 7-24.

TONG, S., ZHU, X., LI, Y., SHI, M., ZHANG, J., BOURGEOIS, M., YANG, H., CHEN, X., RECUENCO, S., GOMEZ, J., CHEN, L. M., JOHNSON, A., TAO, Y., DREYFUS, C., YU, W., MCBRIDE, R., CARNEY, P. J., GILBERT, A. T., CHANG, J., GUO, Z., DAVIS, C. T., PAULSON, J. C., STEVENS, J., RUPPRECHT, C. E., HOLMES, E. C., WILSON, I. A. & DONIS, R. O. 2013. New world bats harbor diverse influenza A viruses. *PLoS Pathog,* 9**,** e1003657.

TSAKIRIDIS, T., TONG, P., MATTHEWS, B., TSIANI, E., BILAN, P. J., KLIP, A. & DOWNEY, G. P. 1999. Role of the actin cytoskeleton in insulin action. *Microsc Res Tech,* 47**,** 79-92.

ULEVITCH, R. J. & TOBIAS, P. S. 1995. Receptor-dependent mechanisms of cell stimulation by bacterial endotoxin. *Annu Rev Immunol,* 13**,** 437-57.

VAN DE SANDT, C. E., KREIJTZ, J. H. & RIMMELZWAAN, G. F. 2012. Evasion of influenza A viruses from innate and adaptive immune responses. *Viruses,* 4**,** 1438-76.

VANHAESEBROECK, B., GUILLERMET-GUIBERT, J., GRAUPERA, M. & BILANGES, B. 2010. The emerging mechanisms of isoform-specific PI3K signalling. *Nat Rev Mol Cell Biol,* 11**,** 329-41.

VANHAESEBROECK, B., LEEVERS, S. J., PANAYOTOU, G. & WATERFIELD, M. D. 1997a. Phosphoinositide 3-kinases: a conserved family of signal transducers. *Trends Biochem Sci,* 22**,** 267-72.

VANHAESEBROECK, B., WELHAM, M. J., KOTANI, K., STEIN, R., WARNE, P. H., ZVELEBIL, M. J., HIGASHI, K., VOLINIA, S., DOWNWARD, J. & WATERFIELD, M. D. 1997b. P110delta, a novel phosphoinositide 3-kinase in leukocytes. *Proc Natl Acad Sci U S A,* 94**,** 4330-5.

VASIN, A. V., TEMKINA, O. A., EGOROV, V. V., KLOTCHENKO, S. A., PLOTNIKOVA, M. A. & KISELEV, O. I. 2014. Molecular mechanisms enhancing the proteome of influenza A viruses: an overview of recently discovered proteins. *Virus Res,* 185**,** 53-63.

VASTRAD, B., VASTRAD, C., GODAVARTHI, A. & CHANDRASHEKAR, R. 2017. Molecular mechanisms underlying gliomas and glioblastoma pathogenesis revealed by bioinformatics analysis of microarray data. *Med Oncol,* 34**,** 182.

WAHLE, E. & KELLER, W. 1996. The biochemistry of polyadenylation. *Trends Biochem Sci,* 21**,** 247-50.

WANG, L., WU, J., LU, J., MA, R., SUN, D. & TANG, J. 2015. Regulation of the cell cycle and PI3K/Akt/mTOR signaling pathway by tanshinone I in human breast cancer cell lines. *Mol Med Rep,* 11**,** 931-9.

WANG, X., LI, M., ZHENG, H., MUSTER, T., PALESE, P., BEG, A. A. & GARCIA-SASTRE, A. 2000. Influenza A virus NS1 protein prevents activation of NF-kappaB and induction of alpha/beta interferon. *J Virol,* 74**,** 11566-73.

WASILENKO, J. L., LEE, C. W., SARMENTO, L., SPACKMAN, E., KAPCZYNSKI, D. R., SUAREZ, D. L. & PANTIN-JACKWOOD, M. J. 2008. NP, PB1, and PB2 viral genes contribute to altered replication of H5N1 avian influenza viruses in chickens. *J Virol,* 82**,** 4544-53.

WATANABE, T., WATANABE, S., NODA, T., FUJII, Y. & KAWAOKA, Y. 2003. Exploitation of nucleic acid packaging signals to generate a novel influenza virus-based vector stably expressing two foreign genes. *J Virol,* 77**,** 10575-83.

WEBSTER, R. G., BEAN, W. J., GORMAN, O. T., CHAMBERS, T. M. & KAWAOKA, Y. 1992. Evolution and ecology of influenza A viruses. *Microbiol Rev,* 56**,** 152-79.

WEBSTER, R. G. & GOVORKOVA, E. A. 2014. Continuing challenges in influenza. *Ann N Y Acad Sci*.

WEI, L., ZHU, S., WANG, J. & LIU, J. 2012. Activation of the phosphatidylinositol 3-kinase/Akt signaling pathway during porcine circovirus type 2 infection facilitates cell survival and viral replication. *J Virol,* 86**,** 13589-97.

WHO/OIE/FAO 2014. Revised and updated nomenclature for highly pathogenic avian influenza A (H5N1) viruses. *Influenza Other Respir Viruses,* 8**,** 384-8.

WISE, H. M., FOEGLEIN, A., SUN, J., DALTON, R. M., PATEL, S., HOWARD, W., ANDERSON, E. C., BARCLAY, W. S. & DIGARD, P. 2009. A complicated message: Identification of a novel PB1-related protein translated from influenza A virus segment 2 mRNA. *J Virol,* 83**,** 8021-31.

YANG, H., CARNEY, P. J., CHANG, J. C., VILLANUEVA, J. M. & STEVENS, J. 2015. Structure and receptor binding preferences of recombinant hemagglutinins from avian and human H6 and H10 influenza A virus subtypes. *J Virol*.

YOON, S. W., WEBBY, R. J. & WEBSTER, R. G. 2014. Evolution and Ecology of Influenza A Viruses. *Curr Top Microbiol Immunol*.

YOUIL, R., SU, Q., TONER, T. J., SZYMKOWIAK, C., KWAN, W. S., RUBIN, B., PETRUKHIN, L., KISELEVA, I., SHAW, A. R. & DISTEFANO, D. 2004. Comparative study of influenza virus replication in Vero and MDCK cell lines. *J Virol Methods,* 120**,** 23-31.

YU, J., ZHANG, Y., MCILROY, J., RORDORF-NIKOLIC, T., ORR, G. A. & BACKER, J. M. 1998. Regulation of the p85/p110 phosphatidylinositol 3'-kinase: stabilization and inhibition of the p110alpha catalytic subunit by the p85 regulatory subunit. *Mol Cell Biol,* 18**,** 1379-87.

ZAMARIN, D., GARCIA-SASTRE, A., XIAO, X., WANG, R. & PALESE, P. 2005. Influenza virus PB1-F2 protein induces cell death through mitochondrial ANT3 and VDAC1. *PLoS Pathog,* 1**,** e4.

ZHANG, D. G., LI, W. Z., WANG, G. F., SU, Y., ZENG, J., ZHANG, C., ZENG, X. X., CHEN, X. X., XU, Y. X. & LI, K. S. 2010. Heterologous SH3-p85beta inhibits influenza A virus replication. *Virol J,* 7**,** 170.

ZHIRNOV, O. P. & KLENK, H. D. 2007. Control of apoptosis in influenza virus-infected cells by up-regulation of Akt and p53 signaling. *Apoptosis,* 12**,** 1419-32.

ZHIRNOV, O. P., KONAKOVA, T. E., WOLFF, T. & KLENK, H. D. 2002. NS1 protein of influenza A virus down-regulates apoptosis. *J Virol,* 76**,** 1617-25.

ZVELEBIL, M. J., MACDOUGALL, L., LEEVERS, S., VOLINIA, S., VANHAESEBROECK, B., GOUT, I., PANAYOTOU, G., DOMIN, J., STEIN, R., PAGES, F. & ET AL. 1996. Structural and functional diversity of phosphoinositide 3-kinases. *Philos Trans R Soc Lond B Biol Sci,* 351**,** 217-23.